UNIVERSITY OF CALIFORNIA, SAN DIEGO

Molecular Regulators of Neurogenesis in Alzheimer's Disease

A dissertation submitted in partial satisfaction of the

requirements for the degree Doctor of Philosophy

in

Molecular Pathology

by

Leslie Anne Crews

Committee in charge:

Professor Eliezer Masliah, Chair
Professor Cristian Achim
Professor Ian Everall
Professor Lawrence Goldstein
Professor Andrew Mizisin
Professor Christina Sigurdson

2010

The Dissertation of Leslie Anne Crews is approved, and it is acceptable in quality and form for publication on microfilm and electronically:

Chair

University of California, San Diego

2010

DEDICATION

To my family : Mom, Dad, Carolynn and Geoff.
I love you all, and am so thankful for your constant support and encouragement.

To Chris : Thank you for always encouraging me to find my confidence, and for reminding me that all obstacles can be broken down and overcome, one step at a time.

TABLE OF CONTENTS

LIST OF FIGURES

LIST OF TABLES

ACKNOWLEDGEMENTS

Throughout the past seven years I have been in the lab here at UCSD—five years of which I have spent working towards my PhD—countless people have helped me in so many ways, for which I am utterly grateful. First, I would like to thank my committee members and Professor Eliezer Masliah for his support as the chair of my committee. His mentorship and guidance over these past years have given me invaluable experience throughout my scientific endeavors. Whether he intended to or not, he is responsible for sparking my interest in science writing and communication, which I hope to be able to incorporate into my future career path. I am grateful for the opportunities I have had to learn from Dr. Masliah's expertise through writing and editing myriad papers and grant applications with him—practice that no doubt has prepared me well for the task of preparing this dissertation.

I would also like to extend my gratitude to the past and present members of the Masliah Lab, without whom my research would have no doubt taken five times as long. Thank you all for providing advice, reagents, laboratory expertise, and for putting up with my countless questions along the way. To my coffee buddy, Anna: Thank you for helping break up the monotony of the daily grind with our coffee breaks, printer shenanigans, and hilarious hamster stories; oh, and thank you for always providing thoughtful advice on scientific matters as well. My immense appreciation also goes to students Esther Kim, Alexandra DeLaney and Rebecca Ruf, without whom I would surely still be doing western blots well into the next decade.

Thank you to my Mol Path (and extended) friends: Katie, Amanda, Heather, Matt, Erin, Miki, Jorge, Cyndi, Anokhi, and Ben. It's been wonderful having friends like you to share this experience of grad school with. To Katie: Thank you for listening, and commiserating, when I needed it, and I must say that I believe I deserve another award, for what you see before you in this dissertation is truly *la Pièce de résistance*.

Thank you to my long-time friends from dancing: Elizabeth and April. I treasure the knowledge that we have always and will always be there for each other, no matter where life takes each of us, and along the many different paths we have traveled. I look forward to having Highland Fusion reunions together when we're old and gray and haven't done a hi-cut in decades.

And finally, I give my love and thanks to my family and to Chris, who all are my emotional foundation and give meaning to my life. I look forward to sharing many happy moments and adventures together especially in the upcoming year, and beyond. To Grandma Jane and Grandpa Cal: I guess I've come a long way from the pre-school work and drawings that Dad would send you years ago. Can you believe your grand-daughter is going to be "Dr. Crews"? To Grandma Goddard: I am so grateful for the constant support that you and Grandpa have given me over the years, and for all of my "Proud Ancestors" who have instilled in me the importance of getting a good education—whether in school or in the classroom of the world. I thank you for fostering my love of travel starting at a young age, and to paraphrase an uncle of mine, "Grandma, it's different when you've been there." And in loving memory of my

Grandpa Goddard: I wish he could be here today to see me reach this milestone in my life; I know he would be proud.

Chapter 1, in part, contains figures and excerpts of the material as it appears in Brain Structure and Function 2009. With kind permission from Springer Science+Business Media: Crews L, Rockenstein E, Masliah E (2009) APP transgenic modeling of Alzheimer's disease: mechanisms of neurodegeneration and aberrant neurogenesis, Springer Berlin/Heidelberg. The dissertation author was the primary author of this paper.

Chapter 2, in part, contains figures and text of the material as it appears in the Journal of Neuroscience 2008. Crews L, Mizuno H, Desplats P, Rockenstein E, Adame A, Patrick C, Winner B, Winkler J, Masliah E (2008) Alpha-synuclein alters Notch-1 expression and neurogenesis in mouse embryonic stem cells and in the hippocampus of transgenic mice. J Neurosci 28:4250-4260, Society for Neuroscience, 2008. The dissertation author was co-lead author and investigator of this paper.

Chapter 2, in part, contains figures and excerpts of the material as it appears in Brain Structure and Function 2009. With kind permission from Springer Science+Business Media: Crews L, Rockenstein E, Masliah E (2009) APP transgenic modeling of Alzheimer's disease: mechanisms of neurodegeneration and aberrant neurogenesis, Springer Berlin/Heidelberg. The dissertation author was the primary author of this paper.

Chapter 3, in full, is currently being prepared for submission for publication of the material. Crews L, Patrick C, Rockenstein EM, Adame A, Masliah E. The dissertation author was the primary investigator and author of this material.

Chapter 4, in full, is currently being prepared for submission for publication of the material. Crews L, Patrick C, Ruf R, Trejo-Morales M, Adame A, Rockenstein EM, Masliah E. The dissertation author was the primary investigator and author of this material.

Chapter 5, in full, has been submitted for publication of the material as it may appear in the Journal of Neuroscience 2010. Crews L, Adame A, Patrick C, DeLaney A, Pham E, Rockenstein EM, Masliah E; Society for Neuroscience, 2010.

Chapter 6, in part, is a reprint of the material as it appears in Acta Neuropathologica 2007. With kind permission from Springer Science+Business Media: Rockenstein E, Mante M, Adame A, Crews L, Moessler H, Masliah E (2007) Effects of Cerebrolysin on neurogenesis in an APP transgenic model of Alzheimer's disease. Acta Neuropathol (Berl) 113:265-275, Springer Berlin/Heidelberg. The dissertation author was co-author of this paper.

Chapter 6, in part, contains figures of the material as it appears in the Journal of Neuroscience Research 2006. With kind permission from John Wiley and Sons: Rockenstein E, Torrance M, Mante M, Adame A, Paulino A, Rose JB, Crews L, Moessler H, Masliah E (2006) Cerebrolysin decreases amyloid-beta production by regulating amyloid protein precursor maturation in a transgenic model of Alzheimer's disease. J Neurosci Res 83:1252-1261, John Wiley and Sons.

VITA

1999	Volunteer Research Assistant, Molecular Biology and Virology Laboratory, The Salk Institute
2000-2001	Undergraduate Intern, BD Pharmingen
2001-2002	University of California Education Abroad Program, University of Glasgow, Scotland
2003	Bachelor of Science, University of California, Los Angeles
2003-2005	Research Associate, University of California, San Diego
2005-2010	Graduate Student Researcher, University of California, San Diego
2010	Doctor of Philosophy, University of California, San Diego

PUBLICATIONS

1. Crews L, Adame A, Patrick C, DeLaney A, Pham E, Rockenstein EM & Masliah E (2010) Increased BMP6 levels in the brains of Alzheimer's disease patients and APP transgenic mice are accompanied by impaired neurogenesis. *J Neurosci* Submitted.

2. Crews L, Patrick C, Ruf R, Trejo-Morales M, Adame A, Rockenstein EM & Masliah E (2010) CDK5-mediated hyperphosphorylation of CRMP2 in models of Alzheimer's disease impairs adult neurogenesis via microtubule destabilization. In preparation.

3. Pham E, Crews L, Hansen L, Adame A, Cartier A, Salmon D, Galasko D, Glabe C & Masliah E (2010) Progressive accumulation of Aβ oligomers in the brains of patients with Alzheimer's disease is associated with selective alterations in synaptic scaffold proteins. *FEBS J* Submitted.

4. Patrick C, Crews L, Achim C, Everall I & Masliah E (2010) Increased CDK5 expression in HIV Encephalitis contributes to neurodegeneration via tau phosphorylation. In preparation.

5. Crews L, Rockenstein E & Masliah E (2009) APP transgenic modeling of Alzheimer's disease: mechanisms of neurodegeneration and aberrant neurogenesis. *Brain Struct Funct*.

6. Masliah E, Rockenstein EM, Mante M, Crews L, Patrick C, Games D, Seubert P, McConlogue L, Buttini M & Schenk D (2010) Immunization with an antibody against the C-terminus of alpha-synuclein promotes clearance via activation of the autophagy pathway in a transgenic model. In preparation.

7. Crews L, Spencer B, Desplats P, Patrick C, Paulino A, Rockenstein EM, Hansen L, Adame A, Galasko D & Masliah E (2010) Selective molecular alterations in the autophagy pathway in patients with Lewy body disease and in models of alpha-synucleinopathy. *PLoS ONE* In press.

8. Crews L, Patrick C, Rockenstein EM, Adame A & Masliah E (2010) Abeta-induced alterations in CDK5 signaling interfere with the maturation of neuronal progenitor cells. In preparation.

9. Ubhi K, Rockenstein E, Doppler E, Mante M, Adame A, Patrick C, Trejo M, Crews L, Paulino A, Moessler H & Masliah E (2009) Neurofibrillary and neurodegenerative pathology in APP-transgenic mice injected with AAV2-mutant TAU: neuroprotective effects of Cerebrolysin. *Acta Neuropathol* 117, 699-712.

10. Rose JB, Crews L, Rockenstein E, Adame A, Mante M, Hersh LB, Gage FH, Spencer B, Potkar R, Marr RA & Masliah E (2009) Neuropeptide Y fragments derived from neprilysin processing are neuroprotective in a transgenic model of Alzheimer's disease. *J Neurosci* 29, 1115-1125.

11. Marongiu R, Spencer B, Crews L, Adame A, Patrick C, Trejo M, Dallapiccola B, Valente EM & Masliah E (2009) Mutant Pink1 induces mitochondrial dysfunction in a neuronal cell model of Parkinson's disease by disturbing calcium flux. *J Neurochem* 108, 1561-1574.

12. Desplats P, Lee HJ, Bae EJ, Patrick C, Rockenstein E, Crews L, Spencer B, Masliah E & Lee SJ (2009) Inclusion formation and neuronal cell death through neuron-to-neuron transmission of alpha-synuclein. *Proc Natl Acad Sci U S A* 106, 13010-13015.

13. Crews L, Tsigelny I, Hashimoto M & Masliah E (2009) Role of synucleins in Alzheimer's disease. *Neurotox Res* 16, 306-317.

14. Crews L, Patrick C, Achim CL, Everall IP & Masliah E (2009) Molecular Pathology of Neuro-AIDS (CNS-HIV). *Int J Mol Sci* 10, 1045-1063.

15. Tsigelny IF, Crews L, Desplats P, Shaked GM, Sharikov Y, Mizuno H, Spencer B, Rockenstein E, Trejo M, Platoshyn O, Yuan JX & Masliah E (2008) Mechanisms of hybrid oligomer formation in the pathogenesis of combined Alzheimer's and Parkinson's diseases. *PLoS ONE* 3, e3135.

16. Spencer B, Marr RA, Rockenstein E, Crews L, Adame A, Potkar R, Patrick C, Gage FH, Verma IM & Masliah E (2008) Long-term neprilysin gene transfer is associated with reduced levels of intracellular Abeta and behavioral improvement in APP transgenic mice. *BMC Neurosci* 9, 109.

17. Kawahara K, Hashimoto M, Bar-On P, Ho GJ, Crews L, Mizuno H, Rockenstein E, Imam SZ & Masliah E (2008) {alpha}-Synuclein Aggregates Interfere with Parkin Solubility and Distribution: ROLE IN THE PATHOGENESIS OF PARKINSON DISEASE. *J Biol Chem* 283, 6979-6987.

18. Doppler E, Rockenstein E, Ubhi K, Inglis C, Mante M, Adame A, Crews L, Hitzl M, Moessler H & Masliah E (2008) Neurotrophic effects of Cerebrolysin in the Mecp2(308/Y) transgenic model of Rett syndrome. *Acta Neuropathol* 116, 425-437.

19. Crews L, Spencer B & Masliah E (2008) Immunotherapy strategies for Lewy body and Parkinson's diseases. In *Handb Neurochem and Mol Neurobiol* (Lajtha A, ed^eds), pp. 599-613. Springer Ref, Orangeburg, NY.

20. Crews L, Spencer B & Masliah E (2008) Role of Abeta-degrading enzymes in synaptic plasticity and neurogenesis in Alzheimer's disease. *Current Hypotheses and Research Milestones in Alzheimer's Disease*.

21. Crews L, Rockenstein E & Masliah E (2008) Biological transgenic mouse models of Alzheimer's disease. *Handb Clin Neurol* 89, 291-301.

22. Crews L, Mizuno H, Desplats P, Rockenstein E, Adame A, Patrick C, Winner B, Winkler J & Masliah E (2008) Alpha-synuclein alters Notch-1 expression and neurogenesis in mouse embryonic stem cells and in the hippocampus of transgenic mice. *J Neurosci* 28, 4250-4260.

23. Crews L, Lentz MR, Gonzalez RG, Fox HS & Masliah E (2008) Neuronal injury in simian immunodeficiency virus and other animal models of neuroAIDS. *J Neurovirol* 14, 327-339.

24. Bar-On P, Crews L, Koob AO, Mizuno H, Adame A, Spencer B & Masliah E (2008) Statins reduce neuronal alpha-synuclein aggregation in in vitro models of Parkinson's disease. *J Neurochem* 105, 1656-1667.

25. Tsigelny IF, Bar-On P, Sharikov Y, Crews L, Hashimoto M, Miller MA, Keller SH, Platoshyn O, Yuan JX & Masliah E (2007) Dynamics of alpha-synuclein aggregation and inhibition of pore-like oligomer development by beta-synuclein. *Febs J* 274, 1862-1877.

26. Spencer B, Rockenstein E, Crews L, Marr R & Masliah E (2007) Novel strategies for Alzheimer's disease treatment. *Expert Opin Biol Ther* 7, 1853-1867.

27. Spencer B, Crews L & Masliah E (2007) Climbing the scaffolds of Parkinson's disease pathogenesis. *Neuron* 53, 469-470.

28. Salaria S, Badkoobehi H, Rockenstein E, Crews L, Chana G, Masliah E & Everall IP (2007) Toll-like receptor pathway gene expression is associated with human immunodeficiency virus-associated neurodegeneration. *J Neurovirol* 13, 496-503.

29. Rockenstein E, Torrance M, Adame A, Mante M, Bar-on P, Rose JB, Crews L & Masliah E (2007) Neuroprotective effects of regulators of the glycogen synthase kinase-3beta signaling pathway in a transgenic model of Alzheimer's disease are associated with reduced amyloid precursor protein phosphorylation. *J Neurosci* 27, 1981-1991.

30. Rockenstein E, Mante M, Adame A, Crews L, Moessler H & Masliah E (2007) Effects of Cerebrolysintrade mark on neurogenesis in an APP transgenic model of Alzheimer's disease. *Acta Neuropathol (Berl)* 113, 265-275.

31. Rockenstein E, Crews L & Masliah E (2007) Transgenic animal models of neurodegenerative diseases and their application to treatment development. *Adv Drug Deliv Rev* 59, 1093-1102.

32. Letendre S, Paulino AD, Rockenstein E, Adame A, Crews L, Cherner M, Heaton R, Ellis R, Everall IP, Grant I & Masliah E (2007) Pathogenesis of hepatitis C virus coinfection in the brains of patients infected with HIV. *J Infect Dis* 196, 361-370.

33. Kuczenski R, Everall IP, Crews L, Adame A, Grant I & Masliah E (2007) Escalating dose-multiple binge methamphetamine exposure results in degeneration of the neocortex and limbic system in the rat. *Exp Neurol* 207, 42-51.

34. Webster B, Hansen L, Adame A, Crews L, Torrance M, Thal L & Masliah E (2006) Astroglial activation of extracellular-regulated kinase in early stages of Alzheimer disease. *J Neuropathol Exp Neurol* 65, 142-151.

35. Tesseur I, Zou K, Esposito L, Bard F, Berber E, Can JV, Lin AH, Crews L, Tremblay P, Mathews P, Mucke L, Masliah E & Wyss-Coray T (2006) Deficiency in

neuronal TGF-beta signaling promotes neurodegeneration and Alzheimer's pathology. *J Clin Invest* 116, 3060-3069.

36. Rockenstein E, Torrance M, Mante M, Adame A, Paulino A, Rose JB, Crews L, Moessler H & Masliah E (2006) Cerebrolysin decreases amyloid-beta production by regulating amyloid protein precursor maturation in a transgenic model of Alzheimer's disease. *J Neurosci Res* 83, 1252-1261.

37. Masliah E, Crews L & Hansen L (2006) Synaptic remodeling during aging and in Alzheimer's disease. *J Alzheimers Dis* 9, 91-99.

38. Masliah E & Crews L (2006) Genetically engineered mouse models of neurodegenerative disorders. In *Protein Misfolding, Aggregation and Conformational Diseases* (Uversky VN, ed^eds). Kluwer Academic/Plenum, New York.

39. Chana G, Everall IP, Crews L, Langford D, Adame A, Grant I, Cherner M, Lazzaretto D, Heaton R, Ellis R & Masliah E (2006) Cognitive deficits and degeneration of interneurons in HIV+ methamphetamine users. *Neurology* 67, 1486-1489.

40. Singer O, Marr RA, Rockenstein E, Crews L, Coufal NG, Gage FH, Verma IM & Masliah E (2005) Targeting BACE1 with siRNAs ameliorates Alzheimer disease neuropathology in a transgenic model. *Nat Neurosci* 8, 1343-1349.

41. Shults CW, Rockenstein E, Crews L, Adame A, Mante M, Larrea G, Hashimoto M, Song D, Iwatsubo T, Tsuboi K & Masliah E (2005) Neurological and neurodegenerative alterations in a transgenic mouse model expressing human alpha-synuclein under oligodendrocyte promoter: implications for multiple system atrophy. *J Neurosci* 25, 10689-10699.

42. Rockenstein E, Schwach G, Ingolic E, Adame A, Crews L, Mante M, Pfragner R, Schreiner E, Windisch M & Masliah E (2005) Lysosomal pathology associated with alpha-synuclein accumulation in transgenic models using an eGFP fusion protein. *J Neurosci Res* 80, 247-259.

43. Rockenstein E, Mante M, Alford M, Adame A, Crews L, Hashimoto M, Esposito L, Mucke L & Masliah E (2005) High beta-secretase activity elicits neurodegeneration in transgenic mice despite reductions in amyloid-beta levels: implications for the treatment of Alzheimer disease. *J Biol Chem* 280, 32957-32967.

44. Rockenstein E, Adame A, Mante M, Larrea G, Crews L, Windisch M, Moessler H & Masliah E (2005) Amelioration of the cerebrovascular amyloidosis in a transgenic model of Alzheimer's disease with the neurotrophic compound cerebrolysin. *J Neural Transm* 112, 269-282.

45. Masliah E, Rockenstein E, Adame A, Alford M, Crews L, Hashimoto M, Seubert P, Lee M, Goldstein J, Chilcote T, Games D & Schenk D (2005) Effects of alpha-Synuclein Immunization in a Mouse Model of Parkinson's Disease. *Neuron* 46, 857-868.

46. Masliah E, Hansen L, Adame A, Crews L, Bard F, Lee C, Seubert P, Games D, Kirby L & Schenk D (2005) Abeta vaccination effects on plaque pathology in the absence of encephalitis in Alzheimer disease. *Neurology* 64, 129-131.

47. Masliah E, Roberts ES, Langford D, Everall I, Crews L, Adame A, Rockenstein E & Fox HS (2004) Patterns of gene dysregulation in the frontal cortex of patients with HIV encephalitis. *J Neuroimmunol* 157, 163-175.

48. Langford D, Grigorian A, Hurford R, Adame A, Crews L & Masliah E (2004) The role of mitochondrial alterations in the combined toxic effects of human immunodeficiency virus Tat protein and methamphetamine on calbindin positive-neurons. *J Neurovirol* 10, 327-337.

49. Hashimoto M, Rockenstein E, Mante M, Crews L, Bar-On P, Gage FH, Marr R & Masliah E (2004) An antiaggregation gene therapy strategy for Lewy body disease utilizing beta-synuclein lentivirus in a transgenic model. *Gene Ther* 11, 1713-1723.

50. Hashimoto M, Kawahara K, Bar-On P, Rockenstein E, Crews L & Masliah E (2004) The Role of alpha-synuclein assembly and metabolism in the pathogenesis of Lewy body disease. *J Mol Neurosci* 24, 343-352.

51. Hashimoto M, Bar-On P, Ho G, Takenouchi T, Rockenstein E, Crews L & Masliah E (2004) Beta-synuclein regulates Akt activity in neuronal cells. A possible mechanism for neuroprotection in Parkinson's disease. *J Biol Chem* 279, 23622-23629.

52. Crews L, Wyss-Coray T & Masliah E (2004) Insights into the pathogenesis of hydrocephalus from transgenic and experimental animal models. *Brain Pathol* 14, 312-316.

53. Hashimoto M, Rockenstein E, Crews L & Masliah E (2003) Role of protein aggregation in mitochondrial dysfunction and neurodegeneration in Alzheimer's and Parkinson's diseases. *Neuromolecular Med* 4, 21-36.

ABSTRACT OF THE DISSERTATION

Molecular Regulators of Neurogenesis in Alzheimer's Disease

by

Leslie Anne Crews

Doctor of Philosophy in Molecular Pathology

University of California, San Diego, 2010

Professor Eliezer Masliah, Chair

Alzheimer's Disease (AD) is characterized by cognitive impairment, progressive neurodegeneration, and formation of amyloid-β (Aβ)-containing plaques. These neuropathological features are accompanied by deregulation of signaling cascades such as the cyclin-dependent kinase-5 (CDK5) pathway. Recent studies have revealed that neurodegeneration in AD is also associated with alterations in hippocampal neurogenesis, which may play a critical role in cognitive impairments and memory loss. The main objectives of this dissertation were to *investigate the cellular mechanisms of defective hippocampal neurogenesis in an animal model of*

AD, and to examine the role of Aβ and CDK5, downstream targets, and other potential candidate regulators in the mechanisms of defective neurogenesis in AD.

To address these aims, *in vitro* and *in vivo* studies designed to inhibit CDK5 activity using pharmacological and genetic approaches demonstrated that CDK5 is critical for hippocampal neurogenesis. In an *in vitro* model of CDK5 hyperactivation, and in the hippocampus of amyloid precursor protein (APP) transgenic (tg) mice, markers of neurogenesis and neurite outgrowth were reduced. I identified the CDK5 substrate collapsin response mediator protein-2 (CRMP2) as a critical regulator of the effects of hyperactive CDK5 on neuronal maturation in AD. CDK5-mediated hyperphosphorylation of CRMP2 contributed to reduced neurite outgrowth by disrupting microtubule polymerization, and this effect could be rescued by down-regulating CDK5 or blocking CRMP2 phoshorylation.

In addition to the role of the CDK5 pathway in neurogenesis in AD, other factors may be involved. In this context, defective hippocampal neurogenesis in AD patients and in APP tg mice was accompanied by increased expression levels of bone morphogenetic protein-6 (BMP6). *In vitro* studies in NPCs showed that Aβ increased BMP6 levels, and that BMP6 treatment reduced proliferation, supporting a role for BMP6 in hippocampal neurogenesis in AD.

Lastly, we found that treatment of APP tg mice with a neurotrophic compound (Cerebrolysin) rescued hippocampal neurogenesis, and this effect was associated with down-regulation of the CDK5 signaling pathway. Taken together, these studies demonstrate that the CDK5 and BMP signaling cascades play important roles in adult

hippocampal neurogenesis. Future therapeutic approaches could target these molecular pathways to rescue defective neurogenesis in AD.

CHAPTER 1

INTRODUCTION

Alzheimer's disease (AD) is a leading cause of dementia in the aging population (Ashford, 2004). Over 5 million people live with this devastating neurological condition and it is estimated that the US will experience an average 50% increase in patients with AD by the year 2025 (Hebert et al., 2004). AD patients experience symptoms including cognitive alterations, memory loss and behavioral changes (Budson and Price, 2005; Katzman, 1986). The neurodegenerative process in AD is characterized by synaptic injury (Masliah et al., 1997; Terry et al., 1994), and neuronal loss (Terry et al., 1981) with overt brain atrophy. This is accompanied by astrogliosis (Beach et al., 1989) and microglial cell proliferation (Masliah et al., 1991; Rogers et al., 1988). The neuropathological features of the disease include altered processing of the amyloid-β (Aβ) precursor protein (APP), resulting in accumulation of extracellular Aβ-containing plaques (Selkoe, 1989) and oligomers (Selkoe, 1999), and the presence of neurofibrillary tangles composed of dystrophic neurites and hyperphosphorylated tau (Terry et al., 1994) (Figure 1.1) (Crews et al., 2009). This neurodegenerative process is followed by reactive astrogliosis (Dickson et al., 1988) and microglial cell proliferation (Masliah et al., 1991; Rogers et al., 1988).

AD generally afflicts patients later in life, with onset of sporadic AD occurring usually between the ages of 60 and 70 (Association, 2010). Although patients with sporadic disease constitute the majority of the affected population, approximately 10-

15% of patients have a genetically-linked familial form of AD (FAD). These patients often have earlier onset of the disease, and it is associated with mutations in several genes, including APP, tau and presenilin-1 (PS1) (Bertoli-Avella et al., 2004; Cruts and Van Broeckhoven, 1998; Hutton and Hardy, 1997; Pastor and Goate, 2004; Rocchi et al., 2003). Animal models of AD have been developed based on these familial mutations, and a number of models that express high levels of mutant APP recapitulate several of the neuropathological, neurodegenerative and behavioral characteristics of the spectrum of disease in human patients (Games et al., 1997; Masliah et al., 1996; Price et al., 2000).

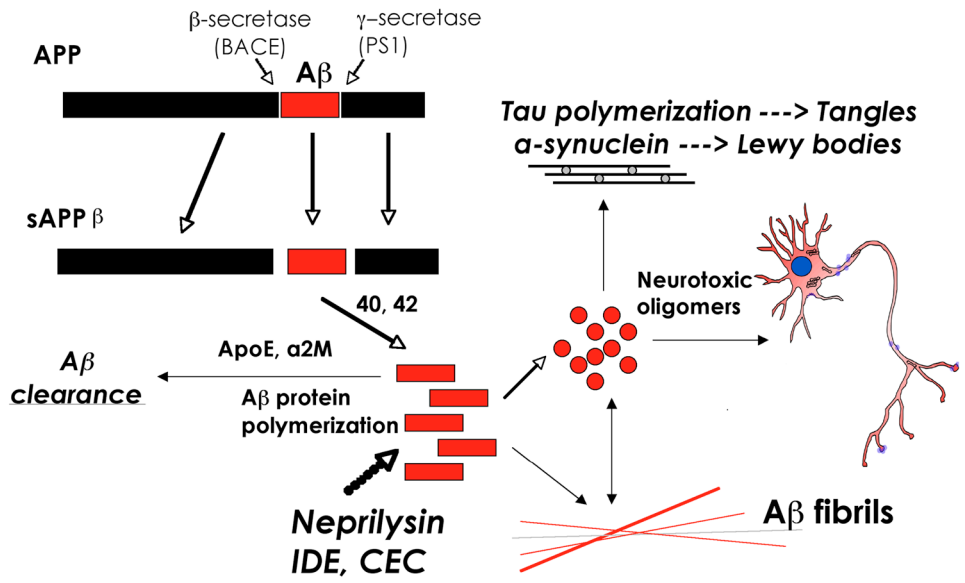

Figure 1.1 *Schematic diagram of APP processing and accumulation of toxic Aβ species.* β- and γ-secretase cleavage of APP results in the production of $A\beta_{1\text{-}40}$ and $A\beta_{1\text{-}42}$, which accumulates into neurotoxic oligomers.

Most efforts towards developing tg models have been focused on overexpression of mutant APP in combination with mutant PS1. A summary of the

FAD mutations of APP reproduced in tg mouse models is presented in Figure 1.2 (Crews et al., 2009). Previously developed tg animal models have shown that it is possible to reproduce certain aspects of AD pathology over a shorter period of time (Games et al., 1997; Masliah et al., 1996; Price et al., 2000).

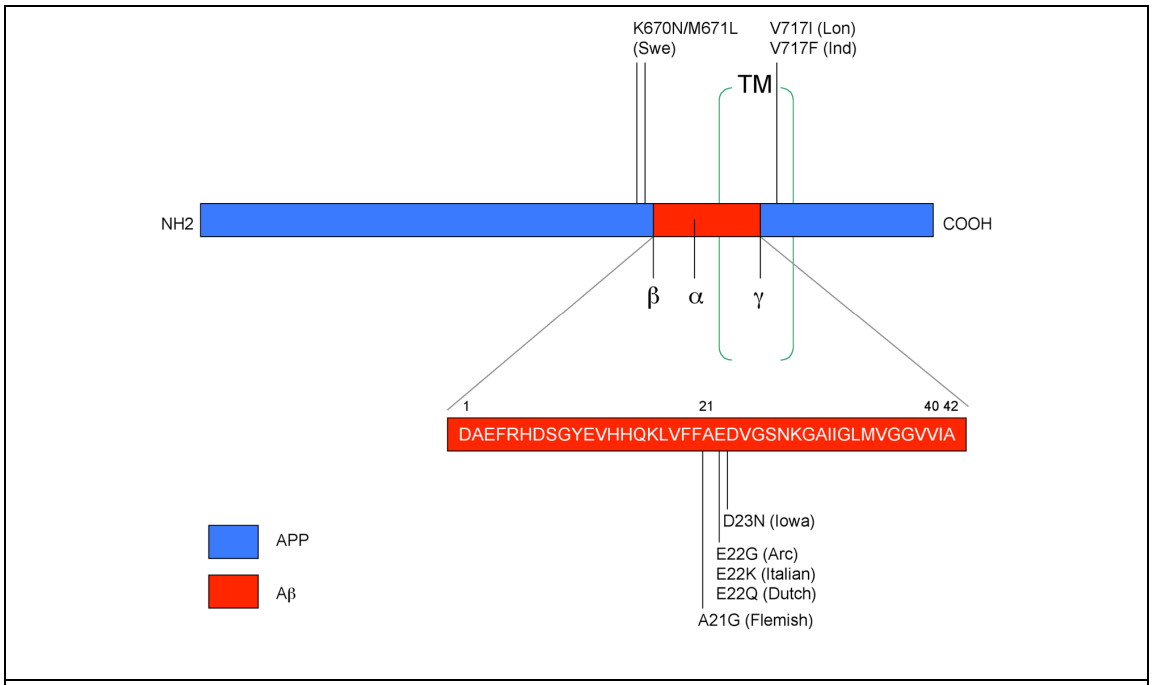

Figure 1.2 *Diagram showing common mutations in the APP gene that are utilized in the generation of animal models of AD.* Mutations in the N- and C-terminal domains of APP result in the accumulation of intracellular and/or extracellular Aβ species, while mutations in the Aβ region lead to the development of amyloid angiopathy. Swe = Swedish mutation, Lon = London mutation, Ind = Indiana mutation, Arc = Arctic mutation, TM = transmembrane domain.

In one such model, we have generated lines of tg mice expressing hAPP751 cDNA containing the London (Lon, V717I) and Swedish (Swe, K670N/M671L) mutations under the regulatory control of the mThy1 gene (mThy1-hAPP751) (Crews et al., 2009; Rockenstein et al., 2001) (Figure 1.3). While expression of mutant hAPP under the PDGF-β promoter results in the production of diffuse (and some mature) plaques (Games et al., 1995; Mucke et al., 2000), tg expression of mutant hAPP under

the mThy1 (Andra et al., 1996) and PrP (Borchelt et al., 1997; Hsiao et al., 1996) promoters favors the formation of mature plaques in the hippocampus and neocortex.

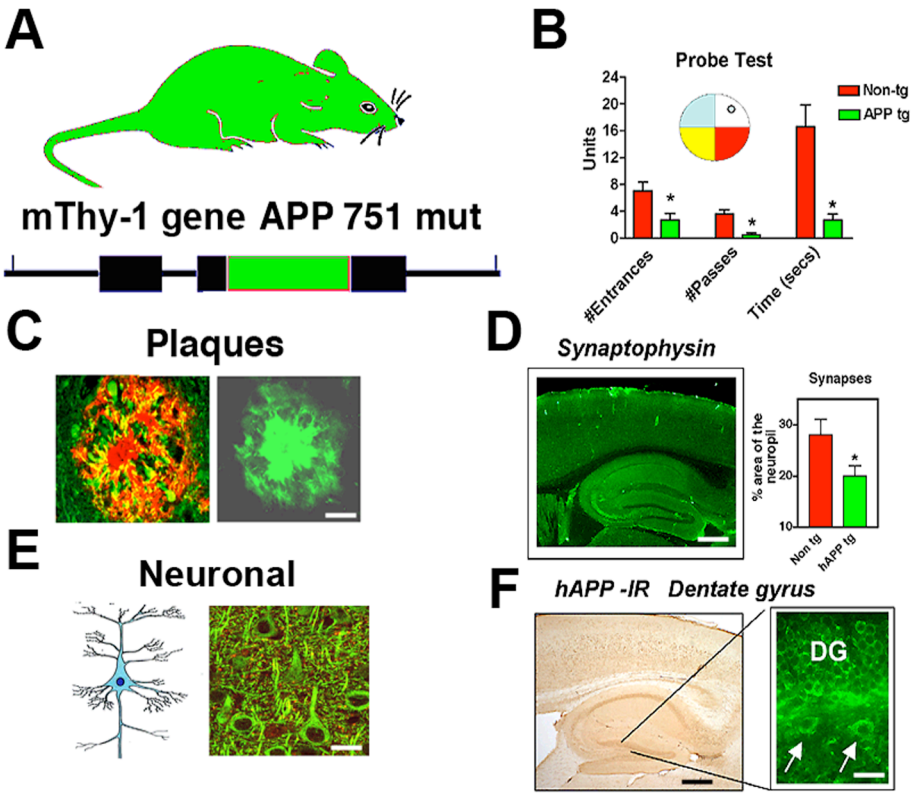

Figure 1.3 *Characterization of cognitive and neuropathological alterations in the brains of mThy1-hAPP tg mice.* (A) Structure of mutant hAPP transgene under the control of the mThy-1 promoter. (B) Memory portion of the water maze behavioral test where the platform was removed (Probe test) to evaluate the number of entrances into the target quadrant where the platform was previously located (# Entrances), the number of times the animal passed over the location where the platform was (# Passes), and time spent (Time) swimming in the target quadrant where the platform was previously located. APP tg mice exhibited reduced performance compared to non-tg controls in all three measures of memory retention in this behavioral test. (C) Aβ-immunoreactive deposits in the cortex of an APP tg mouse. Scale bar = 50μm. (D) Reduced synaptophysin immunoreactivity in the brain of an APP tg mouse. Scale bar = 0.2mm. (E) Degeneration of the MAP2-immunoreactive dendritic arbor in the cortex of an APP tg mouse. Scale bar = 10μm. (F) hAPP immunoreactivity in the dentate gyrus (DG) of an APP tg mouse. Scale bar = 1mm (left panel), 20μm (right panel). *p < 0.05 compared to non-tg controls by Student's t-test (n = 4 mice per group).

This suggests that the differential patterns of Aβ deposition might be dependent on the specific neuronal populations selected by the promoter, levels of

expression and topographical distribution of the transgene, and levels of $A\beta_{1-40}$ and $A\beta_{1-42}$. Extensive investigation of these animal models has led to better understanding of the neuropathological alterations and some of the pathways involved in AD pathogenesis, however the molecular mechanisms are still not entirely clear, and other deficits may play a role in the cognitive alterations in AD.

Loss of synapses (DeKosky and Scheff, 1990; Masliah, 2001; Scheff and Price, 2001) and axonal pathology (Raff et al., 2002) are probably key neuropathological features leading to dementia in these neurodegenerative disorders, however other factors may contribute. In addition to the alterations in synaptic plasticity and neuronal integrity in mature neuronal circuitries, the neurodegenerative process in AD has recently been shown to be accompanied by alterations in neurogenesis (Boekhoorn et al., 2006; Dong et al., 2004; Haughey et al., 2002a; Jin et al., 2004a; Jin et al., 2004b; Lee et al., 2004; Li et al., 2008a). This suggests that the pathogenesis of AD may represent a two-pronged attack on the brain, contributing to degeneration of mature neurons, and disruption of the neurogenic niches in the adult brain (Crews et al., 2009) (Figure 1.4).

In this context, the main objectives of this dissertation are to *i) Investigate the cellular mechanisms involved in defective hippocampal neurogenesis in an animal model of FAD; ii) Elucidate the role of Aβ in altered neurogenesis in AD; iii) Examine the role of cyclin-dependent kinase-5 (CDK5) in neurogenesis and its relationship to Aβ-induced alterations in signaling in NPCs; and iv) Identify molecular targets of CDK5, as well as other potential novel candidate regulators, and investigate their function in the mechanisms of defective neurogenesis in AD.*

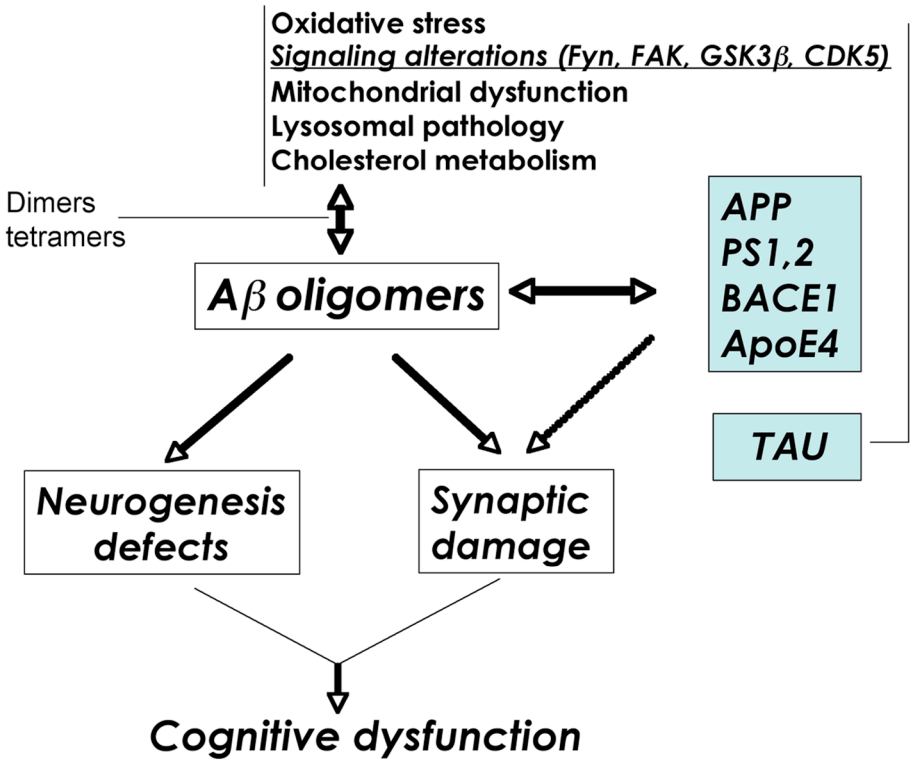

Figure 1.4 *Schematic diagram of factors contributing to Aβ oligomerization.* Defective cellular processes can lead to the accumulation of Aβ dimers, trimers and oligomers, which in turn contribute to neurogenesis defects and synaptic damage.

Neurodegeneration in Alzheimer's disease: The role of Aβ

During aging and in the progression of Alzheimer's disease (AD), synaptic plasticity and neuronal integrity are disturbed (Lee et al., 2004; Masliah et al., 1997; Terry et al., 1994; Terry et al., 1981). Although the precise mechanisms leading to neurodegeneration in AD are not completely clear, most studies have focused on the role of APP and its products in AD pathogenesis (Selkoe, 1989; Selkoe, 1999; Vassar, 2005). Recent studies suggest that alterations in the processing of APP, resulting in the accumulation of Aβ and APP C-terminal products, might play a key role in the pathogenesis of AD (Kamenetz et al., 2003; Sinha et al., 2000) (Figure 1.1). In this

context, previous studies have shown that $A\beta_{1-42}$, a proteolytic product of amyloid precursor protein (APP) metabolism (Figure 1.1), accumulates in the neuronal endoplasmic reticulum (ER) (Cuello, 2005) and extracellularly (Selkoe et al., 1996; Trojanowski and Lee, 2000; Walsh et al., 2000). Several products are derived from APP through alternative proteolytic cleavage pathways, and enormous progress has recently been made in identifying the enzymes involved (Cai et al., 2001; Luo et al., 2001; Selkoe, 1999; Sinha et al., 1999; Vassar et al., 1999) (Figure 1.1).

The primary pathogenic event triggering synaptic loss and selective neuronal cell death in these disorders is not yet completely clear (Masliah, 2000; Masliah, 2001), however recent studies suggest that nerve damage might result from the conversion of normally non-toxic monomers to toxic oligomers (Volles and Lansbury, 2002; Volles et al., 2001; Walsh and Selkoe, 2004) (Figure 1.4), whereas larger polymers and fibers that often constitute the plaques might not be as toxic (Lansbury, 1999; Walsh et al., 2002). Various lines of evidence suggest that the direct abnormal accumulation of Aβ oligomers in the nerve terminals might lead to the synaptic damage and ultimately to neurodegeneration in AD (Selkoe, 1999). More recent studies have uncovered evidence suggesting that another component to the neurodegenerative process in AD might include the possibility of interference with the process of adult neurogenesis in the hippocampus (Boekhoorn et al., 2006; Li et al., 2008a). In transgenic (tg) animal models of AD, previous studies have shown significant alterations in the process of adult neurogenesis in the hippocampus (Chevallier et al., 2005; Dong et al., 2004; Donovan et al., 2006; Jin et al., 2004a; Wen et al., 2004).

Defective neurogenesis in Alzheimer's disease

In addition to the alterations in synaptic plasticity and neuronal integrity in mature neurononal circuitries, the neurodegenerative process in AD has recently been shown to be accompanied by alterations in neurogenesis (Boekhoorn et al., 2006; Dong et al., 2004; Haughey et al., 2002a; Jin et al., 2004a; Jin et al., 2004b; Lee et al., 2004; Li et al., 2008a). Although there is some controversy over whether neurogenesis is increased (Jin et al., 2004b) or decreased (Boekhoorn et al., 2006; Li et al., 2008a) in the pathogenesis of AD, more recent studies suggest that apparent increases in markers of neurogenesis in the brains of AD patients may be related to glial and vasculature-associated changes (Boekhoorn et al., 2006).

Animal models of APP overexpression present a more complex picture, however in support of the more recent studies in human AD patients, a number of animal models of FAD display significantly reduced neurogenesis compared to non-tg controls (Dong et al., 2004; Donovan et al., 2006; Haughey et al., 2002a; Rockenstein et al., 2007a) (for a more comprehensive review of neurogenic alterations in FAD-linked mouse models, please see (Lazarov and Marr, 2009)). Taken together, these studies suggest that the pathogenesis of AD may be characterized by not only a loss of mature neurons but also by alterations in neural progenitor cells (NPCs) in neurogenic niches such as the dentate gyrus (DG) of the hippocampus. However, the molecular mechanisms involved in defective neurogenesis in AD and in animal models of FAD remain to be fully elucidated.

Neurogenesis in the mature healthy CNS occurs throughout adult life (Kempermann et al., 1997) in the olfactory bulb, the subventricular zone (SVZ) and

the DG of the hippocampus (Zhao et al., 2008). Neurogenesis is a complex process characterized by several progressive steps, including NPC *proliferation*, *migration*, *differentiation* (cell fate commitment), and *maturation* (including growth and synaptogenesis) (Figure 1.5). Moreover, during any one of these stages, survival and apoptosis may play a role in the net outcome of neurogenesis and numbers of surviving neural progeny in the adult hippocampus. Furthermore, each of these phases may be regulated by distinct molecular mechanisms, and could be susceptible to changes induced by pathological conditions in disease states.

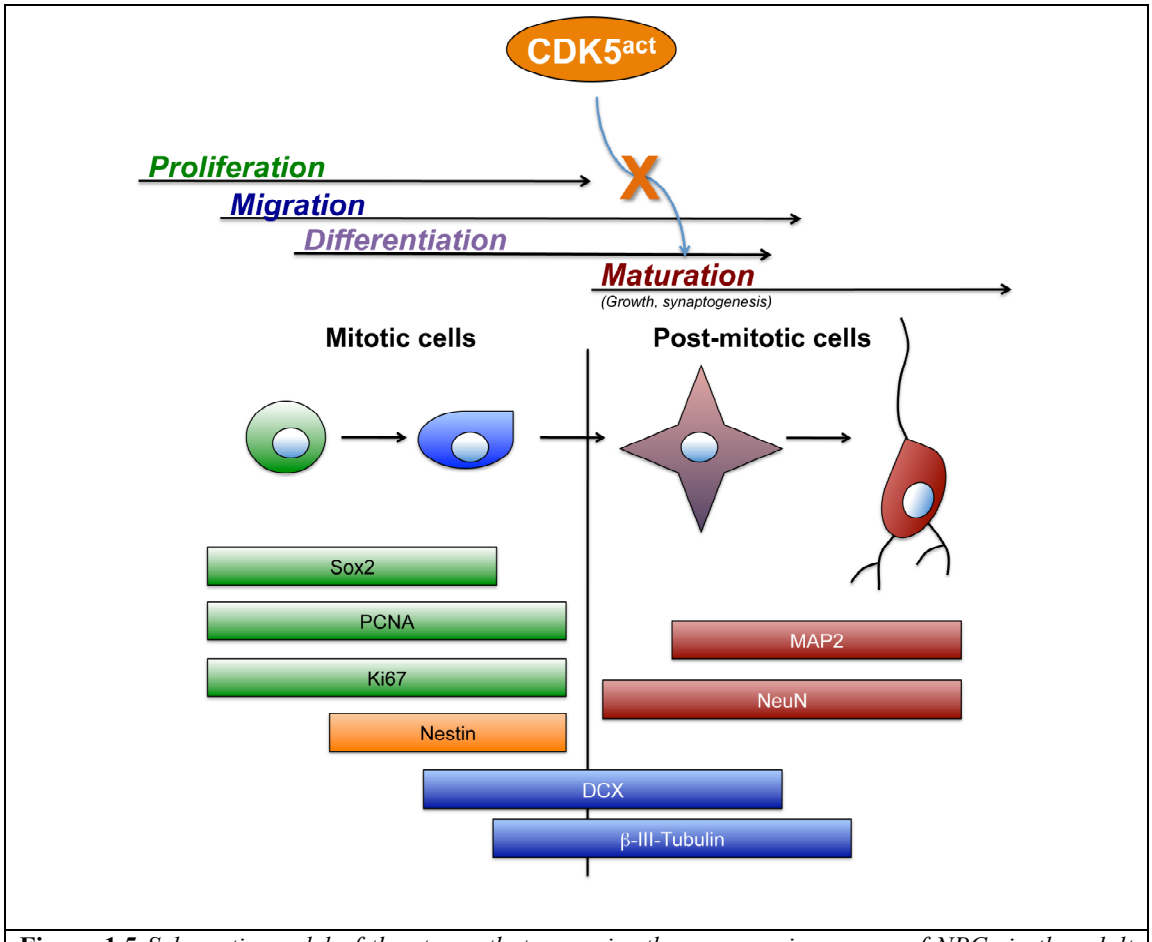

Figure 1.5 *Schematic model of the stages that comprise the neurogenic process of NPCs in the adult brain, and representative markers that can be utilized to identify cells in various phases of development.* Aberrant activation of signaling molecules such as CDK5 ($CDK5^{act}$) might impair adult neurogenesis during the cell maturation stage.

For studies of neurogenesis in both the SVZ and DG, characterization of different markers is used to distinguish between stages of the neurogenic process (Figure 1.5), however there is much overlap in expression of the different markers and phases themselves. Markers of cell division (Sox2, PCNA, Ki67, or BrdU in BrdU-treated cells or animals) or NPC-specific markers (nestin) are often used to identify cells in the progenitor cell (proliferative) phase of neurogenesis (Kempermann et al., 1997; Scholzen and Gerdes, 2000) (Figure 1.5). For later stages in the process, markers such as doublecortin (DCX) or β-III Tubulin are utilized to detect progeny in the early neuroblast phase (newly-born neurons, often migratory) or immature new neurons, respectively (Rao and Shetty, 2004) (Figure 1.5). For cells that are committed to a neuronal fate, eventually these progeny will be immunopositive with markers such as NeuN, MAP2 or synaptic markers (Figure 1.5).

Neurogenesis in the DG is an active process in the mature brain and plays a key role in synaptic plasticity, memory, and learning (Gage et al., 1998). Environmental enrichment has been shown to stimulate neurogenesis and improve performance in memory tasks in mice (Brown et al., 2003; Bruel-Jungerman et al., 2005; Olson et al., 2006). Mechanisms of neurogenesis in the fetal brain have been extensively studied, and pathways such as the wnt (Lie et al., 2005) and Notch (Androutsellis-Theotokis et al., 2006; Beatus and Lendahl, 1998) signaling cascades play an important role in this process. However less is known about the factors regulating neurogenesis in the adult nervous system and their role in neurodegenerative disorders.

While extensive studies have focused in the past on elucidating the signaling pathways and downstream mechanisms involved in the neurodegenerative process in AD, less is known about the factors regulating neurogenesis in the adult nervous system and their role in neurodegenerative disorders. Previous studies have shown that a number of signaling proteins, including glycogen synthase kinase-3β (GSK3β) (Baum et al., 1996; Hooper et al., 2007; Rockenstein et al., 2007b; Rockenstein et al., 2006) and cyclin-dependent kinase-5 (CDK5) (Cruz and Tsai, 2004) are involved in the neurodegenerative progression of AD, however the role of such signal transduction mechanisms in defective neurogenesis in AD is unknown, and other factors may also be involved.

Contribution of the CDK5 Pathway to neurodegeneration in Alzheimer's disease, and potential role for this pathway in the mechanisms of defective neurogenesis

In AD the neurodegenerative process has been linked with hyperactivation of cyclin-dependent kinase-5 (CDK5) and its activators p35 and p25 (Cruz and Tsai, 2004; Liu et al., 2003; Patrick et al., 1999). Furthermore, levels of CDK5 are increased in the brains of AD patients (Lee et al., 1999). CDK5 is the predominant CDK found in the brain, is highly expressed in neurons, and plays an important role in synaptic plasticity and neuronal development (Cicero and Herrup, 2005). CDK5 is a Ser-Thr protein kinase with postmitotic activity that phosphorylates KSP motifs on cytoskeletal (MAP1b, tau, NF, nestin, DCX), synaptic proteins (PSD95, synapsin, cadherin) and transcription factors (MEF2) (Dhavan and Tsai, 2001; Shelton and Johnson, 2004; Tang et al., 2005). While in dividing neurons CDKs are activated by

cyclins, in the nervous system CDK5 is activated by forming a complex with p35 or p39 (Dhavan and Tsai, 2001; Smith et al., 2001). The primary activator of CDK5 is p35 (Tsai et al., 1994), which under high calcium conditions is cleaved by calpain into p25 (Lee et al., 2000). While CDK5 activation via complex formation with p35 is associated with physiological activation of CDK5, the truncated p25 form hyperactivates CDK5 and leads to abnormal phosphorylation of substrates such as tau (Ahlijanian et al., 2000). Through these effects, CDK5 and p35/p25 may play a critical role in neuroplasticity in the pathogenesis of AD.

Although the hyperactivation of CDK5/p35/p25 has been associated with the pathogenesis of neurodegenerative diseases such as AD, its physiological function has been implicated in critical functions such as neuroblast migration (Chae et al., 1997; Hirota et al., 2007; Ohshima et al., 1996) and synaptic plasticity (Fischer et al., 2005; Johansson et al., 2005). Furthermore, the Cdk5/p35 complex localizes to the leading edge of axonal growth cones (Pigino et al., 1997) where it regulates neurite outgrowth in mature cortical neurons (Nikolic et al., 1996). More recently, CDK5 has been shown to be essential for adult neurogenesis (Jessberger et al., 2008; Lagace et al., 2008). In this context, it is possible that the neurogenesis deficits in AD might be related to alterations in CDK5 activity in NPCs.

Recent evidence in support of this possibility suggests that the neurodegenerative process in patients with AD might not only target mature neurons, but also might interfere with the process of neurogenesis (Dong et al., 2004; Haughey et al., 2002a; Jin et al., 2004a). Studies demonstrating that in mice deficient in this kinase and its activator (p35) neuronal development and migration is arrested (Cicero

and Herrup, 2005; Gilmore et al., 1998; Hirota et al., 2007) support the notion that CDK5 plays an important role in neurogenesis in the developing brain. In the adult nervous system the role of the p35-CDK5 signaling pathway in neurogenesis is less well understood. The mechanisms through which AD-related molecular changes interfere with neurogenesis in the adult brain might involve signaling alterations (e.g. CDK5/p35/p25) analogous to those involved in the neurodegenerative process.

In this context, in models of AD, Aβ has been shown to impair neurogenesis via calpain activation and p35 deregulation (Haughey et al., 2002b), however the downstream effectors involved and the consequences of CDK5 and p35/p25 manipulation remain to be revealed. CDK5 may mediate alterations in neurogenesis in AD via aberrant phosphorylation of CDK5 substrates, which include cytoskeletal (neurofilaments, nestin) (Sahlgren et al., 2003) and synaptic proteins (e.g. synapsin, (Matsubara et al., 1996)), among others (Figure 1.6). Previous studies have shown that the Aβ/CDK5 neurotoxic pathway may involve the destabilization of microtubules (Li et al., 2003) since CDK5 can associate with microtubules indirectly (Sobue et al., 2000) and its substrates include microtubule-associated proteins (MAPs). Since CDK5 plays a role both in synaptic function and neuronal integrity, then abnormal activation of this molecule by Aβ might impair the functioning of mature neurons and also contribute to alterations in neurogenesis by impairing cell *maturation* (Figure 1.5, Figure 1.6). Elucidating the signaling pathways and *downstream molecular targets* involved in the deregulation of neurogenesis is important to fully understand the mechanisms of neuroplasticity in AD (Figure 1.6).

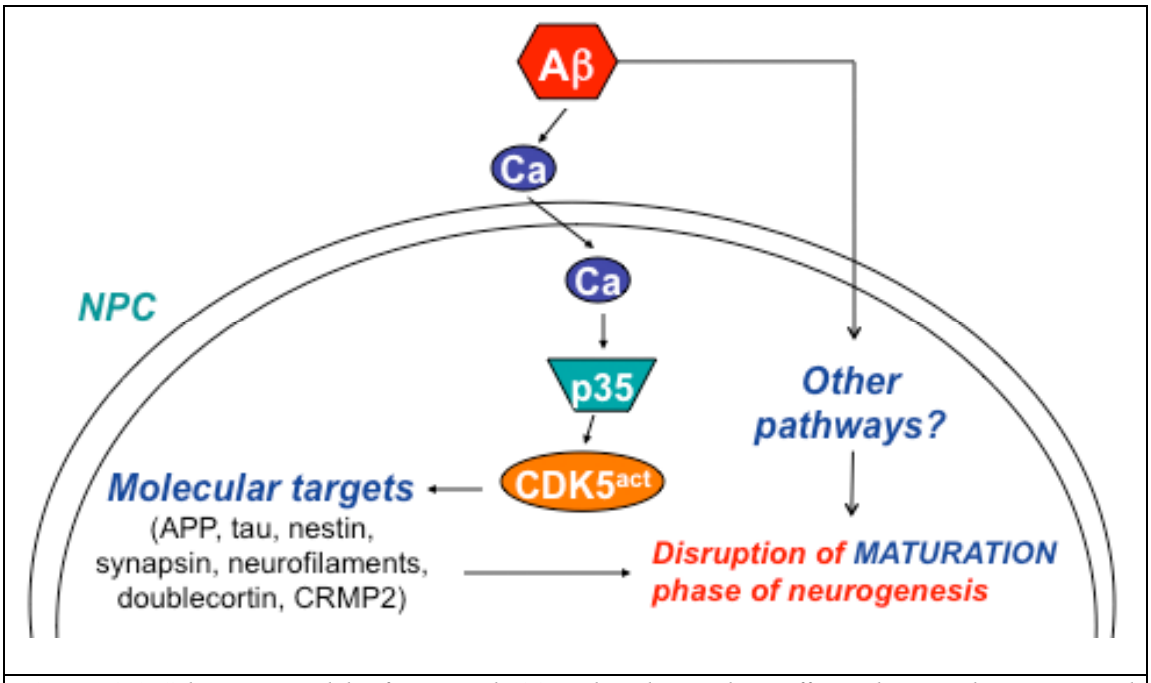

Figure 1.6 *Schematic model of potential Aβ-mediated signaling effects that result in impaired neurogenesis in AD.* Aberrant signaling through CDK5 and other pathways might disrupt the maturation stage of adult neurogenesis in the pathogenesis of AD.

The BMP family of proteins as potential regulators of neurogenesis in Alzheimer's disease

In addition to the potential role that CDK5 may play in neurogenesis in AD, other signaling pathways may contribute to the Aβ-mediated alterations in neurogenesis. In order to determine novel candidate regulators of neurogenesis in AD, we screened published gene array studies focused on neurogenesis and the aging hippocampus (Diez del Corral and Storey, 2001; Rowe et al., 2007). A comparison of these studies revealed that the bone morphogenetic protein (BMP) family of proteins was disproportionately represented; specifically, BMP2, 6 and 7 were deregulated in the aged hippocampus.

BMPs belong to the transforming growth factor-β (TGFβ) superfamily of cytokines. In addition to their role in osteogenesis, BMPs are important regulators of embryonic neurogenesis (Mehler et al., 1997) and they belong to the same family as the AD-related transforming growth factor-β (TGF-β) (Tesseur and Wyss-Coray, 2006). Like CDK5, BMPs also play a role in regulating cytoskeletal organization (Gamell et al., 2008). BMPs have been implicated in embryonic (Mehler et al., 1997) and adult neurogenesis (Colak et al., 2008), however the involvement of BMPs in neurodegenerative disorders such as AD is less well defined.

BMPs are traditionally understood to promote glial differentiation via Smad signaling (Mehler et al., 1997), and during development their *inhibition* promotes neurogenesis (Nakashima and Taga, 2002). However, a recent study showed that BMP signaling is *required* for adult neurogenesis (Colak et al., 2008) and BMP activity has also been implicated in synaptic plasticity in the adult hippocampus (Sun et al., 2007). Interestingly, a recent study showed that BMP signaling is involved in the maintenance of microtubule integrity (Wang et al., 2007), suggesting that, like CDK5, these factors may be involved in regulating neuronal differentiation through modulation of microtubule stability. Taken together, BMPs may have a distinct function during adult neurogenesis and plasticity, however their precise role in neurogenesis in AD is not well understood.

In support of a role for BMPs in the pathogenesis of AD, a recent study showed that BMP4 was associated with reduced hippocampal cell proliferation in a mouse model of AD (Li et al., 2008b), however whether these proteins are deregulated in AD patients is unknown, and the precise signaling pathways that regulate BMP

expression and downstream mechanisms resulting in impaired neurogenesis are unclear. Because of the potential common pathways between CDK5 and BMPs in regulating neurogenesis in AD, we focused on this group to better understand how these molecules play a role in regulating neurogenesis in the adult brain and in AD.

Neurotrophins and neuroprotection in Alzheimer's disease

Interestingly, paralleling the decline in both the pool of neural progenitor cells (NPCs) and their proliferative potential in AD, the levels of various neurotrophic factors, including brain-derived neurotrophic factor (BDNF), stem cell factor (SCF), and neurosteroids among others, are deregulated in AD and FAD-linked models (Laske et al., 2008; Weill-Engerer et al., 2002) (for review see (Schindowski et al., 2008)). These studies suggest that the neurogenic niche is dramatically altered in the pathogenesis of AD, other growth factors may be deregulated as well, as we have investigated in a study aimed at examining BMPs in AD. Furthermore, therapeutic compounds capable of protecting synapses and promoting neurogenesis might hold a serious promise in the development of new treatments for AD.

The nootrophic agent Cerebrolysin™ (CBL, a mixture of peptides and amino acids obtained from porcine brain tissue) has been shown to improve memory in patients with mild to moderate cognitive impairment (Ruther et al., 1994a; Ruther et al., 1994b). In support of these observations, it has also been shown to display neurotrophic activity *in vitro* (Mallory et al., 1999) and in animal models of neurodegeneration (Francis-Turner and Valouskova, 1996; Masliah et al., 1999; Veinbergs et al., 2000). Moreover, CBL has been shown to ameliorate the

neurodegenerative alterations and amyloid burden in an APP model of AD-like pathology (Rockenstein et al., 2002). We have recently shown that CBL might reduce the amyloid pathology by decreasing APP production and proteolysis (Rockenstein et al., 2006). Although the regulatory effects of CBL on APP might contribute to the neuroprotective effects of this compound, it is possible that other mechanisms might also be involved. Among them, considerable interest has developed in the potential role of neurogenesis on the effects of neuroprotective compounds (Chen et al., 2006; Tatebayashi et al., 2003). Thus, therapeutic approaches might be developed and refined using a strategy to ameliorate the neurodegenerative process in AD by stimulating neurogenesis in the adult hippocampus.

MAIN OBJECTIVES AND SIGNIFICANCE

The *main objectives* of this dissertation are to *i) Investigate the cellular mechanisms involved in defective hippocampal neurogenesis in an animal model of FAD; ii) Elucidate the role of Aβ in altered neurogenesis in AD; iii) Examine the role of CDK5 in neurogenesis and its relationship to Aβ-induced alterations in signaling in NPCs; and iv) Identify molecular targets of CDK5, as well as other potential novel candidate regulators, and investigate their function in the mechanisms of defective neurogenesis in AD.*

My *Principal Hypothesis* is that Aβ-mediated alterations in signaling cascades such as the CDK5 and BMP6 pathways are centrally involved in defective maturation and proliferation during neurogenesis in the adult hippocampus in AD. I propose that

aberrant signaling through these pathways might disrupt the *proliferation* or *maturation* stages of neurogenesis.

Identification of signaling pathways and growth factors (such as CDK5, BMPs and other neurotrophins) that might be mediators of the neurogenic alterations in AD may provide a key to broaden our understanding of the mechanisms of defective neurogenesis in the disease. Rescuing neurogenesis by targeting these pathways with selective agents might not only recover physiological levels of neurogenesis in AD but could promote synaptic and neuronal plasticity of the mature cell population. These approaches could be of value toward future human therapies directed at ameliorating the behavioral deficits in patients with AD.

ACKNOWLEDGEMENTS

Chapter 1, in part, contains figures and excerpts of the material as it appears in Brain Structure and Function 2009. With kind permission from Springer Science+Business Media: Crews L, Rockenstein E, Masliah E (2009) APP transgenic modeling of Alzheimer's disease: mechanisms of neurodegeneration and aberrant neurogenesis, Springer Berlin/Heidelberg. The dissertation author was the primary author of this paper.

CHAPTER 2

DEVELOPMENT AND CHARACTERIZATION OF *IN VITRO* AND *IN VIVO* MODELS TO STUDY NEUROGENESIS IN ALZHEIMER'S DISEASE

ABSTRACT

Adult neurogenesis plays an important role in learning and memory in the adult brain, and defects in this process during the progression of Alzheimer's disease (AD) might be associated with the cognitive deficits that characterize this devastating disorder. Previous studies have implicated signal transduction mechanisms such as the wnt and Notch signaling pathways in developmental neurogenesis, however the molecular regulators involved in adult neurogenesis are less well-defined, and the signaling molecules that might contribute to defective neurogenesis in AD are unknown. In order to begin to investigate the molecular mechanisms that regulate this process, we first characterized two *in vitro* cell models of neurogenesis. For the first, a mouse embryonic stem (mES) cell line was differentiated to induce neural progeny over a period of 18 days, and markers of neuronal differentiation were assessed by immunoblot and immunocytochemistry. For the second, adult rat hippocampal neuronal progenitor cells (NPC) were cultured and differentiated to induce neural progeny over a period of 4 days, followed by immunoblot and immunocytochemical analyses. We determined that the NPC model was the most relevant for studying adult neurogenesis *in vitro*, so we then adapted this model to develop a paradigm of adult hippocampal neurogenesis in AD and study the role of the CDK5 signaling pathway in

this process. Next, to establish an *in vivo* model of adult neurogenesis in AD, we utilized a transgenic (tg) mouse model that overexpresses mutant human APP and recapitulates several features of AD. We showed by immunohistochemical analysis that in this model, neurodegenerative alterations and activation of the CDK5 signaling pathway were accompanied by impaired neurogenesis in the adult hippocampus. Subsequent studies will make use of these *in vitro* and *in vivo* models to further examine the molecular mechanisms involved in defective neurogenesis in AD, and the role of the CDK5 signaling pathway and downstream targets might play in these alterations.

INTRODUCTION

Alzheimer's disease (AD) is the most common neurodegenerative disorder in the aging population. It is characterized by the progressive and irreversible deafferentation of the limbic system, association neocortex and basal forebrain (Hof et al., 1990; Hyman et al., 1984; Masliah et al., 1993; Palmer and Gershon, 1990; Perry et al., 1977; Wilcock et al., 1988), accompanied by the formation of neuritic amyloid plaques, amyloid angiopathy, neurofibrillary tangles (NFTs) and neuropil threads (Terry et al., 1994). This neurodegenerative process is followed by reactive astrogliosis (Dickson et al., 1988) and microglial cell proliferation (Masliah et al., 1991; Rogers et al., 1988).

Loss of synapses (DeKosky and Scheff, 1990; Masliah, 2001; Scheff and Price, 2001) and axonal pathology (Raff et al., 2002) are probably key neuropathological features leading to dementia in neurodegenerative disorders such as

AD. The most significant correlate to the severity of the cognitive impairment in AD is the loss of synapses in the frontal cortex and limbic system (DeKosky and Scheff, 1990; DeKosky et al., 1996; Masliah and Terry, 1994; Terry et al., 1991). The pathogenic process in AD involves alterations in synaptic plasticity that include changes in formation of synaptic contacts, changes in spine morphology and abnormal area of synaptic contact (Scheff and Price, 2003). However, other cellular mechanisms necessary to maintain synaptic plasticity might also be affected in AD (Cotman et al., 1993; Masliah, 2000; Masliah et al., 2001). Recent studies indicate that neurogenesis in the mature brain plays an important role maintaining synaptic plasticity and memory formation in the hippocampus (van Praag et al., 2002), and several lines of evidence support the possibility that alterations in the niches for neurogenesis in the adult brain might also contribute to the neurodegenerative process in AD (Boekhoorn et al., 2006; Chevallier et al., 2005; Dong et al., 2004; Donovan et al., 2006; Haughey et al., 2002b; Jin et al., 2004a; Li et al., 2008a; Tatebayashi et al., 2003; Wen et al., 2004).

Neurogenesis in the mature healthy CNS occurs throughout adult life (Kempermann et al., 1997) in the olfactory bulb, the subventricular zone (SVZ) and the DG of the hippocampus (Zhao et al., 2008). Neurogenesis is a complex process characterized by several different steps, including NPC *proliferation*, *migration*, *differentiation* (cell fate commitment), and *maturation* (including growth and synaptogenesis) (Figure 2.1). Moreover, during any one of these stages, survival and apoptosis may play a role in the net outcome of neurogenesis and numbers of surviving neural progeny in the adult hippocampus. Furthermore, each of these phases

may be regulated by distinct molecular mechanisms, and could be susceptible to changes induced by pathological conditions in disease states.

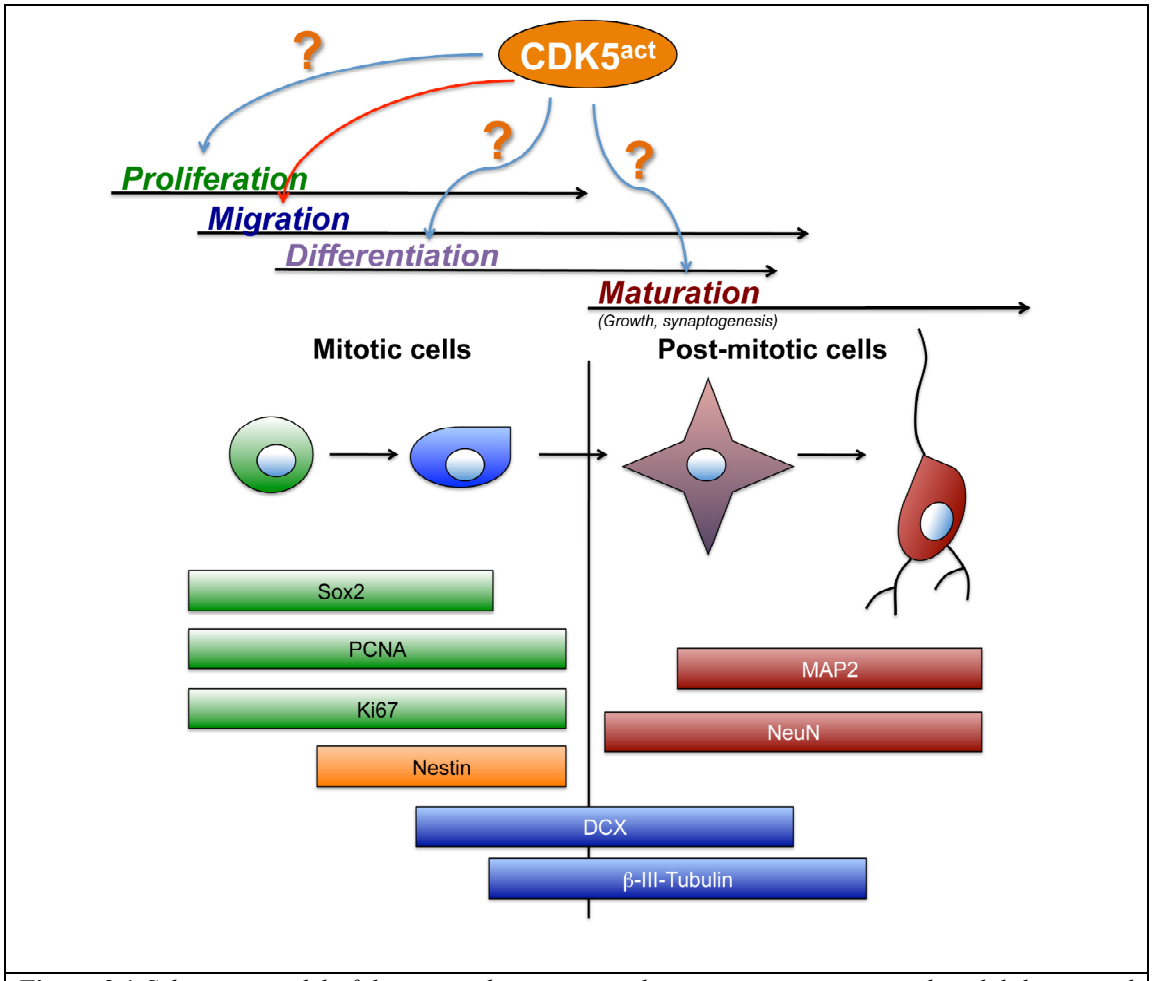

Figure 2.1 *Schematic model of the stages that comprise the neurogenic process in the adult brain, and representative markers that can be utilized to identify cells in various phases of development.* Cyclin-dependent kinase-5 (CDK5) has been previously shown to regulate cell migration during developmental neurogenesis, however it may modulate other stages of neurogenesis as well.

For studies of neurogenesis in both the SVZ and DG, characterization of different markers is used to distinguish between stages of the neurogenic process, however there is much overlap in expression of the different markers and phases themselves. Markers of cell division (Sox2, PCNA, Ki67, or BrdU in BrdU-treated cells or animals) or NPC-specific markers (nestin) are often used to identify cells in

the progenitor cell (proliferative) phase of neurogenesis (Kempermann et al., 1997; Scholzen and Gerdes, 2000) (Figure 2.1). For later stages in the process, markers such as doublecortin (DCX) or β-III Tubulin are utilized to detect progeny in the early neuroblast phase (newly-born neurons, often migratory) or immature new neurons, respectively (Rao and Shetty, 2004) (Figure 2.1). For cells that are committed to a neuronal fate, eventually these progeny will be immunopositive with markers such as NeuN, MAP2 or synaptic markers (Figure 2.1).

In the adult nervous system, motor activity and environmental enrichment (EE) have been shown to stimulate neurogenesis in the hippocampal dentate gyrus (DG) (Gage et al., 1998; van Praag et al., 2002). Physiological neurogenesis in the adult brain is regulated by numerous cell extrinsic and cell intrinsic factors, including local cytokine/chemokine signals and intracellular signal transduction (Johnson et al., 2009). In this context, recent studies have shown that, among other pathways, the Notch (Breunig et al., 2007; Crews et al., 2008), cyclin-dependent kinase-5 (CDK5) (Jessberger et al., 2008; Lagace et al., 2008), and wnt/bone morphogenetic protein (BMP) (Lie et al., 2005; Lim et al., 2000) cascades are involved in regulating adult neurogenesis, however the molecular mechanisms of aberrant neurogenesis in AD are unclear.

Interestingly, separate studies have shown that some signaling pathways that control physiological adult neurogenesis are known to be deregulated in AD, supporting the possibility that these molecules could play a role in defective neurogeneis in AD. In this context, CDK5 has been previously implicated as an important regulator of developmental neurogenesis, specifically during cell *migration*

(Chae et al., 1997; Ohshima et al., 1999; Ohshima et al., 1996), and recent studies have revealed the importance of this kinase in physiological adult neurogenesis (Hirota et al., 2007; Jessberger et al., 2008; Jessberger et al., 2009; Lagace et al., 2008) (Figure 2.1). Moreover, CDK5 is hyperactivated in AD by Aβ peptide-mediated calcium influx (Cruz and Tsai, 2004; Lee et al., 2000). In mature neurons, this contributes to neurodegeneration by promoting aberrant phosphorylation of downstream targets of CDK5 such as tau (Ahlijanian et al., 2000; Cruz and Tsai, 2004), however the direct effects of CDK5 deregulation on NPCs in AD are unknown, and CDK5 may target other phases of neurogenesis in addition to cell migration (Figure 2.1). Taken together, it is possible that kinases such as CDK5 that are disturbed in mature neurons in AD may play an imporant role in the mechanisms of disrupted neurogenesis in the adult AD brain.

In this context, we sought to develop *in vitro* and *in vivo* models to study the molecular mechanisms responsible for the neurogenic alterations associated with the pathogenesis of AD. First, we characterized the process of neurogenesis in an *in vitro* mouse embryonic stem (mES) cell-based model of neuronal differentiation. Then we developed an alternative model more relevant to neurogenesis in the adult hippocampus, namely an *in vitro* neuronal progenitor cell (NPC)-based model derived from adult rat hippocampus. Characterization of this model revealed that cells were differentiated to an enriched culture of immature neurons over a short (4-day) period of time. Using this model, we then developed a paradigm for CDK5 hyperactivation in neurogenesis in AD using a viral vector to express the CDK5 activator, p35, in combination with exogenous Aβ protein treatment.

Since the CDK5 signaling pathway has been shown to be deregulated in the brains of AD patients and in APP tg mice (Cruz et al., 2006), we used a line of mice expressing high levels of APP under the control of the mThy-1 promoter to investigate the potential role of CDK5 in defective adult neurogenesis in AD. First, we characterized the baseline status of adult neurogenesis in BrdU-treated APP tg mice, and found that markers of neurogenesis were significantly reduced compared to non-tg controls. Subsequent studies will employ these *in vitro* and *in vivo* models to further elucidate the molecular and functional mechanisms involved in CDK5 hyperactivation and defective neurogenesis in AD.

MATERIALS AND METHODS

ES cell culture. The D3 mES cell line (purchased from ATCC) was cultured on tissue culture plates coated with 0.1% (v/v) porcine gelatin (Sigma-Aldrich, St. Louis, MO). Cells were cultured in ES medium, consisting of knock-out Dulbecco's modified Eagle's medium (Invitrogen, Carlsbad, CA), 15% knock-out serum replacement (Invitrogen), 55 μM mercaptoethanol, 1 mM sodium pyruvate, 2 mM glutamine, 0.1 mM non-essential amino acids, and 1000 units/ml murine leukemic inhibitory factor (LIF, Chemicon, Temecula, CA), in 5% CO_2, 95% air at 37°C. Cells were trypsinized and replated, or replaced with fresh ES medium every other day.

Neuronal differentiation of mES cells. Neuronal differentiation of ES cells was based on a modification of prior published methods (Bibel et al., 2004). Briefly, for embryoid body formation, 3 x 10^6 mES cells were plated onto nonadherent petri

dishes in EB medium (ES medium without LIF and only 10% serum replacement) and incubated for 8d. Medium was changed every 2 d and 5 μM retinoic acid (Sigma) was added after 4 d. Embryoid bodies were then dissociated with 0.05% trypsin in 0.04% EDTA/PBS (Invitrogen) and the cells were plated on L-ornithine and laminin-coated plates in Neurobasal medium (Invitrogen) in the presence of 1 mM L-glutamine and N2 supplement (Invitrogen) (N2 medium). The following day, the N2 medium was changed, and after two days, the medium was replaced by Neurobasal medium in the presence of 1 mM L-glutamine and B27 supplement (Invitrogen) (B27 medium).

NPC culture and neuronal differentiation assay. Adult rat hippocampal NPCs (generously provided by F. Gage, Salk Institute) were cultured routinely for expansion as previously described (Ray and Gage, 2006; Ray et al., 1995) with some modifications. Briefly, cells were grown as monolayers on poly-ornithine/laminin coated plates in NPC basal media (DMEM/F-12 [Mediatech, Manassas, VA], 2mM L-glutamine, and 1% penicillin-streptomycin [all from Invitrogen, Carlsbad, CA]) supplemented with 1X B27 supplement (without vitamin A) and 20ng/mL fibroblast growth factor-2 (FGF2) (Millipore, Temecula, CA). This media (NPC Growth media) was used to enhance growth conditions for maximal proliferation of cells. For differentiation, cells were plated onto poly-ornithine/laminin (Sigma-Aldrich, St. Louis, MO) coated plates or coverslips in NPC Growth media, and transferred the following day (day 0) to NPC Differentiation media (NPC basal media supplemented with 1X N2 supplement [Invitrogen], 1μM all-*trans* retinoic acid [Sigma], 5μM

forskolin [Sigma] and 1% FBS). Cells were differentiated for four days, with fresh NPC Differentiation media added at day 2.

Adaptation of the adult hippocampal NPC neural induction protocol to model CDK5 hyperactivation in AD. To investigate the role of the CDK5 signaling pathway in the differentiation of NPCs, we studied the effects of activating this pathway in the adult rat hippocampal NPC model by utilizing a viral vector expressing the CDK5 activator, p35. Since Aβ has been shown to abnormally stimulate the activity of this pathway, p35-expressing differentiating cells were treated in combination with exogenous Aβ peptide. For this purpose, cells were infected on day 2 of differentiation with adenovirus expressing human p35 or GFP control (Vector Biolabs, Philadelphia, PA) at a multiplicity of infection (MOI) of 30. Cells were then treated on day 3 with freshly dissolved human $A\beta_{1-42}$ (1-5μM, American Peptide, Sunnyvale, CA) or reverse human $A\beta_{42-1}$ peptide (American Peptide) as a control. Additional controls included vehicle alone or a non-Aβ-amyloidogenic protein, human transthyretin (TTR, 1μM, EMD Chemicals, San Diego, CA).

Biochemical and ultrastructural analyses of Aβ oligomerization state in recombinant protein preparations applied to NPCs in culture. To characterize the species of Aβ aggregates that were present in the recombinant protein preparations utilized in our *in vitro* paradigm of CDK5 activation in neurogenesis in AD, we performed gel electrophoresis and electron microscopy with freshly solubilized solutions of $A\beta_{1-42}$, reverse $A\beta_{42-1}$ or TTR. First, for gel electrophoresis, 15μL of each

peptide (1μM or 10μM solution prepared in basal DMEM/F12 media) was separated under non-reducing conditions on 4-12% Bis-Tris gels (Invitrogen) in MES buffer (Invitrogen). Gels were run in parallel, and one gel was fixed and stained with silver using the SilverQuest kit (Invitrogen) according to the manufacturer's instructions. The second gel was immunoblotted and probed with mouse monoclonal antibodies against Aβ (82E1 clone, 1:1000, specific for aa 1-16 of Aβ, IBL, Minneapolis, MN) or goat polyclonal anti-TTR (C-20, 1:500, Santa Cruz Biotechnology, Santa Cruz, CA).

For ultrastructural characterization of aggregates in each peptide preparation, as previously described (Tsigelny et al., 2008), 1μl aliquots of 1μM $A\beta_{1-42}$, $A\beta_{42-1}$ or TTR prepared under identical conditions as for immunoblotting were pipetted onto formvar coated grids, followed by 2% uranyl acetate staining. Grids were analyzed with a Zeiss OM 10 electron microscope as previously described (Hashimoto et al., 1998).

Immunoblotting of mES cells, NPCs and induced neural progeny. After washing with PBS, cells were harvested and disrupted in cell lysis buffer (20 mM Tris, pH 7.5, 150 mM NaCl, 1% Nonidet P-40, 1 mM ethylenediaminetetraacetate (EDTA), 50 mM NaF, 1 mM Na_3VO_4, 1% Triton X-100) supplemented with protease inhibitor cocktail (Calbiochem, San Diego, CA). The lysed samples were transferred to microcentrifuge tubes and incubated on ice for 20 min, and then cleared by centrifugation (13,000 x g, 15 min) at 4°C. Lysate protein concentration was measured by the D_C protein assay kit (Bio-Rad, Hercules, CA). For electrophoretic analysis, 3X SDS sample buffer was added to cell lysates. The samples were loaded on SDS-

polyacrylamide gels for electrophoresis and subsequently transferred onto polyvinylidene fluoride membranes (Millipore, Bedford, MA). After blocking, the membranes were incubated with gentle agitation overnight at 4°C with the specific primary antibodies against β-III Tubulin (Tuj1-like TU-20 clone, 1:1000, Chemicon), β-Tubulin (1:2000, Sigma-Aldrich), α-Tubulin (1:5000, Sigma-Aldrich), neuron specific enolase (NSE, 1:1000, Abcam, Cambridge, MA), or β-actin (1:1000, Millipore) as a loading control. After washing, the membranes were incubated with horseradish peroxidase (HRP)-conjugated secondary antibody for 1 hr at room temperature. Blots were visualized with enhanced chemiluminescence (ECL, Perkin-Elmer) and detection was performed using the VersaDoc Imaging System (Bio-Rad).

Immunocytochemical analysis of markers of neurogenesis and neuronal differentiation in mES cells, NPCs and neural progeny. Differentiating mES cells grown on coverslips were fixed in 4% paraformaldehyde (PFA) in PBS, washed in TBS and then double labeled with antibodies against doublecortin (DCX, 1:500, Santa Cruz Biotechnology), nestin (1:500, Millipore), or NSE (1:500, Abcam) detected with the Tyramide Signal Amplification™-Direct (Red) system (1:100, NEN Life Sciences, Boston, MA). Then coverslips were incubated with and the mouse monoclonal antibodies against β-III-Tubulin (Tuj1-like TU-20 clone, 1:100), or actin (1:250, Millipore) detected with FITC-conjugated secondary antibodies (1:75, Vector Laboratories) (Masliah et al., 2000).

NPCs and neural progeny grown on coverslips were fixed in 4% PFA in PBS, then washed in TBS. For β-III-Tubulin immunolabling, coverslips were incubated

with the mouse monoclonal antibody against β-III-Tubulin (Tuj1-like TU-20 clone, 1:1000, Chemicon) overnight at 4°C, and then incubated for 1 hr with biotinylated secondary antibody. Following rinses in TBS, avidin-biotin-peroxidase complex was applied for 1 hr, and then peroxidase detection was performed for 10 mins (25 mg/ml diaminobenzidine [DAB], 0.01% H_2O_2, 0.04% NiCl in TBS). For fluorescent immunolabeling of CDK5, coverslips were incubated with the rabbit polyclonal antibody against CDK5 (C-8, 1:1000, Santa Cruz Biotechnology) overnight at 4°C and detected with the Tyramide Signal Amplification™-Direct (Red) system (NEN Life Sciences, Boston, MA).

For each experiment, all coverslips were processed simultaneously under the same conditions and experiments were performed twice to assess reproducibility. Sections stained with fluorescent secondary antibodies were imaged with a Zeiss 63X (N.A. 1.4) objective on an Axiovert 35 microscope (Zeiss, Germany) with an attached MRC1024 LSCM system (Bio-Rad) (Masliah et al., 2000). Sections stained with DAB were imaged with a digital Olympus microscope. To confirm the specificity of primary antibodies, control experiments were performed where sections were incubated overnight in the absence of primary antibody (deleted) or preimmune serum and primary antibody alone.

Fixation of NPC-derived neural progeny for β-Tubulin immunofluorescence. For Tubulin immunofluorescence, a glutaraldehyde-based fixation procedure was utilized, essentially as previously described by Desai and Mitchison (http://mitchison.med.harvard.edu/protocols/gen1.html). For this purpose, media was

gently aspirated from cells growing on glass coverslips, and then cells were extracted for 30 sec in cytoskeletal buffer (CB, 80mM PIPES pH 6.8, 1mM $MgCl_2$, 4mM EGTA) containing 0.5% freshly added Triton-X 100. Glutaraldehyde (Electron Microscopy Sciences, Hatfield, PA) was immediately added to the CB on the coverslips at a final concentration of 0.5%. Coverslips were incubated for 10 min at 37°C. Fixative was then removed and a freshly-prepared solution of 0.1% $NaBH_4$ in PBS was added and samples were incubated for 7 min at room temperature to quench free glutaraldehyde. Coverslips were washed at least 3 times in PBS to remove the $NaBH_4$, and samples were then processed for tubulin immunofluorescence.

For tubulin immunofluorescence, fixed cells on coverslips were washed with Tris buffered saline (TBS, pH 7.4), pre-treated in 3% H_2O_2, and blocked with 10% serum (Vector Laboratories). Samples were incubated with mouse monoclonal anti-β-Tubulin primary antibody (clone B2.1, 1:250, Sigma-Aldrich) for 1 hr at room temperature and detected with FITC-conjugated secondary antibodies (1:75, Vector Laboratories). Samples were mounted under glass coverslips with ProLong Gold antifade reagent with DAPI (Invitrogen) and imaged with a Zeiss 63X (N.A. 1.4) objective on an Axiovert 35 microscope (Zeiss, Germany) with an attached MRC1024 laser scanning confocal microscope system (BioRad) (Masliah et al., 2000). All samples were processed simultaneously under the same conditions and the experiments were performed twice to assess reproducibility. For analysis of neurite outgrowth of NPC-derived neural progeny immunolabeled with β-Tubulin, neurite thicknesses were measured using the ImageJ program (NIH, Bethesda, MD) and neurite lengths were measured using ImageJ with the NeuronJ plugin.

Immunoprecipitation and kinase activity assay. For analysis of CDK5 activity levels, essentially as previously described (Hsiao et al., 2008), 300 μg of total cell lysate from NPC-derived neural progeny was incubated with 1 μg of rabbit polyclonal antibody against CDK5 (C-8, Santa Cruz Biotechnology) in a total volume of 500 μL CDK5 IP buffer (50 mM Tris pH 7.5, 150 mM NaCl, 1 mM EDTA and 1mM EGTA) with freshly-added protease, calpain and phosphatase inhibitors for 1 hr at 4°C with gentle rotation. Then 20 μL of protein A (Roche, Germany) pre-washed beads slurry was added to the lysate, and samples were incubated for 3 hrs at 4°C with gentle rotation. Then samples were centrifuged (12,000 rpm for 30 sec in a microcentrifuge) and washed three times with 1 mL CDK5 IP buffer, with gentle rotation for 10 mins at 4°C between each wash. All supernatant was carefully removed after the final wash. Then, for the kinase activity assay, beads were resuspended in a final volume of 50 μL of CDK5 kinase assay buffer (25 mM Tris pH 7.5, 10 mM MgCl2) containing freshly-added 90 μM ATP and 0.1 mM histone H1 peptide (Promega). Samples were incubated for 30 mins at 30°C, then transferred to wells in an all-white 96-well plate. 50 μL of Kinase-Glo Plus reagent (Promega) was added to each sample and luminescence values were measured on a Beckman Coulter DTX 880 Multimode plate reader. This reagent reacts with the remaining ATP in each sample, and a standard curve of serial dilutions of ATP in kinase buffer alone with Kinase-Glo reagent allowed determination of the concentration of remaining ATP after the kinase reaction.

Quantitative real-time PCR (qRT-PCR) analysis. RNA was purified from cultured cells or the hippocampus from control and tg mice using the RNeasy mini kit (Qiagen, Valencia, CA). Total RNA was reverse transcribed using iScript cDNA Synthesis kit (Bio-Rad, Hercules, CA) with 1 μg of total RNA in accordance with the manufacturer's instructions. Quantitative PCR was performed with primers specific for CDK5, p35, and GAPDH (primer assays, Qiagen) using the iCycler iQ Real-Time PCR Detection System (Bio-Rad). Reactions were performed in a volume of 25 μl using the iQ SYBR Green Supermix (Bio-Rad) according to the manufacturer's instructions.

Animal lines and treatment regimen. The tg mice utilized express mutated human (h)APP751 under the control of the mThy-1 promoter (mThy1-hAPP751) and, for this study, the highest expresser (line 41) tg mice were used (Rockenstein et al., 2001). These tg mice are unique in that, compared to other tg models, amyloid plaques are found in the brain at a much earlier age (beginning at 3 months) (Rockenstein et al., 2001). The first area in the brain to show amyloid deposition is the frontal cortex at 3 months, followed by the hippocampus. In this latter brain region, amyloid deposits occur at 4-6 months of age in the molecular and pyramidal layers but not in the subgranular zone (SGZ) of the dentate gyrus. Genomic DNA was extracted from tail biopsies and analyzed by PCR amplification, as described previously (Rockenstein et al., 1995). Transgenic lines were maintained by crossing heterozygous tg mice with non-transgenic (non tg) C57BL/6 x DBA/2 F1 breeders. All mice were heterozygous with respect to the transgene. A total of 4 (6-month old) tg mice and 4 age-matched

non-tg littermates were utilized for the present study. Each mouse received 5 intraperitoneal injections (one per day) with 5-bromo-2-deoxyuridine (BrdU, Sigma-Aldrich, St. Louis, MO) at 50 mg/kg. One month after the start of BrdU treatement, mice were sacrificed for analysis of neurogenesis. All experiments were approved by the animal subjects committee at the University of California at San Diego (UCSD) and were performed according to NIH recommendations for animal use.

Tissue processing. In accordance with NIH guidelines for the humane treatment of animals, mice were anesthetized with chloral hydrate and flush-perfused transcardially with 0.9% saline. Brains were removed and divided sagitally. One hemibrain was post-fixed in phosphate-buffered 4% paraformaldehyde (pH 7.4) at 4°C for 48 hr and sectioned at 40 μm with a Vibratome 2000 (Leica, Germany), while the other hemibrain was snap frozen and stored at -70°C for protein analysis.

Immunohistochemical analysis of markers of neurogenesis and cell death. For detection of markers of neurogenesis, briefly as previously described (Winner et al., 2004; Winner et al., 2008), vibratome sections oriented in the sagittal plane were incubated with antibodies against BrdU (marker of dividing cells; rat monoclonal, 1:100, Oxford Biotechnology, Oxford, UK), proliferating cell nuclear antigen (PCNA, marker of proliferation; mouse monoclonal, 1:250, Santa Cruz Biotechnology, Santa Cruz, CA) or doublecortin (DCX, marker of migrating neuroblasts; goat polyclonal, 1:500, Santa Cruz Biotechnology) overnight at 4°C. For detection of BrdU-labeled nuclei, the following DNA denaturation steps preceded the incubation with anti-BrdU

antibody: 2 hrs incubation in 50% formamide/ 2xSSC (2xSSC: 0.3 M NaCl, 0.03 M sodium citrate) at 65°C, 5 min rinse in 2xSSC, 30 min incubation in 2 M HCl at 37°C, and 10 min rinse in 0.1M boric acid, pH 8.5. Sections were then incubated with biotinylated secondary antibodies directed against rat, mouse, or goat. Following intermittent rinses in tris-buffered saline (TBS), avidin-biotin-peroxidase complex was applied (ABC Elite kit, Vector) followed by peroxidase detection with diaminobenzidine (DAB) in 0.01% H_2O_2, 0.04% NiCl in TBS.

For detection of apoptosis of neural progenitor cells in the SGZ, the terminal deoxynucleotidyl transferase dUTP Nick End Labeling (TUNEL) detection method using the ApopTag *In Situ* Apoptosis Detection Kit (Millipore) was used with modifications for free floating sections as described previously (Biebl et al., 2000; Biebl et al., 2005; Cooper-Kuhn and Kuhn, 2002). DAB-immunostained sections were imaged with a digital Olympus microscope. All sections were processed simultaneously under the same conditions and the experiments were performed twice to assess reproducibility.

Quantitative analysis of neurogenesis in the hippocampus. For this purpose, a systematic, random counting procedure, similar to the optical disector (Gundersen et al., 1988), was used as described previously (Williams and Rakic, 1988). For the purpose of the present study the morphometric analysis was focused on the subgranular zone (SGZ) of the DG. This area corresponds to the layer of NPCs located directly under the first layer of mature granular cells in the DG, which in addition to the SGZ, includes the granular cell layer and the molecular layer (ML). The analysis

was centered on the SGZ because a previous study has shown that this is the area most consistently affected in APP tg mice (Donovan et al., 2006). To determine the number of BrdU+, DCX+, PCNA+ or TUNEL+ cells in the SGZ of the hippocampus, every sixth section (200-µm interval) of the left hemisphere was selected from each animal and processed for immunohistochemistry. The reference volume was determined by tracing the areas using a semi-automatic stereology system (Stereoinvestigator, MicroBrightField, Colchester, VT). Positive cells were counted within a 60 x 60 µm counting frame, which was spaced in a 300 x 300 µm counting grid. Positive profiles that intersected the uppermost focal plane (exclusion plane) or the lateral exclusion boundaries of the counting frame were not counted. The total counts of positive profiles were multiplied by the ratio of reference volume to sampling volume in order to obtain the estimated number of positive cells for each structure.

Statistical analysis. The data are expressed as mean values ± standard error of the mean (SEM). Statistical analysis was performed using Student's t-test or one-way analysis of variance (ANOVA) followed by post-hoc Dunnett's test to compare test groups to controls (Prism Graph Pad Software, San Diego, CA, USA). The significance level was set at $p < 0.05$.

RESULTS

In vitro generation of mES cell-derived neural progeny

The neuronal differentiation protocol used in this study was adapted from a previously described method (Bibel et al., 2004) and includes 5 stages (A through E)

(Figure 2.2A). Following withdrawal of LIF and treatment with retinoic acid, the mES cells (Figure 2.2B) (Stage A) formed embryoid bodies (Figure 2.2C) (Stages B and C). After 4 days embryoid bodies were dissociated into the putative NPCs (Figure 2.2D) (Stage D). The EB media was then replaced with B27 media, and cells began to differentiate into a neuronal phenotype (Figure 2.2E, F) (Stage E).

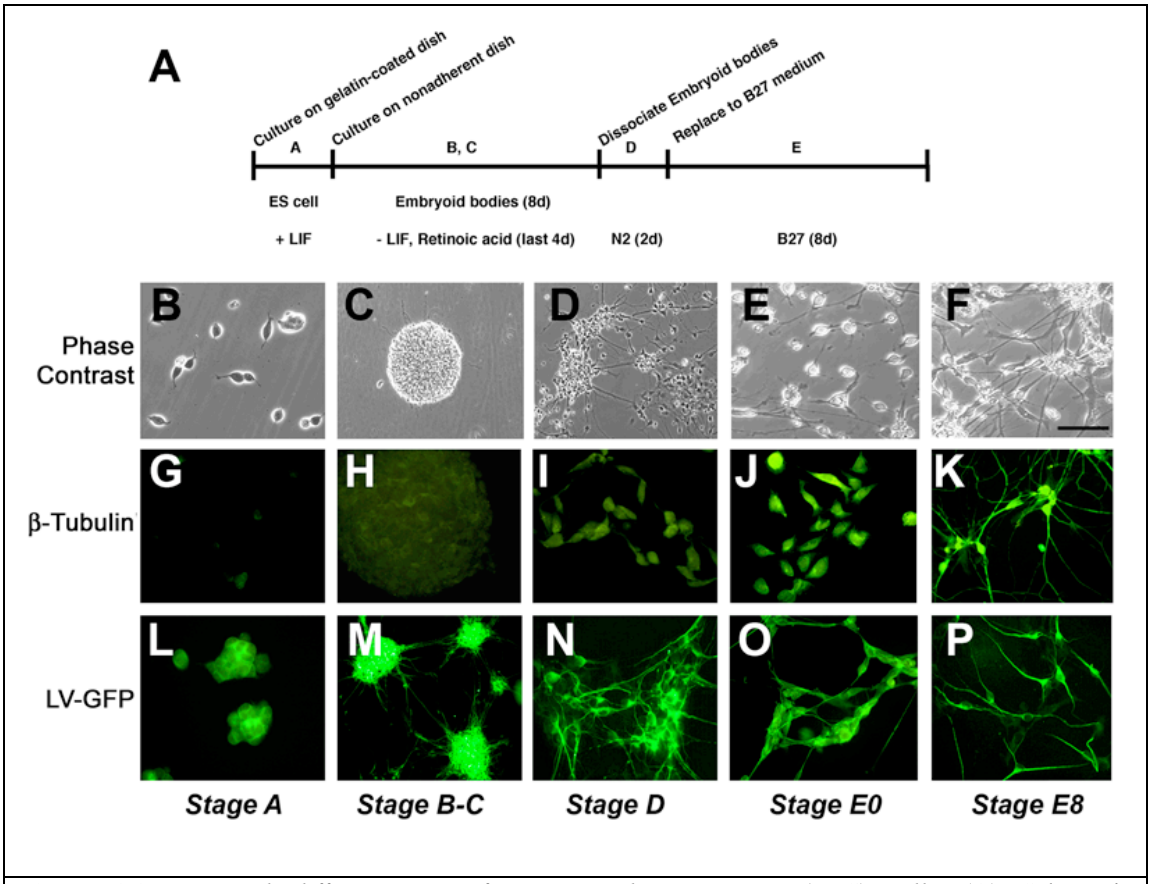

Figure 2.2 *Neuronal differentiation of mouse embryonic stem (mES) cells.* (A) Schematic representation of neuronal differentiation procedure. mES cells were cultured on 0.1% gelatin coated plate and grow as a monolayer (Stage A). mES cells on nonadherent dishes form embryoid bodies (Stage B). After 4d of embryoid body formation, retinoic acid was added (Stage C). Embryoid bodies were dissociated and plated on poly-ornithine/laminin-coated plates in N2 medium (Stage D). After 2d, medium was replaced with B27 medium and cultured for 8d (Stage E). (B-F) Phase contrast images of the mES cells during the differentiation process. (G-K) Expression of the neuronal marker β-Tubulin in the mES cells during differentiation. (L-P) Lentivirus-mediated transduction of GFP into mES cells. *B, E, F, G-P*: scale bar = 30 μm; *C, D:* scale bar = 60 μm.

At early stages of the differentiation protocol (stages A-B) the precursor cells expressed nestin (Figure 2.3A-C) and later on DCX (stage C-D) (Figure 2.3D-F). Over the course of neuronal differentiation (8 d) (Figure 2.2E, F, J, K), low levels of β-Tubulin and neuron-specific enolase (NSE) expression were first noted at Stage D, with a progressive increase during Stage E, reaching their peak at E8 (Figure 2.2G-K, Figure 2.3G-I). This was confirmed by western blot analysis (Figure 2.3J).

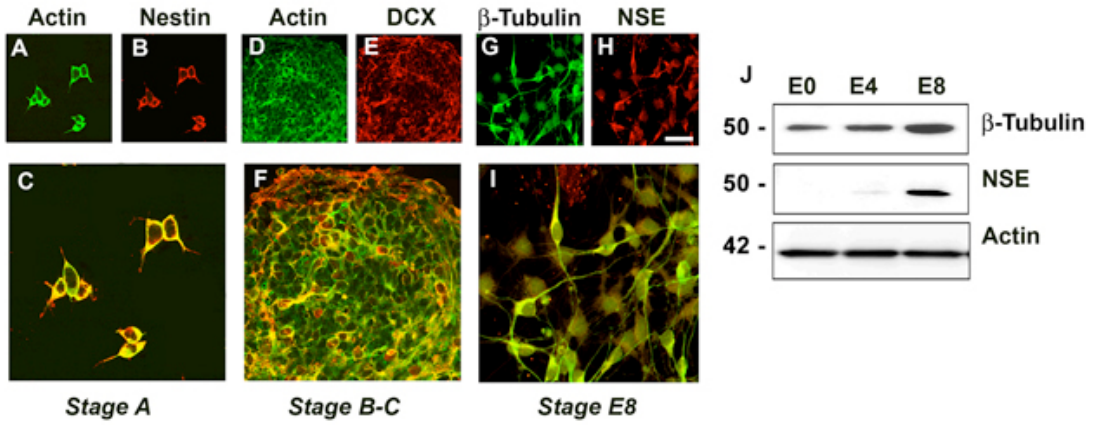

Figure 2.3 *Characterization of the expression of neuronal markers in differentiating mES cells.* (A-C) Expression of the progenitor cell marker, nestin, at Stage A of differentiation. (D-F) Expression of the neuroblast marker, DCX, at Stages B-C of differentiation. (G-I) Expression of the mature neuronal marker, NSE, at the end of Stage E (E8) of differentiation. Panels C, F and I represent merged images. Scale bar = 30 μm.

By the end of stage E, approximately 85% of the cells expressed neuronal markers, including β-Tubulin, MAP2 (not shown) and NSE and displayed polarization with formation of elongated neuritic processes (Figure 2.3I). About 5% of the cells expressed GFAP, while the remaining cells did not express neuronal or astroglial markers (not shown). These heterogeneous cultures were composed primarily of cells expressing immature and mature neuronal markers, with a minority of cells expressing

astroglial markers or markers of proliferating NPCs; therefore we defined these cultures as ‘mES cell-derived neural progeny’.

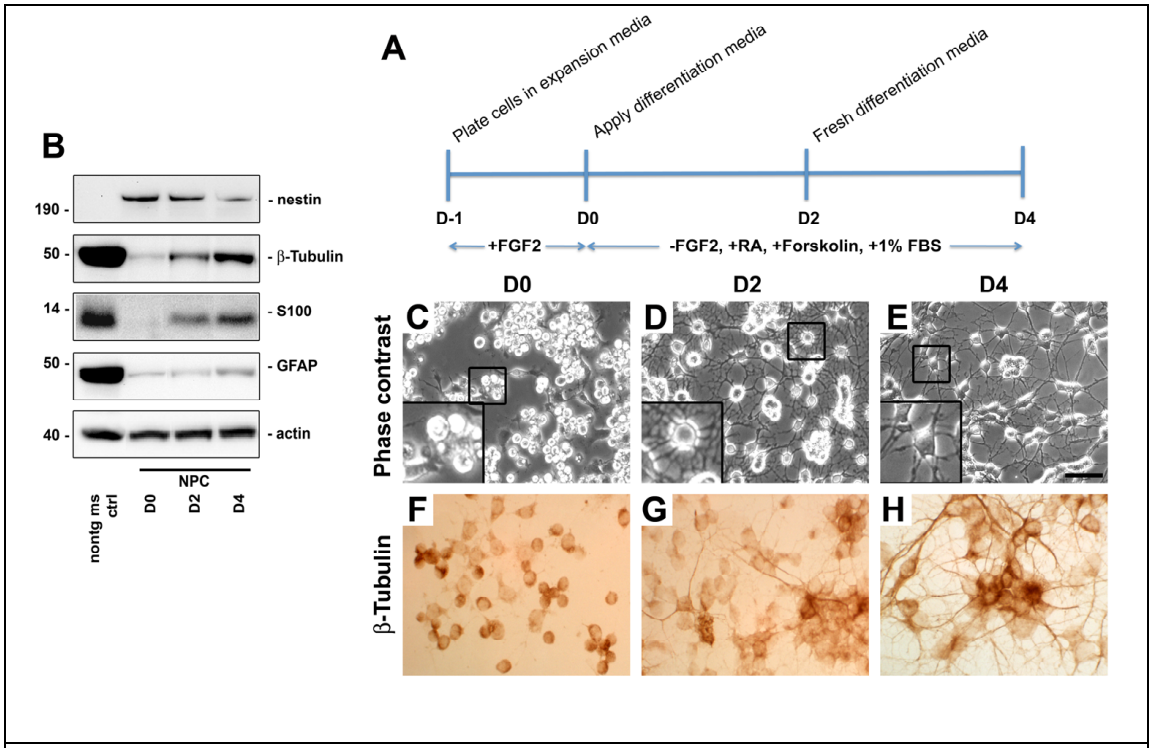

Figure 2.4 *Characterization of neuronal-directed differentiation in adult rat hippocampal NPCs.* (A) Schematic representation of neuronal differentiation procedure. NPCs were plated on poly-ornithine/laminin-coated plates for differentiation induced by fibroblast growth factor-2 (FGF2) withdrawal and application of retinoic acid (RA), forskolin and 1% fetal bovine serum (FBS). (B) Immunoblot characterization of levels of nestin, β-III-Tubulin, S100, GFAP and actin at days 0, 2 and 4 of the differentiation procedure. Non-transgenic (nontg) mouse brain homogenate is shown as a positive control for various lineage markers. (C-E) Live cell imaging of differentiating NPCs at days 0, 2 and 4 of the procedure. (F-H) Immunocytochemical analysis of β-III-Tubulin immunoreactivity at days 0, 2 and 4 of neural induction. Scale bar = 20 μm for low-power images, 10 μm for inset images.

Modeling adult hippocampal neurogenesis *in vitro* and generation of NPC-derived neural progeny

To investigate a potentially more relevant model of adult hippocampal neurogenesis, we modified a previously described *in vitro* model system of neurogenesis and neuronal differentiation where adult rat hippocampal NPCs are

differentiated towards a neuronal phenotype over a period of four days (Ray and Gage, 2006; Ray et al., 1995) (Figure 2.4A).

In order to characterize this neuronal differentiation procedure in our hands, NPCs were grown in NPC Differentiation media for four days and analyzed by western blot and immunocytochemistry. By western blot analysis, levels of progenitor cell markers (nestin) decreased during differentiation and levels of early differentiation (S100) and neuronal markers (β-III Tubulin) increased, while expression of markers of other lineages (GFAP, astrocyte marker) remained low (Figure 2.4B). A representation of relative expression levels of a panel of progenitor cell and mature lineage markers, and members of the CDK5 signaling pathway, in this adult hippocampal NPC model is presented in Table 2.1.

Table 2.1 *Profile of relative expression levels of progenitor cell and mature lineage markers during induced neuronal differentiation of the adult rat hippocampal NPC model system.*

	Proliferation	**Migration**	**Differentiation**	**Maturation**
PCNA	+++	+++	+	+
Sox2	+	-	-	-
Nestin	+++	++	+	-
S100β	+	+	++	++
DCX	+	++	+	-
β-III-Tubulin	+	++	+++	+++
MAP2	-	-	-	+
GFAP	+	+	+	+
CDK5	+	++	+++	+++
p35	+	+	+	+

Live cell imaging of differentiating NPCs showed that undifferentiated cells displayed a small, rounded morphology, the cell bodies having very few or no visible processes (Figure 2.4C). After two days of culture in neuronal differentiating

conditions, most cells acquired a stellate appearance and projected numerous short processes (Figure 2.4D). After two additional days of differentiation, cells displayed a neuronal-like phenotype characterized by processes of increased length (Figure 2.4E). It should be noted that this differentiation procedure generates heterogeneous cultures, and therefore we refer to the cells derived from the differentiation process as 'NPC-derived neural progeny'. Immunocytochemical analysis confirmed the immunoblot results showing that β-III Tubulin (Figure 2.4F-H) expression levels increased steadily to day four of differentiation.

Characterization of CDK5 signaling during induced neuronal differentiation of NPCs

Since previous studies have shown that the CDK5 signaling pathway is deregulated during the pathogenesis of AD and in models of the disorder (Cruz and Tsai, 2004; Lee et al., 1999; Liu et al., 2003; Patrick et al., 1999), and these alterations contribute to neurodegeneration in AD, we sought to develop an *in vitro* model to examine whether this kinase might also contribute to defective neurogenesis in AD models. For this purpose, first we characterized the expression patterns of members of the CDK5 signaling pathway during differentiation of the adult rat hippocampal NPC model (Figure 2.5).

In support of previous studies in other *in vitro* models of neurogenesis (Fu et al., 2002), immunoblot and qRT-PCR analyses showed that protein and mRNA expression of CDK5 increased approximately two-fold over the course of differentiation (Figure 2.5A, B). Levels of p35/p25 remained relatively stable at low

levels at all stages studied (Figure 2.5A, C). Immunocytochemical analysis confirmed the immunoblot and qPCR results showing that CDK5 (Figure 2.5D-F) expression levels increased steadily to day four of differentiation.

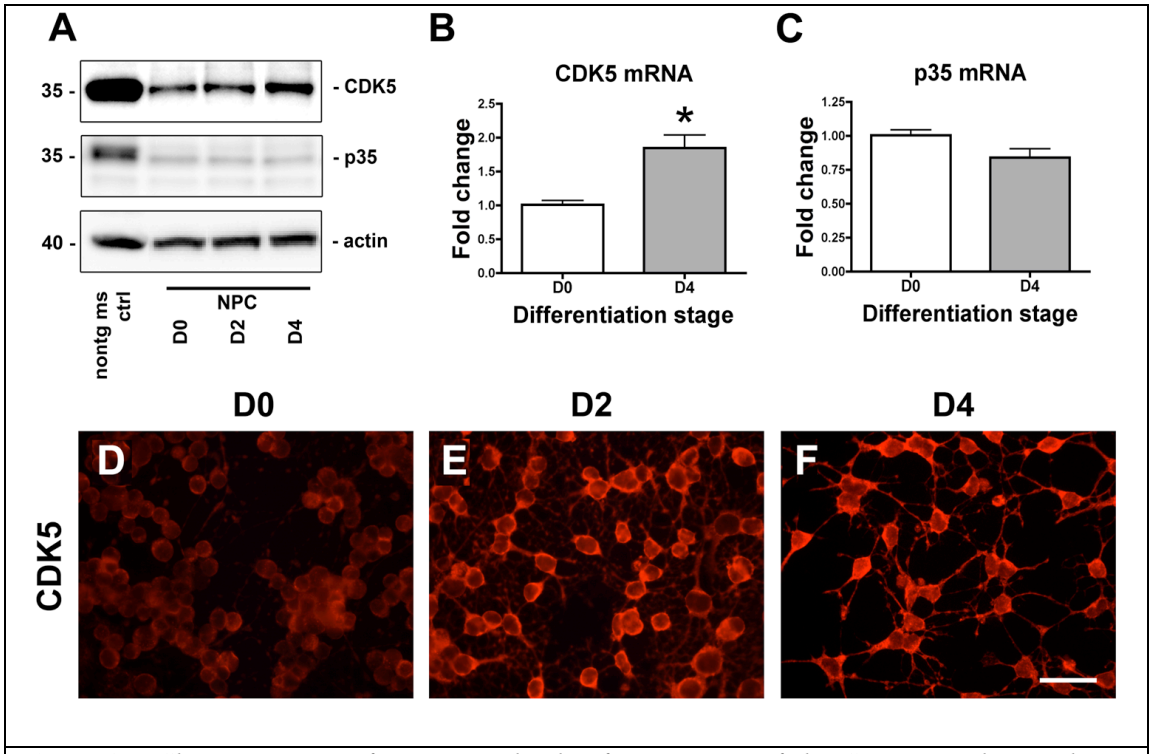

Figure 2.5 *Characterization of expression levels of components of the CDK5 signaling pathways during directed neuronal differentiation of adult rat hippocampal NPCs.* (A) Immunoblot analysis of levels of CDK5, p35 and actin at days 0, 2 and 4 of directed neuronal differentiation of cultured adult rat hippocampal NPCs. (B, C) qRT-PCR analysis of levels of CDK5 and p35 mRNA in undifferentiated NPCs and in D4 NPC-derived neural progeny. (D-F) Immunocytochemical analysis of CDK5 immunoreactivity at days 0, 2 and 4 of directed neuronal differentiation of cultured adult rat hippocampal NPCs. Scale bar = 20 μm. * $p < 0.05$ compared to undifferentiated controls by one-way ANOVA with post-hoc Dunnett's test.

Modeling AD-related CDK5 hyperactivation in adult neurogenesis *in vitro*

To investigate the role of the CDK5 signaling pathway in the differentiation of NPCs, we studied the effects of activating this pathway in the adult rat hippocampal NPC model by utilizing a viral vector expressing the CDK5 activator, p35. Since Aβ has been shown to abnormally stimulate the activity of this pathway, p35-expressing

differentiating cells were treated with Aβ to study the role of this disease-related protein in the CDK5 signaling pathway in neuronal maturation.

Infection of NPCs with an adenoviral (adv) construct expressing p35 resulted in high levels of p35 expression after four days of differentiation (Figure 2.6A). No changes were observed in CDK5 levels or β-III Tubulin expression (Figure 2.6A). Phase contrast microscopy of live cell cultures showed that there were no significant morphological differences in adv-p35 infected cultures compared to uninfected or adv-GFP infected controls (Figure 2.6B-D). In order to investigate the activation of the CDK5 signaling pathway with Aβ, following adv-p35 infection, cultures were treated with sub-toxic concentrations of $A\beta_{1-42}$ for 24 hrs (Figure 2.6E-G). Analysis of kinase activity confirmed that, as expected, in cells expressing p35 or treated with Aβ alone, or in combination, CDK5 activity was significantly increased (Figure 2.6H).

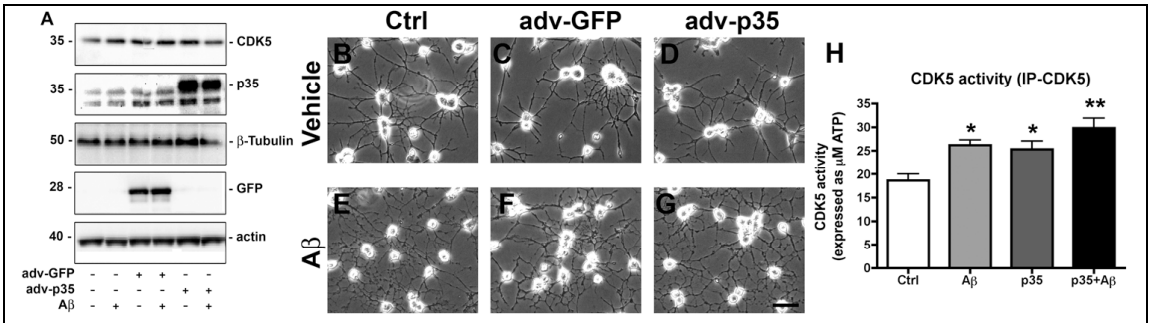

Figure 2.6 *Characterization of an* in vitro *model of adult neurogenesis in AD.* (A) Immunoblot analysis of expression levels of CDK5, p35, β-III-Tubulin, GFP and actin (loading control) in NPC-derived neural progeny expressing p35 or GFP control and treated with Aβ. (B-G) Live cell imaging of morphology of NPC-derived neural progeny expressing p35 or GFP control and treated with Aβ. (H) Increased kinase activity of CDK5 in p35 and Aβ alone and p35/Aβ-treated NPC-derived neural progeny. Scale bar = 10 μm. * $p < 0.05$ compared to vehicle-treated controls by one-way ANOVA with post-hoc Dunnett's test. ** $p < 0.01$ compared to vehicle-treated controls by one-way ANOVA with post-hoc Dunnett's test.

In this model system of CDK5 hyperactivation in neurogenesis in AD, the CDK5 activator p35 was expressed beginning at day 2 of differentiation, when cells were still in the proliferative phase. We selected this time point for expression of p35 because prior to day 2, endogenous levels of both p35 and CDK5 are low (Figure 2.5A-C). While endogenous p35 levels remain low to day 4 of differentiation, CDK5 levels increase about two-fold between days 2 and 4, suggesting that there is more endogenous CDK5 present to interact with the over-expressed p35. By the end of the 4-day differentiation period, the majority (>90%, Figure 2.4H) of progeny are immuno-positive for β-III-Tubulin, suggesting that they are committed to a neuronal fate and represent immature neurons. Therefore, by studying the effects of CDK5 activation during the latter stage of the neuronal differentiation procedure, we are targeting the *maturation* phase of adult NPCs in this culture model.

Characterization of oligomeric species present in peptide preparations used in culture

To characterize the aggregation status of the freshly-solubilized Aβ peptide used in our model system, we performed control experiments using gel electrophoresis and electron microscopy techniques (Figure 2.7). For this purpose, peptide preparations containing 1μM solutions of $A\beta_{1\text{-}42}$, $A\beta_{42\text{-}1}$, TTR, or vehicle control were separated under non-reducing conditions by gel electrophoresis and subjected to silver stain analysis (Figure 2.7A).

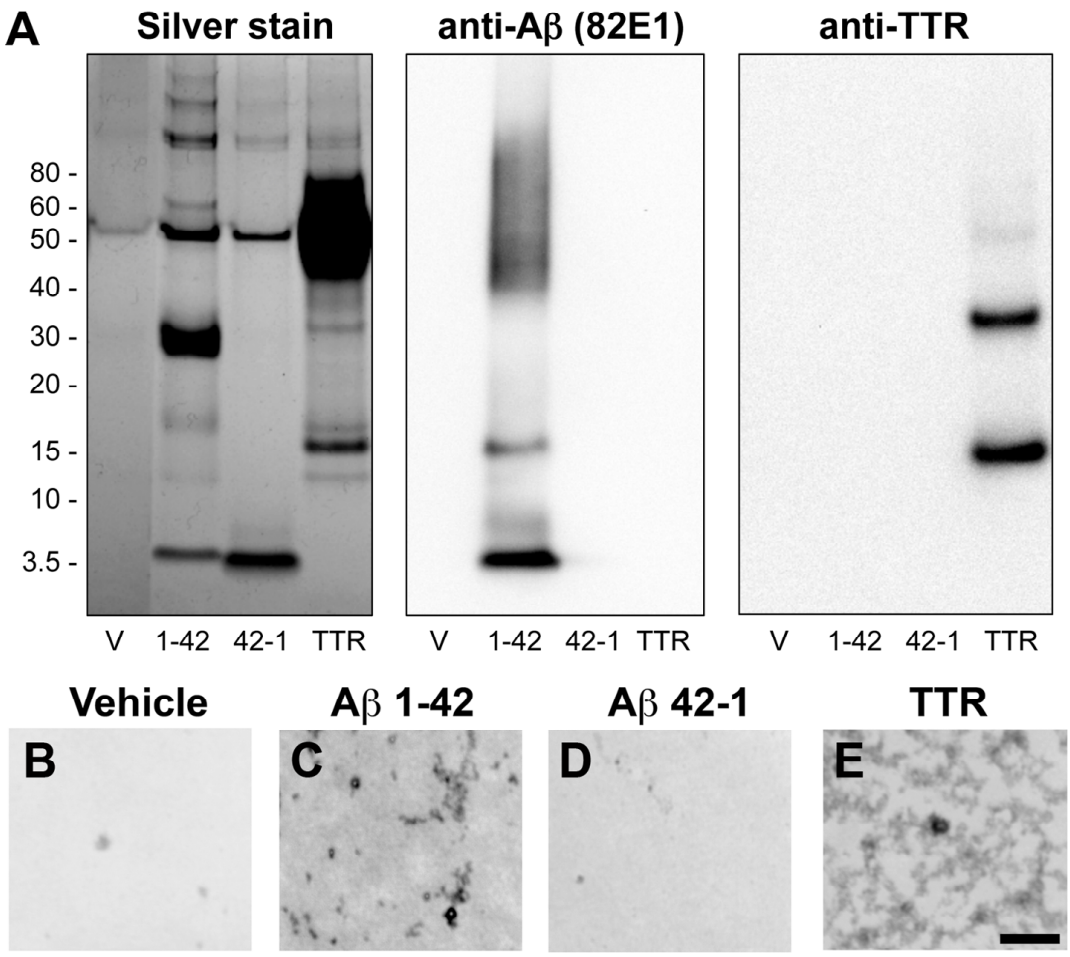

Figure 2.7 *Gel electrophoresis and ultrastructural characterization of aggregation patterns of $A\beta_{1\text{-}42}$ and controls.* Peptide solutions of $A\beta_{1\text{-}42}$, $A\beta_{42\text{-}1}$, transthyretin (TTR) or vehicle control (V) were prepared at 1μM or 10μM concentrations and analyzed by gel electrophoresis or electron microscopy. (A) Silver stain (left panel) analysis of 1μM preparations, or immunoblot analysis of 10μM preparataions probed with antibodies against Aβ (82E1 clone, middle panel) or TTR (right panel). (B-E) Ultrastructural analysis of 1μM solutions of $A\beta_{1\text{-}42}$, $A\beta_{42\text{-}1}$, TTR or vehicle control. Scale bar = 100 nm.

This analysis showed that monomer (4 kDa) and small oligomers were the primary species detected in the $A\beta_{1\text{-}42}$ sample (Figure 2.7A). In contrast, as expected, in the reverse $A\beta_{42\text{-}1}$ solution, only protein deposits consistent with the molecular weight of the monomeric species (4 kDa) were detected, with a few non-specific bands also present in the vehicle control sample. In the TTR solution, monomeric (15

kDa) species and species around a molecular weight of 30-50 kDa were detected (Figure 2.7A). The 50 kDa protein deposit is likely serum albumin because TTR is derived from human plasma.

Next, to confirm protein identities by immunoblot analysis, gels run in parallel were transferred onto membranes and probed with antibodies against Aβ (82E1 clone) or TTR (Figure 2.7A). Immunoblot analysis of 1μM solutions was not sensitive enough to detect protein species with this technique, so for illustration, immunoblot analysis is shown with 10μM peptide solutions. This revealed similar small monomer and oligomeric species in the Aβ1-42 solution, and a diffuse smear of immunoreactivity from about 40-100 kDa (Figure 2.7A). It is unclear what this protein smear represents, as there were several different distinct bands detected in this region by silver stain, including a non-specific background band. Consistent with the known aggregation pattern of TTR into dimeric and tetrameric species, by immunoblot with an antibody against TTR, bands were detected at around 15 kDa (monomer), 30 kDa (dimer) and a fainter band around 45-60 kDa (trimer or tetramer) (Figure 2.7A).

To confirm and provide further characterization of the peptide species detected by gel electrophoresis and immunoblot, ultrastructural analysis was performed (Figure 2.7B-E). Consistent with the gel analyses, electron microscopic images showed that in samples of 1μM $A\beta_{1-42}$, small aggregates were observed (Figure 2.7C) similar to oligomeric species of Aβ described in previous studies (Tsigelny et al., 2008). More diffuse aggregates were observed in samples containing 1μM TTR (Figure 2.7E), and no electron dense deposits were detected in samples containing vehicle control (Figure 2.7B) or reverse $A\beta_{42-1}$ peptide. These results support the contention that the $A\beta_{1-42}$

preparations are composed of primarily small oligomeric and monomeric species, and the reverse $A\beta_{42-1}$ peptide provides an appropriate non-aggregating experimental control.

Taken together, these results support the notion that under the conditions utilized in our model system, the freshly-solubilized $A\beta_{1-42}$ peptide is composed of monomeric and small oligomeric species, while the reverse $A\beta_{42-1}$ peptide does not oligomerize, and TTR forms homodimers and trimers or tetramers.

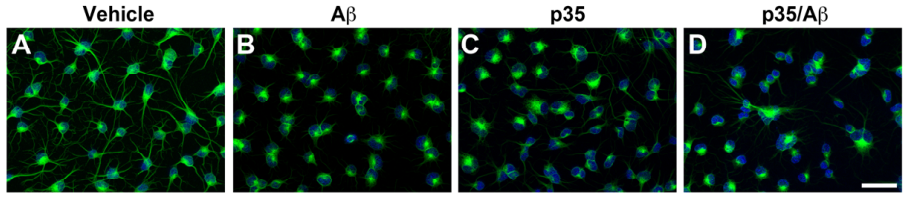

Figure 2.8 *Impaired neurite outgrowth in NPC-derived neural progeny expressing p35 and treated with Aβ.* Differentiating NPCs were infected at day 2 with an adenoviral vector expressing p35, and 24 hrs later cells were exposed to 1 μM $A\beta_{1-42}$. On day 4, cells were briefly extracted, then fixed with glutaraldehyde and processed for β-tubulin immunofluorescence. (A-D) Reduced β-tubulin-immunoreactive neurites in NPC-derived neural progeny with p35 or Aβ treatment alone or in combination. (E) Quantitative image analysis showing reduced neurite lengths in NPC-derived neural progeny with p35 or Aβ treatment alone or in combination. Scale bar = 10 μm. * $p < 0.05$ compared to vehicle-treated controls by one-way ANOVA with post-hoc Dunnett's test.

Increased CDK5 activity in NPC-derived neural progeny expressing p35 and treated with Aβ is associated with reduced neurite outgrowth

In order to determine whether activation of CDK5 was associated with any measurable differences in neuronal *maturation*, neurite outgrowth was assessed in NPC-derived neural progeny expressing p35 and treated with Aβ (Figure 2.8). β-Tubulin immunofluorescence and neurite outgrowth studies revealed that p35 and Aβ treatment alone or in combination resulted in shorter processes in NPC-derived neural progeny (Figure 2.6G, Figure 2.8), however other controls for Aβ (reverse $A\beta_{42-1}$

peptide) and aggregating proteins (TTR) had no significant effects on neurite outgrowth (Figure 2.9). Taken together, this system provides a useful model in which to study the molecular mechanisms involved in CDK5 hyperactivation during neurogenesis in AD.

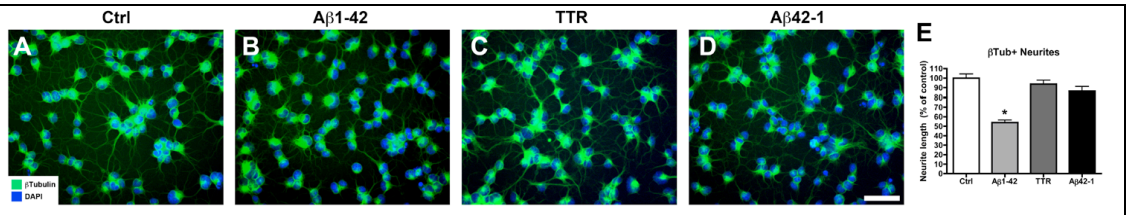

Figure 2.9 In vitro *control treatments for $A\beta_{1\text{-}42}$.* Differentiating NPCs were exposed on day 3 to 1 μM $A\beta_{1\text{-}42}$, TTR or reverse $A\beta_{42\text{-}1}$ peptide. On day 4, cells were briefly extracted, then fixed with glutaraldehyde and processed for β-tubulin immunofluorescence. (A-D) β-Tubulin immunoreactivity in NPC-derived neural progeny treated with vehicle control (ctrl, A), $A\beta_{1\text{-}42}$ (B), TTR (C) or reverse $A\beta_{42\text{-}1}$ peptide (D). (E) Image analysis of neurite lengths of NPC-derived neural progeny. Scale bar = 20 μm. * $p < 0.05$ compared to vehicle-treated controls by one-way ANOVA with post-hoc Dunnett's test.

For subsequent analysis of β-tubulin immunoreactivity by immunoblot (Chapter 4), we performed validation studies of this antibody and an antibody against α-tubulin for semi-quantitative analysis in our digital immunoblot imaging system using the VersaDoc (BioRad). For this purpose, immunoblots were prepared with serial dilutions of lysates from control NPC-derived neural progeny (Figure 2.10). Blots were incubated with antibodies against β-tubulin or α-tubulin and visualized with enhanced chemiluminescence (Figure 2.10A, B). Using the VersaDoc digital imaging system, high-resolution images were obtained at 5-second intervals to generate exposures ranging from 5sec-250sec in length (semi-quantitative analysis of other antibodies requires varying exposure times up to 5 mins in length). Images containing saturated pixels in the bands of interest were not used for quantitation. All analysis was performed with the Quantity One quantitation program (BioRad) (Figure

2.10A), and background signal intensities were subtracted from the intensity values measured for each immunoreactive band.

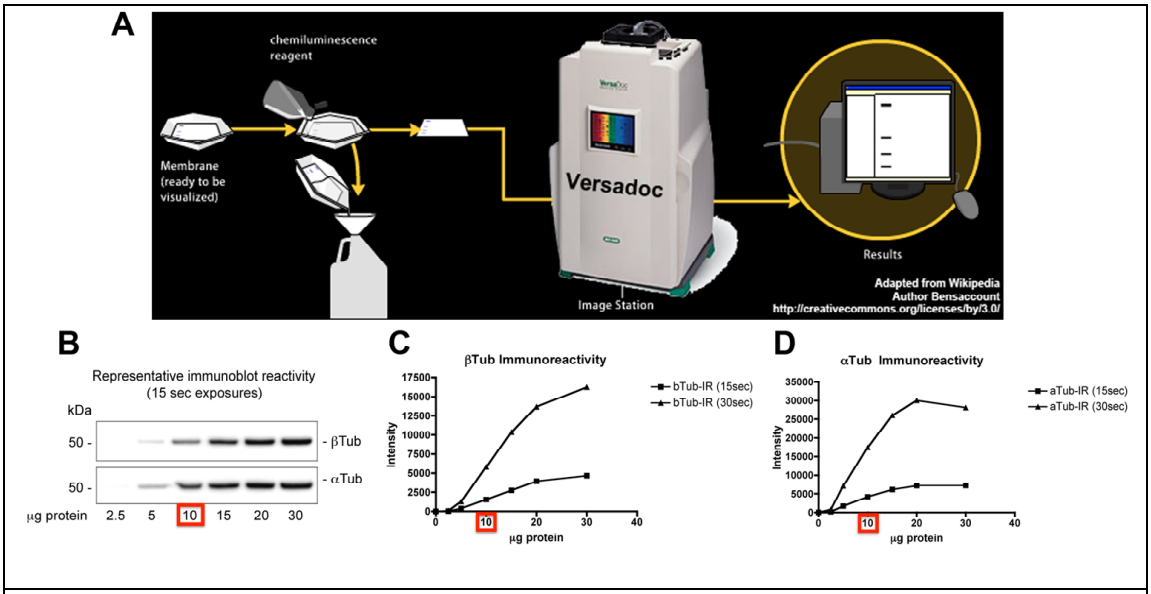

Figure 2.10 *Validation studies of anti-tubulin antibodies for digital imaging and semi-quantitative measurements.* (A) Schematic diagram showing the gel visualization and image capture and analysis procedure utilized for semi-quantitative analysis of tubulin immunoreactivity. (B) Representative immunoblots from gels loaded with serial dilutions of lysates from control NPC-derived neural progeny. Blots were probed with mouse monoclonal antibodies against β-tubulin or α-tubulin (both from Sigma-Aldrich). 10μg indicates the quantity of protein typically loaded for tubulin analysis in subsequent experiments. (C, D) Semi-quantitative image analysis of increasing signal intensity corresponding with increased protein loaded on blots probed with antibodies against β-tubulin (C) or α-tubulin (D). The linear range of signal intensity on 15-sec exposures was detected between 5μg and 20μg. 30-sec exposures showed some pixel saturation and are shown for comparison.

Graphic analysis of signal intensities of β-tubulin immunoreactivity plotted against protein loaded (in μg) demonstrated that with standard exposure times (15sec), increasing signal intensity was detected in a linear range with protein loading quantities from 5μg-20μg (Figure 2.10B, C). Analysis of an image from a 30-sec exposure that displayed saturated pixels is shown for comparison demonstrating that with pixel saturation, the signal sensitivity is reduced and is no longer linear above 20μg. Similar results were obtained with an antibody against α-tubulin (Figure

2.10D). Taken together, these studies confirm the validity of our semi-quantitative image analysis of immunoreactivity using tubulin antibodies on immunoblots loaded with with 5-20μg of protein.

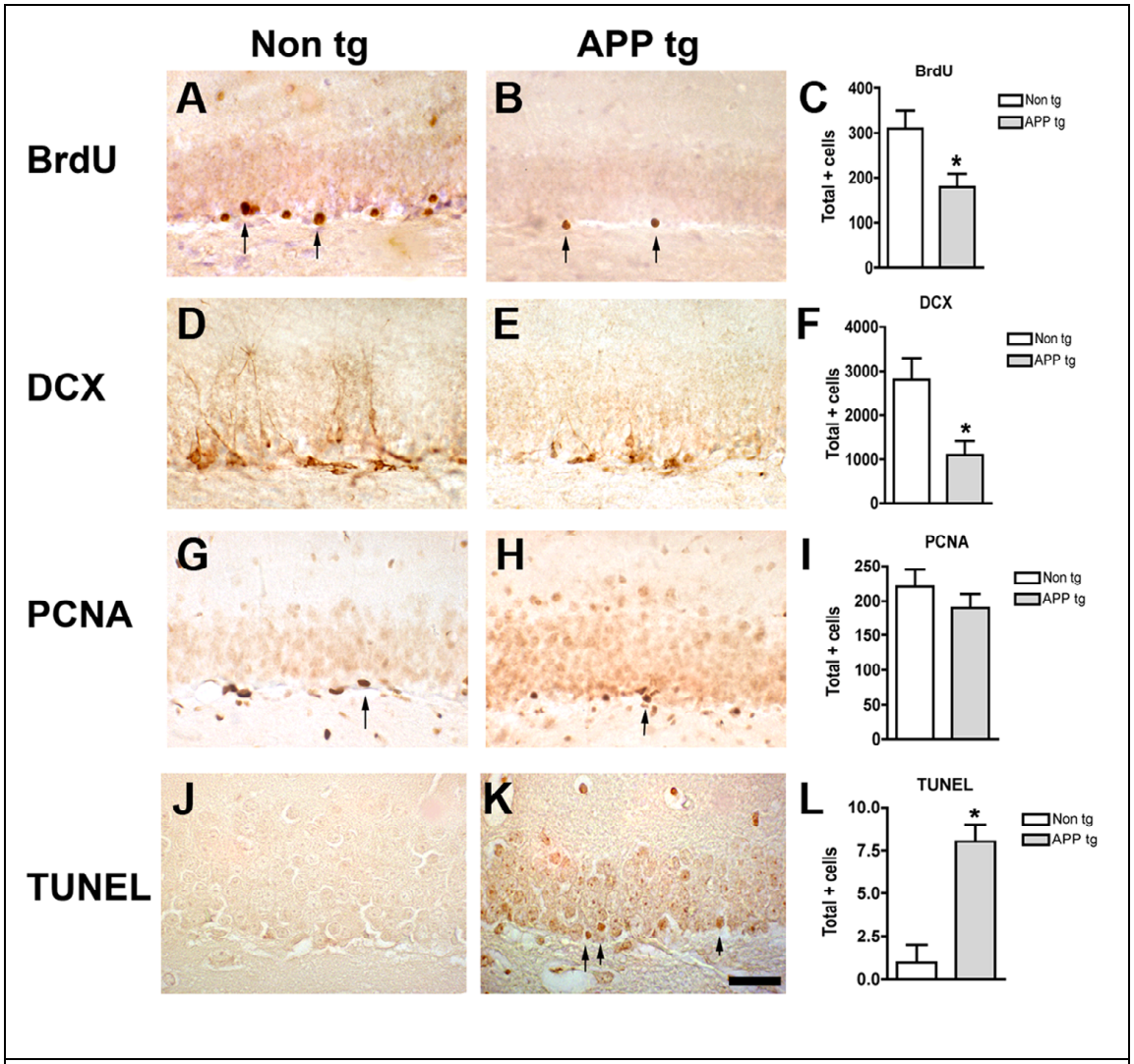

Figure 2.11 *Reduced markers of neurogenesis and increased apoptosis in the hippocampus of APP tg mice.* (A-C) Reduced BrdU immunoreactivity in the hippocampal dentate gyrus of APP tg mice treated with BrdU compared to non-tg controls treated with BrdU. (D-E) Reduced doublecortin (DCX) immunoreactivity in the hippocampal dentate gyrus of APP tg mice compared to non-tg controls. (G-I) Proliferating cell nuclear antigen (PCNA) immunoreactivity in the hippocampal dentate gyrus of APP tg mice and non-tg controls. (J-L) Increased TUNEL-positive cells in the hippocampal dentate gyrus of APP tg mice compared to non-tg controls. Scale bar = 50μm for all panels. *$p < 0.05$ compared to non-tg controls by Student's t-test (n = 4 mice per group).

Neurogenesis is reduced in an *in vivo* APP tg model of AD

To characterize the status of neurogenesis in BrdU-treated APP tg mice expressing mutant human APP under the control of the mThy-1 promoter, we performed immunohistochemical analysis of markers of neurogenesis in the hippocampal DG of non-tg and APP tg mice (Figure 2.11).

Stereological image analysis of brain sections immunolabeling with antibodies against BrdU, DCX or PCNA revealed that numbers of BrdU- and DCX-positive cells were significantly reduced in the SGZ of APP tg mice compared to non-tg controls (Figure 2.11A-F). Numbers of PCNA-positive cells were unchanged (Figure 2.11G-I). Because our BrdU treatment regimen was devised to investigate the survival and maturation of NPCs at one month post-treatment, the changes in BrdU- and DCX-positive cell numbers suggest that there was impaired cell maturation or survival. In support of this possibility, analysis of apoptosis by TUNEL demonstrated increased numbers of TUNEL-positive cells in the DG of APP tg mice compared to non-tg controls (Figure 2.11J-L). Taken together, the neurodegenerative process in APP tg mice may be accompanied by impairments in the maturation or survival of NPCs in the adult hippocampus, and our subsequent studies will utilize these *in vitro* and *in vivo* models to elucidate the role of CDK5 in this process, and other molecular mechanisms that may be involved.

DISCUSSION

Alterations in synaptic plasticity in AD might involve not only direct damage to the synapses but also interference with adult neurogenesis. The mechanisms of

synaptic pathology in AD are the subject of intense investigation. Studies in experimental models of AD and in human brain support the notion that aggregation of Aβ, resulting in the formation of toxic oligomers rather than fibrils, might be ultimately responsible for the synaptic damage that leads to cognitive dysfunction in patients with AD (Glabe, 2005; Glabe and Kayed, 2006; Walsh and Selkoe, 2004). Moreover, a dodecameric Aβ complex denominated *56 has been recently characterized (Lesne et al., 2006) in brains from APP tg mice and shown to contribute to the behavioral alterations in these animals. Supporting this notion, it has been shown that Aβ oligomers reduce synaptic transmission and dendritic spine movement (Lacor et al., 2004; Moolman et al., 2004; Walsh and Selkoe, 2004), and interfere with axoplasmic flow and activate signaling pathways that might lead to synaptic dysfunction, Tau hyperphosphorylation and cell death. Among these pathways, CDK5 has been implicated as an important contributor to neurodegeneration in AD, and is directly targeted by Aβ via calcium influx and calpain-mediated activation (Cruz and Tsai, 2004). However, its role in adult neurogenesis in AD is unclear.

In this context, we aimed to develop *in vitro* and *in vivo* models of neurogenesis in AD to elucidate the role of this kinase in this process. In order to establish models to investigate the molecular mechanisms that regulate this process, we first characterized two *in vitro* cell models of neurogenesis and neuronal maturation. For the first, a mES cell line was differentiated to induce neural progeny over a period of 18 days, and markers of neuronal differentiation were assessed by immunoblot and immunocytochemistry. At the end of the differentiation period, we found that cells displayed a neuronal morphology, and expressed markers of immature

(β-III-Tubulin) and mature (NSE) neuronal states. However, this process was lengthy and the average cell yield from embryoid body dissociation tended to be low. To develop an alternative, more relevant *in vitro* system to study neurogenesis in the *adult* brain, for the second model, adult rat hippocampal neuronal progenitor cells (NPC) were cultured and differentiated to induce neural progeny over a period of 4 days, followed by immunoblot and immunocytochemical analyses. This procedure induced neurite outgrowth and yielded a high proportion of β-III-Tubulin-positive cells.

We determined that the NPC model was the most relevant for studying adult neurogenesis *in vitro*, so we then adapted this model to develop a paradigm of adult hippocampal neurogenesis in AD. To investigate the role of the CDK5 signaling pathway in the differentiation of NPCs, we studied the effects of activating this pathway in the adult rat hippocampal NPC model by utilizing a viral vector expressing the CDK5 activator, p35. Since Aβ has been shown to abnormally stimulate the activity of this pathway, p35-expressing differentiating cells were treated with human $A\beta_{1\text{-}42}$ peptide to study the role of this AD-related protein in the CDK5 signaling pathway in neuronal maturation. First we performed control characterization experiments with $A\beta_{1\text{-}42}$ peptide, reverse $A\beta_{42\text{-}1}$, and a non-Aβ amyloidogenic protein, TTR. These studies confirmed that $A\beta_{1\text{-}42}$ peptide preparations formed small oligomeric aggregates similar to the species implicated in other studies to interfere with synaptic integrity in mature neurons (Glabe, 2005; Glabe and Kayed, 2006; Walsh and Selkoe, 2004).

In our *in vitro* model of CDK5 hyperactivation in adult neurogenesis in AD, expression of p35 resulted in high levels of p35 immunoreactivity by day four of

differentiation, and combined treatment with sub-toxic concentrations of $A\beta_{1-42}$ for 24 hrs demonstrated that CDK5 activity was significantly increased. This was accompanied by a reduction in neurite outgrowth, supporting a role for CDK5 hyperactivation in impaired neurogenesis in AD (Figure 2.12). In this model system, we induced CDK5 activation during the latter stage of the neuronal differentiation procedure, when cells are exiting the proliferative phase and the majority express immature neuronal markers. Therefore we are specifically examining the *maturation* phase of adult NPCs in this culture model.

Next, to characterize an *in vivo* model of adult neurogenesis in AD, we utilized a tg mouse model that overexpresses mutant human APP and recapitulates several features of AD. We showed by immunohistochemical analysis that in this model, there were reduced numbers of BrdU-labeled cells in the adult hippocampus of APP tg mice compared to non-tg controls one month post-treatment, and this was accompanied by increased numbers of TUNEL-positive apoptotic cells in the SGZ. Moreover, there were reduced numbers of DCX-positive immature neuronal cells in the DG of APP tg mice compared to non-tg controls, suggesting that survival or maturation of immature neurons is impaired in these animals. The deficient neurogenesis in the subgranular zone (SGZ) of the DG found in our APP tg mice (Rockenstein et al., 2007a) is consistent with studies in other lines of APP tg mice and other models of AD that have shown decreased markers of neurogenesis, with an increase in the expression of markers of apoptosis (Dong et al., 2004; Feng et al., 2001; Haughey et al., 2002b; Wang et al., 2004). Subsequent studies will make use of these *in vitro* and *in vivo* models to further examine the molecular targets involved in defective neurogenesis in

AD, and the role of the CDK5 signaling pathway and downstream targets might play in these alterations (Figure 2.12).

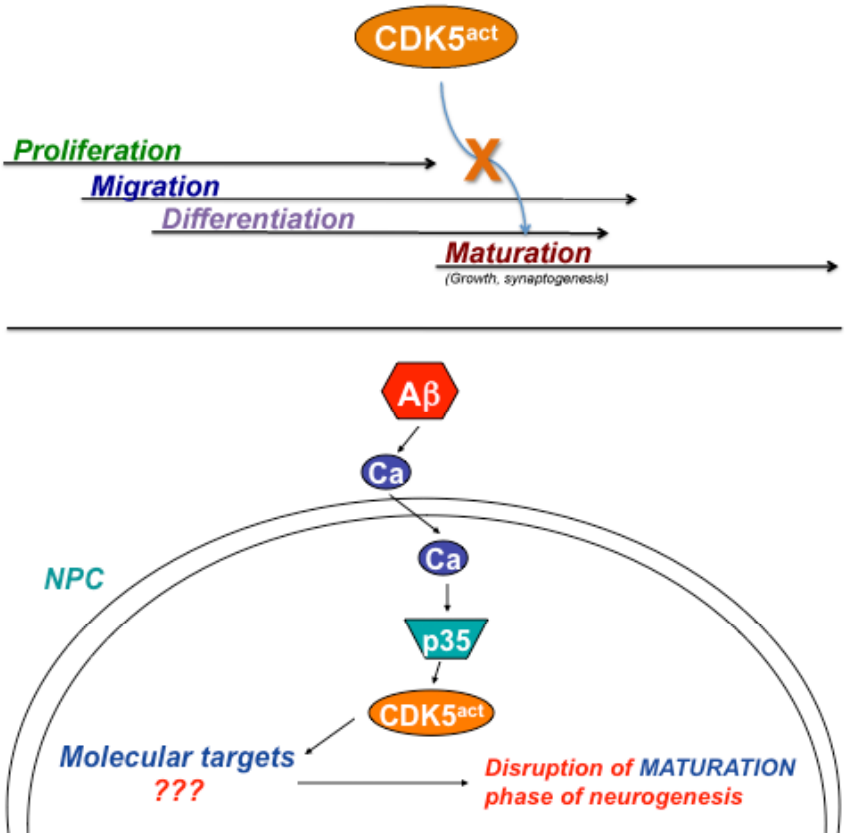

Figure 2.12 *Diagram showing proposed role of CDK5 in defective neurogenesis in AD.* Subsequent studies will utilize the *in vitro* and *in vivo* models described to elucidate the molecular targets that might mediate CDK5-dependent alterations in the maturation of immature neurons.

ACKNOWLEDGEMENTS

Chapter 2, in part, contains figures and text of the material as it appears in the Journal of Neuroscience 2008. Crews L, Mizuno H, Desplats P, Rockenstein E, Adame A, Patrick C, Winner B, Winkler J, Masliah E (2008) Alpha-synuclein alters Notch-1 expression and neurogenesis in mouse embryonic stem cells and in the hippocampus of transgenic mice. J Neurosci 28:4250-4260, Society for Neuroscience, 2008. The dissertation author was co-lead author and investigator of this paper.

Chapter 2, in part, contains figures and excerpts of the material as it appears in Brain Structure and Function 2009. With kind permission from Springer Science+Business Media: Crews L, Rockenstein E, Masliah E (2009) APP transgenic modeling of Alzheimer's disease: mechanisms of neurodegeneration and aberrant neurogenesis, Springer Berlin/Heidelberg. The dissertation author was the primary author of this paper.

The work in Chapter 2 was supported by NIH Grants AG10435, AG022074, AG18440, AG11385, NS44233 and AG5131.

CHAPTER 3

ROLE OF CDK5 IN THE MECHANISMS OF DEFECTIVE NEUROGENESIS IN ALZHEIMER'S DISEASE

ABSTRACT

Recent studies show that in Alzheimer's disease (AD), alterations in neurogenesis contribute to the neurodegenerative process. Neurodegeneration in AD has been associated with aberrant signaling through the cyclin-dependent kinase 5 (CDK5) pathway via its activators p35/p25. Since CDK5 has also been implicated in developmental neurogenesis, we hypothesized that the CDK5 signaling pathway might play an important role in the maintenance and regulation of differentiation of neuronal progenitor cells (NPCs) in the adult brain. To investigate the role of CDK5 in an *in vitro* model system of neurogenesis, CDK5 was inhibited utilizing siRNA knockdown and pharmacological approaches. Immunoblot and immunocytochemical studies demonstrated that CDK5 inhibition arrested neuronal differentiation, reduced the expression of neuronal markers, and dramatically altered neurite outgrowth. These results were confirmed in an *in vivo* animal model that is a heterozygous knockout for CDK5. Next, to study the activation of the CDK5 signaling pathway via p35 overexpression and Aβ treatment, NPCs were infected with a viral vector expressing p35 and exposed to the AD-related amyloid-β protein ($A\beta_{1\text{-}42}$). These conditions modified neuronal differentiation, resulting in the generation of glia-like cells expressing markers of multiple progenitor and differentiated lineages.

Pharmacological inhibition of CDK5 in this model rescued the normal differentiation phenotype *in vitro*. Consistent with the cell culture studies, in double-labeling immunocytochemical studies in mice, CDK5 and p35 were detected in NPCs in the hippocampus of adult non-transgenic mice, while in a transgenic mouse model of AD, glia-like cells similar to those in the *in vitro* model were observed—an effect that was reversed in APP transgenic mice treated with a pharmacological CDK5 inhibitor. Taken together, these data suggest that the CDK5 signaling pathway plays a critical role in neuronal differentiation, and potential therapeutic approaches targeting the neurogenic alterations in AD could focus on normalizing activity of CDK5 or preventing activation of the pathologic CDK5 signaling pathway.

INTRODUCTION

During aging and in the progression of Alzheimer's disease (AD), synaptic plasticity and neuronal integrity are disturbed (Lee et al., 2004). In AD this has been linked with hyperactivation of cyclin-dependent kinase-5 (CDK5) and its activators p35 and p25 (Cruz et al., 2006; Cruz and Tsai, 2004; Liu et al., 2003; Patrick et al., 1999), and levels of CDK5 are increased in the brains of AD patients (Lee et al., 1999). Similarly, CDK5 has been implicated in the pathogenesis of other disorders such as Parkinson's (Smith et al., 2003) and prion disorders (Lopes et al., 2007).

CDK5 is the predominant CDK found in the brain, is highly expressed in neurons, and plays an important role in synaptic plasticity and neuronal development (Cicero and Herrup, 2005) in the mature brain by regulating the phosphorylation of cytoskeletal proteins (e.g. nestin, doublecortin), synaptic proteins (e.g. synapsin I,

PSD) and transcription factors (e.g. MEF2). CDK5 is activated specifically by p35 (Tsai et al., 1994) and by the calpain-mediated cleavage product of p35, p25 (Lee et al., 2000). While CDK5 activation via interactions with p35 is associated with physiological activation of CDK5, the truncated p25 form—which, in AD can be generated by amyloid-β (Aβ)-mediated calpain cleavage of p35 (Lee et al., 2000)—hyperactivates CDK5 and leads to abnormal phosphorylation of substrates such as tau (Ahlijanian et al., 2000). This in turn contributes to neurodegeneration, suggesting that CDK5 signaling plays an important role in neurotoxicity in the pathogenesis of AD.

In addition to the alterations in synaptic plasticity in mature neurons, recent studies have uncovered evidence suggesting that the neurodegenerative process in AD might include deregulation of adult neurogenesis (Boekhoorn et al., 2006; Jin et al., 2004b; Li et al., 2008a). This suggests that both aging and AD may be characterized by not only a loss of mature neurons but also by a decrease in the generation of new neurons from neural progenitor cells (NPCs) in the subventricular zone (SVZ) and dentate gyrus (DG) of the hippocampus in the adult brain. Mechanisms of neurogenesis in the fetal brain have been extensively studied, however less is known about the signaling pathways regulating neurogenesis in the adult nervous system and their role in neurodegenerative disorders.

Although there is some controversy over whether neurogenesis is increased (Jin et al., 2004b) or decreased (Boekhoorn et al., 2006; Li et al., 2008a) in the pathogenesis of AD, some studies suggest that apparent increases in markers of neurogenesis in the brains of AD patients may be related to glial and vasculature-associated changes (Boekhoorn et al., 2006). Animal models of APP overexpression

present a more complex picture, however in support of the more recent studies in human AD patients, a number of animal models of familial AD (FAD) display significantly reduced neurogenesis compared to non-tg controls (Dong et al., 2004; Donovan et al., 2006; Haughey et al., 2002a; Rockenstein et al., 2007a) (for a more comprehensive review of neurogenic alterations in FAD-linked mouse models, please see (Lazarov and Marr, 2009)). However, the molecular mechanisms involved in producing these effects remain to be fully defined.

Although the hyperactivation of CDK5/p35/p25 has been associated with the pathogenesis of neurodegenerative diseases such as AD, its physiological function has been implicated in critical functions such as neuroblast migration in the cerebral cortex (Chae et al., 1997; Hirota et al., 2007; Ohshima et al., 1996) and synaptic plasticity (Fischer et al., 2005; Johansson et al., 2005). Furthermore, the Cdk5/p35 complex localizes to the leading edge of axonal growth cones (Pigino et al., 1997) where it regulates neurite outgrowth in mature cortical neurons (Nikolic et al., 1996). More recently, CDK5 has been shown to be essential for adult neurogenesis (Jessberger et al., 2008; Lagace et al., 2008). In this context, it is possible that the neurogenesis deficits in AD might be related to alterations in CDK5 activity in NPCs.

In support of this idea, in models of AD, Aβ has been shown to impair neurogenesis via calpain activation and p35 deregulation (Haughey et al., 2002b), however the consequences of CDK5 and p35/p25 manipulation on neuronal *maturation* remain to be revealed (Figure 3.1). Elucidating the signaling pathways involved in the deregulation of neurogenesis is important to fully understand the mechanisms of neuroplasticity in aging and AD.

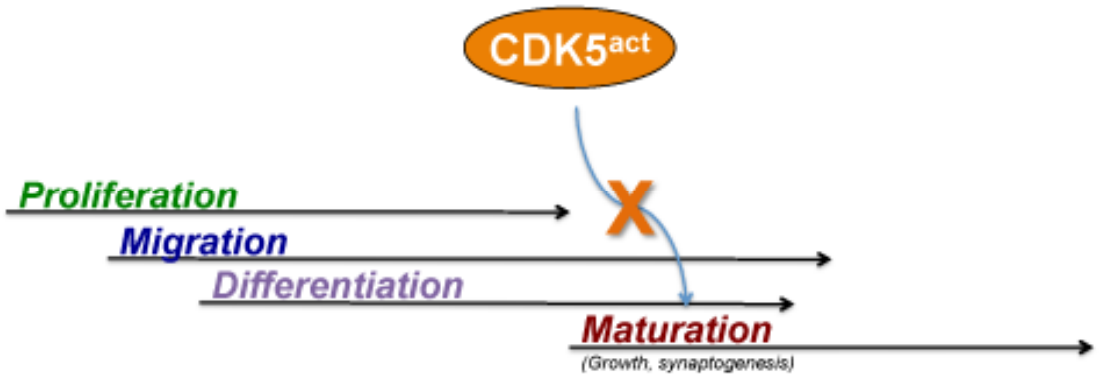

Figure 3.1 *Schematic diagram showing proposed role of pathological CDK5 in the maturation phase of neurogenesis in adult hippocampal NPCs.*

In this context, in the present study we showed in an *in vitro* model system of neuronal differentiation that CDK5 is critical for neuronal differentiation, and hyperactivation of this pathway via adenoviral expression of p35 combined with Aβ treatment resulted in the generation of glia-like cells that fail to complete neuronal differentiation. These results were supported by *in vivo* studies in a transgenic (tg) mouse model of AD that overexpresses the amyloid precursor protein (APP), where cells similar to the hybrid glial cells detected *in vitro* were also observed in the dentate gyrus of the hippocampus. Taken together, these studies suggest that while CDK5 is a critical factor for proper neuronal differentiation, hyperactivation of this kinase interferes with the tightly-regulated process of neuronal maturation.

MATERIALS AND METHODS

Pharmacological treatments and siRNA knockdown. For inhibition of the CDK5 signaling pathway, cells were treated at day 2 of differentiation with either the pharmacological CDK5 inhibitor Roscovitine (1-10μM, Calbiochem, San Diego, CA)

or transfected with siRNA against CDK5 or control non-targeting fluorescent-tagged siRNA (37.5-150 ng, Qiagen, Valencia, CA) using the HiPerfect transfection reagent (Qiagen) according to the manufacturer's protocol.

Viral infection and Aβ treatment. For activation of the CDK5/p35 pathway, cells were infected on day 2 of differentiation with adenovirus expressing human p35 or GFP control (Vector Biolabs, Philadelphia, PA) at a multiplicity of infection (MOI) of 30. Cells were then treated on day 3 with freshly dissolved $A\beta_{1-42}$ (1-5μM, American Peptide, Sunnyvale, CA) or reverse $A\beta_{42-1}$ peptide (American Peptide) as a control.

Animal models, treatments, and tissue processing. To study the effects of genetic CDK5 inhibition *in vivo*, CDK5 heterozygous deficient mice were used ($CDK5^{+/-}$) (Ohshima et al., 1996). Full ablation of both copies of CDK5 ($CDK5^{-/-}$) in mice is embryonic lethal, so in order to study CDK5 knockdown in the adult mouse brain, the $CDK5^{+/-}$ animals were used as a model of reduced CDK5 activity. $CDK5^{+/-}$ mice were kindly provided by the laboratory of Dr. Joseph Gleeson (UCSD). The tg mice utilized in this study express mutated human (h)APP751 under the control of the mThy-1 promoter (mThy1-hAPP751) (Rockenstein et al., 2001).

For pharmacological treatments, nontg and APP tg animals (N=6 per group) received intra-cerebral infusions of Roscovitine (Calbiochem) at a concentration of 20 mg/kg into the lateral ventricle. For this purpose, mice were anesthetized and under sterile conditions a 26 gauge stainless steel cannula was implanted stereotaxically into

the lateral ventricle using the bregma as a reference (Franklin and Paxinos, bregma 0.5mm; 1.1mm lateral; depth 3mm) and secured to the cranium using superglue. The cannula was connected via a 5 mm coil of V3 Biolab vinyl to a model 1007D osmotic minipump (Alzet, Cupertino, CA) surgically placed subcutaneously beneath the shoulder. The solutions were delivered at a flow rate of 0.5μl per hour for 2 weeks. The pump was left for an additional 2 weeks and mice were euthanized one month after the initiation of the infusions.

For studies of neurogenesis, 6-month old nontg, $CDK5^{+/-}$, APP tg, or $CDK5^{+/-}$ /APP tg crossed mice (N=8 per group) received 5 injections (one per day) with 5-bromo-2-deoxyuridine (BrdU, Sigma-Aldrich, St. Louis, MO) at 50 mg/kg or vehicle control (saline) (N=4 per group per treatment). After 1m, mice were sacrificed for analysis of neurogenesis. All experiments described were approved by the animal subjects committee at the University of California at San Diego (UCSD) and were performed according to NIH recommendations for animal use. In accordance with NIH guidelines for the humane treatment of animals, mice were anesthetized with chloral hydrate and flush-perfused transcardially with 0.9% saline. Brains were removed and divided sagitally. One hemibrain was post-fixed in phosphate-buffered 4% paraformaldehyde at 4°C for 48 hr and sectioned at 40 μm with a Vibratome 2000, while the other hemibrain was snap frozen and stored at -70°C for protein analysis.

Immunoblot analysis. For preparation of homogenates from mouse brains, briefly as previously described (Cole et al., 1988; Masliah et al., 2000), 0.1 g of frozen tissue was homogenized in 500 μL of a detergent-free HEPES-based lysis buffer (1.0 mM HEPES, 5.0 mM Benzamidine, 2.0 mM 2-Mercaptoethanol, 3.0 mM EDTA, 0.5

mM Magnesium Sulfate, 0.05% Sodium Azide; final pH 8.8) that facilitates separation of membrane and cytosolic fractions. Fresh protease and phosphatase inhibitor cocktails (Calbiochem, San Diego, CA) were added to all lysis buffers. Following a brief centrifugation step to clear nuclei and cell debris, total homogenates were then centrifuged for 1 hr at 100,000 rpm at 4°C. Supernatants were saved (cytosolic fraction) and the pellets (membrane fraction) were resuspended in 500 μL HEPES lysis buffer. For preparation of total cell lysates, adherent cells in culture were lysed in buffer composed of 10 mM Tris-HCl (pH 7.4), 150 mM NaCl, 5 mM EDTA (TNE) containing 1% Triton-X 100 to obtain total cell lysates.

For immunoblot analysis, cytosolic and membrane fractions from brain homogenates or total cell lysates were separated by gel electrophoresis on 4-12% Bis-Tris gels (Invitrogen, Carlsbad, CA) and blotted onto 0.45 μm PVDF membranes (Millipore, Temecula, CA). Immunoblots were probed with rabbit polyclonal antibodies against CDK5 (1:500, C-8, Santa Cruz Biotechnology, Santa Cruz, CA), p35/p25 (1:500, C-19, Santa Cruz Biotechnology), or mouse monocloncal antibodies against the immature neuronal marker β-III Tubulin (1:10,000, Tuj1 clone, Covance, Princeton, NJ), the NPC marker nestin (1:1000, Millipore), the NPC/radial glia marker S100-β (1:1000, Sigma-Aldrich, St. Louis, MO), or actin (Millipore) as a loading control as previously described (Rockenstein et al., 2001). Blots were developed with enhanced chemiluminescence (Perkin-Elmer), and images were obtained and semi-quantitative analysis was performed with the VersaDoc gel imaging system and Quantity One software (Bio-Rad).

Immunohistochemical analysis. For analysis of levels of components of the CDK5 signaling pathway and markers of neurogenesis in NPC-derived neural progeny, adherent cells on coverslips were fixed in 4% paraformalehyde in PBS, and then processed for immunofluorescence or immunocytochemical analysis with diaminobenzidine (DAB). For immunofluorescence, coverslips were blocked in 10% serum (Vector Laboratories, Burlingame, CA), and then immunolabeled with the rabbit polyclonal antibodies against CDK5 (1:1000, C-8, Santa Cruz Biotechnology), p35 (1:1000, C-19, Santa Cruz Biotechnology), or the mouse monoclonal antibodies against nestin (1:200, Millipore), or S100-β (1:250, Sigma-Aldrich) detected with the Tyramide Signal Amplification™-Direct (Red) system (NEN Life Sciences, Boston, MA). For double-immunolabeling analysis, some samples were co-labeled with mouse monoclonal antibodies against β-III Tubulin (1:250, Tuj1 clone, Covance) or the mature astrocyte marker glial fibrillary acidic protein (GFAP, 1:500, Millipore) detected with FITC-conjugated secondary antibodies (1:75, Vector Laboratories). For immunocytochemical analysis with DAB, coverslips were blocked and incubated in primary mouse monoclonal antibody against β-III-Tubulin (1:250, Tuj1 clone, Covance) and incubated with biotinylated secondary antibodies detected with DAB.

For analysis of levels of components of the CDK5 signaling pathway and markers of neurogenesis in the brains of nontg or APP tg mice, brain sections were processed for double-labeling immunofluorescence or immunocytochemical analysis with DAB. For immunofluorescence, sections were blocked in 10% serum (Vector Laboratories), and then immunolabeled with the rabbit polyclonal antibodies against CDK5 (1:1000, C-8, Santa Cruz Biotechnology), p35 (1:1000, C-19, Santa Cruz

Biotechnology), or the goat polyclonal antibodies against doublecortin (DCX, 1:100, Millipore), a marker of migrating neuroblasts, detected with the Tyramide Signal Amplification™-Direct (Red) system (NEN Life Sciences, Boston, MA). Sections were co-labeled with mouse monoclonal antibodies against the mature neuronal marker microtubule-associated protein-2 (MAP2, 1:250, Millipore) or human APP (8E5, 1:2000, courtesy of ELAN Pharmaceuticals, San Francisco, CA), or the rabbit polyclonal antibodies against CDK5 (1:500, C-8, Santa Cruz Biotechnology) detected with FITC-conjugated secondary antibodies (1:75, Vector Laboratories). For immunocytochemical analysis with DAB, sections were blocked and incubated in primary mouse monoclonal antibody NeuN (1:500, Millipore), rabbit polyclonal antibodies against CDK5 (1:500, C-8, Santa Cruz Biotechnology) or p35 (1:500, C-19, Santa Cruz Biotechnology), rat antibody against BrdU (1:100, rat monoclonal, AbD Serotec, Raleigh, NC), or goat polyclonal antibody against DCX (1:50, Santa Cruz Biotechnology) and incubated with biotinylated secondary antibodies detected with DAB. For sections immunostained for BrdU, pre-treatments were performed essentially as previously described (Winner et al., 2004).

DAB-immunostained sections were imaged with a digital Olympus microscope. Coverslips or sections were mounted under glass coverslips with VectaShield (Vector Biolabs) and imaged with a Zeiss 63X (N.A. 1.4) objective on an Axiovert 35 microscope (Zeiss, Germany) with an attached MRC1024 laser scanning confocal microscope system (BioRad) (Masliah et al., 2000). All sections were processed simultaneously under the same conditions and the experiments were performed twice to assess reproducibility.

For all immunolabeling studies, assessment of levels of immunoreactivity was performed utilizing the Image-Pro Plus program (Media Cybernetics, Silver Spring, MD). For each case or mouse a total of three sections (10 images per section) were analyzed in order to estimate the average number of immunolabeled cells per unit area (mm^2) or the average intensity of the immunoreactive signal (corrected pixel intensity).

Quantitative real-time PCR (qPCR) analysis. RNA was purified from cultured cells or the hippocampus from control and tg mice using the RNeasy mini kit (Qiagen, Valencia, CA). Total RNA was reverse transcribed using iScript cDNA Synthesis kit (Bio-Rad, Hercules, CA) with 1 μg of total RNA in accordance with the manufacturer's instructions. Quantitative PCR was performed with primers specific for CDK5 or GAPDH as a housekeeping gene control (primer assays, Qiagen) using the iCycler iQ Real-Time PCR Detection System (Bio-Rad). Reactions were performed in a volume of 25 μl using the iQ SYBR Green Supermix (Bio-Rad) according to the manufacturer's instructions.

Statistical analysis. All experiments were performed blind coded and in triplicate. Values in the figures are expressed as means ± SEM. To determine the statistical significance, values were compared by one-way ANOVA with post-hoc Dunnett's or Tukey-Kramer test when comparing APP tg mice to controls or among groups. The differences were considered to be significant if p values were less than 0.05.

RESULTS

Inhibition of CDK5 signaling interferes with NPC maturation

Since we found that CDK5 levels increased during neuronal differentiation, to investigate the role of this kinase in this process, we studied the effects of modulation of CDK5 on neuronal maturation in our NPC model system. Since basal levels of CDK5 were relatively high in these cells, we inhibited CDK5 by utilizing a pharmacological approach (Roscovitine) to inhibit CDK5 activity or an siRNA approach to knock down CDK5 expression (Figure 3.2).

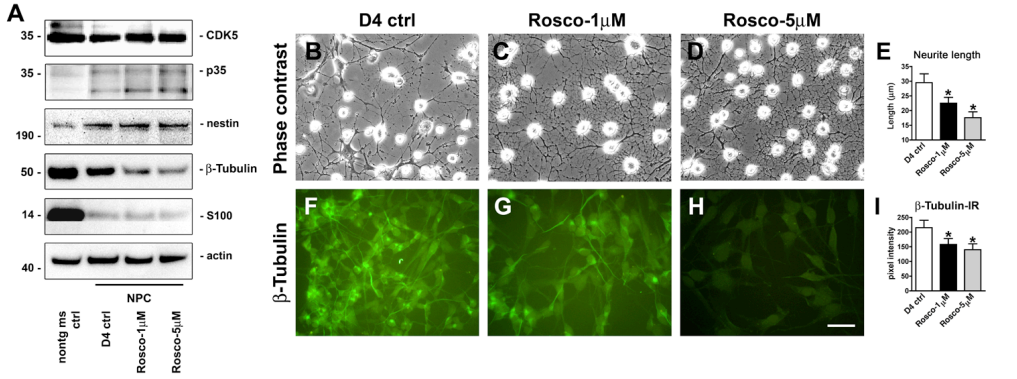

Figure 3.2 *Pharmacological inhibition of CDK5 impairs neuronal maturation in adult rat hippocampal NPCs.* Adult rat hippocampal NPCs were cultured under neuronal differentiation conditions, and treated with Roscovitine starting at day 2. Cells were imaged at day 4 (D4) and processed for immunoblot or immunocytochemical analyses. (A) Immunoblot analyses of levels of CDK5, p35, nestin, β-III-Tubulin, S100 and actin in D4 NPC-derived neural progeny treated with 1 μM or 5 μM Roscovitine for 48 hrs. Brain homogenate from a non-tg mouse is shown as a comparative positive control for various lineage markers. (B-E) Phase contrast live cell imaging and reduced neurite outgrowth in NPC-derived neural progeny treated with 1 μM or 5 μM Roscovitine for 48 hrs. * $p < 0.05$ compared to vehicle-treated controls by one-way ANOVA with post-hoc Dunnett's test. Scale bar = 10 μm.

These studies showed that pharmacological inhibition of CDK5 with exposure to Roscovitine for four days resulted in decreased expression of neuronal markers such as β-III Tubulin (Figure 3.2). As expected, no changes were observed in the levels of CDK5 protein expression in cells treated with Roscovitine (Figure 3.2A). Live cell

imaging demonstrated that compared to vehicle-treated controls, inhibition of endogenous CDK5 activity with Roscovitine altered the morphological appearance of NPC-derived neural progeny after four days of differentiation (Figure 3.2B-D), and Roscovitine-treated NPC-derived neural progeny displayed shorter (Figure 3.2E), abundant neurites reminiscent of untreated cells at the second day of differentiation (Figure 2.4D).

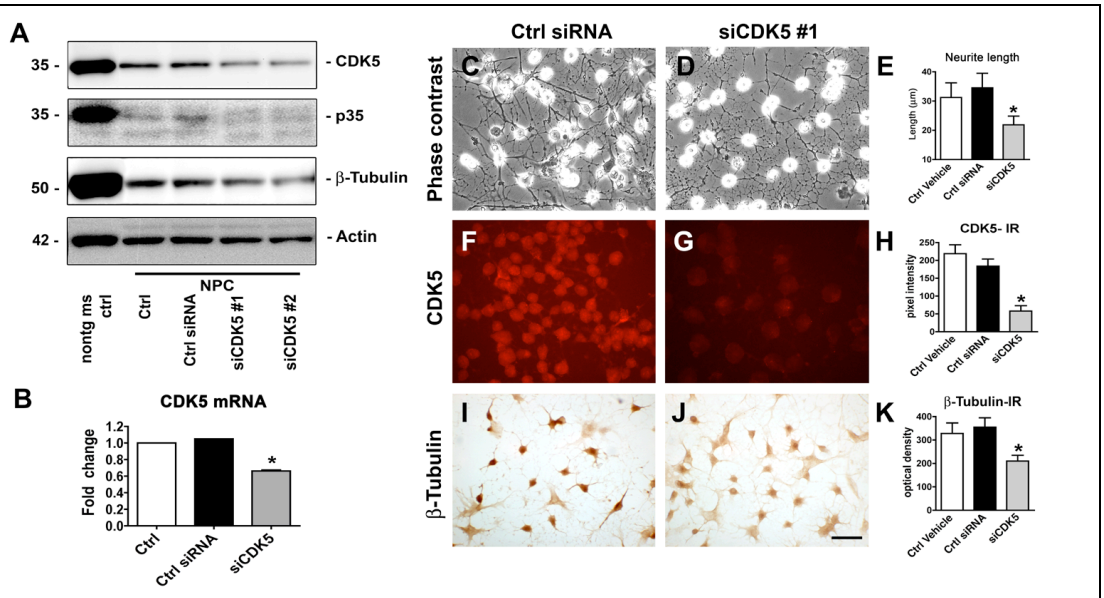

Figure 3.3 *siRNA knockdown of CDK5 expression impairs neuronal maturation in adult rat hippocampal NPCs.* Adult rat hippocampal NPCs were cultured under neuronal differentiation conditions, and transfected with 5 nM siRNA against CDK5 (siCDK5) or a control (Ctrl) non-targeting fluorescent-tagged siRNA at day 2. Cells were imaged at day 4 (D4) and processed for immunoblot, qRT-PCR or immunocytochemical analyses. (A) Immunoblot analysis of levels of CDK5, p35, β-III-Tubulin and actin in NPC-derived neural progeny treated with siCDK5. Brain homogenate from a non-tg mouse is shown as a comparative positive control. (B) qRT-PCR of levels of CDK5 mRNA in NPC-derived neural progeny treated with siCDK5. (C-E) Phase contrast live cell imaging and reduced neurite outgrowth in NPC-derived neural progeny treated with siCDK5. (F-H) Reduced CDK5 immunoreactivity in NPC-derived neural progeny treated with siCDK5. (I-K) Reduced β-III-Tubulin immunoreactivity in NPC-derived neural progeny treated with siCDK5. * $p < 0.05$ compared to non-targeting siRNA-treated controls by one-way ANOVA with post-hoc Dunnett's test. Scale bar = 20 μm.

Similarly, treatment of differentiating NPCs with siRNAs specific for CDK5 resulted in reduced expression levels of neuronal markers (β-III Tubulin, Figure 3.3)

after four days in culture compared to cells transfected with a non-targeting siRNA. Immunoblot (Figure 3.3A) and qPCR (Figure 3.3B) analyses of CDK5 expression demonstrated that CDK5 mRNA and protein levels were reduced by more than 50%.

As with pharmacological inhibition of CDK5 with Roscovitine, siRNA knockdown of CDK5 during differentiation generated progeny characterized by reduced neurite density (Figure 3.3C-E) and reduced β-III Tubulin expression (Figure 3.3A, I-K). Immunocytochemical analysis (Figure 3.3F-H) analysis confirmed that CDK5 levels were significantly reduced by siRNA treatment. The concomitant reduction in expression of neuronal markers when CDK5 expression was knocked down suggests that endogenous CDK5 is a critical factor for neuronal differentiation. Taken together, these studies suggest that modulation of the CDK5 signaling pathway has a significant impact on neuronal differentiation in the adult brain.

CDK5 deficiency in a mouse model impairs adult neurogenesis

To examine the effects of CDK5 inhibition on adult neurogenesis in an animal model, we investigated the status of neurogenesis in CDK5 heterozygous-deficient ($CDK5^{+/-}$) mice. For this purpose, $CDK5^{+/-}$ mice were treated with BrdU to label dividing cells, and brain sections from these animals were then analyzed by immunoblot and immunocytochemistry for markers of neurogenesis and neuronal differentiation. Immunocytochemical analysis confirmed that levels of CDK5 expression in total brain homogenates from $CDK5^{+/-}$ mice were approximately 50% lower than levels in the brains of age-matched control mice possessing two copies of the CDK5 gene ($CDK5^{+/+}$) (Figure 3.4A-D).

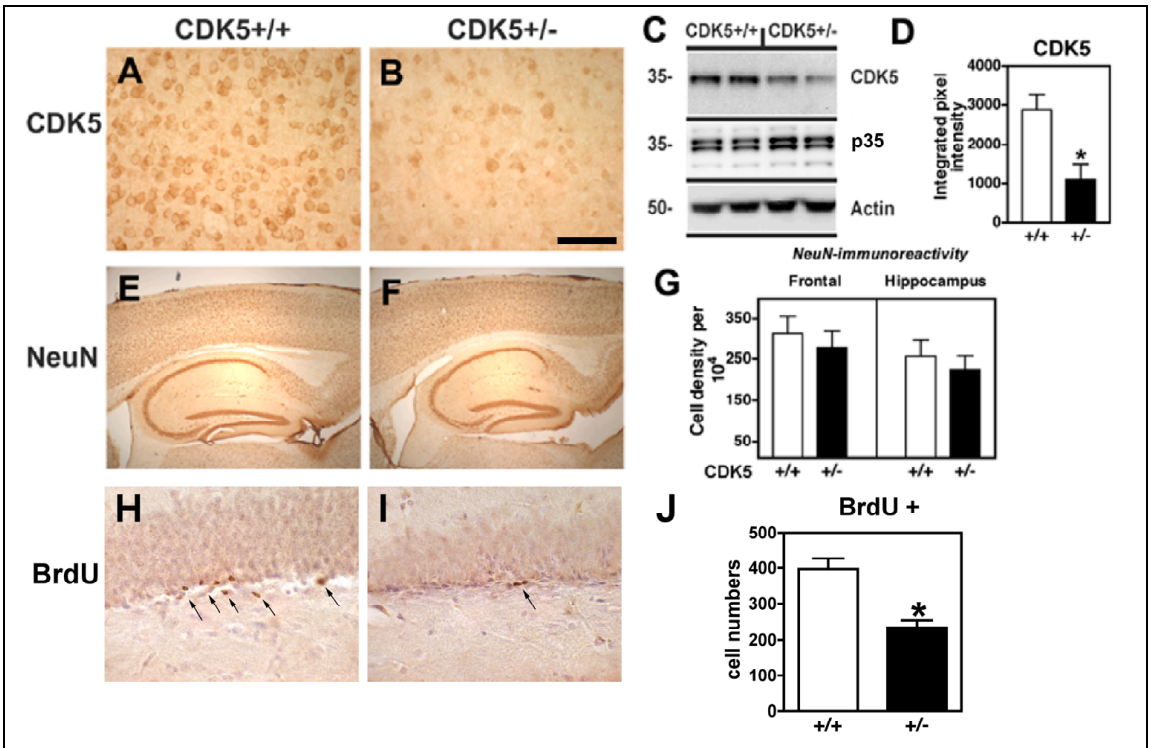

Figure 3.4 In vivo *CDK5 heterozygous deficiency impairs adult neurogenesis.* Brain sections from 6-month old CDK5+/- mice and wild-type controls treated with BrdU were processed for immunohistochemistry and immunoblot analysis. (A-B) Immunohistochemical analysis of CDK5 immunoreactivity in the frontal cortex of CDK+/- mice and wild-type controls. (C, D) Immunoblot analysis of levels of CDK5, p35 and actin immunoreactivity in brain homogenates from CDK5+/- mice and wild-type controls. (E-G) Immunohistochemical analysis of NeuN immunoreactivity in the brains of CDK5+/- mice and wild-type controls. (H-J) Reduced numbers of BrdU-positive cells (arrows, H, I) in the SGZ of the hippocampus in CDK5+/- mice compared to wild-type controls. * $p < 0.05$ compared to wild-type controls by one-way ANOVA with post-hoc Dunnett's test (N=4 animals per group). Scale bar = 50 μm (panels A, B); 3 mm (panels E, F), 100 μm (panels H, I).

To determine whether CDK5 deficiency might impair adult neurogenesis in these animals and potentially result in reduced neuronal numbers in the adult brain, immunocytochemical analysis was performed with an antibody against the neuronal marker NeuN. This showed a trend towards reduced neuronal numbers in the frontal cortex and the neurogenic hippocampus, as demonstrated by NeuN immunoreactivity (Figure 3.4E-G), however the differences were not significant at the age analyzed.

Interestingly, several studies have recently shown that CDK5 ablation results in impaired adult hippocampal neurogenesis (Jessberger et al., 2008; Lagace et al., 2008). This suggests that CDK5 plays a critical role in adult neurogenesis, but it is unclear whether there may also be alterations in neurogenesis in animals expressing reduced levels of CDK5. To determine whether $CDK5^{+/-}$ mice display impaired hippocampal neurogenesis, animals treated with BrdU were analyzed by immunocytochemistry. This showed that there was a significant decrease in the numbers of BrdU-positive cells in the hippocampal DG of $CDK5^{+/-}$ mice compared to $CDK5^{+/+}$ controls (Figure 3.4H-J). Taken together, these results suggest that CDK5 deficiency impairs adult neurogenesis and that sufficient levels of expression of this kinase are required for neurogenesis to proceed in the adult brain.

Abnormal activation of CDK5 signaling re-directs differentiation and promotes the generation of glia-like progeny in vitro

In addition to the deleterious effects of CDK5 deficiency, previous studies have shown that hyper-activation of CDK5 is also harmful and has been associated with neurodegerative processes. To characterize the effects of activating CDK5 via p35 overexpression and Aβ treatment on neuronal differentiation, double-labeling immunocytochemical analysis was performed. Immunolabeling with a p35-specific antibody confirmed that p35 was expressed at high levels in >95% of the cells after four days of culture under differentiating conditions (Figure 3.5). In cultures that received combined infection with adv-p35 and treatment with Aβ, there were

increased numbers of NPC-derived neural progeny that expressed markers of neuronal and glial lineages as well as progenitor cell markers (Figure 3.5).

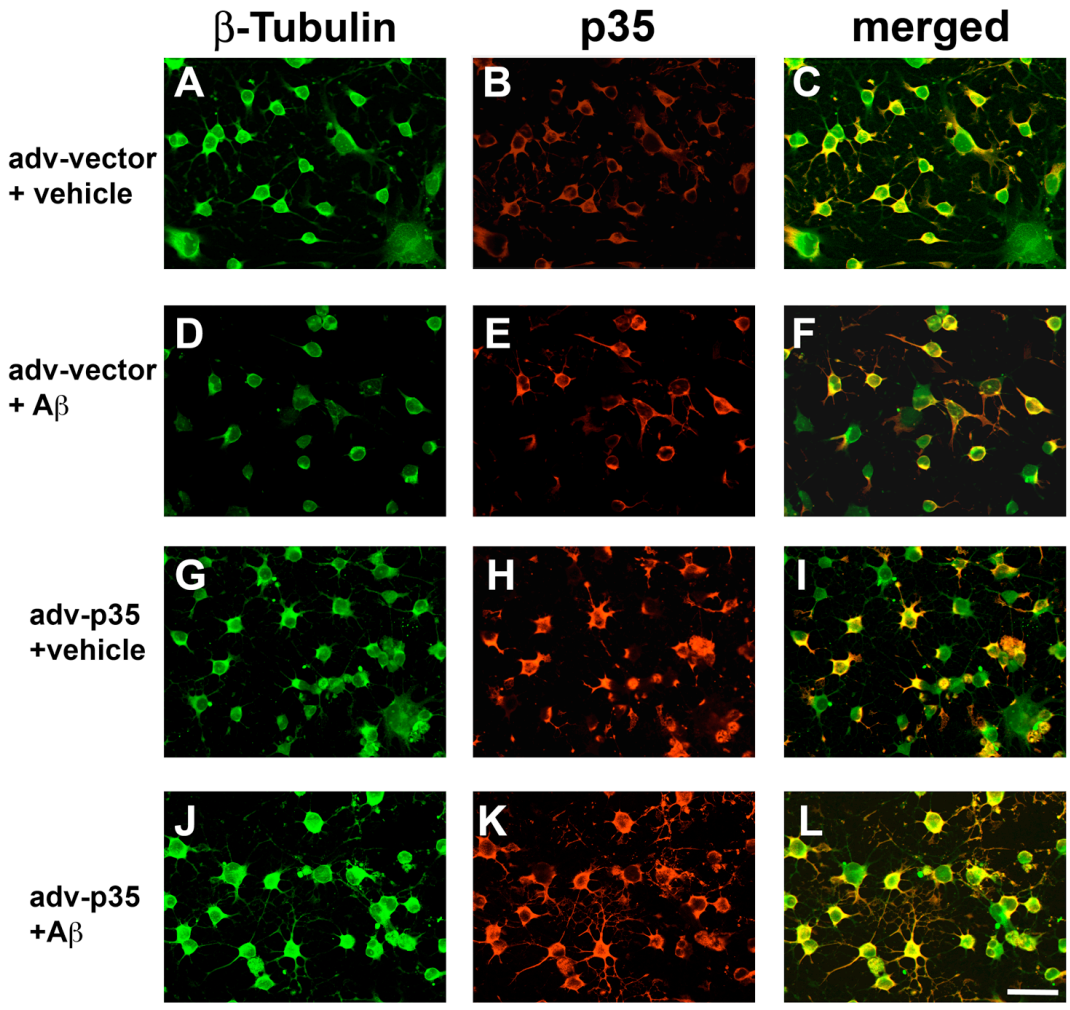

Figure 3.5 *Morphological alterations in NPC-derived neural progeny expressing p35 and treated with Aβ.* Differentiating NPCs were infected with an adenoviral (adv) vector expressing p35 or vector control on day 2 of differentiation, then treated with 1 μM Aβ or vehicle control on day 3 for 24 hrs, and processed for double-immunolabeling with antibodies against β-III-Tubulin and p35. (A-F) Double-labeling analysis of β-III-Tubulin and p35 in vector-infected NPC-derived neural progeny treated with vehicle control (A-C) or Aβ (D-F) for 24 hrs. (G-L) Double-labeling analysis of β-III-Tubulin and p35 in p35-expressing NPC-derived neural progeny treated with vehicle control (A-C) or Aβ (D-F) for 24 hrs. Scale bar = 20 μm.

After four days in culture under differentiating conditions, cells in adv-p35/Aβ cultures were immunoreactive for the neuronal marker β-III Tubulin, the astroglial

markers S100 and GFAP, and the progenitor cell marker nestin (Figure 3.6). Moreover, these hybrid cells had an aberrant morphology characterized by large cell bodies surrounded by a reticular pattern of small processes. The presence of both undifferentiated and differentiated markers suggests that conditions that constitutively activate CDK5 signaling might promote the generation of cells that are unable to fully complete differentiation.

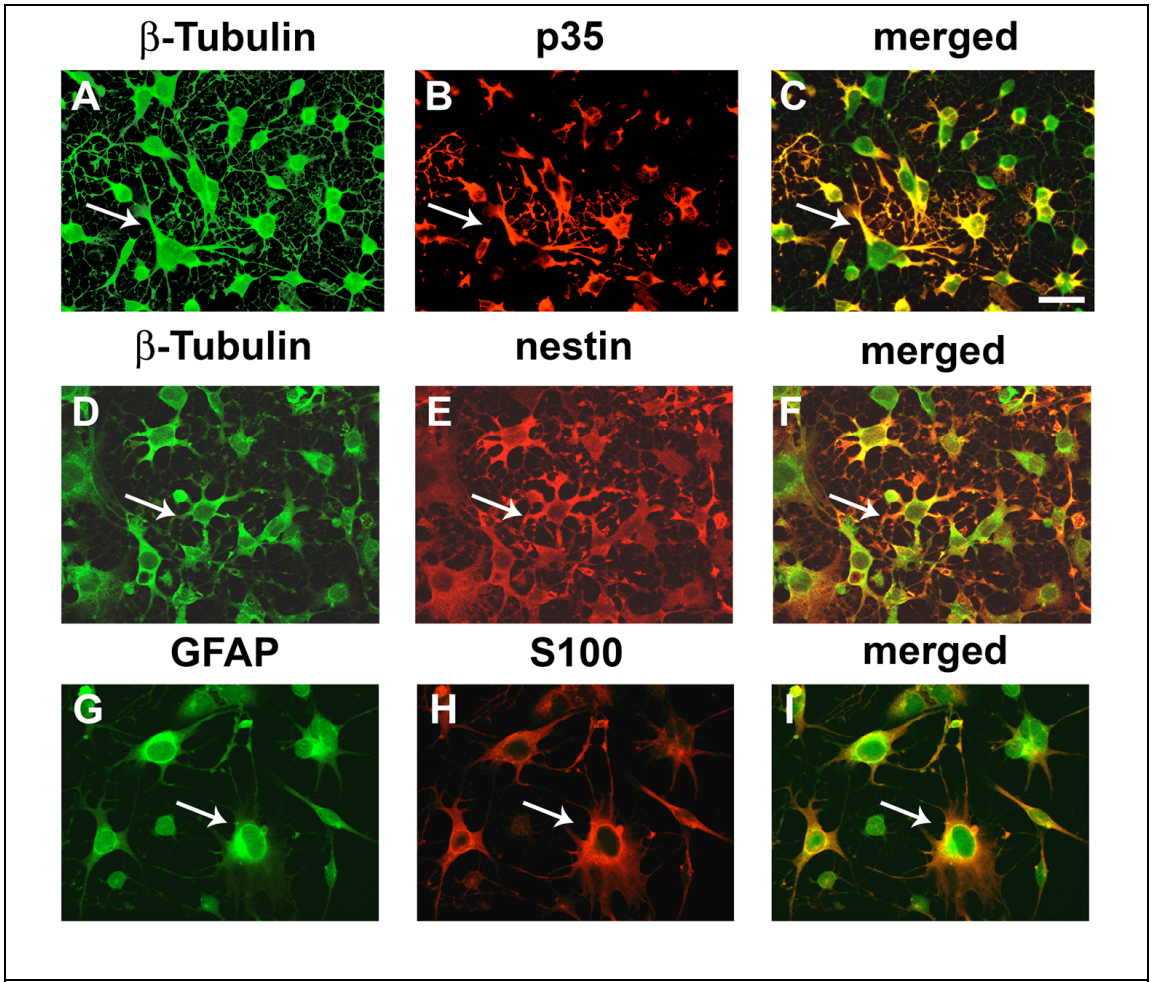

Figure 3.6 *Co-expression of progenitor cell and neuronal/glial markers in NPC-derived neural progeny expressing p35 and treated with Aβ.* Differentiating NPCs were infected with an adenoviral (adv) vector expressing p35 on day 2 of differentiation, then treated with 1 μM Aβ on day 3 for 24 hrs, and processed for double-immunolabeling with antibodies against β-III-Tubulin and p35 (A-C), β-III-Tubulin and nestin (D-F) or GFAP and S100 (G-I). Numerous cells double-positive for markers of multiple progenitor and lineage markers (arrows) were detected. Scale bar = 10 μm.

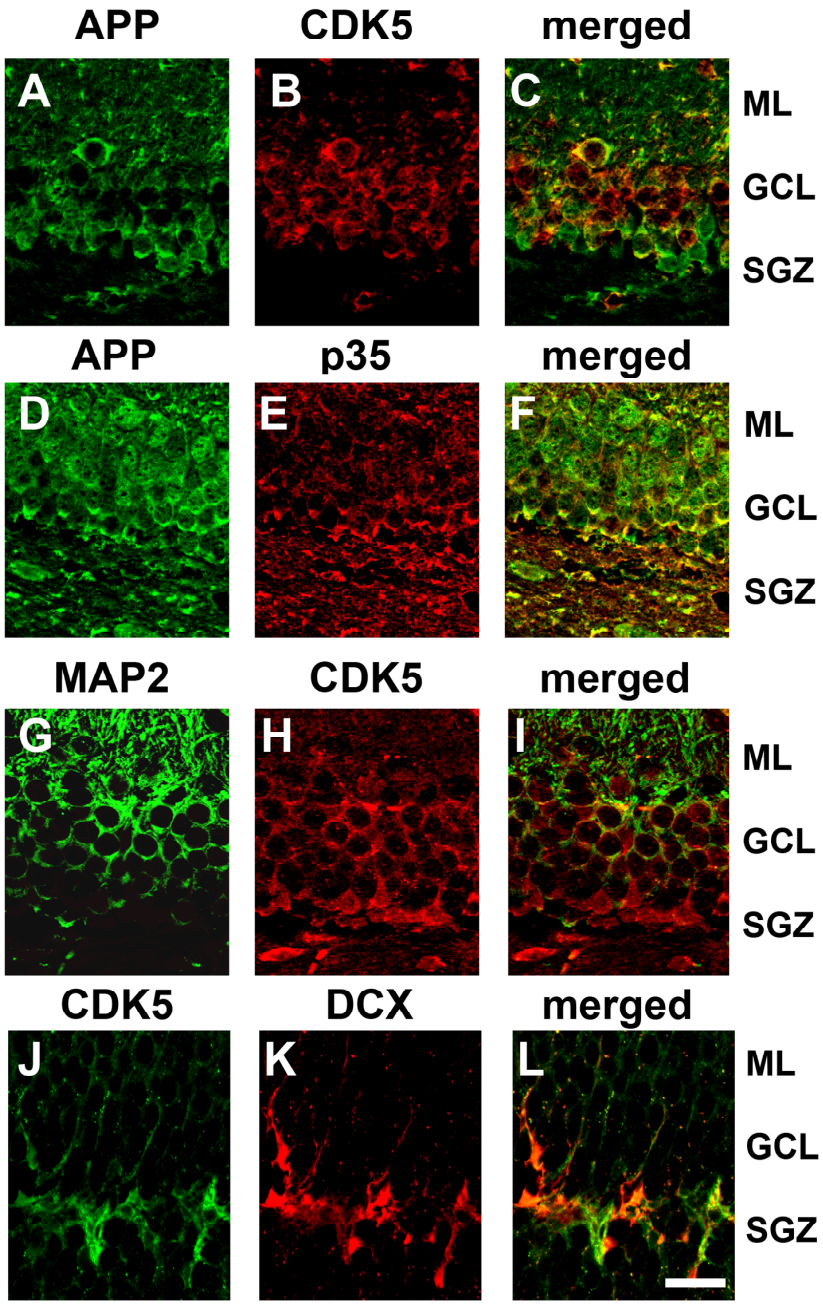

Figure 3.7 *Components of the CDK5 signaling pathway are expressed in the neurogenic niche of the adult hippocampus in APP tg mice.* Brain sections from APP tg mice were double-labeled with antibodies against APP and CDK5 or p35, and CDK5 and the mature neuron marker microtubule-associated protein-2 (MAP2) or the immature neuron marker doublecortin (DCX). All images are from the dentate gyrus (DG) of the hippocampus. (A-C) Double-labeling analysis of APP and CDK5 showing co-expression in cells of the DG, particularly in the granular cell layer (GCL). (D-F) Double-labeling analysis of APP and p35 showing co-expression of these markers throughout the neuropil of the DG. (G-I) Double-labeling analysis of MAP2 and CDK5 showing CDK5 expression localized primarily to the granular cell layer and subgranular zone (SGZ), while MAP2 was detected more predominantly in the molecular layer (ML). (J-L) Double-labeling analysis of CDK5 and DCX showing co-expression localized to cells in the SGZ. Scale bar = 20 μm.

Alterations in neurogenesis in APP tg mice and rescue with pharmacological or genetic CDK5 inhibition

To further elucidate the role of CDK5 and p35/p25 and Aβ interactions *in vivo*, we first characterized the CDK5 signaling pathway in the dentate gyrus of APP tg mice. For this purpose, we used animals that express mutated human (h)APP751 under the control of the mThy-1 promoter and, for this study, the highest expresser (line 41) tg mice were used (Rockenstein et al., 2001). These tg mice produce high levels of $A\beta_{1\text{-}42}$, and amyloid plaques are found in the brain at an early age (beginning at 3 months) (Rockenstein et al., 2001). We have previously shown that neurogenesis is impaired in the brains of these animals, as demonstrated by reduced numbers of dividing cells (BrdU), which was accompanied by a significant increase in apoptosis, as detected by TUNEL staining (Rockenstein et al., 2006).

To examine the expression levels and localization of CDK5 signaling molecules and neurogenic markers in the DG of the hippocampus, double-labeling studies were performed in sections from the brains of APP tg mice. In support of a role for CDK5 in the adult murine hippocampal, these analyses demonstrated that APP, CDK5 and p35 (Figure 3.7) are expressed in this neurogenic region of the dentate gyrus, and that CDK5 localizes to cells immunopositive for the NPC marker DCX (Figure 3.7).

To investigate whether there are any alterations in CDK5 signaling in this region of the brain in APP tg mice, additional immunohistochemical studies were performed. This showed that compared to non-tg animals, CDK5 (Figure 3.8A, B, D)

and p35 (Figure 3.8E, F, H) immunoreactivity was increased in the hippocampal subgranular zone (SGZ) of APP tg mice.

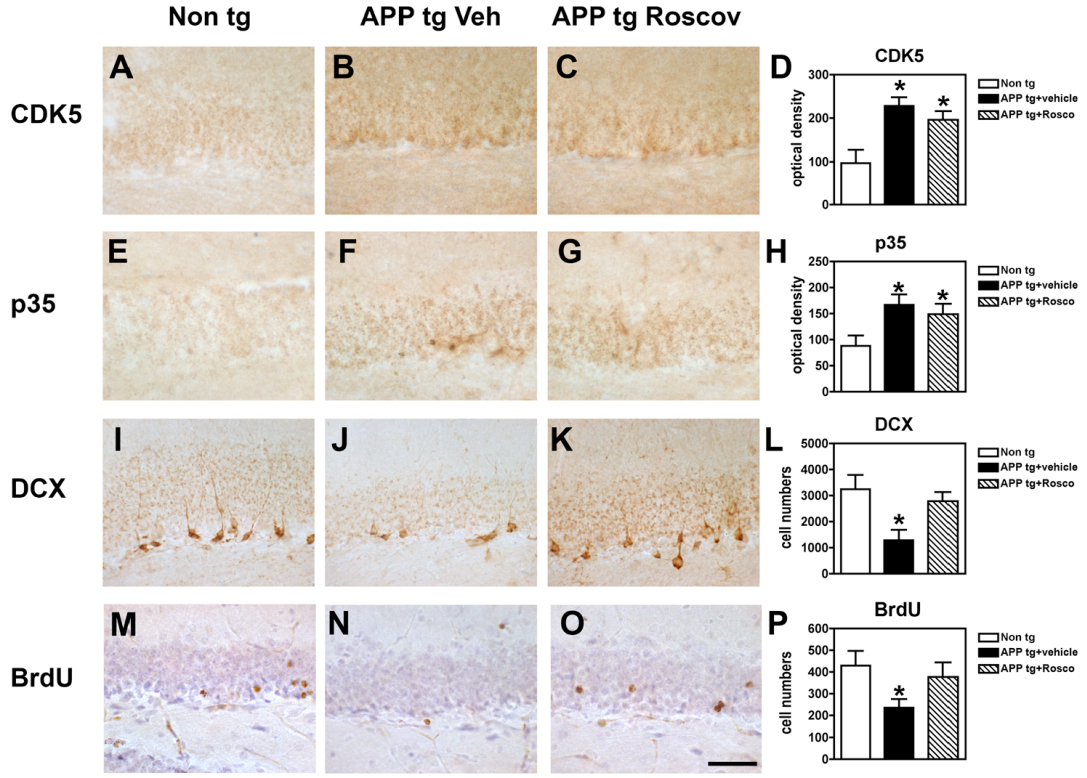

Figure 3.8 *Roscovitine treatment rescues neurogenic deficits in the hippocampus of APP tg mice.* Brain sections from 6-month old APP tg mice and non-tg controls treated with Roscovitine or vehicle control and BrdU were processed for immunohistochemical analysis with antibodies against CDK5, p35, doublecortin (DCX) or BrdU. All images are from the dentate gyrus of the hippocampus. (A-D) Immunohistochemical analysis of CDK5 immunoreactivity in non-tg and APP tg mice treated with vehicle control or Roscovitine. (E-H) Immunohistochemical analysis of p35 immunoreactivity in non-tg and APP tg mice treated with vehicle control or Roscovitine. (I-L) Immunohistochemical analysis of DCX immunoreactivity in non-tg and APP tg mice treated with vehicle control or Roscovitine. (M-P) Immunohistochemical analysis of BrdU immunoreactivity in non-tg and APP tg mice treated with vehicle control or Roscovitine. * $p < 0.05$ compared to vehicle-treated controls by one-way ANOVA with post-hoc Dunnett's test (N=6 animals per group). Scale bar = 100 μm.

These alterations were accompanied by a reduction in numbers of DCX-positive (Figure 3.8I, J, L) and BrdU-positive cells (Figure 3.8M, N, P) in the APP tg mice compared to nontg controls, suggesting that abnormal CDK5 activity in the neurogenic DG might be involved in regulating the proliferation and migration of

neurogenic cells and newborn neurons. Remarkably, inhibition of CDK5 activity by treatment with Roscovitine rescued the neurogenic alterations in APP tg mice (Figure 3.8K, L, O, P). These effects were most likely related to a reduction in kinase activity, as levels of CDK5 and p35 were only modestly reduced (Figure 3.8D, H).

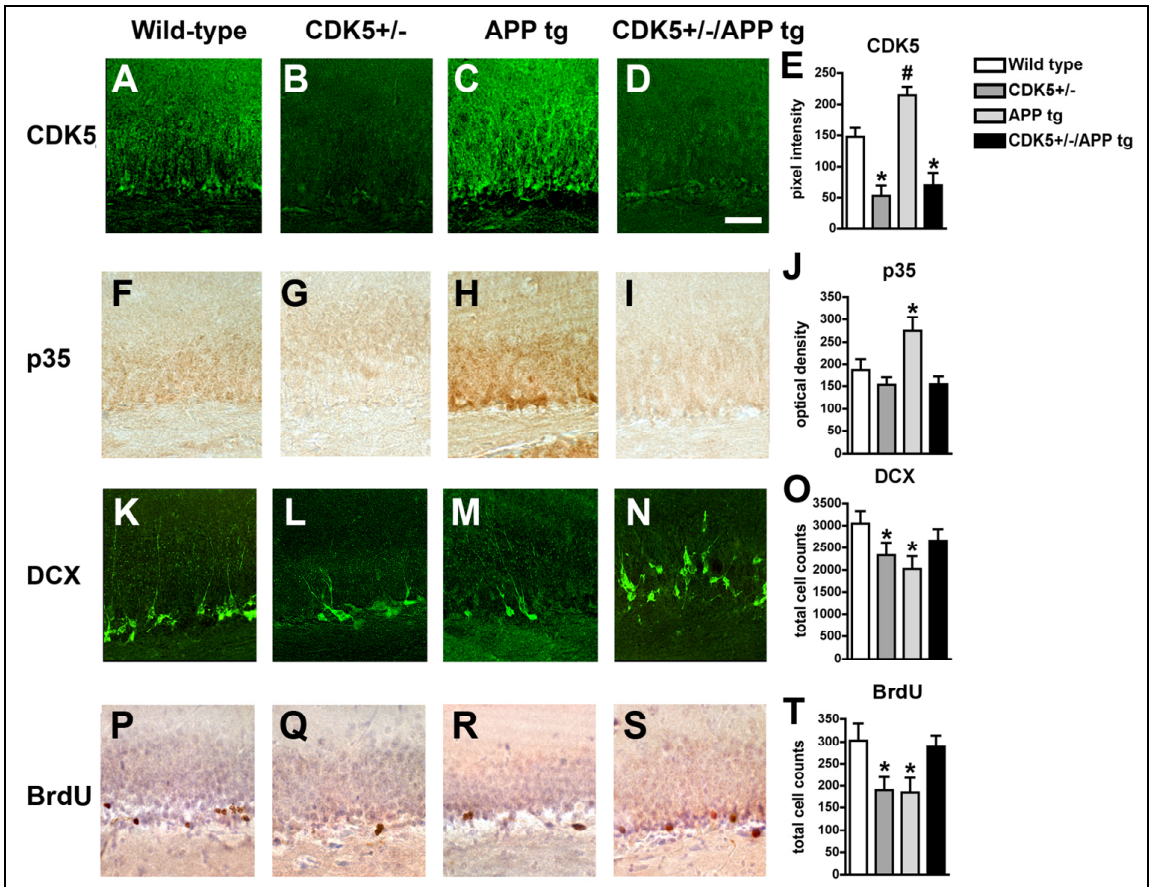

Figure 3.9 In vivo *reduction of CDK5 levels rescues neurogenic deficits in the hippocampus of APP tg mice.* Brain sections from 6-month old wild-type controls, CDK5 heterozygous deficient ($CDK5^{+/-}$), or APP tg mice, or crosses treated with BrdU. Brain sections were processed for immunohistochemical analysis with antibodies against CDK5, p35, doublecortin (DCX) or BrdU. For panels A-D, K-N and P-S, images are from the dentate gyrus of the hippocampus. For panels F-I, images are from the pyramidal cell layer of the hippocampus. (A-E) Immunohistochemical analysis of levels of CDK5 immunoreactivity in wild-type, $CDK5^{+/-}$, APP tg mice or $CDK5^{+/-}$/APP crosses. (F-J) Immunohistochemical analysis of levels of p35 immunoreactivity in wild-type, $CDK5^{+/-}$, APP tg mice or $CDK5^{+/-}$/APP crosses. (K-O) Immunohistochemical analysis of DCX-immunoreactive cells in wild-type, $CDK5^{+/-}$, APP tg mice or $CDK5^{+/-}$/APP crosses. (P-T) Immunohistochemical analysis of BrdU-immunoreactive cells in wild-type, $CDK5^{+/-}$, APP tg mice or $CDK5^{+/-}$/APP crosses. * $p < 0.05$ compared to wild-type controls by one-way ANOVA with post-hoc Dunnett's test. # $p < 0.05$ compared to APP tg mice by one-way ANOVA with post-hoc Dunnett's test. N=4 animals per group. Scale bar = 50 μm (panels A-D, K-N, P-S), 15 μm (panels F-I).

A similar rescue effect was observed when APP tg mice were crossed with CDK5 heterozygous deficient ($CDK5^{+/-}$) animals to genetically reduce CDK5 levels (Figure 3.9). Consistent with the results presented in Figure 3.4, we observed that reduction of baseline CDK5 levels (Figure 3.9A, B, E) resulted in decreased numbers of DCX- and BrdU-positive cells in the dentate gyrus of the hippocampus (Figure 3.9K, L, O, P, Q, T). However, in $CDK5^{+/-}$/APP tg crosses there was a recovery of markers of neurogenesis compared to APP tg mice (Figure 3.9). These results are consistent with the possibility that when CDK5 levels or activity are de-regulated to lower or higher than physiological levels, neurogenesis is impaired. Taken together, these data support a potential role for CDK5 in regulating neurogenesis and neuronal differentiation in the pathogenesis of AD.

DISCUSSION

In the present study we showed that in an *in vitro* model system of neurogenesis in AD, CDK5 activity was necessary for neuronal maturation, however stimulation of the CDK5/p35 signaling pathway resulted in alterations in the fate of NPC-derived neural progeny. This supports a role for CDK5 in neuronal differentiation and suggests the necessity of physiological expression levels and activity of CDK5 in order for proper neuronal maturation to proceed. Previous studies have implicated CDK5 in several processes related to embryonic neuronal development, migration, and synapse formation. Early studies of CDK5 in the central nervous system showed that CDK5 and p35 are present in the growth cones of developing neurons (Pigino et al., 1997), and expression of dominant-negative CDK5

inhibited neurite outgrowth, suggesting that CDK5/p35 is essential for neurite outgrowth during neuronal differentiation (Nikolic et al., 1996). Furthermore, and supporting a role for CDK5 not only in neurogenesis but in the migration of developing neurons, another previous study using *in vitro* and *in vivo* conditional knock-out experiments showed that CDK5 deletion impaired the speed, directionality and other factors involved in neuroblast migration in the postnatal subventricular zone (Hirota et al., 2007). In addition to the neurogenesis-related functions of CDK5 during development, previous studies have shown that expression of dominant-negative CDK5 results in a significant reduction of synaptic activity in a neuroblastoma-glioma cell line (Johansson et al., 2005).

Although the role of CDK5 has been investigated in detail in developmental neurogenesis, less is known about this signaling pathway in adult neurogenesis in the context of neurodegenerative disease. Previous studies have shown in detail the mechanism through which hyperactivation of CDK5 plays a causal role in the pathogenesis of AD. In this process, Aβ triggers calcium influx into neurons, which activates calpain activity and subsequent cleavage of p35 to p25, which is a more stable activator of CDK5 that promotes the hyperphosphorylation of downstream substrates of CDK5 (Lee et al., 2000). This shows a clear role for CDK5 in Aβ-mediated neurotoxicity of mature neurons, and while a previous study demonstrates similar toxic effects in an NPC line exposed to high concentrations of Aβ, lower sub-toxic concentrations interfere with the ability of NPCs to differentiate into mature neurons via a mechanism that involves calpain activation and p25 generation (Haughey et al., 2002b).

It is important to note that while CDK5 pathological activation associated with AD is detrimental, too little CDK5 activity has a significant negative impact as well (Figure 3.10). A previous work has aptly labeled CDK5 as a "Jekyll and Hyde kinase" (Cruz and Tsai, 2004). This reflects both the pathological hyperphosphorylation of CDK5 substrates associated with neurodegeneration in the pathogenesis of AD (Cruz et al., 2006) as well as the necessity of its physiological function in neuronal migration (Ohshima et al., 1996) and in synaptic functions (Dhavan and Tsai, 2001; Matsubara et al., 1996) (Figure 3.10).

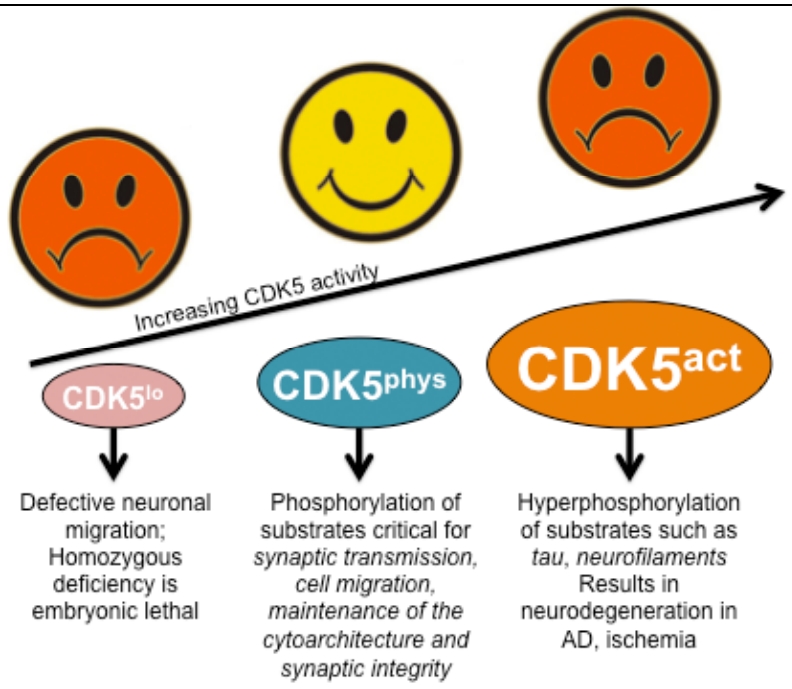

Figure 3.10 *Schematic model of the two "faces" of CDK5 activity.* Reduced CDK5 activity (CDK5 low, or $CDK5^{lo}$) impairs critical neuronal functions, while over-active CDK5 ($CDK5^{act}$) results in hyperphosphorylation of substrates contributing to neurodegeneration and defective neurogenesis in AD.

In support of this notion, the present study shows that inhibition of CDK5 arrests neuronal differentiation in an *in vitro* model of neuronal differentiation and in a

mouse model of reduced CDK5 activity. Pharmacological and siRNA knockdown approaches showed that reduced levels of CDK5 resulted in lower levels of neuronal markers such as β-III tubulin. Moreover, NPCs were arrested in their differentiation phenotype and continued to display numerous short processes even after 4 days of differentiation. This could be related to the involvement of CDK5 in the multipolar-to-bipolar transition of developing neurons (Ohshima et al., 2007), however it remains unclear what the downstream regulators of this feature of neuronal differentiation may be.

Previous studies (Ohshima et al., 1996; Tanaka et al., 2001) and the results of the present study show that inhibition of CDK5 activity is by itself deleterious to neuronal survival and differentiation. Moreover, two recent studies have demonstrated that CDK5 is critical for adult neuronal differentiation (Jessberger et al., 2008; Lagace et al., 2008), however the role of this kinase in mediating neurogenic alterations in AD is unclear. In this context, we focused on the activation of this pathway to further probe the role of CDK5 in neuronal differentiation. Interestingly, a previous study showed that Aβ leads to reduced neuronal differentiation via CDK5 activation (Haughey et al., 2002b), and here we show that enhanced activation of the CDK5 pathway via combined p35 expression and Aβ treatment results in the generation of morphologically distinct progeny.

Both *in vitro* and *in vivo* results show that p35 overexpression combined with Aβ treatment promotes the generation of NPC-derived glia-like progeny, suggesting that aberrant activation of this pathway may redirect neuronal maturation. This is consistent with a recent study demonstrating that although neuroproliferation may be

increased in the brains of AD patients, these progenitor cells fail to differentiate into mature MAP2 positive neurons (Li et al., 2008a). The present study supports this finding, and furthermore suggests a role for hyperactivation of CDK5 in preventing the appropriate maturation of NPCs in AD (Figure 3.11).

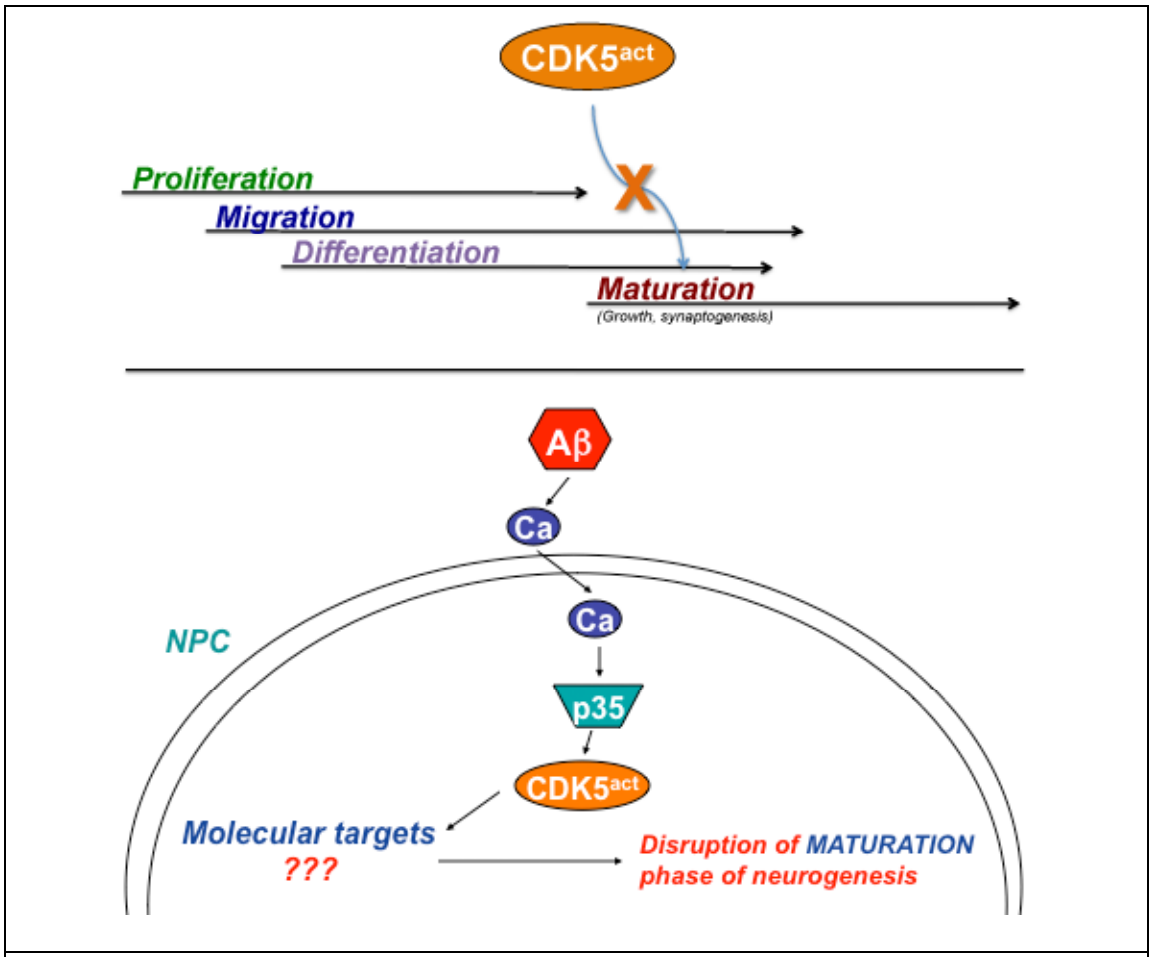

Figure 3.11 *Schematic model of potential role of Aβ and CDK5 in defective maturation during adult neurogenesis in AD.*

Further studies will be necessary to delineate the precise mechanisms through which CDK5 hyperactivation interferes with the maturation of NPCs in AD and promotes the generation of arrested glia-like progeny, however one possibility is that this effect may be related to the roles of CDK5 in neurofilament metabolism (Grant et

al., 2001) and p35 in modulating microtubule dynamics (Hou et al., 2007). In this context, several downstream targets of CDK5 play a role in cytoskeletal dynamics, so analysis of the phosphorylation states of these substrates might provide important information as to the molecular mechanisms involved in CDK5-mediated defective neuronal maturation in the hippocampus in AD. Taken together, the present study suggests a role for hyperactivation of CDK5 in the regulation of the maturation of immature neurons in the hippocampus. Therapeutic approaches targeting at normalizing, but not eradicating, CDK5 activity may prove useful to protect against excessive CDK5 activity in NPCs in AD and promote the completion of differentiation without the potential negative side effects of abolishing CDK5 function entirely.

ACKNOWLEDGEMENTS

Chapter 3, in full, is currently being prepared for submission for publication of the material. Crews L, Patrick C, Rockenstein EM, Adame A, Masliah E. The dissertation author was the primary investigator and author of this material.

This work was supported by NIH grants AG10435 and MH62962 and NIA Training Grant AG00216.

CHAPTER 4

CDK5-MEDIATED MODULATION OF CRMP2 IN THE MECHANISMS OF DEFECTIVE NEUROGENESIS IN ALZHEIMER'S DISEASE

ABSTRACT

Recent studies have suggested that the pathogenic process in Alzheimer's disease (AD) may damage not only mature neuronal circuitries, but may also target neuronal progenitor cells (NPCs) in the neurogenic niches of the adult brain. The CDK5 signaling pathway has been shown to be deregulated during neurodegeneration in AD, and because this kinase plays an important role in developmental neurogenesis-related processes, CDK5 may also play a role in regulating defective neurogenesis in AD. Most studies have focused on the role of tau hyperphosphorylation in mediating the neurodegenerative effects of CDK5, however given the large number of substrates of this kinase, other downstream targets may be involved in disrupting adult neurogenesis in AD. Here we identify and characterize collapsin-response mediator protein-2 as a critical regulator of this process in an *in vitro* model of CDK5 hyperactivation in neurogenesis in AD. To stimulate CDK5 activity in the adult neurogenesis model, we overexpressed the activator of CDK5, p35, with a viral vector, in combination with treatment with the AD-related $A\beta_{1-42}$ protein. We demonstrate that activation of CDK5 resulted in reduced neurite outgrowth in NPC-derived neural progeny, and this effect was accompanied by hyperphosphorylation of CRMP2. Pharmacological or siRNA-mediated inhibition of CDK5 rescued the

defective neurite outgrowth with a concomitant reduction in CRMP2 phosphorylation. To determine whether CRMP2 phosphorylation was required for the alterations in neurite outgrowth observed in this model of adult neurogenesis in AD, we generated a non-phosphorylatable CRMP2 construct mutated at the CDK5 epitope (S522A). Compared to WT-CRMP2, expression of the mutant construct dramatically reduced phosphorylation of CRMP2 in NPC-derived neural progeny, and furthermore protected against the neurite outgrowth defects induced by CDK5 hyperactivation with p35/Aβ. In order to better understand the mechanisms involved in CDK5/CRMP2-mediated defective neurite outgrowth in adult neurogenesis in AD, we used biochemical, immunofluorescence, and electron microscopic methods to assess the integrity of microtubules in p35/Aβ-treated NPC-derived neural progeny. We found that microtubule polymerization was impaired under conditions of CDK5 hyperactivation, which likely occurs because phosphorylation of CRMP2 impairs microtubule polymerization. Taken together, these results support a role for aberrant CDK5 activation and CRMP2 modulation with impaired microtubule polymerization during adult neurogenesis in AD.

INTRODUCTION

During aging and in the progression of Alzheimer's disease (AD), synaptic plasticity and neuronal integrity are disturbed (Lee et al., 2004). Although the precise mechanisms leading to neurodegeneration in AD are not completely clear, most studies have focused on the role of amyloid-β protein (Aβ) precursor (APP) and its products in AD pathogenesis (Selkoe, 1989; Selkoe, 1999; Vassar, 2005). In AD this

has been linked with hyperactivation of cyclin-dependent kinase-5 (CDK5) and its activators p35 and p25 (Liu et al., 2003; Patrick et al., 1999). Furthermore, levels of CDK5 are increased in the brains of AD patients (Lee et al., 1999).

In addition to the alterations in synaptic plasticity in mature neurons, recent studies have uncovered evidence suggesting that the neurodegenerative process in AD might include deregulation of adult neurogenesis (Boekhoorn et al., 2006; Jin et al., 2004b; Li et al., 2008a). This suggests that both aging and AD may be characterized by not only a loss of mature neurons but also by a decrease in the generation of new neurons from neural progenitor cells (NPCs) in the subventricular zone (SVZ) and dentate gyrus (DG) of the hippocampus in the adult brain. Mechanisms of neurogenesis in the fetal brain have been extensively studied, however less is known about the signaling pathways regulating neurogenesis in the adult nervous system and their role in neurodegenerative disorders.

Although the hyperactivation of CDK5/p35/p25 has been associated with the pathogenesis of neurodegenerative diseases such as AD, recent studies have shown that physiological CDK5 activity is essential for adult neurogenesis (Jessberger et al., 2008; Lagace et al., 2008). In this context, it is possible that the neurogenesis deficits in AD might be related to alterations in CDK5 activity in NPCs. In support of this possibility, we have previously shown that CDK5 hyperactivation impairs neurite outgrowth and neurogenesis in an *in vitro* model of adult neurogenesis and in APP tg mice (Crews et al., 2010). However, the downstream regulators mediating CDK5-associated defective neurogenesis in AD are unknown.

In this context, CDK5 may mediate alterations in neurogenesis in AD via aberrant phosphorylation of CDK5 substrates, which include cytoskeletal (neurofilaments, nestin)(Sahlgren et al., 2003) and synaptic proteins (e.g. synapsin, (Matsubara et al., 1996)), among others. During adult neurogenesis in AD, it is possible that CDK5 may modulate structural elements of the cytoskeleton of developing NPCs, which may contribute to defective neurogenesis in this disorder. Elucidating the signaling pathways and downstream molecular targets involved in the deregulation of neurogenesis is important to fully understand the mechanisms of neuroplasticity in AD.

In order to better understand the molecular mechanisms involved in CDK5-mediated deregulation of adult neurogenesis, here we utilized biochemical, immunocytochemical and electron microscopic methods to identify and characterize collapsin-response mediator protein-2 as a critical downstream regulator of this process in an *in vitro* model of CDK5 hyperactivation in neurogenesis in AD. We demonstrate that activation of CDK5 resulted in reduced neurite outgrowth in NPC-derived neural progeny, and this effect was accompanied by hyperphosphorylation of CRMP2. Pharmacological or siRNA-mediated inhibition of CDK5 rescued the defective neurite outgrowth with a concomitant reduction in CRMP2 phosphorylation, and using a non-phosphorylatable CRMP2 construct mutated at the CDK5 epitope (S522A), we showed that CRMP2 phosphorylation was required for the alterations in neurite outgrowth observed in this model of adult neurogenesis in AD. In order to better understand the mechanisms involved in CDK5/CRMP2-mediated defective neurite outgrowth in adult neurogenesis in AD, we assessed the integrity of

microtubules in p35/Aβ-treated NPC-derived neural progeny. We found that microtubule polymerization was impaired under conditions of CDK5 hyperactivation. Taken together, these results support a role for aberrant CDK5 activation and CRMP2 modulation with impaired microtubule polymerization during adult neurogenesis in AD.

MATERIALS AND METHODS

NPC culture and neuronal differentiation assay. Adult rat hippocampal (ARH) NPCs (generously provided by F. Gage, Salk Institute) were cultured routinely for expansion essentially as previously described (Ray and Gage, 2006) with some modifications. Briefly, cells were grown for expansion in DMEM/F12 media (Mediatech, Manassas, VA) containing B27 supplement, 1X L-glutamine and 1X antibiotic-antimycotic (all from Invitrogen, Carlsbad, CA). For induction of neuronal differentiation, cells were plated onto poly-ornithine/laminin (Sigma-Aldrich, St. Louis, MO) coated plates or coverslips and transferred the next day to differentiation media containing N2 supplement (Invitrogen), 1 μM all-trans retinoic acid (Sigma-Aldrich), 5 μM forskolin (Sigma-Aldrich) and 1% FBS. Cells were differentiated for four days, and fresh differentiation media was added at day 2. It should be noted that this differentiation procedure generates heterogeneous cultures, and therefore we refer to the cells derived from the differentiation process as "NPC-derived neural progeny."

Phospho-protein purification, 2D gel electrophoresis, gel staining and mass spectrometry analysis. For purification of phosphorylated proteins in NPC-derived

neural progeny, uninfected cells and cells expressing p35 were harvested and purified and concentrated using a PhosphoProtein Purification kit (Qiagen, Valencia, CA) according to the manufacturer's instructions. Next, 10 μg of total protein from purified control or p35-expressing NPC-derived neural progeny were separated on an isoelectric focusing (IEF) Novex gel to separate proteins according to their isoelectric point from pH 3-10 (Invitrogen). Proteins on the gel were visualized by staining with a colloidal blue gel staining kit (Invitrogen) according to the manufacturer's instructions. Each lane was then cut out of the gel and transferred into the well of a 2-dimensional (2D) 4-12% Bis-Tris gel (Invitrogen). 2 gels for each sample were run in parallel, with one for subsequent immunoblotting analysis onto PVDF membranes, and one for silver staining and mass spectrometry. For highly-sensitive visualization of protein spots on the 2D gels, gels were fixed and processed for silver stain analysis using the SilverQuest staining kit (Invitrogen) according to the manufacturer's directions. All steps were performed with new staining and washing containers, and solutions were made with ultrapure water to prevent potential contamination of the samples. Spots were then cut out, destained using the provided SilverQuest reagents, and samples were sent to the UCSD Biomolecular/Proteomics Mass Spectrometry facility for analysis by MALDI-TOF mass spectrometry (with technical advice kindly provided by Dr. Majid Ghassemian, UCSD). Peptides detected in each sample were identified using the ProteinPilot 3.0 software.

Site-directed mutagenesis and generation of hCRMP2 mutant constructs. The wild-type hCRMP2/pCMV6-XL4 plasmid DNA (Origene, Rockville, MD) was

maintained in *E. coli* TOP10 cells (*dam*$^+$/*dcm*$^+$ strain). Using plasmid DNA isolated from the *E. coli* strain as a template, site-directed mutagenesis of *hCRMP2* was carried out using a QuickChange® Lightning Site-Directed Mutagenesis Kit (Stratagene, La Jolla, CA) with the primers 5'-ctcggccaagacggctcctgccaagcag-3' (sense) and 5'-ctgcttggcaggagccgtcttggccgag-3' (antisense) for S522A single point mutation. The PCR reaction was performed according to the manufacturer's instructions, with 10-min extension cycles at 68 °C. In order to remove the parental DNA template, PCR products were subjected to DpnI restriction enzyme digestion reaction and then directly transformed into *E. coli* TOP10 cells. After selection on LB medium supplemented with ampicillin, plasmid DNA was extracted from positive transformants using a QIAprep Spin Miniprep kit (Qiagen) according to the manufacturer's instructions. Purified plasmids were subjected to DNA sequencing with hCRMP2 specific primers: 5'-atcaaggcaaggagcaggct-3' (sense), and 5'-aatgttgtcatcaatctgagcacca-3' (antisense). After sequence confirmation, the pCMV6-XL4 vector constructs containing either the wild-type hCRMP2, or the S522A construct were used for transformation and amplification in XL10 *E. coli* cells (Stratagene).

Cell culture treatments—Viral infection, Aβ treatment, plasmid DNA transfection, and microtubule chemical treatments. For activation of the CDK5/p35 pathway, cells were infected on day 2 of differentiation with adenovirus expressing human p35 or GFP control (Vector Biolabs, Philadelphia, PA) at a multiplicity of infection (MOI) of 30. Cells were then treated on day 3 with freshly dissolved $A\beta_{1-42}$

(1-5μM, American Peptide, Sunnyvale, CA) or reverse $A\beta_{42-1}$ peptide (1-5μM, American Peptide) as a control.

For overexpression of wild-type or mutant human (h)CRMP2 in NPCs, cells were differentiated from day 0 in medium without antibiotics, and transfected on day 2 of differentiation (6 hrs prior to virus infection) with pCMV6-XL4 plasmids hCRMP2-WT, or hCRMP2-S522A, or pCMV-GFP control. Transfection was performed using Lipofectamine 2000 transfection reagent (Invitrogen) at a concentration of 2.5 μL/mL according to the manufacturer's instructions. For transfection of cells in 6-well plates, 4.0 μg plasmid DNA was applied per well, and for transfection of cells on coverslips in 6 cm dishes, 8.0 μg plasmid DNA was applied per dish. Six hrs after transfection, fresh differentiation medium without antibiotics was applied with or without viral vectors. Cells were then lysed for biochemical analyses or fixed for immunocytochemical analysis.

For stabilization of microtubules *in vitro*, cells were treated with paclitaxel (100 nM, Sigma-Aldrich) or vehicle for 6hrs or 24hrs prior to harvest. For disruption of microtubules, cells were treated with nocodazole (5 μg/mL, Sigma-Aldrich) for 3 hrs. Then, cultures were washed with differentiation media three times, followed by incubation in fresh media for 10 mins, 20 mins or 30 mins. Cells were then fixed for tubulin immunofluorescence analysis.

Immunoblot analysis. For immunoblot analysis of total cell homogenates, adherent cells in culture were lysed in buffer composed of 10 mM Tris-HCl (pH 7.4), 150 mM NaCl, 5 mM EDTA (TNE) containing 1% Triton-X 100 to obtain total cell

lysates. Cytosolic and membrane fractions from brain homogenates or total cell lysates were separated by gel electrophoresis on 4-12% Bis-Tris gels (Invitrogen) and blotted onto 0.45 μm PVDF membranes (Millipore, Temecula, CA). All immunoblots were incubated in primary antibodies diluted in 5% BSA in PBS-Tween (PBS-T) overnight at 4°C. Immunoblots were probed with rabbit polyclonal antibodies against phosphorylated (pThr316) Nestin (1:500, Santa Cruz Biotechnology, Santa Cruz, CA), phosphorylated (pSer522) CRMP2 (1:1000, ECM Biosciences, Versailles, KY), phosphorylated (pThr514) CRMP2 (1:1000, Cell Signaling Technology, Danvers, MA), phosphorylated (pThr555) CRMP2 (1:1000, ECM Biosciences), or total CRMP2 (1:1000, Millipore). For immunoblot analysis with a panel of antibodies against different epitopes of full-length Nestin, blots were probed with primary antibodies described in Table 4.1 at a dilution of 1:1000 for all antibodies.

Table 4.1. *Antibodies and reactive epitopes against full-length Nestin.*

Company	**Species**	**Clone**	**Reactivity**	**Epitope**	**Immunogen**
Chemicon	Mouse	Rat-401	Rat, mouse	Full-length nestin	Nestin from embryonic rat spinal cord
BD Transduction	Mouse	25/Nestin	Rat, mouse, human	aa 402-604	Rat nestin aa 402-604
Rockland	Rabbit	N/A	Human, rat, mouse	aa 1484-1500	Human nestin aa 1484-1500
DSHB	Mouse	4E2	Rat	46-48 kDa nestin fragment	membrane vesicles from lower hind-limb muscles from 5-6 day-old rats

For immunoblot analysis with a panel of different phosphorylated or total CRMP proteins, blots were probed with antibodies described in Table 4.2 at a dilution of 1:1000 for all antibodies. For immunoblot analysis of various tubulin proteins, blots

were probed with mouse monoclonal antibodies against β-Tubulin (1:1000, clone B2.1, Sigma-Aldrich), α-Tubulin (1:1500, clone B-5-1-2, Sigma-Aldrich), β-III Tubulin (1:5000, clone Tuj1, Covance), acetylated-Tubulin (1:5000, Sigma-Aldrich) or actin (Millipore) as a loading control as previously described (Rockenstein et al., 2001). After incubation with primary antibodies, all immunoblots were incubated for 45 mins at room temperature in secondary antibodies diluted in 5% non-fat milk with 1% BSA in PBS-T. Blots were developed with enhanced chemiluminescence (Perkin-Elmer, Waltham, MA), and images were obtained and semi-quantitative analysis was performed as described in Chapter 2 (Figure 2.10) using the VersaDoc gel imaging system and Quantity One software (Bio-Rad, Hercules, CA).

Table 4.2. *Antibodies and reactive epitopes against phosphorylated and total CRMP proteins.*

Antibody	**Epitope**	**Company**	**Species**	**Reactivity**
CRMP2	pThr514	Cell Signaling	Rabbit	Human, mouse, rat
CRMP2	pThr514	Kinasource	Sheep	Human, mouse
CRMP2	pThr509, pThr514	Kinasource	Sheep	Human, mouse, rat
CRMP2	pSer522	ECM Biosciences	Rabbit	Human, mouse, rat
CRMP2	pSer522	Kinasource	Sheep	Human, mouse, rat
CRMP2	pThr555	ECM Biosciences	Rabbit	Human, mouse, rat
CRMP2	total (C-terminus)	ECM Biosciences	Rabbit	Human, mouse, rat
CRMP2	total (peptide)	Millipore	Rabbit	Rat
CRMP2	total (recombinant)	Kinasource	Sheep	Human, mouse CRMP1,2,4
CRMP1	pThr509	Kinasource	Sheep	Human
CRMP4	pThr509	Kinasource	Sheep	Human, mouse, rat
CRMP4 (TUC4)	total (peptide)	Millipore	Rabbit	Human, mouse, rat

Tubulin fractionation and quantitative analysis of cellular microtubules vs. free tubulin. Essentially as previously described (Davis et al., 2005; Vogl et al., 2004), to isolate the free and polymerized fractions of tubulin from NPC-derived neural progeny, all of the assay components (e.g., samples, rotors, centrifuge tubes, and buffers) were maintained at 37°C throughout the isolation procedure. Cells were grown in 10 cm dishes and harvested and lysed in a cell lysis/microtubule stabilization buffer (MTSB) of the following composition: 100 mM PIPES (pH 6.9), 5 mM MgCl2, 1 mM EGTA, 30% glycerol, 0.1% nonidet P-40 alternative, 0.1% Triton X-100, 0.1% Tween 20, 0.1% β-mercaptoethanol, 0.001% antifoam, 1 mM dithiothrietol, 0.1 mM GTP, 1 mM ATP, containing protease, phosphatase and calpain inhibitors (Calbiochem, San Diego, CA). Buffer was made fresh before each assay. Cell homogenization and centrifugation were performed at 37°C to maintain microtubule stability.

For homogenization, media was gently aspirated from cultures, pre-warmed MTSB was added (400 μL per dish) and cells were immediately scraped and transferred into pre-warmed microcentrifuge tubes. Total cell lysates were incubated in a 37C water bath for 10 min, during which they were gently homogenized with a microgrinder pestle attachment for microcentrifuge tubes. Three hundred μL of the total cell lysates were transferred to ultracentrifuge tubes and centrifuged at 100,000 *g* for 30 min at 37C. Supernatants containing soluble tubulin were separated immediately from the pellets containing microtubules (polymerized tubulin plus microtubule-associated proteins). The supernatant volumes were determined, and the pellets were dissolved in the same volume of double-distilled deionized water

(ddH2O) containing 200μM CaCl2. Pellets were dissociated by incubation on ice with frequent vortex for 1 h. Protein concentration of the total cell lysates, supernatant, and pellet fractions, were determined with the detergent-compatible bicinchoninic acid reagent kit (Pierce, Rockford, IL). 10 μg of each fraction was loaded per well on 4-12% Bis-Tris gels (Invitrogen), and Western blot analyses were conducted as described above for immunoblot analysis to determine β-tubulin and α-tubulin levels associated with free and polymerized fractions.

Fixation procedure for the preservation of microtubules. To preserve the integrity of intact microtubules in cultured cells, a glutaraldehyde-based fixation procedure was utilized, essentially as previously described by Desai and Mitchison (http://mitchison.med.harvard.edu/protocols/gen1.html). For this purpose, media was gently aspirated from cells growing on glass coverslips, and then cells were extracted for 30 sec in cytoskeletal buffer (CB, 80mM PIPES pH 6.8, 1mM $MgCl_2$, 4mM EGTA) containing 0.5% freshly added Triton-X 100. Glutaraldehyde (Electron Microscopy Sciences, Hatfield, PA) was immediately added to the CB on the coverslips at a final concentration of 0.5%. Coverslips were incubated for 10 min at 37°C. Fixative was then removed and a freshly-prepared solution of 0.1% $NaBH_4$ in PBS was added and samples were incubated for 7 min at room temperature to quench free glutaraldehyde. Coverslips were washed at least 3 times in PBS to remove the $NaBH_4$, and samples were then processed for tubulin immunofluorescence.

Immunocytochemical analysis. For double-immunocytochemical analysis, briefly, as previously described (Masliah et al., 2003), cells on coverslips were fixed in 4% paraformaldehyde (PFA) in PBS, then washed with Tris buffered saline (TBS, pH 7.4), pre-treated in 3% H_2O_2, and blocked with 10% serum (Vector Laboratories, Burlingame, CA). Samples were incubated in a rabbit polyclonal primary antibody against phospho-Nestin (Thr316, 1:500, Santa Cruz Biotechnology) and detected with the Tyramide Signal Amplification™-Direct (Red) system (NEN Life Sciences, Boston, MA). Coverslips were co-labeled with the mouse monoclonal antibody against β-III-Tubulin (clone TU-20, 1:250, Millipore) detected with FITC-conjugated secondary antibodies (1:75, Vector Laboratories). For tubulin immunofluorescence, fixed cells on coverslips were washed with Tris buffered saline (TBS, pH 7.4), pre-treated in 3% H_2O_2, and blocked with 10% serum (Vector Laboratories). Samples were incubated with primary anti-Tubulin antibodies (mouse anti-β-Tubulin clone B2.1, 1:250, Sigma-Aldrich; mouse anti-α-Tubulin clone B-5-1-2, 1:250, Sigma-Aldrich) for 1 hr at room temperature and detected with FITC-conjugated secondary antibodies (1:75, Vector Laboratories).

Samples were mounted under glass coverslips with ProLong Gold antifade reagent with DAPI (Invitrogen) and imaged with a Zeiss 63X (N.A. 1.4) objective on an Axiovert 35 microscope (Zeiss, Germany) with an attached MRC1024 laser scanning confocal microscope system (BioRad) (Masliah et al., 2000). All samples were processed simultaneously under the same conditions and the experiments were performed twice to assess reproducibility. To confirm the specificity of primary antibodies, control experiments were performed where sections were incubated

overnight in the absence of primary antibody (deleted) or primary antibody pre-incubated with blocking peptide. For analysis of neurite outgrowth of NPC-derived neural progeny immunolabeled with β-Tubulin, neurite lengths were measured using the ImageJ Program with the NeuronJ Plugin.

Ultrastructural analysis by electron microscopy. Briefly, as previously described (Marongiu et al., 2009), NPCs were plated in 35 mm dishes with a coverslip in the bottom (MatTek, Ashland, MA) and infected with p35 adenovirus and treated with Aβ as described in the cell culture conditions. After 4 days of differentiation, cells were fixed in 1% glutaraldehyde in media, then fixed in osmium tetraoxide and embedded in epon araldite. Once the resin hardened, blocks with the cells were detached from the coverslips and mounted for sectioning with an ultramicrotome (Leica, Germany). Grids were analyzed with a Zeiss OM 10 electron microscope as previously described (Rockenstein et al., 2001).

Statistical Analysis. All experiments were performed blind coded and in triplicate. Values in the figures are expressed as means ± SEM. To determine the statistical significance, values were compared by one-way ANOVA with post-hoc Dunnett's test when comparing differences to controls, or with post-hoc Tukey-Kramer test when comparisons were made among groups. The differences were considered to be significant if p values were less than 0.05.

RESULTS

CDK5 hyperactivation in an in vitro model of adult neurogenesis in Alzheimer's disease results in reduced neurite outgrowth and enhanced phosphorylation of an unknown protein

We have shown in an *in vitro* model of adult neurogenesis that CDK5 is important in the process of adult neurogenesis and that hyperactivation of CDK5 impairs neurogenesis (Chapter 3, (Crews et al., 2010)). In this model, neuronal differentiation of ARH-NPCs is chemically induced, and in order to model the hyperactivation of CDK5 that has been reported in AD, at the midpoint (day 2) during differentiation, the CDK5 pathway is stimulated by virus-mediated expression of the CDK5 activator p35 in combination with exposure to $A\beta_{1\text{-}42}$ (Crews et al., 2010). In this model system, Aβ treatment or p35 expression alone or in combination dramatically reduced neurite outgrowth of β-Tubulin-positive processes compared to vehicle-treated controls (Figure 4.1A-E).

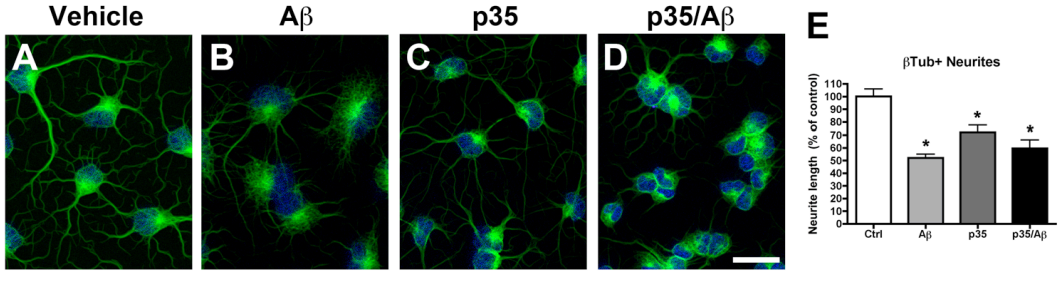

Figure 4.1 *Impaired neurite outgrowth in NPC-derived neural progeny expressing p35 and treated with Aβ.* Differentiating NPCs were infected at day 2 with an adenoviral vector expressing p35, and 24 hrs later cells were exposed to 1 μM $A\beta_{1\text{-}42}$. On day 4, cells were briefly extracted, then fixed with glutaraldehyde and processed for β-tubulin immunofluorescence. (A-D) Reduced β-tubulin-immunoreactive neurites in NPC-derived neural progeny with p35 or Aβ treatment alone or in combination. (E) Quantitative image analysis showing reduced neurite lengths in NPC-derived neural progeny with p35 or Aβ treatment alone or in combination. * $p < 0.05$ compared to vehicle-treated controls by one-way ANOVA with post-hoc Dunnett's test. Scale bar = 10 μm.

In order to investigate the molecular mechanisms downstream of CDK5 that might be involved in this process, we assessed the phosphorylation status of substrates of CDK5 that might have a functional role in neuronal maturation. One of the first substrates we investigated was the intermediate filament protein nestin. Immunoblot analysis showed that while there were no significant changes in phosphorylation levels of full-length (FL) nestin at Thr316 (an epitope known to be phosphorylated by CDK5) in NPC-derived neural progeny with hyperactivated CDK5 (Figure 4.2A), in NPCs expressing p35 and treated with Aβ we observed a remarkable upregulation in immunoreactivity levels of an unknown cross-reactive (CR) protein at an approximate molecular weight of 62 kDa (Figure 4.2A).

We hypothesized that this unknown protein could be either a novel fragment or alternatively spliced form of nestin, or an unrelated protein that could be a putative substrate for CDK5. First, to assess the specificity of the antibody immunoreactivity to the 62-kDa band, we incubated western blot membranes with the pThr316-nestin antibody with or without pre-incubation with an epitope-specific blocking peptide. In support of the specificity of the antibody interaction, pre-incubation of the antibody with blocking peptide abolished the immunoreactivity to the 62-kDa band (Figure 4.2B, upper panel). Next, since the antibody is phospho-specific, it is possible that the CR band is a phosphorylated protein or fragment itself, so to determine whether the reactive epitope is phosphorylated, we incubated lysates with alkaline phosphatase to dephosphorylate total proteins. As expected, this treatment dramatically reduced the immunoreactive signal of FL phosphorylated nestin, and moreover the immunoreactive band at 62-kDa was no longer detectable (Figure 4.2A). Taken

together, these results support the possibility that the protein is phosphorylated at the epitope that the antibody recognizes.

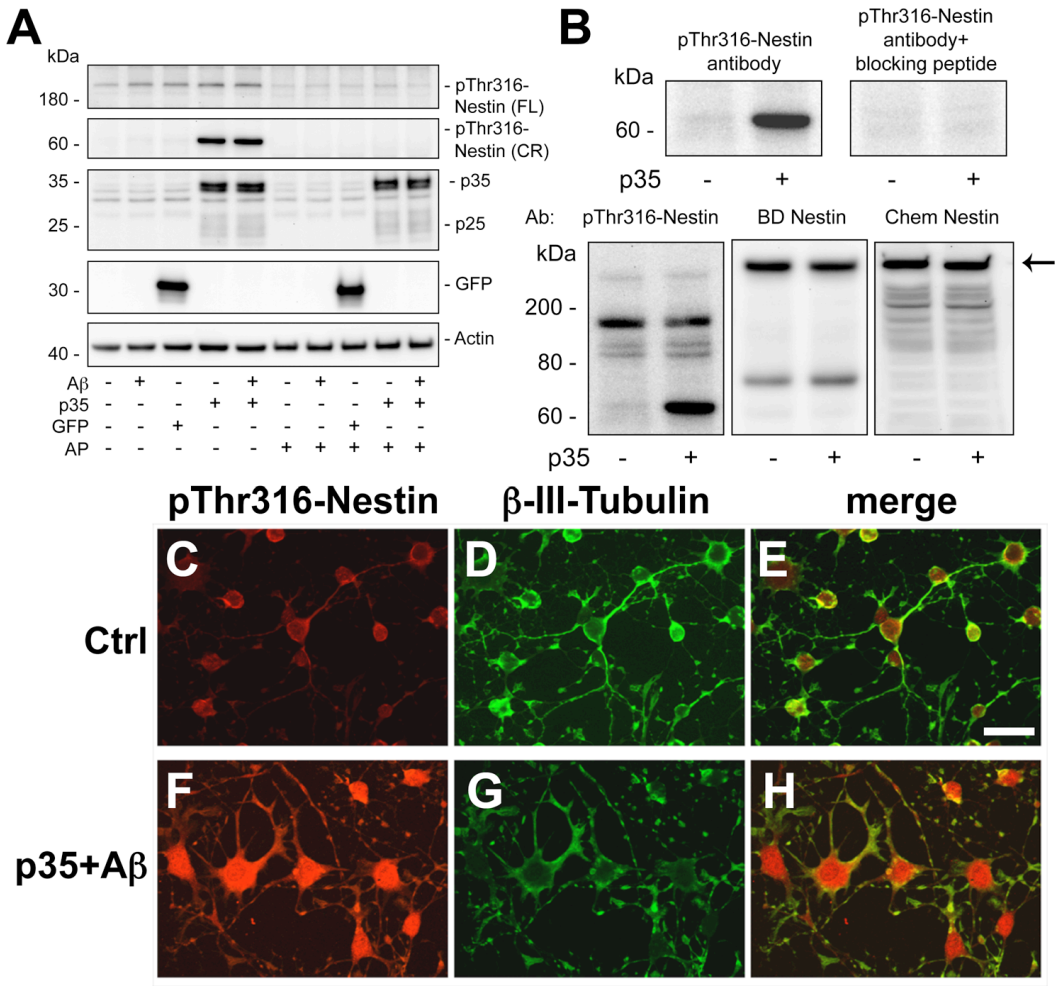

Figure 4.2 *Detection of an upregulated phospho-protein of unknown identity in NPC-derived neural progeny expressing p35 and treated with Aβ.* After differentiation, infection with p35 adenovirus and treatment with Aβ, cells were lysed and processed for immunoblot analysis (panels A and B) or fixed with PFA and processed for double-immunocytochemistry (panels C-H). (A) Immunoblot analysis of full-length (FL) Thr316 phosphorylated-nestin (pThr316-Nestin) and the detection of an unidentified cross-reactive (CR) 62-kDa protein upregulated in NPC-derived neural progeny expressing p35 alone or in combination with Aβ treatment. This band was not detected in control samples infected with GFP adenovirus. Treatment of lysates with alkaline phosphatase (AP) abolished the immunoreactivity of the antibody with the CR protein. (B) *Upper panel,* Incubation of immunoblots with pThr316-Nestin antibody pre-incubated with specific blocking peptide abolished the signal at 62-kDa. *Lower panel,* Incubation of immunoblots with different antibodies against total nestin recognized the FL protein (arrow) but failed to detect any immunoreactive signal around 62 kDa. (C-H) Increased pThr316-Nestin immunoreactivity compared to controls (Ctrl) in β-III-Tubulin-positive NPC-derived neural progeny expressing p35 and treated with Aβ. Scale bar = 10 μm.

Next, to further investigate the possibility that this unknown protein could be a phosphorylated fragment of nestin, we analyzed levels of total nestin by immunoblot using a panel of nestin-specific antibodies against different regions of the full-length protein (Table 4.1). This analysis demonstrated that of the antibodies tested, none detected a band at a similar molecular weight to the pThr316-nestin antibody (Figure 4.2B, lower panel). Moreover, there were no changes in levels of total nestin in NPC-derived neural progeny expressing p35 and treated with Aβ (Figure 4.2B, lower panel), suggesting that there was no enhanced cleavage of full-length nestin that may have generated an increase in the 62-kDa band. Taken together, these results support the possibility that the unknown 62-kDa protein is not nestin, but an alternative putative substrate for CDK5 phosphorylation. Immunocytochemical analysis with the pThr316-nestin antibody confirmed that increased immunoreactivity was detected in NPC-derived neural progeny with hyperactivated CDK5 (Figure 4.2C-H).

Identification of CRMP2 as the protein substrate of CDK5 in NPC-derived neural progeny with p35/Aβ

To definitively ascertain the identity of the unknown phosphorylated 62-kDa protein that was dramatically upregulated in NPC-derived neural progeny upon activation of the CDK5 signaling pathway, we utilized an approach involving purification and concentration of the phosphorylated proteins, followed by 2D gel electrophoresis and mass spectrometry analysis. Immunoblot analysis with the pThr316-nestin antibody confirmed that the 62kDa protein was successfully

concentrated in lysates from cells expressing p35 that were isolated over a phospho-purification column (Figure 4.3A).

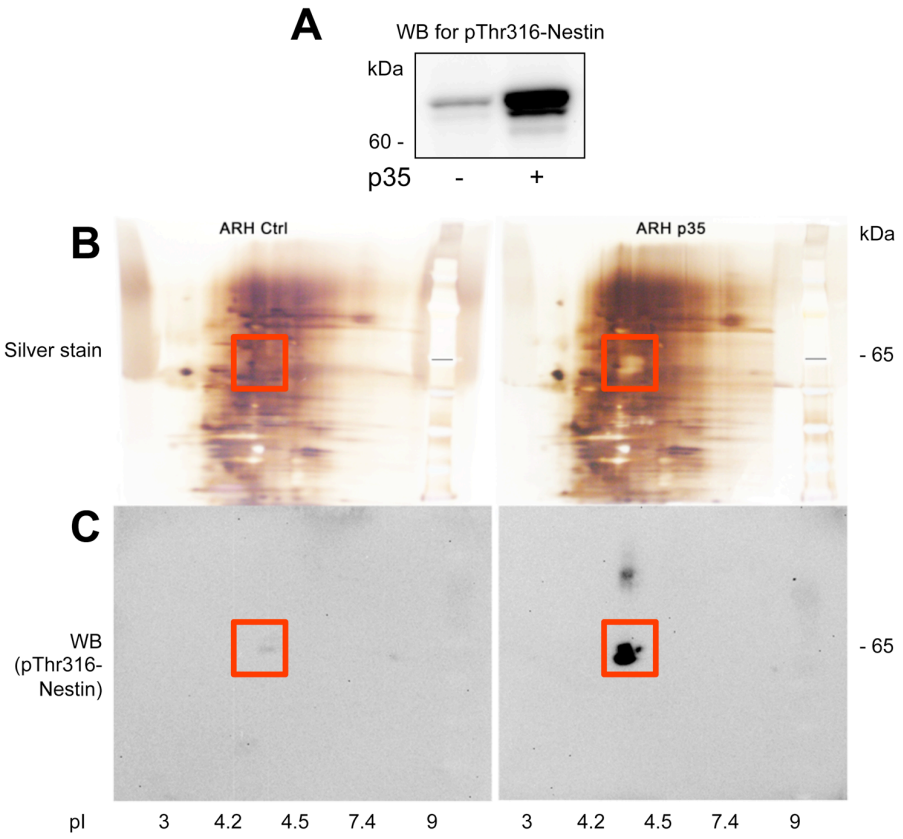

Figure 4.3 *Purification of phosphorylated proteins, and immunoblot and silver stain gel analysis of 2-dimensional gels.* Total cell lysates from NPC-derived neural progeny +/- p35 were purified and concentrated to enrich phosphorylated proteins in each sample. Proteins were then separated on isoelectric focusing (IEF) gels, following by 2-dimensional (2D) gel analysis and silver staining of the gels, or immunoblot analysis with the pThr316-Nestin antibody. (A) Confirmation by immunoblot that the phospho-purification procedure substantially enriched the 62-kDa protein in the p35-expressing cells that immunoreacted with the pThr316 antibody. (B) Silver-stained 2D gels showing lysates from adult rat hippocampal (ARH) NPC-derived neural progeny from uninfected control (Ctrl) cells (left panel) or p35-infected cells (right panel). A highly protein-dense deposit was detected around a pI of 4.3 and a molecular weight of about 65 kDa in overexposed gels of lysates from cells expressing p35, but not in control samples (box). (C) A pThr316-Nestin-immunoreactive spot was detected only on 2D immunoblots from lysates of p35-expressing cells and not in control cells (box), and corresponded with the pI and molecular weight of the protein-dense deposit detected on silver-stained 2D gels.

2D gel electrophoresis and silver stain analysis of gels run with phospho-purified samples from control and p35-expressing NPC-derived neural progeny

revealed a hyper-saturated protein deposit around 62 kDa on the gel with p35-infected samples that was not prominent on the control gel (Figure 4.3B). This protein-dense deposit that excluded the silver pigment corresponded with the immunoreactive 62 kDa spot on 2D gels that were run in parallel and immunoblotted with the pThr316-nestin antibody (Figure 4.3C).

Next, the protein-dense spot on the silver-stained gel from p35-expressing cells was cut out, destained, digested with trypsin, and analyzed by MALDI-TOF mass spectrometry. This analysis detected only a few proteins in the sample, and of these, the proteins identified with the highest percent coverage were Dpysl2 (CRMP2) (Figure 4.4A) and Dpysl3 (CRMP4).

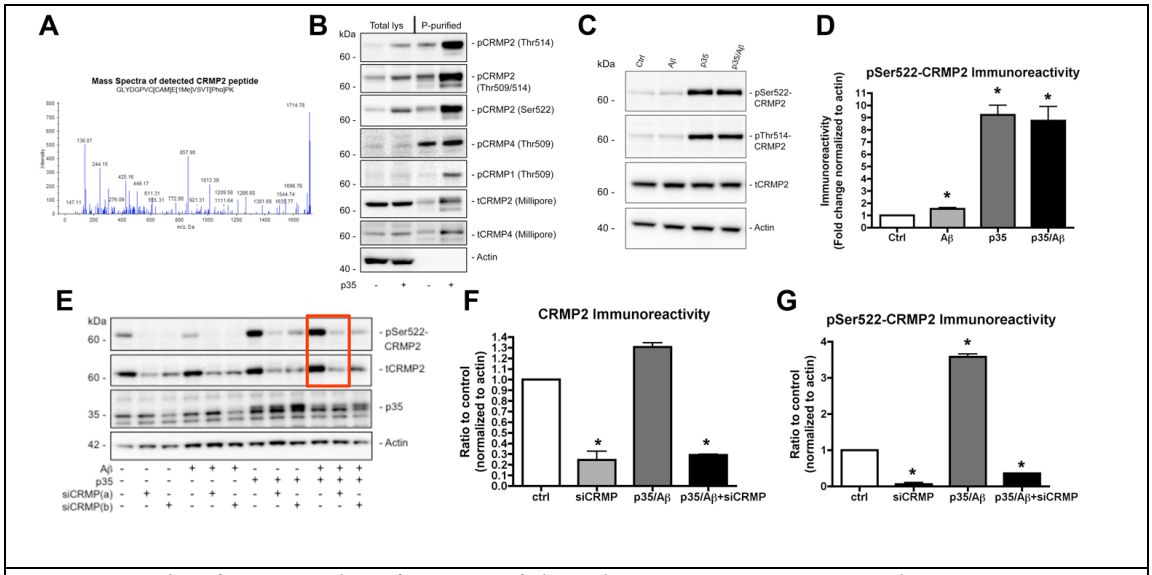

Figure 4.4 *Identification and confirmation of the unknown protein as CRMP2 by mass spectrometry and immunoblot analysis.* Spots from 2D gels of p35-expressing NPC-derived neural progeny were carefully excised, and analyzed by MALDI-TOF mass spectrometry. For confirmation by immunoblot, levels of phosphorylated and total CRMP proteins were analyzed, and a set of samples were prepared from NPC-derived neural progeny treated with siRNA against CRMP2. (A) Sample mass spectra of a CRMP2 peptide detected in the sample from a 2D gel of p35-expressing NPC-derived neural progeny. (B) Immunoblot analysis of total lysates and phospho-purified samples demonstrating increased phosphorylation of CRMP2 in p35-expressing NPC-derived neural progeny compared to control cells. (C, D) Immunoblot analysis of total cell lysates showing that CRMP2 phosphorylation was increased in p35/Aβ NPC-derived neural progeny. (E-G) siRNA knockdown of CRMP2 reduced levels of total and phosphorylated (Ser522) CRMP2 (pSer522-CRMP2). * $p < 0.05$ compared to vehicle-treated controls by one-way ANOVA with post-hoc Dunnett's test.

To confirm whether one of these proteins was in fact the protein we observed to be dramatically upregulated in p35/Ab NPC-derived neural progeny, we obtained a set of antibodies from various sources (Table 4.2) to narrow down the possible species involed. These antibodies were specific for different phosphorylated forms of CRMP proteins (CRMP2, CRMP4, CRMP1) or total non-phosphorylated forms (Figure 4.4B). This analysis confirmed that CRMP2 was the most likely candidate target of CDK5 in this model, which is consistent with previous reports showing that CDK5 phosphorylates CRMP2 at Ser522 (Figure 4.4B). Taken together, these analyses established that CRMP2 is a very likely candidate for CDK5 hyperphosphorylation in NPC-derived neural progeny expressing p35 and treated with Aβ.

CDK5 hyperactivation in an in vitro model of adult neurogenesis in Alzheimer's disease results enhanced CRMP2 phosphorylation

To assess the levels of CRMP2 phosphorylation with antibodies specific for pSer522-CRMP2 and pThr514-CRMP2, which is an epitope phosphorylated by GSK3β following priming phosphorylation of Ser522 by CDK5, we performed immunoblot analysis with NPC-derived neural cells. We found that phosphorylation of the CDK5 target Ser522 in CRMP2 was significantly upregulated, particularly in cells expressing p35 (Figure 4.4C, D). We found that the CRMP2 epitopes targeted by CDK5 and GSK3β were specifically hyperphosphorylated (Figure 4.4C), while phosphorylation at another non-CDK5 epitope (Thr555) was undetectable (data not shown).

To verify that CRMP2 is the identity of the 62-kDa protein, we used siRNA to knock down expression of the endogenous CRMP2 protein, and performed immunoblot analysis to assess levels of pSer522-CRMP2 and total CRMP2 (Figure 4.4E). We found that treatment with siCRMP decreased total levels of CRMP2 expression by approximately 80% compared to controls in both untreated and p35/Aβ-treated NPC-derived neural progeny (Figure 4.4F). Moreover, transfection of siCRMP dramatically reduced levels of pSer522-CRMP2 by over 90% in control cells, and completely reversed the hyperphosphorylation of CRMP2 observed in p35/Aβ-treated NPC-derived neural progeny (Figure 4.4G). Taken together, these studies confirmed the identity of the 62-kDa protein as CRMP2, and demonstrated that it is phosphorylated at CDK5- (Ser522) and GSK3β- (Thr514) specific residues.

Pharmacological inhibition of CDK5 or siRNA knockdown of CDK5 rescues neurite outgrowth defects and reduces CRMP2 phosphorylation

Our initial observations showed that CDK5 hyperactivation in NPC-derived neural progeny impaired neurite outgrowth and development (Figure 4.1). In order to determine whether CDK5 expression and activity was required for the defects in neurite outgrowth and the concomitant increase in CRMP2 phosphorylation, we used a pharmacological inhibitor of CDK5 (Roscovitine) or an siRNA-based approach to inhibit CDK5 activity or expression, respectively. For this purpose, differentiating NPCs were pre-treated with Roscovitine or transfected with siRNA targeting CDK5 for 6 hrs, followed by infection with virus expressing p35 and Aβ treatment. As we have observed previously (Crews et al., 2010), because physiological levels of CDK5

activity are necessary for neurogenesis, treatment with Roscovitine or siCDK5 alone modestly reduced neurite outgrowth compared to vehicle-treated controls (Figure 4.5A-C, J).

Also consistent with our previous observations, combined p35/Aβ treatment significantly reduced neurite outgrowth compared to vehicle-treated controls (Figure 4.5D, J). However, NPC-derived neural progeny with a hyperactive CDK5 pathway from combined p35/Aβ treatment showed a recovery of neurite outgrowth following Roscovitine or siCDK5 pre-treatment (Figure 4.5D-F, J).

Moreover, rescued neurite outgrowth by Roscovitine or siCDK5 treatment in p35/Aβ NPC-derived neural progeny was accompanied by reduced levels of CRMP2 phosphorylation by immunocytochemical (Figure 4.5G-I) and immunoblot analyses (Figure 4.5K, L) of the CDK5 epitope. Taken together, these results support the possibility that CDK5 hyperactivation specifically targets CRMP2, and the resulting aberrant phosphorylation may play a role in impaired neurite outgrowth in models of adult neurogenesis in AD.

Expression of a non-phosphorylatable CRMP2 construct reduces CRMP2 phosphorylation by CDK5 and rescues neurite outgrowth defects

In order to determine whether CRMP2 phosphorylation is directly related to the neurite outgrowth defects observed in our cellular model of CDK5 hyperactivation in adult neurogenesis, we utilized site-directed mutagenesis to generate a construct encoding a mutant (S522A) form of CRMP2 (S522A-CRMP2) that is not phosphorylatable by CDK5 at the Ser522 epitope (Figure 4.6A).

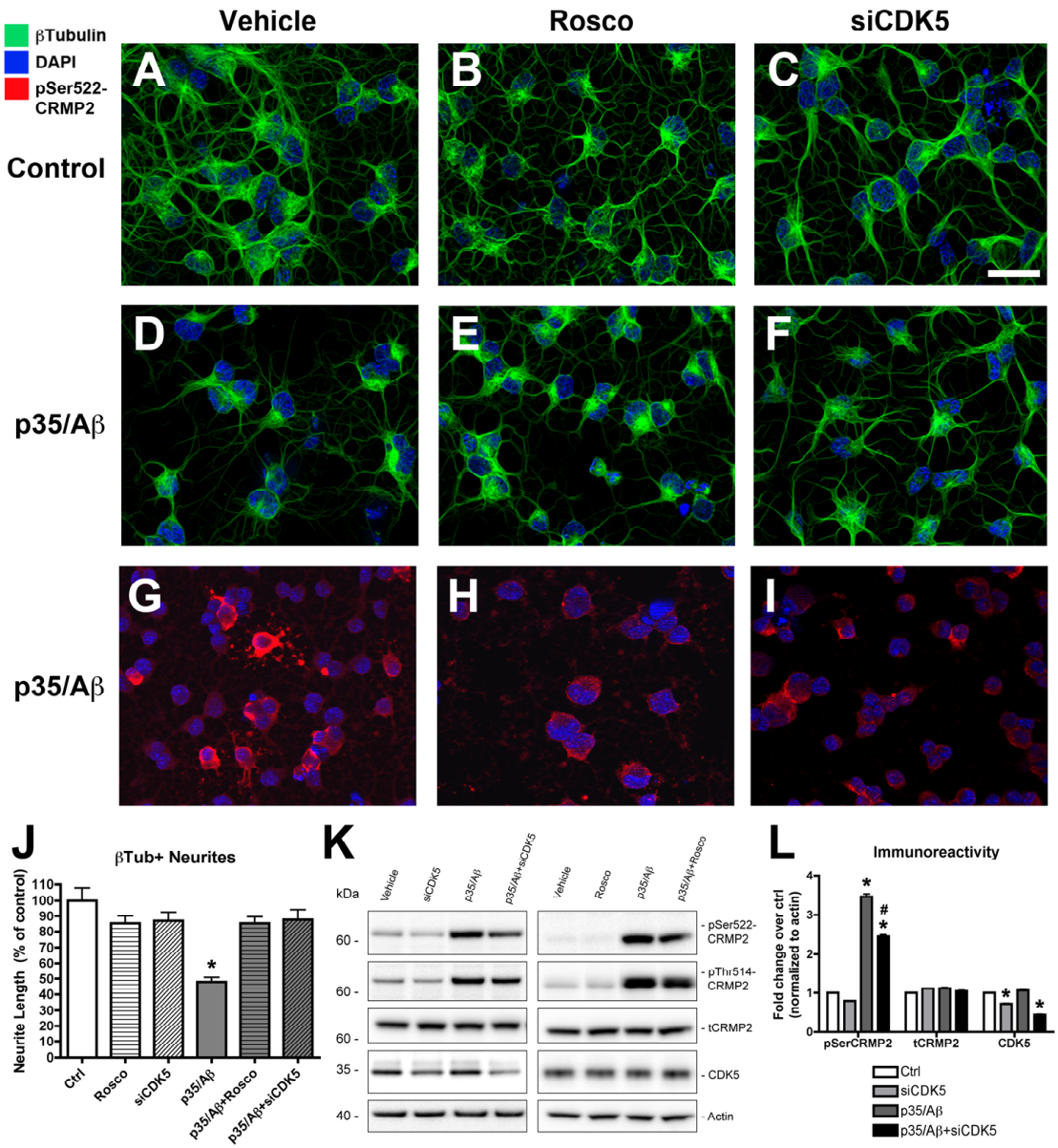

Figure 4.5 *Inhibition of CDK5 rescues neurite deficits and reduces CRMP2 phosphorylation.* Differentiating NPCs were treated on day 2 with the pharmacological inhibitor Roscovitine (Rosco) or siRNA against CDK5 (siCDK5), then infected with p35-adenovirus, followed by treatment with Aβ on day 3. On day 4, NPC-derived neural progeny were fixed for immunofluorescence or lysed for immunoblot analysis. (A-C) Compared to controls (A), uninfected NPC-derived neural progeny treated with Rosco (B) or siCDK5 (C) showed a mild reduction in β-tubulin-positive neurites. (D-F) NPC-derived neural progeny with p35/Aβ treatment showed a notable decrease in β-tubulin-positive neurites (D); this was rescued by treatment with Rosco (E) or siCDK5 (F). (G-I) CRMP2 hyperphosphorylation in p35/Aβ NPCs (G) was reversed by treatment with Rosco (H) or siCDK5 (I). (J) Rescue of neurite lengths with CDK5 inhibition. (K, L) Immunoblot and semi-quantitative analysis of levels of CRMP2 phosphorylation in NPCs treated with p35/Aβ with or without Rosco or siCDK5. * $p < 0.05$ compared to vehicle-treated controls by one-way ANOVA with post-hoc Dunnett's test. # $p < 0.05$ compared to p35/Aβ-treated NPCs by one-way ANOVA with post-hoc Tukey-Kramer test. Scale bar = 10 μm.

As expected, immunoblot analysis confirmed that transfection of differentiating NPCs with the S522A-CRMP2 construct or WT-CRMP2 resulted in similar levels of total CRMP2 expression (Figure 4.6B), while levels of pSer522-CRMP2 immunoreactivity were dramatically reduced in NPC-derived neural progeny expressing S522A-CRMP2 compared to WT-CRMP2-transfected controls (Figure 4.6B, C). Controls including transfection agent (Lipofectamine) alone or CMV-GFP vector control showed levels of pSerCRMP2 and total CRMP2 immunoreactivity similar to non-transfected controls (Figure 4.6B, C).

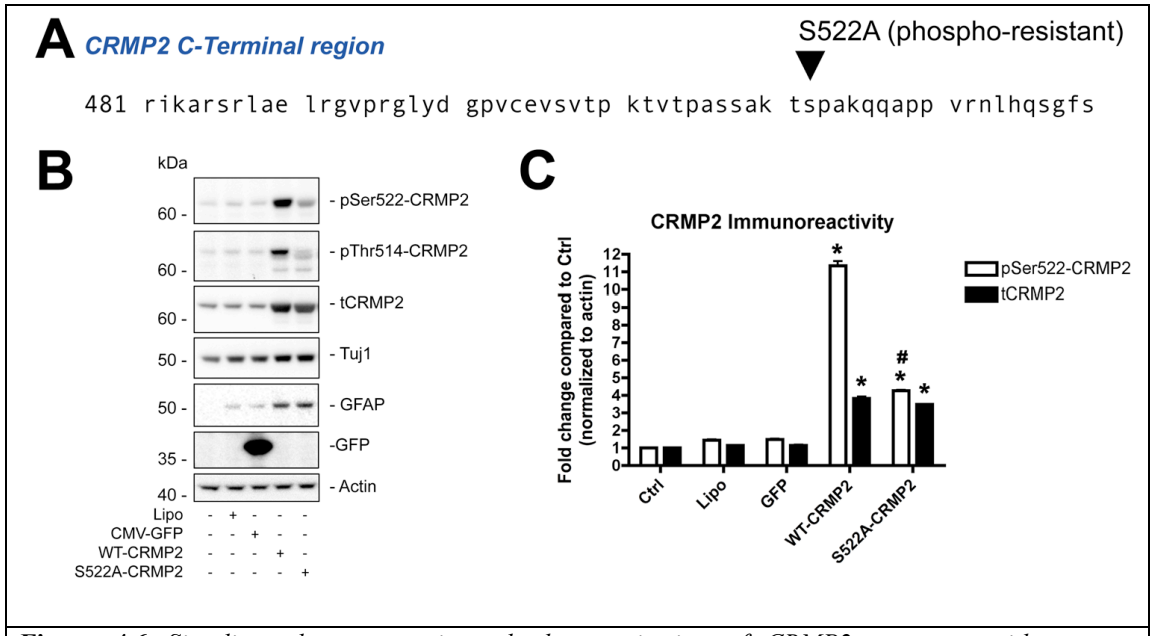

Figure 4.6 *Site-directed mutagenesis and characterization of CRMP2 construct with a non-phosphorylatable CDK5 Ser522 epitope.* A pCMV6-XL4 plasmid containing wild-type (WT) human CRMP2 was mutated at Ser522 to Ala (S522A-CRMP2) to prevent CDK5-mediated phosphorylation of this epitope. Differentiating NPCs were transfected on day 2 with plasmids containing WT or S522A-CRMP2, and on day 4 NPC-derived neural progeny were lysed for immunoblot analysis. (A) Diagram showing a portion of the Ser/Thr-rich C-terminal region of hCRMP2 where Ser522 was mutated to Ala. (B) Immunoblot analysis of lysates from NPC-derived neural progeny expressing WT-CRMP2, S522A-CRMP2, or CVM-GFP or transfection reagent (Lipofectamine, Lipo) controls. (C) Image analysis showing reduced pSer522-CRMP2 immunoreactivity in NPC-derived neural progeny expressing S522A-CRMP2 compared to WT-CRMP2. Levels of total CRMP2 (tCRMP2) were similarly increased in cells expressing WT-CRMP2 and S522A-CRMP2 compared to vector-infected controls. * $p < 0.05$ compared to vehicle-treated controls by one-way ANOVA with post-hoc Dunnett's test. # $p < 0.05$ compared to p35/Aβ-treated NPCs by one-way ANOVA with post-hoc Tukey-Kramer test.

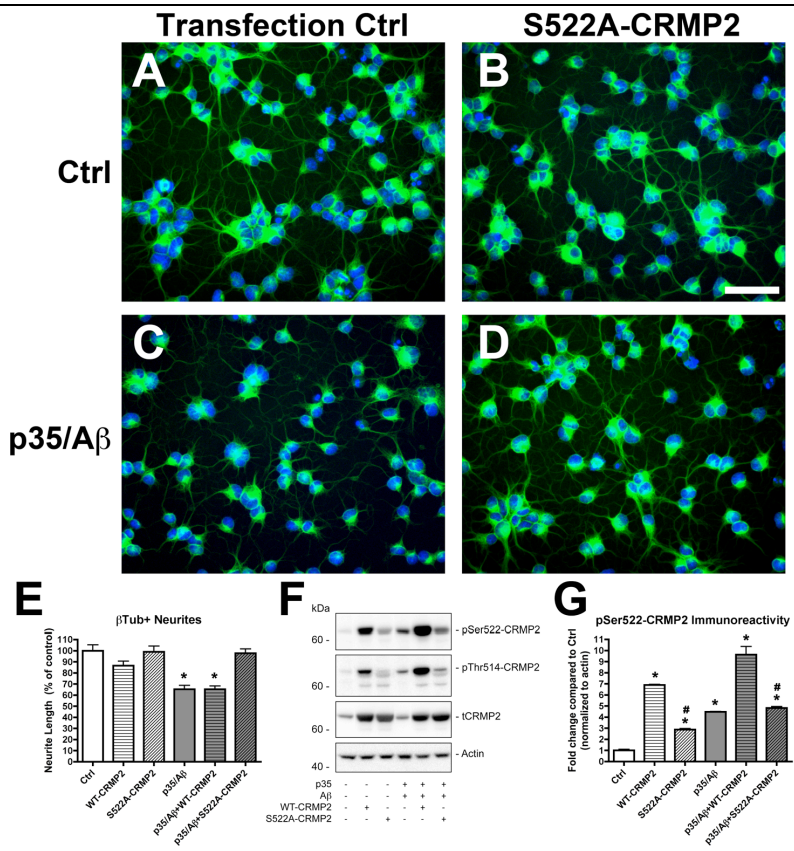

Figure 4.7 *Expression of S522A-CRMP2 mutant construct rescues neurite deficits and reduces CRMP2 phosphorylation in p35/Aβ-treated NPC-derived neural progeny.* Differentiating NPCs were transfected on day 2 with wild-type (WT) human CRMP2 or mutated S522A-CRMP2 plasmids, followed by infection with p35 adenovirus, and then treatment with Aβ on day 3. Cells were then fixed with glutaraldehyde for β-tubulin immunofluorescence, or lysed for immunoblot analysis. (A-D) Immunocytochemical analysis of β-tubulin immunoreactivity showed reduced β-tubulin-positive neurites in NPC-derived neural progeny treated with p35/Aβ and rescue with co-expression of S522A-CRMP2 plasmid. (E) Image analysis showing reduced β-tubulin-positive neurite lengths in p35/Aβ treated and p35/Aβ+WT-CRMP2 NPC-derived neural progeny that was recovered with co-expression of S522A-CRMP2. (F, G) Immunoblot analysis showing reduced CRMP2 phosphorylation in p35/Aβ NPC-derived neural progeny transfected with a S522A-CRMP2 plasmid compared to WT-CRMP2. * $p < 0.05$ compared to vehicle-treated controls by one-way ANOVA with post-hoc Dunnett's test. # $p < 0.05$ compared to WT-CRMP2-transfected NPCs by one-way ANOVA with post-hoc Tukey-Kramer test. Scale bar = 25 μm.

In order to assess whether blocking CDK5-mediated phosphorylation of CRMP2 at Ser522 by expression of a mutant construct might have a protective effect on the neurite alterations in NPC-derived neural progeny, immunocytochemical analysis with an antibody against β-Tubulin was performed (Figure 4.7A-D). This

demonstrated that expression of the mutant S522A-CRMP2 construct rescued the neurite deficits in NPC-derived neural progeny expressing p35 and treated with Aβ, whereas expression of the WT-CRMP2 construct was not protective under these conditions (Figure 4.7A-E).

Immunoblot analysis confirmed that expression of S522A-CRMP2 reduced CRMP2 phosphorylation in p35/Aβ-treated NPC-derived neural progeny compared to WT-CRMP2, and levels of total CRMP2 were similar (Figure 4.7F, G). Taken together, these data support the possibility that phosphorylation of CRMP2 by CDK5 at the Ser522 epitope plays critical role in impaired neurite outgrowth under conditions of CDK5 hyperactivity in cultured NPCs.

CDK5 hyperactivation results in impaired microtubule polymerization

Previous studies have shown that phosphorylation of CRMP2 regulates its interactions with tubulin heterodimers (Fukata et al., 2002). Taken together with our present observations, it is possible that CDK5-mediated hyperphosphorylation of CRMP2 in our *in vitro* system might impair neurite outgrowth by disrupting microtubule polymerization in developing neuronal processes. To further investigate this possibility, and to better understand the functional mechanisms involved in CDK5/CRMP2-mediated alterations in neurite outgrowth in NPCs expressing p35 and treated with Aβ, we performed a biochemical fractionation assay that facilitates the separation of soluble tubulin from polymerized (microtubule-bound) tubulin. Then, immunoblot analysis was utilized to quantify tubulin levels in each fraction.

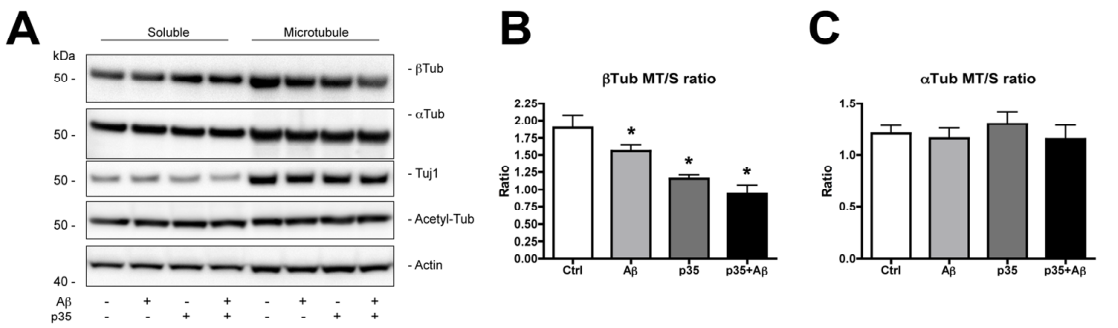

Figure 4.8 *Tubulin fractionation analysis of tubulin distribution in soluble and microtubule fractions.* NPC-derived neural progeny with p35/Aβ were fractionated by ultra-centrifugation in cytoskeletal-stabilizing buffer, then analyzed by immunoblot for levels of α-tubulin (αTub), β-tubulin (βTub), acetylated-tubulin (Acetyl-Tub), or Actin as a loading control. (A-C) Tubulin fractionation analysis of proportion of tubulin in soluble or microtubule fractions showing a reduction in the βTub MT/S ratio in p35/Aβ-treated NPC-derived neural progeny (B). Levels of other tubulin molecules (αTub) were unchanged among different treatment groups (C). * $p < 0.05$ compared to vehicle-treated controls by one-way ANOVA with post-hoc Dunnett's test.

To determine whether *in vitro* conditions modeling AD-like conditions during adult neurogenesis might alter cell maturation via disruption of microtubule polymerization, we assessed the distribution of tubulin immunoreactivity by immunoblot in total, soluble and microtubule fractions from NPC-derived neural progeny infected with p35 and treated with Aβ (Figure 4.8). For semi-quantitative analysis of immunoblots probed with tubulin antibodies, images were obtained and semi-quantitative analysis was performed as described in Chapter 2 (Figure 2.10) using the VersaDoc gel imaging system and Quantity One software. Validation of our quantitation methods was performed as described in Chapter 2 (Figure 2.10). This analysis revealed that compared to vehicle-treated controls, there was a reduction in microtubule-bound β-tubulin levels in cells with p35 or Aβ alone, and a more dramatic reduction in cells exposed to the combined p35/Aβ treatment (Figure 4.8A, B). This was accompanied by a corresponding increase in β-tubulin levels in soluble

fractions (Figure 4.8A, B), suggesting that under conditions of CDK5 hyperactivation there may be a redistribution of β-tubulin from microtubules to the soluble intracellular pool of tubulin.

To assess whether this effect was specific to β-tubulin, or other tubulin proteins were altered as well, we measured levels of α-tubulin and acetylated-tubulin in soluble and microtubule fractions. This analysis showed that levels of α-tubulin and acetylated-tubulin were similar across all samples in each fraction, suggesting that the altered tubulin distribution was specific to β-tubulin and not other components involved in microtubule polymerization. Taken together, these results are consistent with the possibility that hyperactivation of the CDK5 signaling pathway in AD might disrupt adult neurogenesis by impairing microtubule polymerization.

Ultrastructural analysis of p35/Aβ-mediated microtubule alterations in NPC-derived neural progeny

To investigate the underlying ultrastructural basis of the neurite and microtubule alterations observed in combined p35/Aβ treated NPC-derived neural progeny, cells on coverslips were fixed in glutaraldehyde and analyzed by electron microscopy (Figure 4.9). These studies showed that control NPC-derived neural progeny displayed long electron-dense microtubule structures distributed along neuritic processes in a parallel, organized arrangement (Figure 4.9A, B). In contrast, in processes of p35/Aβ-treated NPC-derived neural progeny, filamentous and tubule-like structures were less abundant, and those that were observed were shorter and more disorganized in arrangement than in control cells (Figure 4.9C, D).

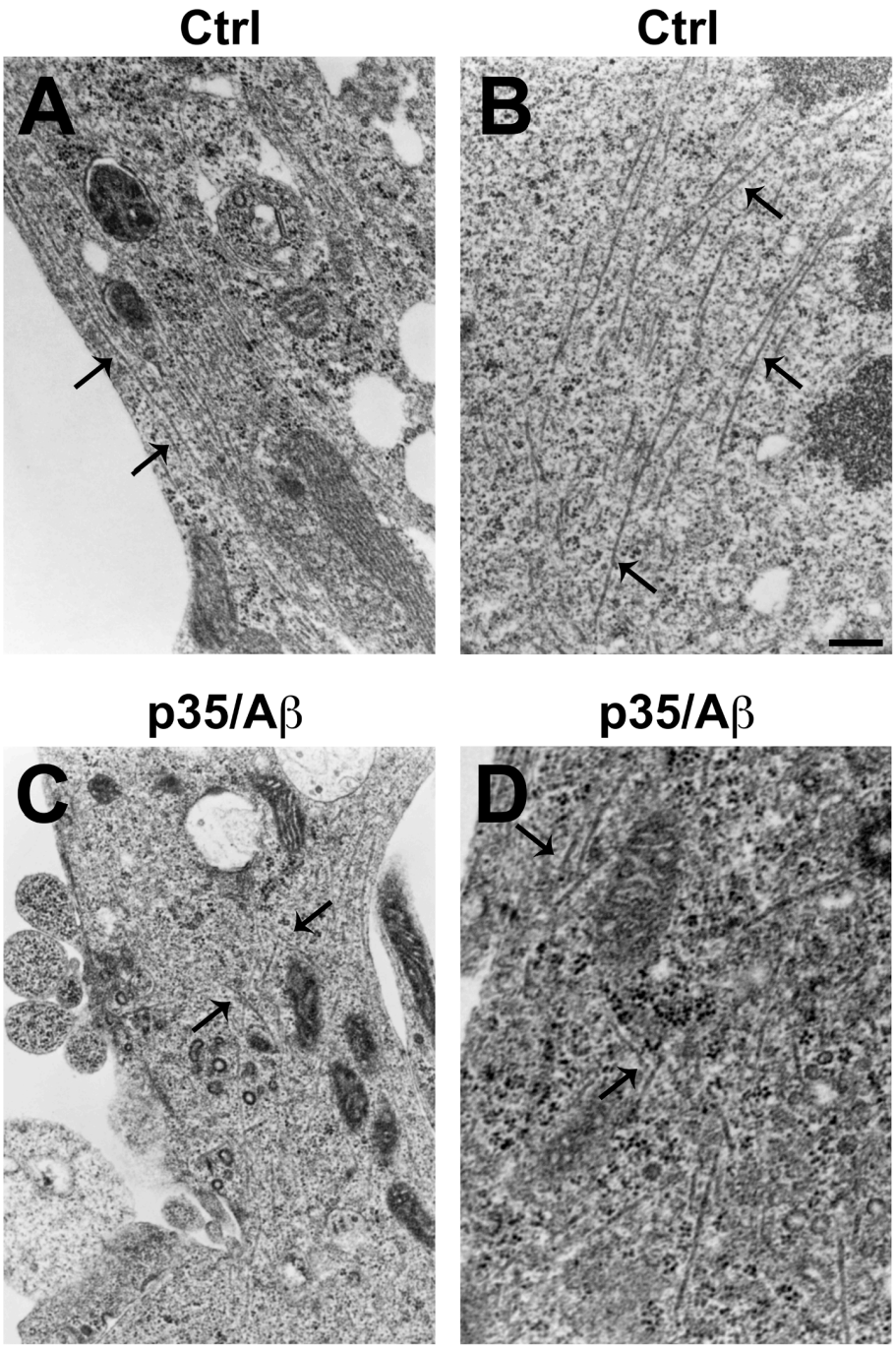

Figure 4.9 *Ultrastructural analysis of cytoskeletal alterations in p35/Aβ-treated NPC-derived neural progeny*. Differentiating NPCs were grown on coverslips embedded in 35mm dishes and infected with p35 adenovirus and treated with Aβ. Cells were fixed in glutaraldehyde and processed for electron microscopic analysis. (A, B) Organized cytoskeletal structure in control NPC-derived neural progeny showed long, parallel tubule structures (arrows) along the processes of cells. (C, D) NPC-derived neural progeny with p35/Aβ displayed a disorganized cytoskeleton with less abundant, short and web-like filamentous structures (arrows) in the processes of cells. Scale bar = 0.5 μm (A, C); 0.25 μm (B, D).

Taken together, these results support the possibility that stimulation of the CDK5 pathway during neurogenesis in AD might disrupt microtubule polymerization and disrupt the organization of these important structural components of the cytoskeleton.

NPC-derived neural progeny with hyperactivated CDK5 show disrupted microtubule dynamics in the presence of microtubule stabilizing and destabilizing agents

In order to determine whether microtubule stabilization might rescue the microtubule and neurite defects observed in NPC-derived neural progeny with p35/Aβ, cultured cells were treated with paclitaxel for 6 hrs prior to harvest and processed for β-tubulin immunofluorescence (Figure 4.10A-F).

This study showed that stabilization of microtubules with paclitaxel resulted in the appearance of dense, thick β-tubulin-immunoreactive microtubule structures in both control and p35/Aβ-treated NPC-derived neural progeny (Figure 4.10A-D). In both vehicle-treated control and p35/Aβ-treated cells, the average thickness of neurites was significantly increased (Figure 4.10E), however neurite lengths were not rescued compared to controls (Figure 4.10F). This suggests that paclitaxel treatment promotes microtubule polymerization under both control and p35/Aβ treatment conditions, however short-term treatment is unable to rescue the neurite outgrowth damage in p35/Aβ NPC-derived neural progeny that are cultured under these disease-simulating conditions from days 2-4 of differentiation.

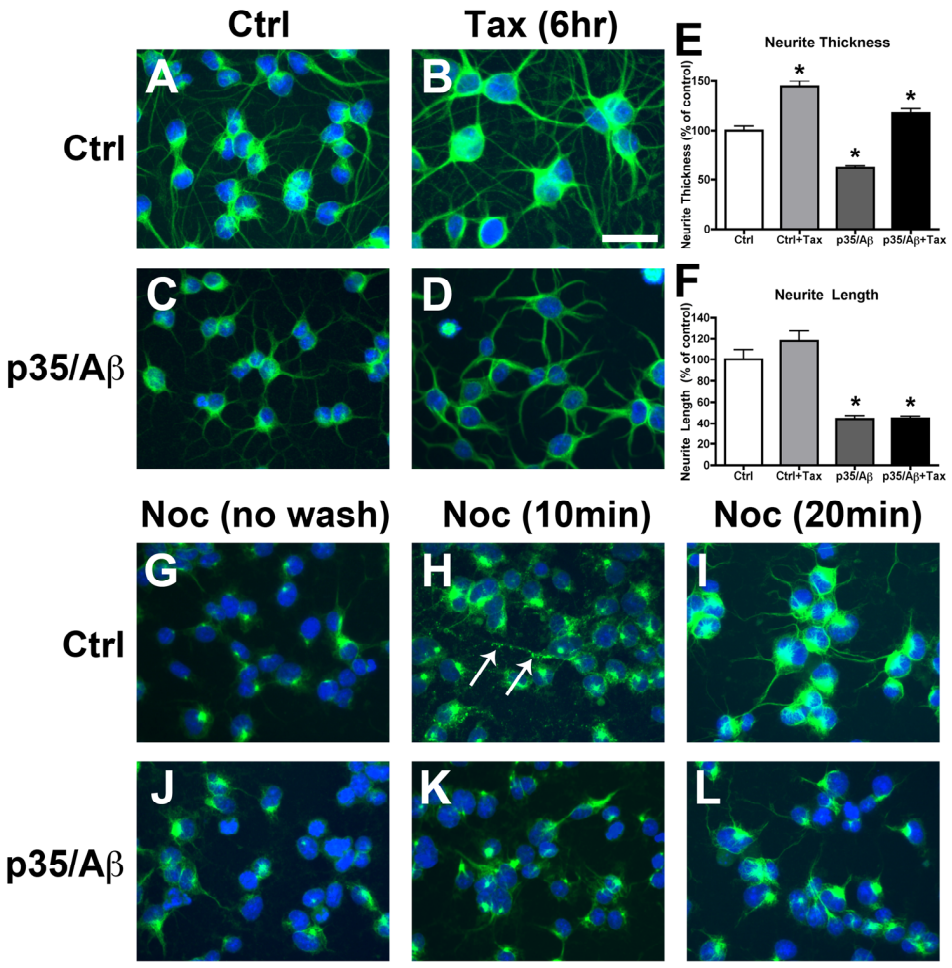

Figure 4.10 *Disrupted microtubule polymerization in p35/Aβ-treated NPC-derived neural progeny.* For chemically-induced microtubule stabilization, differentiating NPCs were treated with 100 nM paclitaxel (Tax) for 6hr prior to fixation. For chemical disruption of microtubules, cultures were treated with 5 μg/mL nocodazole (Noc) for 3hr, followed by washout and incubation in fresh differentiation media for 10 or 20mins. After chemical treatments, NPC-derived neural progeny were fixed with glutaraldehyde and processed for β-tubulin immunofluorescence. (A-D) Compared to vehicle-treated control (Ctrl) NPC-derived neural progeny (A), Tax treatment enhanced microtubule formation under baseline conditions (B), and in cells treated with p35/Aβ (C, D). (E) Image analysis of average neurite thickness in cultures of NPC-derived neural progeny treated with vehicle control or Tax. ImageJ was used to measure the width of each process within 5μm of the cell body before any branch points. (F) Image analysis of average neurite length in cultures of NPC-derived neural progeny treated with vehicle control or Tax. The NeuronJ plugin in ImageJ was used to measure the length of each process extending from the cell body. (G-I) Disruption of microtubule structure in nocodazole-treated control NPC-derived neural progeny (G) was partially recovered by 10min post-washout, and β-tubulin-immunoreactive punctae (arrows) were detected in processes where microtubules reformed (H). By 20min post-washout, microtubule structure was recovered (I) and morphology resembled untreated controls. (J-L) Disruption of microtubule structure in nocodazole-treated p35/Aβ NPC-derived neural progeny (J) was only moderate recovered by 10min (K) or 20min (L) post-washout. * $p < 0.01$ compared to vehicle-treated controls by one-way ANOVA with post-hoc Dunnett's test. Scale bar = 15 μm.

Longer-term treatment of cultures with paclitaxel at earlier stages in the differentiation procedure (24 or 48 hrs, not shown) resulted in nuclear disruption and many apoptotic nuclei, probably due to the fact that most of the cells in these cultures at day 2 are in a proliferative stage. Taken together, these results support the possibility that hyperactivation of CDK5 might impair microtubule polymerization, and paclitaxel can rescue the microtubule polymerization and neurite deficits to some extent.

To further investigate the process of microtubule polymerization in NPC-derived neural progeny, we performed a series of nocodazole washout experiments to visualize the formation of microtubules over a period of 30 mins. For this purpose, NPC-derived neural progeny were incubated with nocodazole for 3 hrs, followed by no washout, or washout for 10, 20 or 30 mins (Figure 4.10G-L). Cells were processed for β-tubulin immunofluorescence and imaged on a fluorescent microscope. This showed, as expected, that directly following nocodazole treatment (no washout), both control and p35/Aβ-treated NPC-derived neural progeny displayed a dramatic reduction of β-tubulin immunoreactivity (Figure 4.10G, J). Microtubule structure was almost completely ablated in both groups (Figure 4.10G, J). However, 10 mins after nocodazole washout, in both control and p35/Aβ NPC-derived neural progeny we observed the appearance of perinuclear microtubule organizing centers (Figure 4.10H, K).

In addition, in control NPC-derived neural progeny, we noted the presence of distinct β-tubulin immunoreactive punctae not associated with the nucleus (Figure 4.10H), suggesting that perhaps under control conditions, microtubules originate in

established neuritic processes as well as at the centrosome. Such punctate immunoreactivity was not observed in p35/Aβ NPC-derived neural progeny, which is consistent with the possibility that microtubule polymerization is impaired under these conditions. By 20 mins post-washout, the majority of control cells (Figure 4.10I) resembled untreated control NPC-derived neural progeny (Figure 4.10A), while p35/Aβ cells only displayed diffuse β-tubulin immunoreactivity in processes (Figure 4.10L). Only very fine processes were detected under these conditions up to 30 mins post-washout (not shown). Taken together, these results support the possibility that CDK5 deregulation impairs the development of microtubules in NPC-derived neural progeny.

DISCUSSION

During the pathogenesis of AD, both CDK5 and GSK3β have been shown to be deregulated, triggering a cascade of hyperphosphorylation of downstream targets of these kinases. Most studies have focused on the role of tau hyperphosphorylation in mediating the neurodegenerative effects of these hyperactive kinases (Cruz and Tsai, 2004), however given the large number of substrates phosphorylated by CDK5 alone, other downstream targets may be involved. In this context, we show here that deregulation of the growth cone signaling protein CRMP2 by CDK5 hyperactivation in an *in vitro* model of adult neurogenesis contributes to defective neurite outgrowth during neuronal differentiation (Figure 4.11). Inhibition of CDK5 with the chemical compound Roscovitine or siRNA knockdown, or expression of a non-

phosphorylatable S522A-CRMP2 mutant construct rescued the neurite defects associated with p35/Aβ-mediated activation of CDK5 in NPC-derived neural progeny.

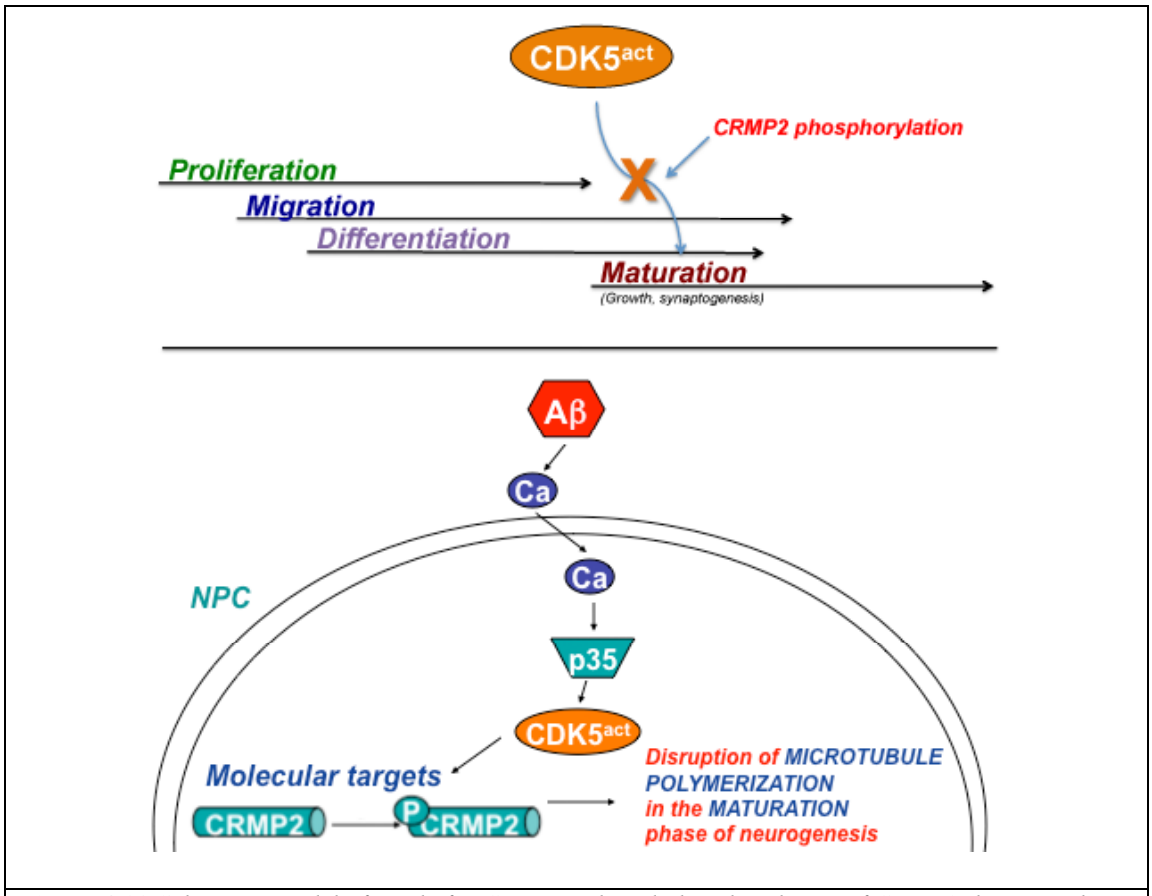

Figure 4.11 *Schematic model of a role for CDK5-mediated phosphorylation of CRMP2 that contributes to defective maturation of immature neurons during neurogenesis in AD.*

In support of a role for CRMP2 in neurodegeneration in AD, previous studies have revealed that in AD patients and in the triple transgenic mouse model of FAD, hyperphosphorylated CRMP2 accumulates as a result of CDK5 hyperactivity (Soutar et al., 2009). In AD brains, phosphorylated CRMP2 associates with damaged neurites and neurofibrillary tangles (Cole et al., 2007; Yoshida et al., 1998), and builds up in neurons surrounding cortical amyloid plaques, an effect that has been associated with the activation of Rho kinase by Aβ (Petratos et al., 2008). However the role of CDK5

in this process is less clear, and the effects of AD-related, CDK5-directed CRMP2 hyperphosphorylation in adult neurogenesis have not been previously investigated.

CRMP2 (also known as Dpysl2) is a signaling protein that has been shown to play a role in growth cone collapse and axon development (Goshima et al., 1995). It is a member of a group of related proteins including CRMP1 and CRMP4, all of which are highly abundant in the brain. CRMP2 has no known enzymatic activity (Wang and Strittmatter, 1997), however its C-terminal region is highly Ser and Thr-rich, and is targeted for phosphorylation by a number of kinases, including CDK5, GSK3β (Cole et al., 2004; Uchida et al., 2005), and Rho kinase (Arimura et al., 2000; Arimura et al., 2004), among others. Phosphorylation of CRMP2 has been reported for at least five amino acid residues in the C-terminal region, namely Thr509, Thr514, Ser518, Ser522 and Thr555. Phosphorylation by CDK5 at Ser522 acts as a priming site for subsequent phosphorylation by GSK3β at Thr514 (Cole et al., 2006; Uchida et al., 2005), while other residues can be phosphorylated independently of CDK5 activity. While the functional effects of phosphorylation at these various resides is not entirely clear, previous studies have shown that some of these post-translational modifications dramatically modulate protein-protein interactions between CRMP2 and its binding partners, including tubulin heterodimers (Fukata et al., 2002).

Aberrant phosphorylation of CDK5 cytoskeletal substrates may also have an effect on structural elements of developing neurons, such as microtubules. In support of this possibility, we showed that the alterations in neurite outgrowth in p35/Aβ NPC-derived neural progeny were accompanied by defective microtubule polymerization compared to controls, as shown by a redistribution of β-tubulin from

polymerized microtubule fractions to the soluble free-tubulin intracellular pool. This is in accordance with previous studies of CDK5 hyperactivation in neurodegeneration showing that CDK5 can associate with microtubules indirectly (Sobue et al., 2000) and its substrates include microtubule-associated proteins (MAPs). Moreover, the Aβ/CDK5 neurotoxic pathway may involve the destabilization of microtubules (Li et al., 2003). Taken together, abnormal activation of CDK5 by Aβ, resulting in hyperphosphorylation of CRMP2 during the pathogenesis of AD, might impair the functioning of mature neurons and also contribute to alterations in neurogenesis by disturbing the development of stable microtubules in differentiating neurons (Figure 4.11).

ACKNOWLEDGEMENTS

Chapter 4, in full, is currently being prepared for submission for publication of the material. Crews L, Patrick C, Ruf R, Trejo-Morales M, Adame A, Rockenstein EM, Masliah E. The dissertation author was the primary investigator and author of this material.

The work in Chapter 2 was supported by NIH Grants AG022074, AG18440 and MH62962.

CHAPTER 5

ROLE OF BMP6 IN THE MECHANISMS OF DEFECTIVE NEUROGENESIS IN ALZHEIMER'S DISEASE

ABSTRACT

During aging and in the progression of Alzheimer's disease (AD), synaptic plasticity and neuronal integrity are disturbed. In addition to the alterations in plasticity in mature neurons, the neurodegenerative process in AD has been shown to be accompanied by alterations in neurogenesis. Members of the bone morphogenetic protein (BMP) family of growth factors have been implicated as important regulators of neurogenesis and neuronal cell fate determination during development, however their role in adult neurogenesis and in AD is less clear. We show here by qRT-PCR analysis that BMP6 mRNA levels were significantly increased in the hippocampus of patients with AD and in APP transgenic mice compared to controls. Immunoblot and immunohistochemical analyses confirmed that BMP6 protein levels were increased in AD and APP transgenic mouse brains compared to controls and accumulated around hippocampal plaques. The increased levels of BMP6 were accompanied by defects in hippocampal neurogenesis in AD patients and APP transgenic mice. In support of a role for BMP6 in defective neurogenesis in AD, we show in an *in vitro* model of adult neurogenesis that treatment with amyloid-$\beta_{1\text{-}42}$ protein (Aβ) resulted in increased expression of BMP6, and that exposure to recombinant BMP6 resulted in reduced proliferation with no toxic effects. Taken together, these results suggest that Aβ-

associated increases in BMP6 expression in AD may have deleterious effects on neurogenesis in the hippocampus, and therapeutic approaches could focus on normalization of BMP6 levels to protect against AD-related neurogenic deficits.

INTRODUCTION

Alzheimer's disease (AD) is a leading cause of dementia in the aging population. Neuropathologically, AD is characterized by synaptic injury (Masliah et al., 1997; Terry et al., 1994), neuronal loss (Terry et al., 1981), and amyloid deposition (Selkoe, 1989). Although the precise mechanisms leading to neurodegeneration in AD remain unclear, many studies have focused on the role of amyloid-β (Aβ) precursor protein (APP) and its products, including Aβ oligomers, in AD pathogenesis (Selkoe, 1989; Selkoe, 1999).

Recent studies have revealed a deregulation of adult neurogenesis in AD patients and in mouse models of the disease (Boekhoorn et al., 2006; Dong et al., 2004; Jin et al., 2004a; Jin et al., 2004b; Li et al., 2008a; Tatebayashi et al., 2003). Neurogenesis in the mature healthy CNS occurs in the olfactory bulb, subventricular zone, and dentate gyrus (DG) of the hippocampus, and plays a role in memory and learning (Gage et al., 1998). There is some controversy over whether neurogenesis is increased (Jin et al., 2004b) or decreased (Boekhoorn et al., 2006; Li et al., 2008a) in AD. A recent study suggests that apparent increases in markers of neurogenesis in AD brains may be related to glial and vasculature-associated changes (Boekhoorn et al., 2006), and another study reports a potential association between higher Braak stage in AD and reduced expression of doublecortin, a marker of neurogenesis (Verwer et al.,

2007). In support of this possibility, a number of mouse models of familial AD (FAD) also display reduced neurogenesis (Dong et al., 2004; Donovan et al., 2006; Haughey et al., 2002a; Lazarov and Marr, 2009; Rockenstein et al., 2007a). We have shown that cyclin-dependent kinase-5 (CDK5) plays an important role in the maturation phase of neurogenesis in AD (Chapters 2-4). However other signaling pathways may contribute to the Aβ-mediated alterations in adult neurogenesis at different stages, and the molecular mechanisms involved in defective neurogenesis in AD and in animal models of FAD remain to be fully elucidated.

Interestingly, paralleling the decline in both the pool of neural progenitor cells (NPCs) and their proliferative potential in AD, the levels of various neurotrophic factors, including brain-derived neurotrophic factor (BDNF), stem cell factor (SCF), and neurosteroids among others, are deregulated in AD and FAD-linked models (Laske et al., 2008; Weill-Engerer et al., 2002) (for review see (Schindowski et al., 2008)). These studies suggest that the neurogenic niche is dramatically altered in the pathogenesis of AD, and other growth factors may be deregulated as well.

In order to determine novel candidate regulators of neurogenesis in AD, we screened gene array studies of neurogenesis in the aging hippocampus (Diez del Corral and Storey, 2001; Rowe et al., 2007). A comparison of these results revealed that the bone morphogenetic protein (BMP) family of proteins was disproportionately represented; specifically, BMP2, 6 and 7 were deregulated in the aged hippocampus.

BMPs belong to the transforming growth factor-β (TGFβ) superfamily of cytokines, and have been implicated in embryonic (Mehler et al., 1997) and adult neurogenesis (Colak et al., 2008). However the involvement of BMPs in

neurodegenerative disorders such as AD is less well defined. A recent publication has demonstrated that increased BMP4 levels correlated with reduced hippocampal cell proliferation in a mouse model of AD (Li et al., 2008b), however whether other related proteins are affected, and if they are deregulated in AD patients is unknown.

To investigate this possibility, we analyzed expression levels of BMP2, 6 and 7 in AD hippocampus and in APP tg mouse brains by qRT-PCR. This analysis revealed that BMP6 levels were significantly increased in the hippocampus of patients with AD and in the brains of APP tg mice, while levels of BMP2 and BMP7 were similar to controls. Immunoblot and immunohistochemical analyses confirmed that BMP6 protein levels were similarly increased, and that BMP6 protein accumulated surrounding diffuse and mature Aβ-containing plaques in the brains of AD patients and in APP tg mice. *In vitro* studies in a model of adult neurogenesis showed that $A\beta_{1-42}$ treatment increased BMP6 expression, and recombinant BMP6 reduced cell proliferation. Taken together, these results suggest that accumulation of Aβ during AD pathogenesis may upregulate BMP6 expression, and that increased levels of BMP6 in AD may have deleterious effects on adult hippocampal neurogenesis.

MATERIALS AND METHODS

Specimen processing, neuropathological evaluation and criteria for disease stage. A total of 9 human cases (N=3 non-demented controls; N=6 AD, of which N=3 early AD and N=3 severe AD) were included for the present study (Table 5.1). Brain tissue was obtained at autopsy from patients studied at the Alzheimer Disease Research Center/University of California, San Diego (ADRC/UCSD). The last

Table 5.1. *Summary of clinico-pathological characteristics of human cases.*

Group	N	Age (yrs)	Gender (M/F)	PMD (hrs, mean)	Duration (yrs)	Education (yrs)	Blessed score (range)	DRS (mean)	MMSE (mean)	Brain weight (grs)	Braak Stage
Control	3	83.4±7.5	1/2	12.7±6.4	0	10.0±0	1-2	133.5±6.5	27.5±1.5	1073±24.9	0-I
Early/ Moderate AD	3	82.7±1.3	2/1	12.0±6.0	4.0±4.0	14.3±2.3	1-9	122.0±13.4	25.3±4.2	1231±34.4	I-II
Severe AD	3	79.3±3.7	1/2	8.3±1.7	10.0±2.7	16.7±1.8	16-33	47.0± 22.9	11.0±7.0	950±110.8	VI

neurobehavioral evaluation was performed within 12 months before death and included Blessed score, Mini Mental State Examination (MMSE) and dementia-rating scale (DRS), and autopsies were performed within 24 hrs of death whenever possible (Table 5.1). Brains were processed and evaluated according to standard methods. At autopsy, brains were divided sagittally; the left hemibrain was fixed in formalin of 4% paraformaldehyde (PFA) for subsequent neuropathological and immunohistochemical analysis and the right was frozen at -80˚C for biochemical analyses.

Animal treatments and tissue processing. The tg mice utilized in this study express mutated (London V717I and Swedish K670M/N671L) human (h)APP751 under the control of the mThy-1 promoter (mThy1-hAPP751, line 41) (Rockenstein et al., 2001). In the hippocampus of mice from line 41, the highest hAPP levels were detected in neurons of the DG and in the CA1 region (Rockenstein et al., 2001).

This tg model was selected because these mice produce high levels of $A\beta_{1-42}$, which is accompanied by a significant reduction in levels of synaptic markers by 6-9 months of age (Rockenstein et al., 2001). Starting at 3-4 months of age, these mice display dense amyloid deposits in the frontal cortex, and by 5-7 months of age, increased size (average diameter of 25-30 μm) and numbers of plaques in the frontal cortex are detected, and dense amyloid deposits are also observed in the subiculum of the hippocampus, thalamus and olfactory region (Rockenstein et al., 2001). The increase in plaque numbers observed at 5-7 months of age was associated with a progressive increase in levels of $A\beta_{1-42}$, which measured approximately 2-3μg/g by ELISA at this age (Rockenstein et al., 2001). Moreover, at 6 months of age, APP tg

mice showed significant performance deficits not related to motor impairments compared to non-tg mice in the spatial learning portion of the water maze test (Rockenstein et al., 2003). In sum, these animals exhibit behavioral deficits, synaptic damage, and plaque formation at an early age (beginning at three months) (Rockenstein et al., 2002; Rockenstein et al., 2001). Transgenic lines were maintained by crossing heterozygous tg mice with non-tg C57BL/6 x DBA/2 F1 breeders. All mice were heterozygous with respect to the transgene and the nontg littermates served as controls.

For measurements of BMP6 expression levels, mice (N=4 non-tg; N=4 APP tg) were maintained until six months of age, followed by biochemical and neuropathological studies. For studies of neurogenesis, 6-month old mice (N=4 non-tg; N=4 APP tg) received five intraperitoneal injections (one per day) with 5-bromo-2-deoxyuridine (BrdU, Sigma-Aldrich, St. Louis, MO) at 50 mg/kg. After one month, mice were sacrificed for analysis of levels of BMP expression and markers of neurogenesis. All experiments described were approved by the animal subjects committee at the University of California at San Diego (UCSD) and were performed according to NIH recommendations for animal use. In accordance with NIH guidelines for the humane treatment of animals, mice were anesthetized with chloral hydrate and flush-perfused transcardially with 0.9% saline in order to preserve one hemibrain for biochemical analysis and the other for fixation and subsequent immunohistochemical analysis. Brains were removed and divided sagitally. One hemibrain was post-fixed in phosphate-buffered 4% PFA at 4°C for 48 hours and

sectioned at 40 μm with a Vibratome 2000, while the other hemibrain was snap frozen and stored at -70°C for biochemical analyses.

qRT-PCR and immunoblot analyses. For qRT-PCR of brain tissue, mRNA was extracted from frozen samples from the hippocampus of human brains (N=3 non-demented controls; N=3 early AD and N=3 severe AD) or mouse brains (N=4 non-tg; N=4 APP tg) using TriReagent (Molecular Research Center, Cincinnati, OH) according to the manufacturer's protocols. For qRT-PCR of cultured neuronal progenitor cells (NPCs), cells were lysed and RNA was purified using the RNeasy kit (Qiagen, Valencia, CA). 2 μg of total RNA from each sample was reverse transcribed using the iScript cDNA Supermix Synthesis kit (Bio-Rad, Hercules, CA) in accordance with the manufacturer's instructions. Primer sequences used are detailed in Table 5.2. For brain tissue samples, actin was used as a reference gene, and for NPCs, hypoxanthine-guanine phosphoribosyltransferase (HPRT) was used as a reference gene due to the relatively low baseline levels of BMP6 in these cells. The HPRT gene is reported as a constitutively expressed housekeeping gene with low mRNA levels, which makes it suitable as an endogenous mRNA control in RT-PCR for highly sensitive quantification of low copy mRNAs (Pernas-Alonso et al., 1999). Quantitative RT-PCR was performed using the iCycler iQ Real-Time PCR Detection System (Bio-Rad). Reactions were performed in a volume of 25 μl using the iQ SYBR Green Supermix (Bio-Rad) according to the manufacturer's instructions.

For immunoblot analysis of samples from human or mouse brains, briefly as previously described (Cole et al., 1988; Masliah et al., 2000), 0.1 g of frozen tissue

Table 5.2. *Oligonucleotide sequences used as primers for qRT-PCR in human and mouse brains, and rat NPCs.*

Gene ID	Accession	Primer F (5'→ 3')	Primer R (5'→ 3')
BMP2 (human)	NM 001200	GCCCTCATCAAGGGTTGGAA	TGCGTGTTGGGCAAAAAGTT
BMP2 (rat)	NM 017178	ATGCTGTGTCCCCACTGAGC	GCAACCCTCCACAACCATGT
BMP6 (human)	NM 001718	CGTGAAGGCAATGCTCACCT	CCTGTGGCGTGGTATGCTGT
BMP6 (rat)	NM 013107.1	GCACACATGAATGCCACCAA	CAGCATGGTTTGGGGACGTA
BMP6 (murine)	NM 007556	AAGACCCGGTGGTGGCTCTA	CTGTGTGAGCTGCCCTTGCT
BMP7 (human)	NM 001719.2	CAAGCTGTGCAGGCAAAACC	TGGCTGGTAGGCGCTCATAA
BMP7 (rat)	XM 342591	TCTCTCACTGCCCACCTTGG	CCACGGTGTGCTCAGGTTTC
β-Actin (human)	NM 001101.3	CTATCCAGGCTGTGCTATC	TACTCGAGGCACAGTGTGGGTGACC
β-Actin (murine)	NM 007393	CCGTGAAAAGATGACCCAGA	AGGCATACAGGGACAGCACA
HPRT (rat)	NM 012583	GACAGCGGCAAGTTGAATCTACA	CAAAAGGGACGCAGCAACAG

was homogenized in 500 μL of a detergent-free HEPES-based lysis buffer (1.0 mM HEPES, 5.0 mM Benzamidine, 2.0 mM 2-Mercaptoethanol, 3.0 mM EDTA, 0.5 mM Magnesium Sulfate, 0.05% Sodium Azide; final pH 8.8) that facilitates separation of membrane and cytosolic fractions. Fresh protease and phosphatase inhibitor cocktails (Calbiochem, San Diego, CA) were added to all lysis buffers. Following a brief centrifugation step to clear nuclei and cell debris, total homogenates were then centrifuged for 1 hr at 100,000 rpm at 4°C. Supernatants were saved (cytosolic fraction) and the pellets (membrane fraction) were resuspended in 500 μL HEPES lysis buffer. For immunoblot analysis of cell homogenates, adherent cells in culture were lysed in buffer composed of 10 mM Tris-HCl (pH 7.4), 150 mM NaCl, 5 mM EDTA (TNE) containing 1% Triton-X 100 to obtain total cell lysates. For immunoblot analysis, cytosolic and membrane fractions from brain homogenates or total cell lysates were separated by gel electrophoresis on 4-12% Bis-Tris gels (Invitrogen, Carlsbad, CA) and blotted onto 0.45 μm PVDF membranes (Millipore, Temecula, CA). Immunoblots were probed with antibodies against secreted BMP6 (mouse monoclonal, RnD Systems, Minneapolis, MN) or BMP6 precursor (mouse monoclonal, Morph 6.1 clone, Millipore; or rabbit polyclonal, Abgent, San Diego, CA), Aβ (82E1 clone, specific for aa 1-16 of Aβ, IBL, Minneapolis, MN), or actin (Millipore) as a loading control as previously described (Rockenstein et al., 2001). Blots were imaged and analyzed with the VersaDoc gel imaging system and Quantity One software (Bio-Rad).

Immunohistochemical analysis. For analysis of levels of BMP6 and markers of neurogenesis in the hippocampus or cortex of AD patients and APP tg mice, brain sections were immunolabeled with the antibodies against BMP6 (mouse monoclonal from Millipore, or rabbit polyclonal from Abgent), doublecortin (DCX, marker of migrating neuroblasts, goat polyclonal, Santa Cruz Biotechnology, Santa Cruz, CA), sex-determining region Y-box 2 (SOX2, marker of undifferentiated NPCs, mouse monoclonal), or BrdU (marker of proliferating cells labeled with BrdU, rat monoclonal, AbD Serotec, Raleigh, NC). BMP6 (1:500) and SOX2 (1:500) antibodies were detected with the Tyramide Signal Amplification™-Direct (Red) system (NEN Life Sciences, Boston, MA). DCX (1:50) and BrdU (1:100) antibodies were detected with fluorescein isothiocyanate (FITC)-conjugated secondary antibodies (1:75, Vector Laboratories, Burlingame, CA). A subset of sections immunolabeled with the monoclonal BMP6 antibody (1:500, Millipore) were co-labeled with the mouse monoclonal antibody against Aβ (clone 6E10, 1:500, Signet Laboratories, Dedham, MA) or DCX (1:50, Santa Cruz Biotechnology) detected with FITC-conjugated secondary antibodies (1:75, Vector Laboratories).

Sections were mounted under glass coverslips with ProLong Gold antifade reagent with DAPI (Invitrogen) and imaged with a Zeiss 63X (N.A. 1.4) objective on an Axiovert 35 microscope (Zeiss, Germany) with an attached MRC1024 laser scanning confocal microscope system (BioRad) (Masliah et al., 2000). All sections were processed simultaneously under the same conditions and the experiments were performed twice to assess reproducibility. To confirm the specificity of primary antibodies, control experiments were performed where sections were incubated

overnight in the absence of primary antibody (deleted) or primary antibody pre-incubated with blocking peptide.

For all immunolabeling studies, assessment of levels of immunoreactivity was performed utilizing the Image-Pro Plus program (Media Cybernetics, Silver Spring, MD). For each case or mouse a total of three sections (10 images per section) were analyzed in order to estimate the average number of immunolabeled cells per unit area (mm^2) or the average intensity of the immunoreactive signal (corrected pixel intensity).

NPC culture and neuronal differentiation assay. Adult rat hippocampal NPCs (generously provided by F. Gage, Salk Institute) were cultured routinely for expansion essentially as previously described (Ray and Gage, 2006) with some modifications. Briefly, cells were grown for expansion in DMEM/F12 media (Mediatech, Manassas, VA) containing B27 supplement, 1X L-glutamine and 1X antibiotic-antimycotic (all from Invitrogen). For induction of neuronal differentiation, cells were plated onto poly-ornithine/laminin (Sigma-Aldrich) coated plates or coverslips and transferred the next day to differentiation media containing N2 supplement (Invitrogen), 1 μM all-trans retinoic acid (Sigma-Aldrich), 5 μM forskolin (Sigma-Aldrich) and 1% FBS. Cells were differentiated for four days, and fresh differentiation media was added at day 2.

In vitro *cell treatments and proliferation, viability and toxicity assays.* For determination of the effects of Aβ exposure on BMP6 expression levels, cultured

NPCs were treated with recombinant Aβ. Adult rat hippocampal NPCs were plated for differentiation and cultures were exposed on day 3 of differentiation (24 hr incubation) with freshly solubilized $A\beta_{1-42}$ (1 μM, American Peptide, Sunnyvale, CA). This concentration of Aβ was selected because it was determined to be sub-lethal in this cell type and is within the range of Aβ concentrations utilized in previous *in vitro* studies investigating the effects of Aβ on neurogenesis (Haughey et al., 2002a; Haughey et al., 2002b). Cells were harvested on day 4 by cell lysis and total protein or RNA was harvested and prepared for immunoblot or qRT-PCR analyses, respectively.

For determination of the effects of BMP6 on cell proliferation, viability and toxicity, NPCs were exposed to recombinant BMP6 (50-100 ng/mL, BioVision, Mountain View, CA) throughout the duration of *in vitro* differentiation (four days). Media was changed and fresh recombinant BMP6 added at day 2 of differentiation. A subset of samples were treated with BrdU for 24 hours prior to the differentiation endpoint and analyzed using a Cell Proliferation Assay kit (Calbiochem) according to the manufacturer's instructions. Additional experiments were performed to assess potential toxicity of BMP6 treatment using the CellTiter MTT-based Viability Assay (Promega, Madison, WI) and the LDH-based CytoTox Assay (Promega).

Statistical analysis. All experiments were performed blind coded and in triplicate. Values in the figures are expressed as means ± SEM. To determine the statistical significance, values were compared by student's t-test or by one-way ANOVA with post-hoc Dunnett's test when comparing differences in AD cases or

APP tg mice compared to controls. The differences were considered to be significant if p values were less than 0.05.

Results

BMP6 Levels are Elevated in the Dentate Gyrus of AD Patients and Accumulate Around Plaques in the Hippocampus

In order to analyze the expression levels of a panel of BMPs in the brains of AD patients, samples from the hippocampus were homogenized and processed for qRT-PCR and immunoblot analyses. Since our comparison of gene array studies from the literature identified BMPs 2, 6 and 7 as potential candidate regulators of neurogenesis in the adult brain, we focused on these three for analysis in human brain.

In order to first screen mRNA levels of these BMPs, qRT-PCR analysis was performed with primers specific for BMP2, BMP6, BMP7, and actin as a control (Table 5.2, Figure 5.1). This analysis showed that of the three BMPs measured, only BMP6 mRNA levels (Figure 5.1B) were significantly increased in the brains of patients with early and severe AD compared to non-demented controls. There was a trend towards increased BMP2 levels only in patients with severe AD, but the differences were not significant compared to controls (Figure 5.1A). BMP7 levels were similar among all three groups (Figure 5.1C). Because of the significant, and trend towards a stage-dependent, increase in BMP6 mRNA levels in patients with AD, we selected this protein for further analysis of protein levels by immunohistochemistry and immunoblot.

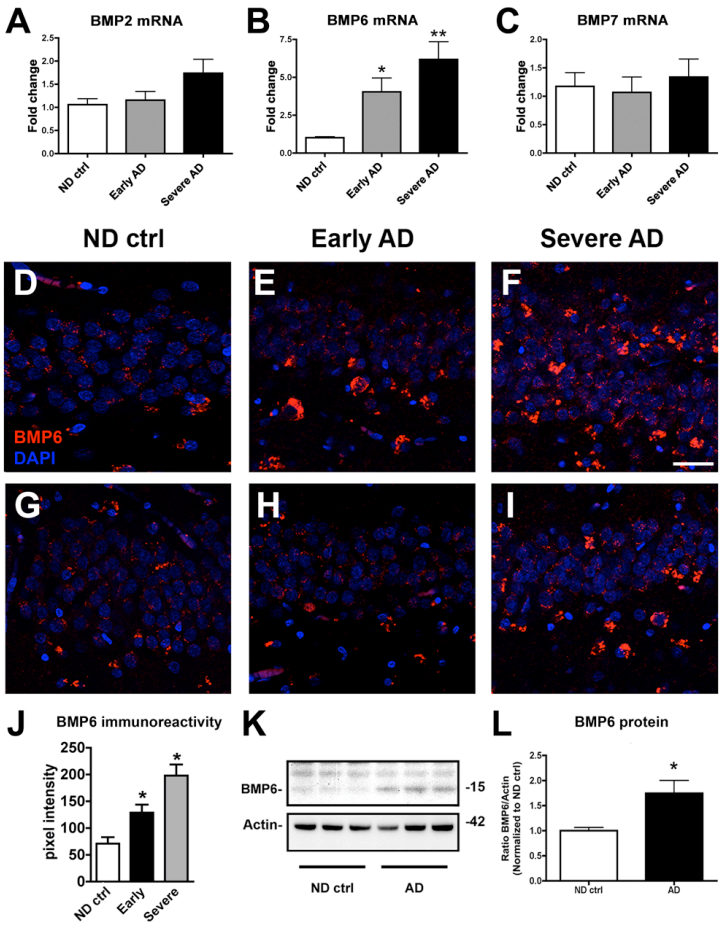

Figure 5.1 *qRT-PCR, immunohistochemical and immunoblot analyses of BMP levels in the hippocampus of AD patients.* In order to screen for changes in BMP expression levels in AD brains, mRNA was extracted from the hippocampus of age-matched non-demented control (ND ctrl) and AD brains and prepared for qRT-PCR analysis. (A-C) Levels of BMP2 (A), BMP6 (B) and BMP7 (C) mRNA were measured and corrected for β-actin levels as a control. Of the three BMPs studied, only levels of BMP6 mRNA (B) were significantly increased in the brains of AD patients compared to non-demented control cases. For immunohistochemical analysis, panels D-F depict representative immunolabeling with a mouse monoclonal antibody against BMP6 (Millipore), and panels G-I show representative immunolabeling with a rabbit polyclonal antibody against BMP6 (Abgent). All images are from the dentate gyrus, and sections were co-stained with DAPI (blue) to label cell nuclei. Scale bar = 40 μm for all images. (D-F) Immunohistochemical analysis with a monoclonal antibody against BMP6 (detected with Tyramide Red) showed that BMP6 protein levels were increased in the hippocampus of AD brains in a severity-dependent manner compared to non-demented controls (ND ctrl). (G-I) Immunohistochemical analysis with a polyclonal antibody against BMP6 (detected with Tyramide Red) showed a similar pattern of immunoreactivity and confirmed that BMP6 protein levels were increased in the hippocampus of AD brains compared to controls. (J) Semi-quantitative analysis of levels of BMP6 immunoreactivity by immunohistochemistry with the Millipore antibody. (K) Representative immunoblot analysis with the Millipore antibody showing increased BMP6 expression in homogenates from the hippocampus of AD patients compared to non-demented controls. (L) Semi-quantitative analysis of levels of BMP6 as measured by immunoblot in hippocampal brain homogenates confirmed increased BMP6 immunoreactivity in the hippocampus of AD patients compared to controls. (N=3 cases per group, *$p < 0.05$ and **$p < 0.01$ compared to non-demented controls by one-way ANOVA with post-hoc Dunnett's test).

To characterize the patterns of upregulation of BMP6 expression in the brains of AD patients, immunohistochemical analysis was performed. For this purpose, sections from human brains were immunolabeled with monoclonal or polyclonal antibodies against BMP6 (Figure 5.1D-I).

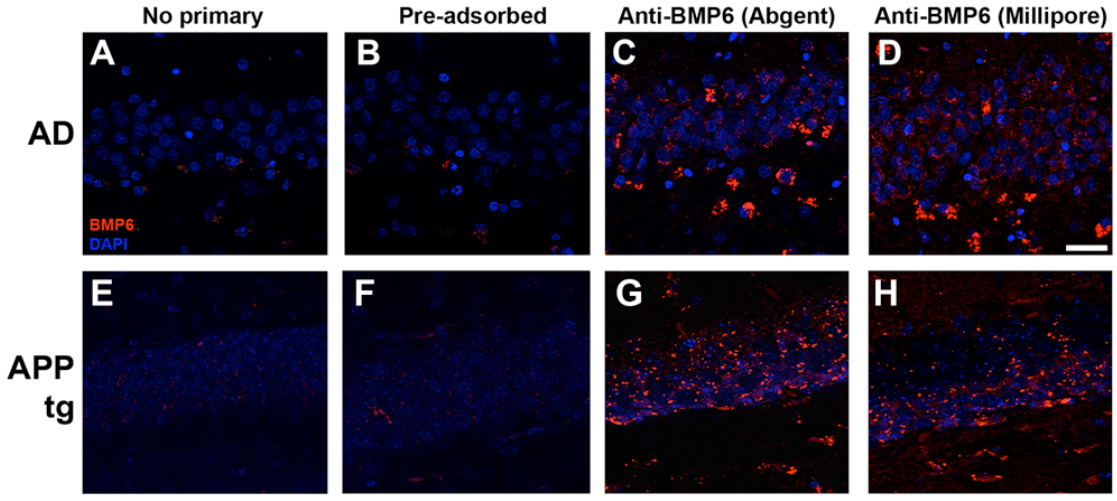

Figure 5.2 *Validation studies to examine the specificity of the BMP6 antibodies for immunohistochemistry.* Panels A-D depict immunolabeling of hippocampal sections from a representative AD case, and panels E-H show immunolabeling of sections from the brain of a representative APP tg mouse. Sections were incubated with no primary antibody (A, E), or with polyclonal antibody pre-incubated with a specific blocking peptide (B, F), or with polyclonal (Abgent, C, G) or monoclonal (Millipore, D, H) antibodies against BMP6. All images are from the dentate gyrus, and sections were co-stained with DAPI (blue) to label cell nuclei. Scale bar = 30 μm for all images. (A, B) Immunolabeling of AD hippocampal sections with no primary antibody (A), or with primary polyclonal BMP6 antibody pre-adsorbed with blocking peptide (B) showed only background immunoreactive signal. (C, D) Immunolabeling of AD hippocampal sections with polyclonal (C) or monoclonal (D) BMP6 antibodies showed similar patterns of immunoreactivity in the dentate gyrus. (E, F) Immunolabeling of APP tg mouse brain sections with no primary antibody (E), or with primary polyclonal BMP6 antibody pre-adsorbed with blocking peptide (F) showed only background immunoreactive signal. (G, H) Immunolabeling of APP tg mouse brain sections with polyclonal (G) or monoclonal (H) antibodies showed similar patterns of immunoreactivity in the dentate gyrus.

In order to verify the specificity of these antibodies in human brain tissue, control experiments were performed without primary antibody or with the antibody pre-adsorbed with blocking peptide (Figure 5.2A-D). Incubation of sections with no primary antibody (Figure 5.2A), or with primary polyclonal antibody pre-incubated with blocking peptide (Figure 5.2B) abolished the signal detected in hippocampal

sections from the brain of an AD patient. Similar patterns of immunoreactivity were observed with both a polyclonal (Figure 5.2C) and monoclonal (Figure 5.2D) antibody against BMP6.

In human brain sections from the hippocampus, BMP6 expression was detected in the cytoplasm of granular cells in the DG, and increased immunoreactivity with the BMP6 monoclonal antibody was observed in sections from patients with early or severe AD compared to non-demented controls (Figure 5.1D-F). Immunolabeling with a polyclonal antibody against BMP6 (Figure 5.1G-I) showed a similar pattern of immunoreactivity and increased levels of BMP6 in AD cases. Semi-quantitative image analysis of BMP6 immunoreactivity with the monoclonal antibody showed significantly increased levels of BMP6 protein in the hippocampus of AD patients compared to non-demented controls (Figure 5.1J). Moreover, increased levels of BMP6 corresponded with increased severity of disease in patients with early and severe AD (Figure 5.1J). Immunoblot analysis confirmed that levels of BMP6 were significantly increased in the hippocampus of AD patients compared to controls (Figure 5.1K, L).

To determine whether increased BMP6 levels in AD might be related to any pathological features of the disease, we assessed the localization of BMP6 immunoreactivity in relation to Aβ-containing plaques in hippocampal sections from the brains of AD patients (Figure 5.3A-F). Interestingly, double-immunohistochemical analysis with a monoclonal antibody against BMP6 and an antibody against Aβ (6E10) showed a striking halo-like pattern of BMP6 immunoreactivity surrounding

both diffuse (Figure 5.3A-C) and mature (Figure 5.3D-F) plaques located in the molecular and pyramidal layers of the hippocampus.

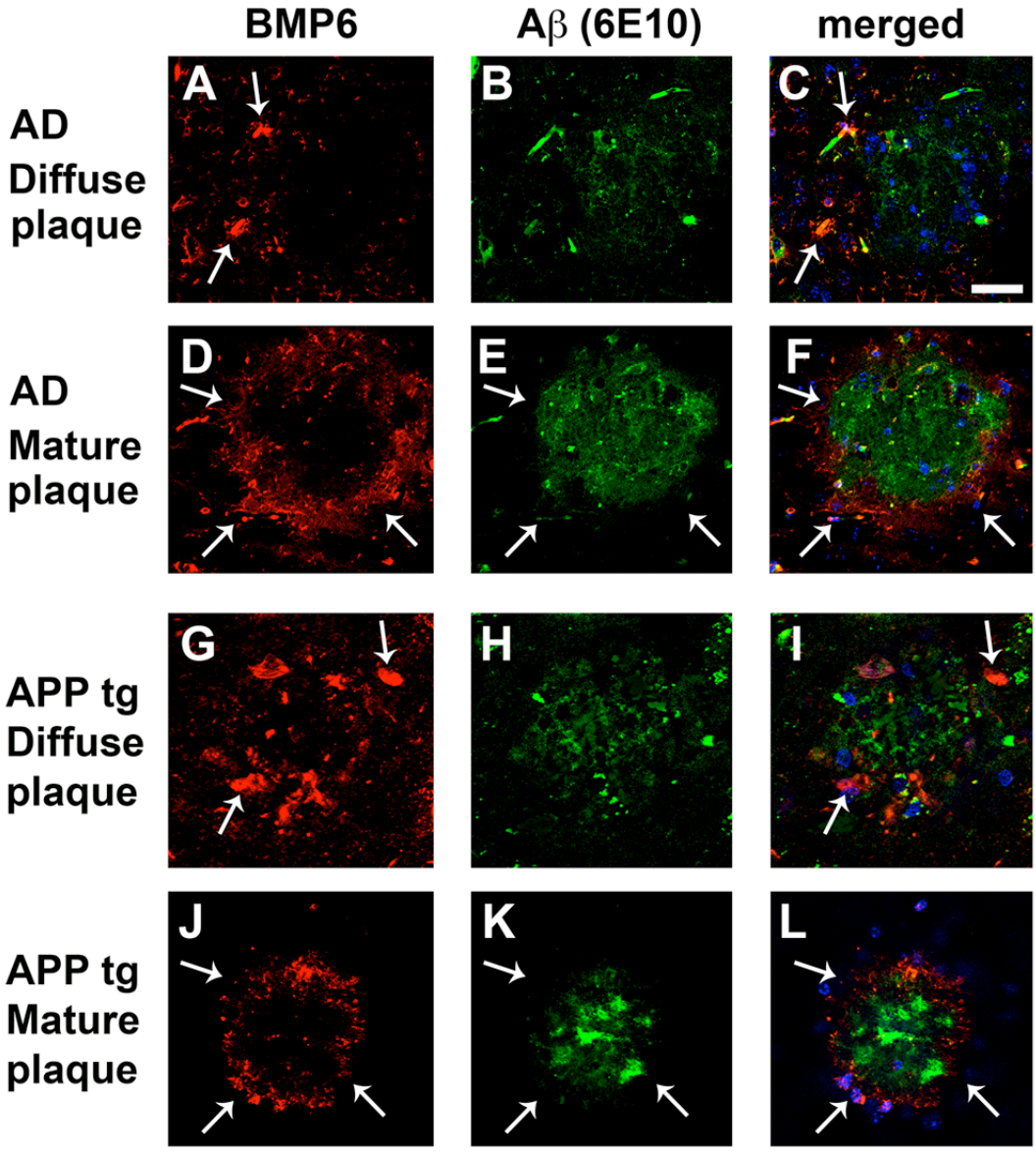

Figure 5.3 *BMP6 immunoreactivity surrounds plaques in the hippocampus of AD patients and APP tg mice.* Sections from the brains of severe AD cases or APP tg mice were immunolabeled with the monoclonal antibody against BMP6 (Millipore) detected with Tyramide Red and co-labeled with an antibody against Aβ (6E10, Signet) detected with a FITC-tagged secondary antibody. All images are from the hippocampus (molecular and pyramidal cell layers), and sections were co-stained with DAPI (blue) to label cell nuclei. Scale bar = 100 μm for all images. (A-F) Representative images showing BMP6 immunoreactivity (arrows, A, C, D, F) in a ring-like pattern surrounding Aβ-immunoreactive diffuse (A-C) and mature (D-F) plaques (arrows, E, F) in the brain of a human case with severe AD. (G-L) Representative images showing BMP6 immunoreactivity (arrows, G, I, J, L) surrounding Aβ-immunoreactive diffuse (G-I) and mature (J-L) plaques (arrows, K, L) in the brain of an APP tg mouse.

To assess whether the alterations in BMP6 expression levels were specific to the human hippocampus, or whether this effect could be detected in other non-neurogenic regions of the brain such as the cortex, immunohistochemical analysis was performed with samples from the cortex (layer V) of patients with AD and non-demented controls.

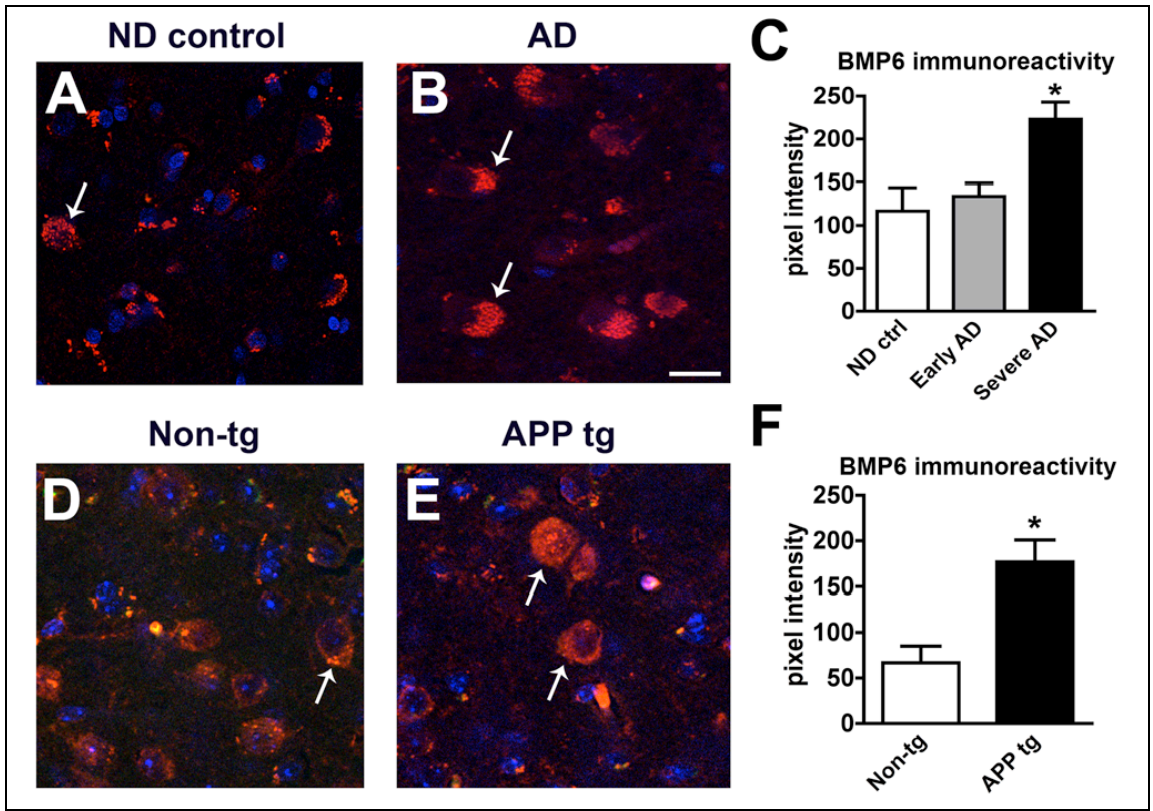

Figure 5.4 *Immunohistochemical analysis of BMP6 levels in the cortex of AD brains and APP tg mice.* Panels A and B show representative sections from the brains of human non-demented (ND) control and AD cases, and panels D and E show representative sections from the brains of non-tg and APP tg mice. Sections were immunolabeled with a monoclonal antibody against BMP6 (Millipore) detected with Tyramide Red. All images are from layer V of the cortex, and sections were co-stained with DAPI (blue) to label cell nuclei. Scale bar = 10 μm for all images. (A-C) BMP6 immunoreactivity (arrows, A, B) was increased in the cortex of AD cases compared to non-demented controls (N=3 cases per group, *$p < 0.05$ compared to non-demented controls by one-way ANOVA with post-hoc Dunnett's test). (D-F) BMP6 immunoreactivity (arrows, D, E) was increased in the cortex of APP tg mice compared to non-tg controls (N=4 animals per group, *$p < 0.05$ compared to non-tg controls by one-way ANOVA with post-hoc Dunnett's test).

Similar to the upregulation of BMP6 expression detected in the hippocampus, immunolabeling studies with the monoclonal antibody against BMP6 showed increased BMP6 immunoreactivity in the cortex of AD patients compared to controls (Figure 5.4A-C). Taken together, these results suggest that BMP6 levels may be increased across multiple brain regions.

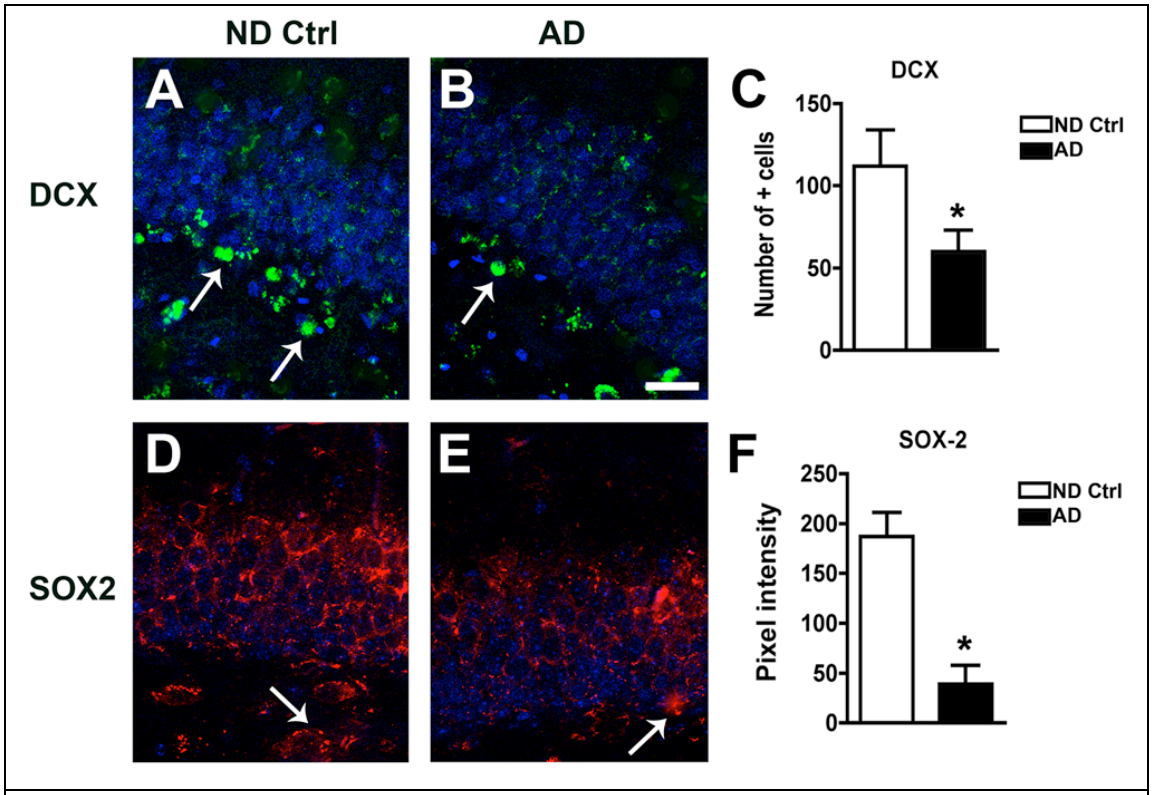

Figure 5.5 *Markers of neurogenesis are reduced in the brains of AD patients.* Sections from the hippocampus of age-matched non-demented control (ND ctrl) patients and severe AD cases were immunolabeled with antibodies against doublecortin (DCX) detected with a FITC-tagged secondary antibody, or sex-determining region Y-box 2 (SOX2) detected with Tyramide Red, and imaged by confocal microscopy. All images are from the dentate gyrus, and sections were co-stained with DAPI (blue) to label cell nuclei. Scale bar = 30 μm for all images. (A-B) Representative immunolabeling of sections from control and AD hippocampus show fewer DCX-positive cells (arrows) in AD brains compared to non-demented control brains. (C) Reduced numbers of DCX-positive cells were detected in the dentate gyrus of AD brains compared to controls. (D-F). Reduced SOX2 immunoreactivity (arrows, D, E) in AD brains compared to non-demented control brains. (N=3 cases per group, *$p < 0.05$ compared to non-demented controls by one-way ANOVA with post-hoc Dunnett's test).

Increased Hippocampal BMP6 Expression is Accompanied by Reduced Markers of Neurogenesis in AD

Given that BMPs have been shown to play an important role in embryonic neurogenesis (Mehler et al., 1997), it is possible that the increased hippocampal expression levels of the secreted protein BMP6 might directly target NPCs in this region. In order to determine whether increased BMP6 expression levels in AD brains might be accompanied by alterations in markers of neurogenesis, sections from the hippocampus of AD patients and non-demented controls were analyzed by immunohistochemistry with antibodies against the neuroblast marker DCX and the early NPC marker SOX2 (Figure 5.5). Image analysis showed that the numbers of DCX-positive cells (Figure 5.5A-C) and SOX2 immunoreactivity (Figure 5.5D-F) were significantly reduced in the DG of AD hippocampus compared to non-demented control cases.

In support of a role for increased BMP6 expression in defective neurogenesis in AD, double-immunohistochemical analysis of sections from the hippocampus of an AD patient showed that BMP6 immunoreactivity was detected in close proximity to, and within, some neurogenic DCX-positive cells in the SGZ (Figure 5.6A-C). Taken together, these results suggest that the impaired neurogenesis observed in the hippocampus of AD patients may be related to elevated levels of BMP6.

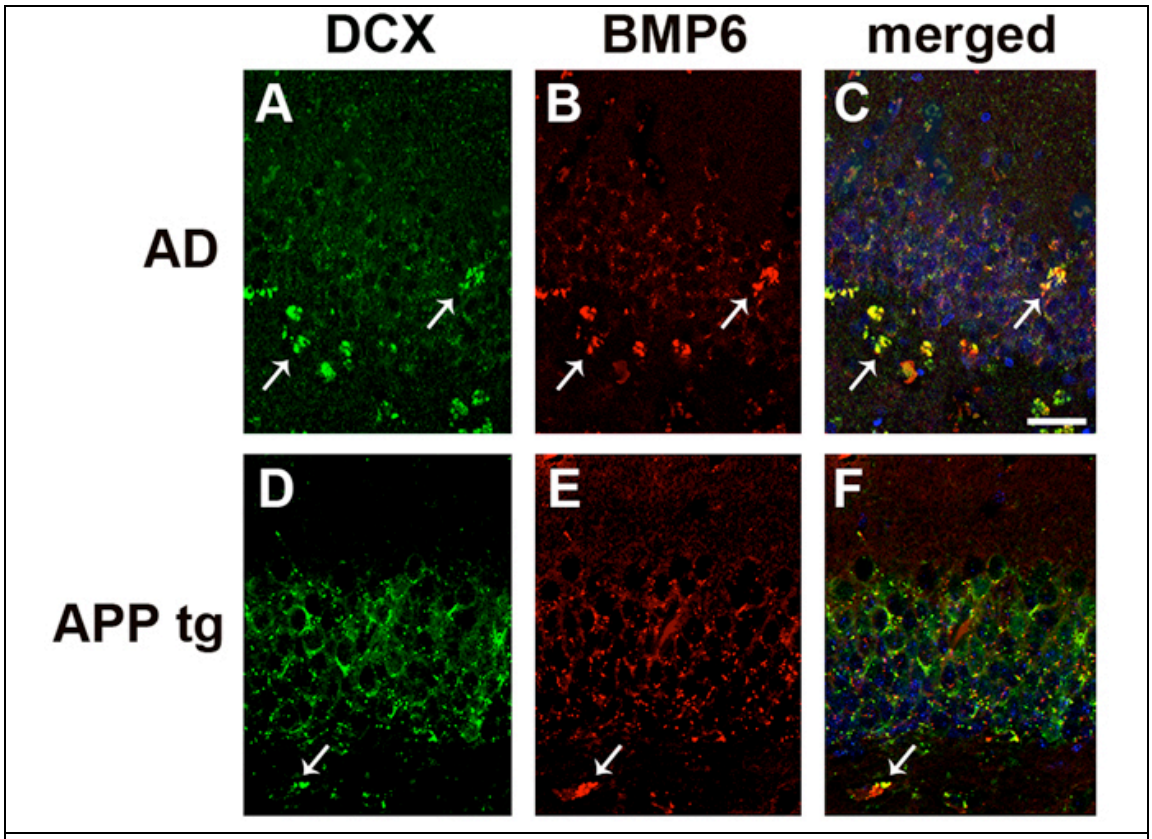

Figure 5.6 *Double-immunohistochemical analysis of BMP6 immunoreactivity and a marker of neurogenesis in the hippocampus of human AD cases and APP tg mice.* Panels A-C show a representative section from the brain of a human AD case, and panels D-F show a representative section from the brain of an APP tg mouse. Sections were immunolabeled with a monoclonal antibody against BMP6 (Millipore) detected with Tyramide Red and co-labeled with a polyclonal antibody against DCX (Santa Cruz) detected with a FITC-tagged secondary antibody. All images are from the hippocampal dentate gyrus, and sections were co-stained with DAPI (blue) to label cell nuclei. Scale bar = 30 μm for all images. (A-C) In the hippocampus of an AD patient, BMP6 immunoreactivity (arrows) was detected within and surrounding cells that were DCX-positive. (D-F) In the hippocampus of an APP tg mouse, BMP6 immunoreactivity (arrows) was detected within and surrounding cells that were DCX-positive.

Increased BMP6 Expression in the Dentate Gyrus of APP Tg Mice is Accompanied by Reduced Hippocampal Neurogenesis

To begin to understand the mechanisms involved in AD-associated elevation of BMP6 expression, protein and mRNA levels were measured in the brains of mice that express high levels of the human form of the Aβ precursor, APP. Similar to the results obtained in the brains of AD patients, qRT-PCR analysis showed that BMP6

mRNA levels were significantly increased in the brains of APP tg mice compared to non-tg controls (Figure 5.7B), but levels of BMP2 and BMP7 were unchanged (Figure 5.7A, C).

To assess protein levels of BMP6, immunohistochemical analysis was then performed with monoclonal or polyclonal antibodies against BMP6 (Figure 5.7D-G). In order to verify the specificity of these antibodies in mouse brain tissue, control experiments were performed without primary antibody or with the antibody pre-adsorbed with blocking peptide (Figure 5.2E-H). Incubation of brain sections with no primary antibody (Figure 5.2E) or with primary antibody pre-incubated with blocking peptide (Figure 5.2F) abolished the signal detected in sections from the brain of APP tg mice. Similar patterns of immunoreactivity were observed with both a polyclonal (Figure 5.2G) and monoclonal (Figure 5.2H) antibody against BMP6.

Immunohistochemical analysis with the monoclonal antibody against BMP6 demonstrated increased protein levels of BMP6 in the cytoplasm of DG granular cells in the hippocampus of APP tg mice compared to non-tg controls (Figure 5.7D, E). Additional analysis with a polyclonal antibody against BMP6 showed a similar pattern of immunoreactivity and increased expression in APP tg mice (Figure 5.7F, G).

Semi-quantitative image analysis of sections immunolabeled with the monoclonal antibody demonstrated a significant increase in BMP6 immunoreactivity in APP tg mouse hippocampus compared to non-tg controls (Figure 5.7G). Immunoblot analysis confirmed that BMP6 protein levels were increased in APP tg brains compared to controls (Figure 5.7H, I).

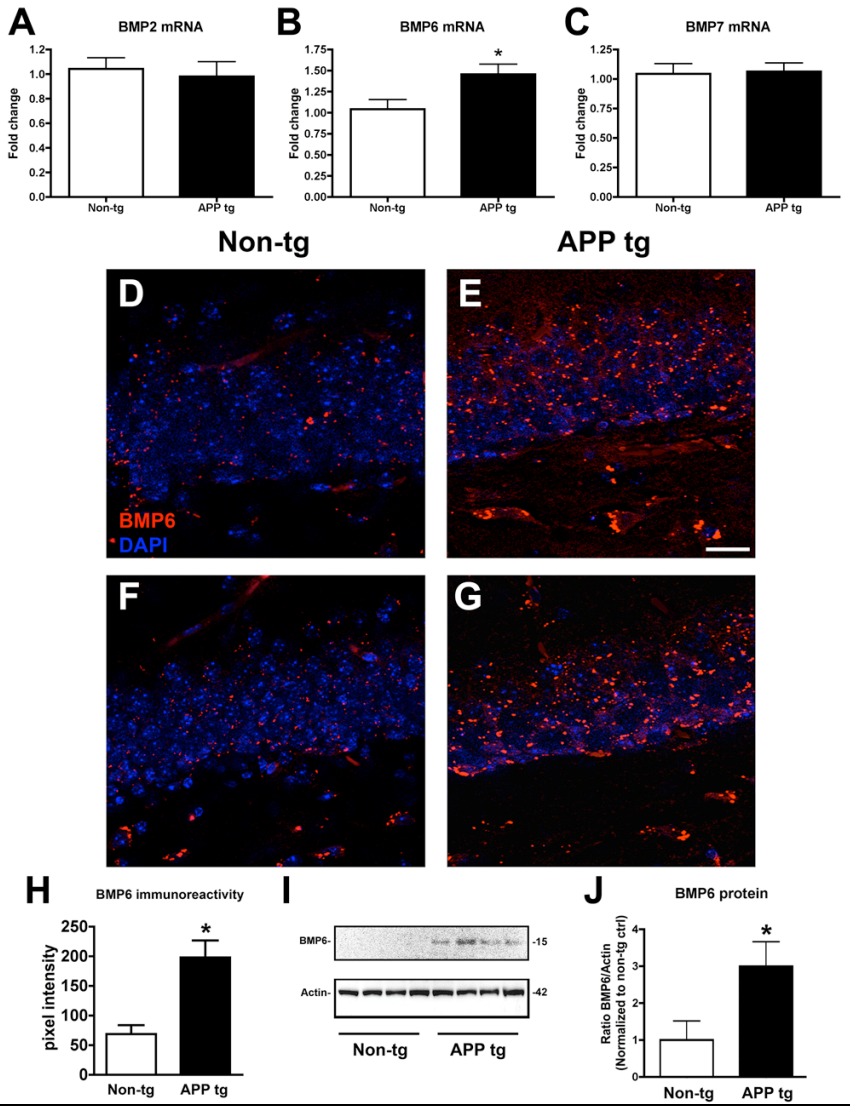

Figure 5.7 *qRT-PCR, immunohistochemical and immunoblot analyses of BMP levels in the brains of APP tg mice.* In order to screen for changes in BMP expression levels in APP tg mice, mRNA was extracted from the brains of 6-month old non-tg and APP tg mice and prepared for qRT-PCR analysis. (A-C) Levels of BMP2 (A), BMP6 (B) and BMP7 (C) mRNA were measured and corrected for β-actin levels as a control. Of the three BMPs studied, only levels of BMP6 mRNA (B) were significantly increased in the brains of APP tg mice compared to non-tg controls. For immunohistochemical analysis, panels D and E show representative immunolabeling with a mouse monoclonal antibody against BMP6 (Millipore), and panels F and G show representative immunolabeling with a rabbit polyclonal antibody against BMP6 (Abgent). All images are from the dentate gyrus, and sections were co-stained with DAPI (blue) to label cell nuclei. Scale bar = 30 μm for all images. (D, E) Immunohistochemical analysis with a monoclonal antibody against BMP6 showing increased BMP6 levels in the hippocampus of APP tg mice (E) compared to non-tg controls (D). (F, G) Immunohistochemical analysis with a polyclonal antibody against BMP6 showed a similar pattern of immunoreactivity and confirmed that BMP6 protein levels were increased in the hippocampus of APP tg mice (G) compared to non-tg controls (F). (H) Semi-quantitative analysis of levels of BMP6 immunoreactivity by immunohistochemistry with the Millipore antibody. (I, J) Immunoblot analysis showing that BMP6 protein levels were significantly increased in the hippocampus of APP tg mice compared to non-tg controls. (N=4 animals per group, *$p < 0.05$ compared to non-tg controls by one-way ANOVA with post-hoc Dunnett's test).

To determine whether BMP6 accumulated surrounding plaques in the hippocampus of APP tg mice similar to the distribution observed in AD patients, we characterized the patterns of BMP6 immunoreactivity in relation to Aβ-containing plaques in the hippocampus of APP tg mice (Figure 5.3G-L). Similar to the expression patterns observed in the hippocampus of AD patients, double-immunohistochemical analysis of brain sections from APP tg mice with a monoclonal antibody against BMP6 and an antibody against Aβ (6E10) showed a ring-like pattern of BMP6 immunoreactivity surrounding both diffuse (Figure 5.3G-I) and mature (Figure 5.3J-L) plaques located in the molecular and pyramidal layers of the hippocampus.

To assess whether the alterations in BMP6 expression levels were specific to the mouse hippocampus, or whether changes in BMP6 expression could be detected in other non-neurogenic regions of the brain such as the cortex, immunofluorescent images were obtained from the cortex (layer V) of non-tg and APP tg mouse brain sections immunolabeled with an antibody against BMP6 (Figure 5.4D-F). Similar to the upregulation of BMP6 expression observed in the hippocampus, immunolabeling studies with the monoclonal antibody against BMP6 showed increased BMP6 immunoreactivity in the cortex of APP tg mice compared to non-tg controls (Figure 5.4D-F).

To determine whether markers of neurogenesis were reduced in the hippocampus of APP tg mice as in the AD patients, immunohistochemical analysis was performed with antibodies against BrdU, DCX, and SOX2 (Figure 5.8). In animals treated with BrdU, numbers of BrdU-positive cells were significantly reduced in the DG of APP tg mice compared to non-tg controls (Figure 5.8A-C). Similarly, the

numbers of DCX-positive cells (Figure 5.8D-F) and SOX2 immunoreactivity (Figure 5.8G-I) were reduced in the DG of APP tg mice compared to non-tg controls.

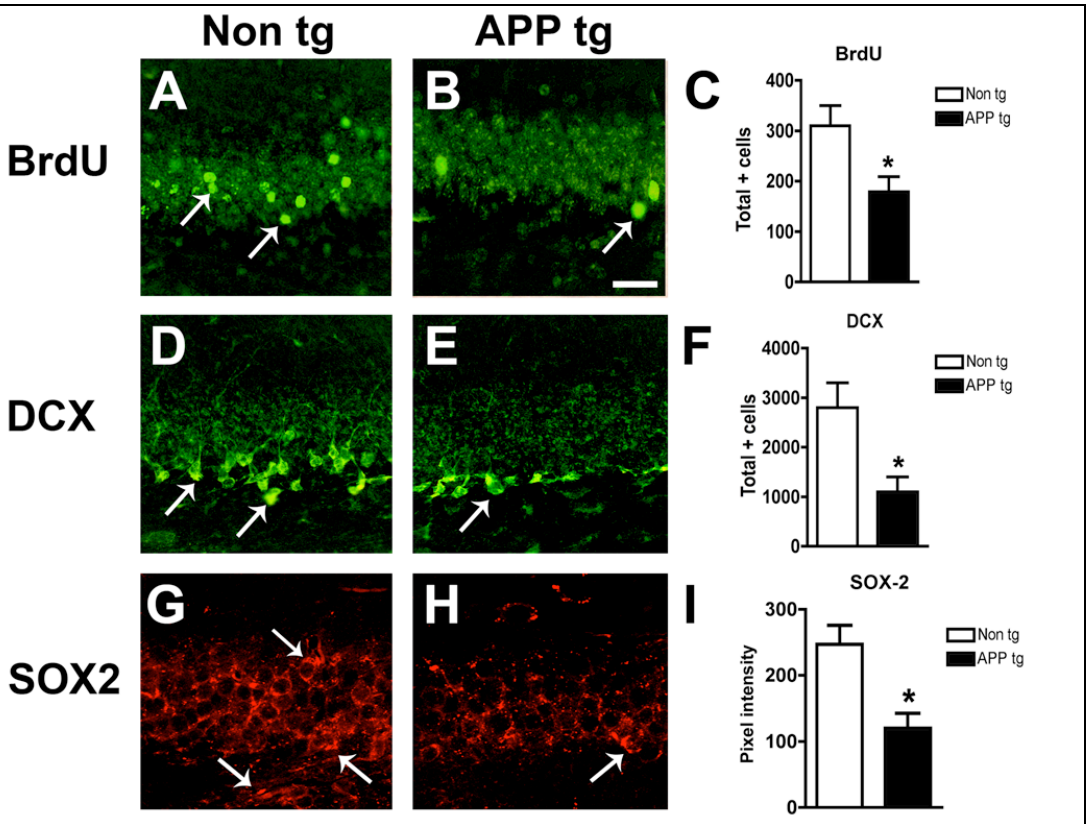

Figure 5.8 *Markers of neurogenesis are reduced in the brains of APP tg mice.* Sections from the brains of 6-month old non-tg control and APP tg mice treated with BrdU were immunolabeled with antibodies against BrdU or doublecortin (DCX) detected with FITC-tagged secondary antibodies, or sex-determining region Y-box 2 (SOX2) detected with Tyramide Red and imaged by confocal microscopy. All images are from the hippocampal dentate gyrus. Scale bar = 30 μm for all images. (A-C) Fewer BrdU-positive cells (arrows, A, B) were detected in the brains of APP tg mice compared to non-tg controls. (D-E) Fewer DCX-positive cells (arrows, D, E) were detected in the brains of APP tg mice compared to non-tg controls. DCX-positive cells and processes were observed throughout the granular cell layer in non-tg control brains (D), but in APP tg mice DCX-positive cells and processes were less prominent, and were primarily observed only in the subgranular zone (E, arrow). (F) Reduced numbers of DCX-positive cells in the dentate gyrus of APP tg mice compared to non-tg controls. (G-I) Reduced SOX2 immunoreactivity in the dentate gyrus of APP tg mice compared to non-tg controls. SOX2-immunoreactivity (arrows, G) was observed throughout the granular cell layer in the hippocampus of non-tg mice (uppermost arrow in G) but to a lesser extent in APP tg mice (arrow, H). (N=4 animals per group, *$p < 0.05$ compared to non-tg controls by one-way ANOVA with post-hoc Dunnett's test).

In support of a role for increased BMP6 expression in defective neurogenesis in APP tg mice, double-immunohistochemical analysis of brain sections from APP tg

mice showed that BMP6 immunoreactivity was detected in close proximity to, and within, some neurogenic DCX-positive cells in the SGZ (Figure 5.6D-F). Taken together, these results in APP tg mice suggest that abnormal elevation of BMP6 expression in the pathogenesis of AD may play a role in defective adult hippocampal neurogenesis.

Aβ Exposure Results in Increased BMP6 Expression in NPCs *In Vitro*

To further investigate the molecular mechanisms that mediate increased BMP6 expression in AD hippocampus and in APP tg mouse brains, we sought to determine whether BMP6 expression might be augmented as a direct result of exposure to Aβ protein. For this purpose, cultured adult rat hippocampal NPCs were treated with recombinant $A\beta_{1-42}$ for 24 hrs, and BMP6 mRNA and protein levels were measured by qRT-PCR and immunoblot, respectively. These studies showed that treatment with $A\beta_{1-42}$ resulted in a significant approximately 25% increase in BMP6 mRNA levels compared to vehicle-treated controls (Figure 5.9A) and a concomitant increase in protein levels (Figure 5.9B), suggesting that Aβ may directly modulate BMP6 expression. In the cell lysates of NPCs exposed to exogenous recombinant Aβ, multimeric forms (dimer, trimer) of Aβ were detected after 24 hrs exposure in addition to the Aβ monomer (Figure 5.9B), suggesting that aggregation of Aβ into small oligomers may play a role in the upregulation of BMP6 expression. These results support the possibility that increased levels of BMP6 may be regulated by the accumulation of Aβ protein in the brains of AD patients and in APP tg mice.

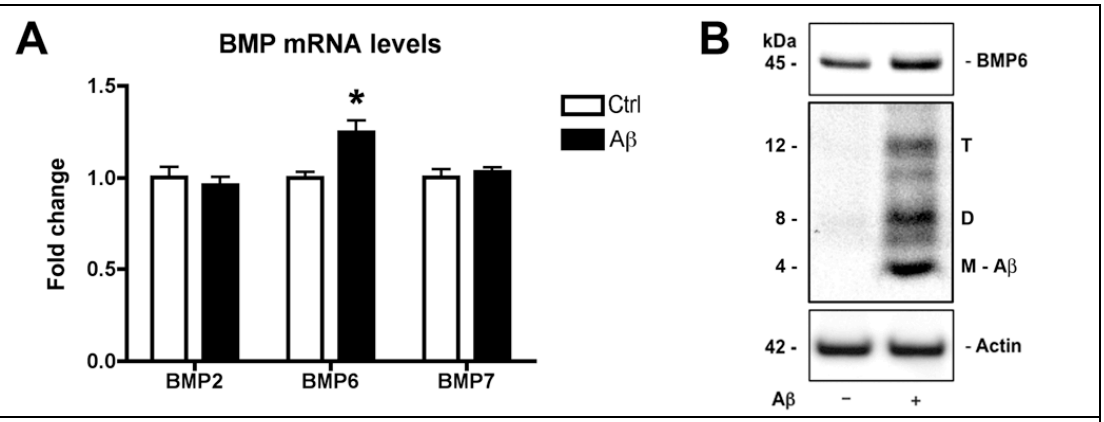

Figure 5.9 *Increased BMP6 expression in cultured NPCs treated with recombinant Aβ.* Adult rat hippocampal NPCs were cultured for four days under neuronal differentiation conditions, and treated with recombinant $A\beta_{1\text{-}42}$ or vehicle control (Ctrl) for the final 24 hrs of differentiation. mRNA levels of BMPs were analyzed by qRT-PCR and BMP6 protein expression was assessed by immunoblot. (A) mRNA levels of BMP2, BMP6 and BMP7 in Aβ-treated NPCs (normalized to levels of the reference gene hypoxanthine-guanine phosphoribosyltransferase [HPRT]). Only BMP6 levels were significantly increased in cultures exposed to Aβ (*$p < 0.05$ compared to vehicle-treated controls by Student's t-test). (B) Immunoblot analysis of BMP6 protein expression and Aβ accumulation. Increased levels of the BMP6 precursor protein were observed in Aβ-treated cell cultures. Multiple Aβ species (M, monomer; D, dimer; T, trimer) were detected in the cell lysates of cultures treated with Aβ. Actin was used as a loading control.

BMP6 Reduces Proliferation of NPCs *In Vitro*

In order to further investigate the possibility that increased BMP6 levels in the hippocampus *in vivo* might have an effect on endogenous NPCs, we studied the effects of recombinant BMP6 on cell proliferation and viability in an *in vitro* cell culture model of adult neurogenesis. For this purpose, cultured adult rat hippocampal NPCs were exposed to 50 or 100 ng/mL of recombinant BMP6 for four days under neuronal differentiation conditions. Live cell imaging demonstrated that treatment with BMP6 at both concentrations resulted in cultures with no noticeable morphological differences compared to controls (Figure 5.10A-C). Treatment with BMP6 resulted in a significant and dose-dependent reduction in cell proliferation as measured by BrdU

uptake (Figure 5.10D), and a decrease in overall mitochondrial activity as measured by MTT assay only with the higher dose of BMP6 (100 ng/mL) (Figure 5.10E).

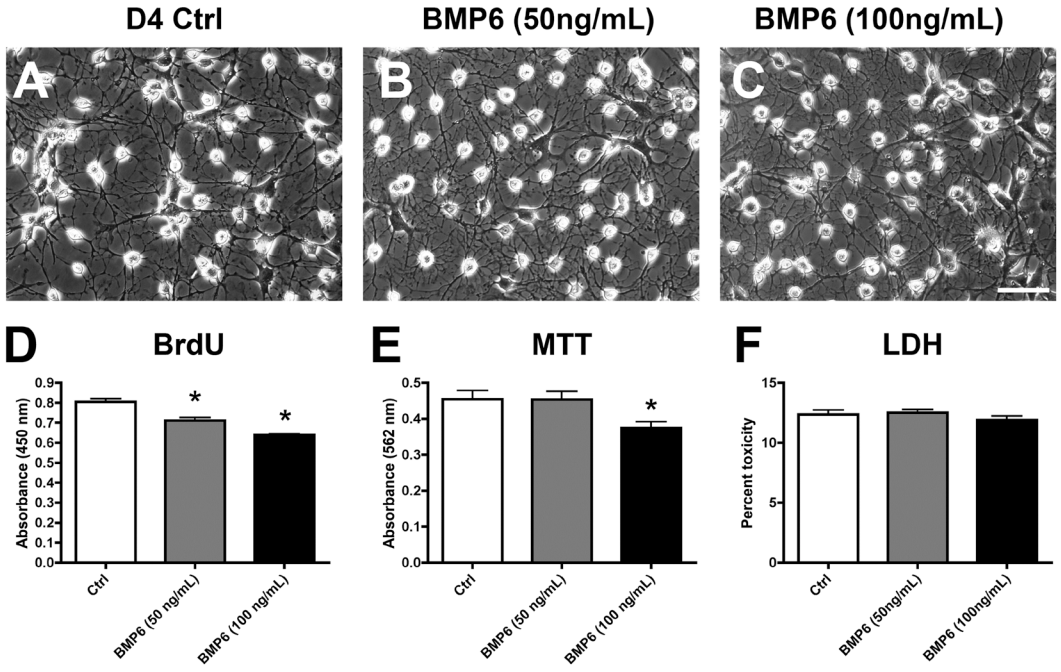

Figure 5.10 *Cell morphology and proliferation, viability and toxicity studies in cultured NPCs treated with BMP6.* Adult rat hippocampal NPCs were cultured for four days under neuronal differentiation conditions in the presence of recombinant human BMP6 or vehicle control (Ctrl), and analyzed by proliferation (BrdU uptake), viability (MTT) and toxicity (LDH release) assays. (A-C) Phase contrast images showing the morphology of live cell cultures after four days of differentiation and treatment with BMP6. Scale bar = 30 μm for all images. (D) BMP6 exposure resulted in a reduction of cell proliferation compared to vehicle-treated controls, as shown by reduced BrdU uptake. (E) Mitochondrial activity was reduced only in cultures treated with the higher (100 ng/mL) dose of BMP6, as shown by MTT assay. (F) BMP6 treatment did not significantly affect cell toxicity, as shown by LDH assay (*$p < 0.05$ compared to vehicle-treated controls by one-way ANOVA with post-hoc Dunnett's test).

These results suggest that BMP6 treatment might decrease cell numbers by reducing proliferation or because of a toxic effect. In order to test the latter possibility, measurements of levels of LDH release were taken and showed no significant differences (Figure 5.10F). Taken together, these results support the possibility that BMP6 directly interferes with neurogenesis by modulating NPC proliferation.

DISCUSSION

The present study showed that levels of BMP6 were increased approximately two to four-fold in the hippocampus of patients with AD and in APP tg mice compared to controls, however no significant differences were detected in the mRNA levels of two other BMPs, BMP2 and BMP7. A striking pattern of BMP6 distribution was also observed in plaque-containing regions of the hippocampus in both AD patients and APP tg mice, where Aβ-containing plaques were surrounded by a ring-like pattern of BMP6 immunoreactivity. Since BMP6 is a secreted protein, and its primary reported role in the brain is in regulating developmental neurogenesis, it is possible that abnormally elevated levels of this protein in AD might affect adult neurogenesis in the hippocampus.

It is important to note that neurogenesis persists in the aged brain, however its rate declines with increasing age, as revealed by previous studies in rodents (Kempermann et al., 1998; Kuhn et al., 1996), non-human primates (Gould et al., 1999), and humans (Cameron and McKay, 1999). Despite this natural decline with age, previous studies have shown that the adult brain remains responsive to therapeutic interventions that enhance neurogenesis (Jin et al., 2003; Wise, 2003). Understanding the molecular mechanisms involved in AD-related alterations in neurogenesis might help guide the development of new therapies in this direction. Interestingly, paralleling the decline in both the pool of NPCs and their proliferative potential in AD, the levels of various neurotrophic factors, including brain-derived neurotrophic factor (BDNF), stem cell factor (SCF), and neurosteroids among others, are deregulated in AD and FAD-linked models (Laske et al., 2008; Weill-Engerer et al., 2002); for review see

(Schindowski et al., 2008)). These studies suggest that the neurogenic niche is dramatically altered in the pathogenesis of AD, and other growth factors may be aberrantly expressed as well.

In support of the possibility that alterations in BMP6 expression in AD may deregulate adult neurogenesis, we showed that markers of neurogenesis were altered in the hippocampus of AD patients and APP tg mice compared to controls. Furthermore, in an *in vitro* model of adult hippocampal neurogenesis, we showed that exposure to Aβ protein upregulated BMP6 expression levels, and treatment with recombinant BMP6 reduced NPC proliferation.

The members of the BMP family of growth factors belong to various subclasses distinguished by amino acid sequence similarity, and approximately 20 unique BMP ligands have been identified to date (Wordinger and Clark, 2007). Although the primary function of many of the BMPs is in osteogenesis, the class 1 (BMP2/4) and class 2 (BMP5/6/7/8) families have been previously implicated in CNS development and disease. For example, BMPs are important regulators of embryonic neurogenesis (Mehler et al., 1997) and during embryonic brain development, the inhibition of these growth factors promotes neurogenesis (Nakashima and Taga, 2002). The canonical role of BMPs in the developing brain is to promote glial differentiation via Smad signaling (Mehler et al., 1997), and previous studies have shown that BMP2 induces astrocyte differentiation in mouse embryonic neuroepithelial cell cultures (Fukuda et al., 2007; Fukuda and Taga, 2005; Gross et al., 1996). BMPs have been implicated in embryonic (Mehler et al., 1997) and adult neurogenesis (Colak et al., 2008), and BMP activity has been shown to regulate

synaptic plasticity in the adult hippocampus (Sun et al., 2007), however the role of BMPs in neurodegenerative disorders in less clear.

In support of a role for BMPs in AD, two recent publications have shown that BMP4 levels are increased in the brains of an animal model of AD (Li et al., 2008b; Tang et al., 2009). High levels of BMP4 were associated with reduced neurogenesis in the DG of mice expressing mutant forms of APP and presenilin-1 (PS1) (Li et al., 2008b; Tang et al., 2009). Increased BMP4 expression was accompanied by reduced expression of the BMP inhibitor Noggin (Tang et al., 2009), however the precise mechanisms through which BMP4 levels are increased during the pathogenesis of AD remain unclear.

In contrast to the defective neurogenesis observed in association with elevated levels of BMPs in AD (present study and (Li et al., 2008b; Tang et al., 2009)), another related protein, BMP7 (osteogenic protein-1), has been proposed to have neuroregenerative capacity in acute CNS injury. BMP7 has been shown to be neuroprotective against nigrostriatal toxicity in a 6-hydroxydopamine rat model of Parkinson's disease (Harvey et al., 2004) and is under investigation as a potential therapy in acute CNS injuries such as stroke (Chou et al., 2006; Kawabata et al., 1998; Ren et al., 2000). Interestingly, both BMP7 and its receptors are upregulated after acute CNS injury or stroke (Chang et al., 2003; Charytoniuk et al., 2000; Harvey et al., 2005; Lewen et al., 1997), suggesting that the increased expression of BMP7 post-injury might represent a protective response. Interestingly, another recent study showed that BMP6, but not BMP7, is protective against apoptosis triggered by acute potassium withdrawal in cerebellar granule neurons (Barneda-Zahonero et al., 2009).

Taken together, it is possible that acute upregulation of BMP expression may be a compensatory response that is protective in the short term, while chronic upregulation of BMPs in the AD mouse models may result in defective neurogenesis possibly via modification of expression or function of receptors and downstream signaling pathways. Moreover, it may be important to exercise caution in long-term therapeutic studies utilizing BMPs in acute CNS injury, as it is possible that elevated levels of these factors may have negative side-effects on adult neurogenesis.

Since our results show that BMP6 is specifically increased in a mouse model overexpressing APP, it is possible that APP or APP products such as Aβ might play a role in producing the abnormal levels of BMP6. The precise transcriptional regulators involved remain to be determined, however the present data show that treatment with exogenous Aβ up-regulates expression of BMP6, and it is possible that Aβ may stimulate signaling pathways that activate transcription of BMP6. In the *in vitro* Aβ preparations, multiple species including monomers, dimers and trimers were detected after 24 hours of exposure. This is consistent with the predominant Aβ species detected in human AD and APP tg mouse brains, where most recent studies suggest that relatively small oligomers are responsible for the synaptotoxic effects of Aβ (Lacor et al., 2004). In this context, it is possible that these smaller oligomeric species may also be responsible for alterations in neurogenesis, however future studies will be necessary to elucidate the precise species that modulate BMP6 expression and neurogenesis. Previous studies have shown that BMP6 production is transcriptionally regulated by hormones such as estrogen (Zhang et al., 2005) and glucocorticoids (Liu et al., 2004). Although increased glucocorticoid production has been identified as an

early feature in AD pathogenesis that specifically targets the hippocampus (Dhikav and Anand, 2007), it is unknown whether Aβ or its oligomeric aggregates might interact with glucocorticoid receptors, and future studies will be necessary to elucidate the precise transcription factors involved in Aβ-mediated regulation of BMP6 expression.

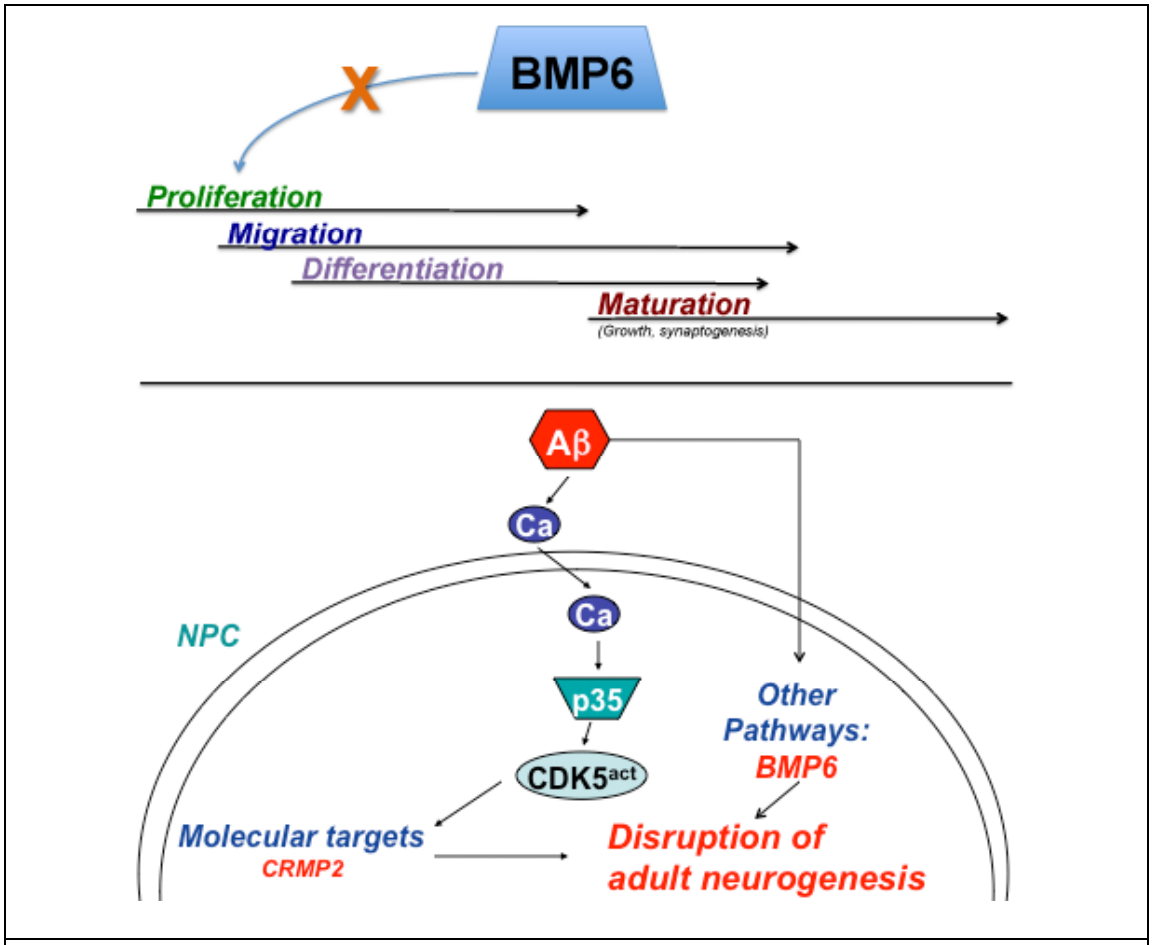

Figure 5.11 *Schematic model of the role of BMP6 in Aβ-mediated defective proliferation of NPCs that might contribute to impaired neurogenesis in AD.*

In addition to uncovering a potential link between elevated levels of BMP6 and reduced neurogenesis in AD brains and APP tg mice, the present study suggests that the increased levels of BMP6 observed in the hippocampus of AD patients and APP tg

mice might directly impair the proliferation of hippocampal NPCs (Figure 5.11). In this context, we showed that treatment with recombinant BMP6 in an *in vitro* model of adult neurogenesis reduced proliferation without an overt toxic effect, however understanding the precise downstream pathways that impair NPC proliferation will require further investigation. We propose that normalization of BMP expression in models of AD may present a novel therapeutic approach for protecting against the neurogenic alterations in AD.

Taken together, the data presented here suggest that increased levels of BMP6 in AD might directly interfere with the process of adult neurogenesis in the hippocampus (Figure 5.11). We also demonstrated that BMP6 protein levels were increased in the non-neurogenic cortex, suggesting that the observed changes in BMP6 expression may occur in multiple brain regions. This could be specific to regions that are more severely affected by AD-related pathological alterations, or it could be a global effect. For the present study, we focused on the effects of increased BMP6 expression on neurogenic cells because of the known role of BMP6 in embryonic neurogenesis, however future studies will be necessary to elucidate the impact of increased BMP6 expression on mature neuronal circuitries in non-neurogenic brain regions.

In both neurogenic and non-neurogenic regions of the brain, APP products such as Aβ may be responsible for increased BMP production, possibly via receptor-mediated transcriptional regulation. Moreover, BMPs might have a neuroprotective effect during the acute phase of CNS injury, but in chronic neurodegenerative processes such as AD they may contribute to pathophysiology. Further investigation

will be necessary to elucidate the precise mechanisms involved in regulating BMP expression in AD and the effects on NPCs in the adult hippocampus, and in future studies BMPs may be important targets for therapeutic intervention to rescue the neurogenic deficits associated with the pathogenesis of AD.

ACKNOWLEDGEMENTS

Chapter 5, in full, has been submitted for publication of the material as it may appear in the Journal of Neuroscience 2010. Crews L, Adame A, Patrick C, DeLaney A, Pham E, Rockenstein EM, Masliah E; Society for Neuroscience, 2010.

The work in Chapter 5 was supported by NIH grants AG18440, AG5131, AG022074 and AG11385.

CHAPTER 6

DEFECTIVE NEUROGENESIS IN AN ANIMAL MODEL OF FAD IS RESCUED BY TREATMENT WITH A NEUROTROPHIC COMPOUND

ABSTRACT

Cerebrolysin (CBL) is a peptide mixture with neurotrophic effects that might reduce the neurodegenerative alterations in Alzheimer's disease (AD). We have previously shown that in the amyloid precursor protein (APP) tg mouse model of AD, CBL improves synaptic plasticity and behavioral performance. However the mechanisms are not completely clear. The neuroprotective effects of CBL might be related to its ability to promote neurogenesis in the hippocampal subgranular zone (SGZ) of the dentate gyrus (DG). To study this possibility, tg mice expressing mutant APP under the Thy-1 promoter were injected with BrdU and treated with CBL for 1 and 3 months.

Compared to non tg controls, vehicle-treated APP tg mice showed decreased numbers of BrdU-positive (+) and doublecortin+ (DCX) neural progenitor cells (NPC) in the SGZ. In contrast, APP tg mice treated with CBL showed a significant increase in BrdU+ cells, DCX+ neuroblasts and a decrease in TUNEL+ and activated caspase-3 immunoreactive NPC. Cerebrolysin did not change the number of proliferating cell nuclear antigen+ (PCNA) NPC or the ratio of BrdU+ cells converting to neurons and astroglia in the SGZ cells in the APP tg mice. The neurogenic effects of CBL were accompanied by reduced levels of active cyclin-dependent kinase-5 (CDK5) and

glycogen synthase kinase-3β (GSK3β) (but not stress-activated protein kinase-1 [SAPK1]). Taken together, these studies suggest that CBL might rescue the alterations in neurogenesis in APP tg mice by protecting NPC, decreasing the rate of apoptosis, and normalizing the activity of some signaling pathways that contribute to neurodegneration and defective neurogenesis in AD. Moreover, the improved neurogenesis in the hippocampus of CBL-treated APP tg mice might play an important role in enhancing synaptic formation and memory acquisition.

INTRODUCTION

Considerable progress has been made in recent years towards better understanding the pathogenesis of Alzheimer's disease (AD), a common dementing disorder of the aging population that affects over 2.5 million individuals in the US and Europe alone. This neurological condition is characterized by widespread neurodegeneration throughout the association cortex and limbic system, deposition of Aβ in the neuropil and around the blood vessels, and formation of neurofibrillary tangles (NFT) (Terry et al., 1994). The neurodegenerative process in the initial stages of AD targets the synaptic terminals (Masliah, 1995) and then propagates to axons and dendrites, leading to neuronal dysfunction and eventually to neuronal death in later stages of disease (Hyman and Gomez-Isla, 1994). Although the precise mechanisms leading to neurodegeneration in AD are not completely understood, recent studies suggest that alterations in the processing of amyloid precursor protein (APP), resulting in the accumulation of amyloid-β protein (Aβ) and APP C-terminal products, might play a key role in the pathogenesis of AD (Kamenetz et al., 2003; Sinha et al., 2000).

Several products are derived from APP through alternative proteolytic cleavage pathways, and enormous progress has recently been made in identifying the enzymes involved (Cai et al., 2001; Luo et al., 2001; Selkoe, 1999; Sinha et al., 1999; Vassar et al., 1999).

Various lines of evidence suggest that the direct abnormal accumulation of Aβ oligomers in the nerve terminals might lead to the synaptic damage and ultimately to neurodegeneration in AD (Selkoe, 1999). More recent studies have uncovered evidence suggesting that another component to the neurodegenerative process in AD might include the possibility of interference with the process of adult neurogenesis in the hippocampus (Tatebayashi et al., 2003). In transgenic (tg) animal models of AD, previous studies have shown significant alterations in the process of adult neurogenesis in the hippocampus (Chevallier et al., 2005; Dong et al., 2004; Donovan et al., 2006; Jin et al., 2004a; Wen et al., 2004). Moreover, previous studies have shown that neurogenesis in the mature brain is important in the process of synaptic plasticity and memory formation in the hippocampus (van Praag et al., 2002). Therefore, compounds capable of protecting synapses and promoting neurogenesis might hold a serious promise in the development of new treatments for AD.

The nootrophic agent Cerebrolysin™ (CBL, a mixture of peptides and amino acids obtained from porcine brain tissue) has been shown to improve memory in patients with mild to moderate cognitive impairment (Ruther et al., 1994a; Ruther et al., 1994b). In support of these observations, it has also been shown to display neurotrophic activity *in vitro* (Mallory et al., 1999) and in animal models of neurodegeneration (Francis-Turner and Valouskova, 1996; Masliah et al., 1999;

Veinbergs et al., 2000). Moreover, CBL has been shown to ameliorate the neurodegenerative alterations and amyloid burden in an APP model of AD-like pathology (Rockenstein et al., 2002). We have recently shown that CBL might reduce the amyloid pathology by decreasing APP production and proteolysis (Rockenstein et al., 2006). Although the regulatory effects of CBL on APP might contribute to the neuroprotective effects of this compound, it is possible that other mechanisms might also be involved. Among them, considerable interest has developed in the potential role of neurogenesis on the effects of neuroprotective compounds (Chen et al., 2006; Tatebayashi et al., 2003). Thus, CBL might ameliorate the neurodegenerative process in AD by stimulating neurogenesis in the adult hippocampus. In this context, the main objective of this study was to investigate the effects of CBL on neurogenesis in the hippocampus of APP tg mice and to better understand the mechanisms involved.

MATERIALS AND METHODS

Generation of APP tg mice, BrdU regimen and CBL treatment. The tg mice generated express mutated human (h)APP751 under the control of the mThy-1 promoter (mThy1-hAPP751) and, for this study, the highest expresser (line 41) tg mice were used (Rockenstein et al., 2001). These tg mice are unique in that, compared to other tg models, amyloid plaques are found in the brain at a much earlier age (beginning at 3 months) (Rockenstein et al., 2001). The first area in the brain to show amyloid deposition is the frontal cortex at 3 months, followed by the hippocampus. In this latter brain region, amyloid deposits occur at 4-6 months of age in the molecular and pyramidal layers but not in the subgranular zone (SGZ) of the dentate gyrus.

Genomic DNA was extracted from tail biopsies and analyzed by PCR amplification, as described previously (Rockenstein et al., 1995). Transgenic lines were maintained by crossing heterozygous tg mice with non-transgenic (non tg) C57BL/6 x DBA/2 F1 breeders. All mice were heterozygous with respect to the transgene. A total of 24 (3-month old) tg mice and 12 non tg littermates were utilized for the present study. Each mouse received 5 injections (one per day) with 5-bromo-2-deoxyuridine (BrdU, Sigma-Aldrich, St. Louis, MO) at 50 mg/kg followed by treatment with vehicle or CBL. For all experiments, saline was utilized as the vehicle control. The 24 tg mice were divided into two groups, for the first, mice were treated for one month with daily intraperitoneal (IP) injections of either vehicle (n=6) or CBL (5 ml/kg) (n=6); for the second mice were treated for 3 months with either vehicle (n=6) or CBL (5 ml/kg) (n=6). The non tg mice were treated for one month with either vehicle (n=6) or CBL (5 ml/kg) (n=6). At the end of this period mice were sacrificed for analysis of neurogenesis and neuropathological assessment. All experiments described were approved by the animal subjects committee at the University of California at San Diego (UCSD) and were performed according to NIH recommendations for animal use.

Tissue processing. In accordance with NIH guidelines for the humane treatment of animals, mice were anesthetized with chloral hydrate and flush-perfused transcardially with 0.9% saline. Brains were removed and divided sagitally. One hemibrain was post-fixed in phosphate-buffered 4% paraformaldehyde (pH 7.4) at 4°C

for 48 hr and sectioned at 40 μm with a Vibratome 2000 (Leica, Germany), while the other hemibrain was snap frozen and stored at -70°C for protein analysis.

Analysis of neurodegeneration and Aβ deposits. To evaluate neurodegeneration and response to CBL, blind-coded 40 μm thick vibratome sections were immunolabeled with the mouse monoclonal antibodies against synaptophysin (SYN, presynaptic terminal marker, 1:40, Chemicon, Temecula, CA), NeuN (general neuronal marker, 1:1000, Chemicon), and glial fibrillary acidic protein (GFAP, marker of astrogliosis, 1:1000, Chemicon), as previously described (Rockenstein et al., 2003; Rockenstein et al., 2006). After overnight incubation with the primary antibodies, sections were incubated with FITC-conjugated horse anti-mouse IgG secondary antibody (1:75, Vector Laboratories, Burlingame, CA), transferred to SuperFrost slides (Fisher Scientific, Tustin, CA) and mounted under glass coverslips with anti-fading media (Vector). All sections were processed under the same standardized conditions. The immunolabeled blind-coded sections were imaged with the laser-scanning confocal microscope (LSCM, MRC1024, BioRad, Hercules, CA) and analyzed with the Image 1.43 program (NIH), as previously described (Mucke et al., 1995; Toggas et al., 1994) to determine the percent area of the neuropil covered by SYN-immunoreactive terminals and the levels of GFAP immunoreactivity (pixel intensity) in the dentate gyrus (DG). For counting of NeuN cells in the DG, digitized confocal images collected according to the optical disector method were analyzed with the Image-Pro Plus 4.0 (Media Cybernetics, Silver Spring, MD) software as previously described (Chana et al., 2006; Chana et al., 2003).

For detection of Aβ deposits, briefly as previously described, vibratome sections were incubated overnight at 4°C with the mouse monoclonal antibody 4G8 (1:600, Senetek, Napa, CA), followed by incubation with a fluorescein isothiocyanate (FITC)-conjugated anti-mouse IgG (Vector Laboratories). Sections were imaged with the LSCM (MRC1024, BioRad) as described previously (Mucke et al., 2000) and digital images were analyzed with the NIH Image 1.43 program to determine the percent area occupied by Aβ deposits. Three immunolabeled sections were analyzed per mouse and the average of individual measurements was used to calculate group means.

Immunocytochemical analysis of markers of neurogenesis and cell death. For detection of markers of neurogenesis, briefly vibratome sections oriented in the sagittal plane were pre-treated with 50% formamide/ 2xSSC (2xSSC: 0.3 M NaCl, 0.03 M sodium citrate) at 65°C, rinsed for 5 minutes in 2xSSC, then incubated for 30 minutes in 2M HCl at 37°C, followed by a 10-minute rinse in 0.1M boric acid, pH 8.5. Then sections were incubated with antibodies against BrdU (marker of dividing cells; rat monoclonal, 1:100, Oxford Biotechnology, Oxford, UK), proliferating cell nuclear antigen (PCNA, marker of proliferation; mouse monoclonal, 1:250, Santa Cruz Biotechnology, Inc., Santa Cruz, CA) or doublecortin (DCX, marker of migrating neuroblasts; goat polyclonal, 1:500, Santa Cruz Biotechnology) overnight at 4°C. Sections were then incubated with biotinylated secondary antibodies directed against rat, mouse, or goat. Following intermittent rinses in tris-buffered saline (TBS), avidin-biotin-peroxidase complex was applied (ABC Elite kit, Vector) followed by

peroxidase detection with diaminobenzidine (DAB) in 0.01% H_2O_2, 0.04% NiCl in TBS.

For analysis of the proportion of BrdU-positive (+) cells converting into neurons or astroglial cells, double immmunofluorescence labeling was performed with antibodies against BrdU and NeuN, and BrdU and GFAP. For this purpose, vibratome sections were treated to denaturate the DNA as described above. Afterwards a combination of the two antibodies was applied in TBS-donkey serum for 48 hours at 4°C, followed by incubation with secondary fluorochrome antibodies as previously described, transferred to SuperFrost slides (Fisher Scientific, Tustin, CA) and mounted under glass coverslips with anti-fading media (Vector). To investigate the relationship between neurogenesis and markers of AD-like pathology, vibratome sections were double-labeled with monoclonal antibodies against Aβ (4G8, 1:500, Senetek) or human APP (8E5, 1:5000, courtesy of Elan Pharmaceuticals) and the polyclonal antibody against DCX (1:500, Santa Cruz Biotechnology). All sections were processed under the same standardized conditions. The immunolabeled blind-coded sections were imaged with the LSCM (MRC1024, BioRad).

For detection of apoptosis of neural progenitor cells, the terminal deoxynucleotidyl transferase dUTP Nick End Labeling (TUNEL) detection method using the ApopTag *In Situ* Apoptosis Detection Kit (Chemicon) was used with modifications for free floating sections as described previously (Biebl et al., 2000; Biebl et al., 2005; Cooper-Kuhn and Kuhn, 2002). Detection was performed with Avidin-FITC and sections were mounted under glass coverslips with anti-fading media (Vector) for confocal microscopy analysis. To verify that NPC undergo

apoptosis, sections were double-labeled with a monoclonal antibody against activated caspase-3 (1:200, Stressgen Bioreagents, Ann Arbor, MI) and the polyclonal antibody against DCX (1:500, Santa Cruz Biotechnology), followed by incubation with fluorochrome-labeled secondary antibodies and imaging on the LSCM.

Quantitative analysis of neurogenesis in the hippocampus. For this purpose, a systematic, random counting procedure, similar to the optical disector (Gundersen et al., 1988), was used as described previously (Williams and Rakic, 1988). For the purpose of the present study the morphometric analysis was focused on the subgranular zone (SGZ) of the DG. This area corresponds to the layer of NPCs located directly under the first layer of mature granular cells in the DG, which in addition to the SGZ, includes the granular cell layer and the molecular layer (ML). The analysis was centered on the SGZ because a previous study has shown that this is the area most consistently affected in APP tg mice (Donovan et al., 2006). To determine the number of BrdU+, DCX+, PCNA+ or TUNEL+ cells in the SGZ of the hippocampus, every sixth section (200-µm interval) of the left hemisphere was selected from each animal and processed for immunohistochemistry. The reference volume was determined by tracing the areas using a semi-automatic stereology system (Stereoinvestigator, MicroBrightField, Colchester, VT). Positive cells were counted within a 60 x 60 µm counting frame, which was spaced in a 300 x 300 µm counting grid. Positive profiles that intersected the uppermost focal plane (exclusion plane) or the lateral exclusion boundaries of the counting frame were not counted. The total counts of positive

profiles were multiplied by the ratio of reference volume to sampling volume in order to obtain the estimated number of positive cells for each structure.

To determine the frequency of neuronal and astroglial differentiation of newborn cells, as previously described (Chevallier et al., 2005; Winner et al., 2004), a series of every sixth section (200-µm interval) was examined using the LSCM equipped with a 63 x PL APO oil objective (1.25 numeric aperture) and a pinhole setting that corresponded to a focal plane of 2 µm or less. On average, 50 BrdU+ cells were analyzed in the SGZ for neuronal differentiation. BrdU+ cells were randomly selected and analyzed by moving through the z-axis of each cell, in order to exclude false double labeling due to an overlay of signals from different cells.

Immunoblot Analysis of Kinases. Briefly as previously described (Rockenstein et al., 2005b), levels of activation of enzymes that phosphorylate APP and regulate APP maturation and processing was determined by Western blot analysis with antibodies that detect the phosphorylated forms of SAPK1 (SAPK1-p, 1:1000, Cell Signaling Technology, Beverly, MA), CDK5 (CDK5-p, rabbit polyclonal, 1:1000, Santa Cruz Biotechnology) and GSK3β (GSK3β-p, mouse monoclonal, 1:1000, Cell Signaling Technology). While the antibodies against SAPK1-p (phosphorylated at amino acid residues threonine 183 and tyrosine 185) and CDK5-p (phosphorylated at amino acid residues tyrosine 15) recognize the activated forms of these enzymes, the one against GSK3β-p (phosphorylated at amino acid residue serine 9) identifies the inactivated kinase. Additional immunoblot analysis was performed with antibodies against total SAPK1 (rabbit polyclonal, 1:1000, Cell Signaling Technology), total

CDK5 (rabbit polyclonal, 1:1000, Santa Cruz Biotechnology), the CDK5 activator p35 (1:1000, Santa Cruz Biotechnology), and total GSK3β (mouse monoclonal, 1:1000, Santa Cruz Biotechnology). After overnight incubation with primary antibodies, membranes were incubated with secondary antibodies tagged with horseradish peroxidase (HRP, 1:5000, Santa Cruz Biotechnology, Inc., Santa Cruz, CA) and visualized by enhanced chemiluminescence and analyzed with a Versadoc XL imaging apparatus (BioRad, Hercules, CA). Analysis of actin levels was used as loading control.

Statistical analysis. Analyses were carried out with the StatView 5.0 program (SAS Institute Inc., Cary, NC). Differences among means were assessed by one-way ANOVA with post-hoc Dunnett's (when comparing to the non tg control group) or Tukey-Kramer (when comparing between treatment groups). Comparisons between 2 groups were done with the two-tailed unpaired Student's t-test. Correlation studies were carried out by simple regression analysis and the null hypothesis was rejected at the 0.05 level. All values are expressed as mean +/- SEM.

RESULTS

Cerebrolysin's neuroprotective effects are associated with increased numbers of BrdU+ and DCX+ cells in the SGZ of APP tg mice

To investigate the effects of CBL in hippocampal neurogenesis, 3 month old APP tg mice received a series of five BrdU injections and then were treated for 1 and 3 months with CBL, and levels of markers of neurogenesis were analyzed in the SGZ.

Compared to vehicle-treated non tg mice (Figure 6.1a, b; 6a, b), vehicle-treated APP tg mice displayed a significant decrease in the numbers of BrdU+ (Figure 6.1a, d) [$F(2,11) = 6.24$, $p<0.02$] and DCX+ (Figure 6a, d) [$F(2,11) = 4.94$, $p<0.05$] cells. In contrast, APP tg mice treated with CBL displayed comparable numbers of BrdU+ (Figure 6.1a, e) and DCX+ (Figure 6.2a, e) cells compared to CBL-treated non tg controls (Figure 6.1a, c; 6.2a, c).

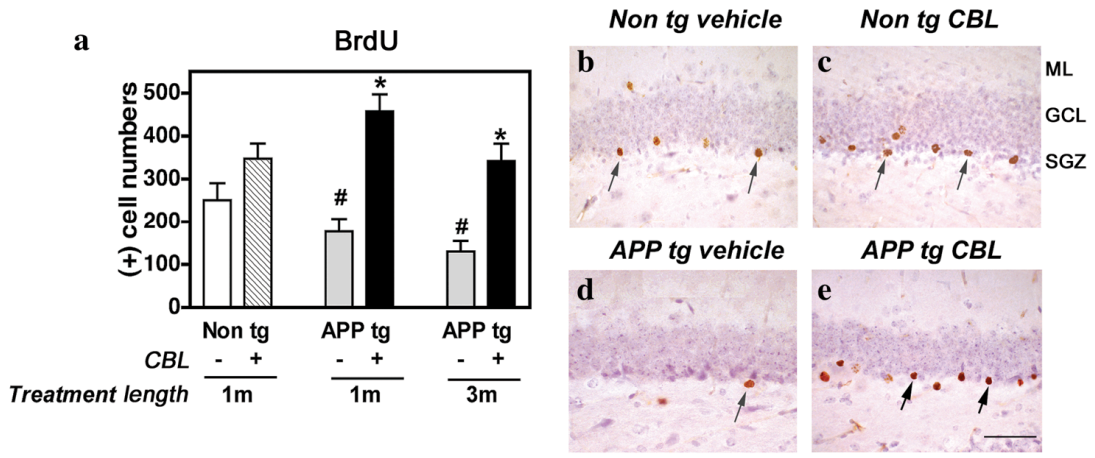

Figure 6.1 *Immunocytochemical analysis of 5-bromo-2-deoxyuridine (BrdU)-positive (+) cells in non transgenic (non tg) and amyloid precursor protein (APP) tg mice treated with Cerebrolysin (CBL).* **a** Quantitative analysis using the disector method in the subgranular zone (SGZ) shows decreased numbers of BrdU+ neurons in vehicle-treated APP tg mice compared to non tg animals, while CBL-treated APP tg mice at 1 and 3 months (m) show increased levels of BrdU+ neurons compared to vehicle-treated APP tg animals. #$p < 0.05$ compared to vehicle-treated non tg control by one-way ANOVA with post-hoc Dunnett's ($n = 6$); *$p < 0.05$ compared to vehicle-treated APP tg mice by one-way ANOVA with post-hoc Tukey-Kramer ($n = 6$). **b-e** All panels are representative images displaying the molecular layer (ML), GCL (granular cell layer), and SGZ at 400X magnification of mice treated for 1 month. BrdU+ neurons in the SGZ of vehicle-treated non tg mice (**b**), CBL-treated non tg mice (**c**), vehicle-treated APP tg mice (**d**), CBL-treated APP tg mice (**e**). Scale bar = 60 μm.

Similar effects were observed after 1 and 3 months of treatment. Moreover, the numbers of BrdU+ cells [$F(3,18) = 21.05$, $p<0.001$] and DCX+ cells [$F(3,18) = 6.51$, $p<0.01$] were different between vehicle- and CBL-treated APP tg mice. In some cases, CBL-treated APP tg mice showed numbers of BrdU+ cells greater than the numbers in

vehicle-treated non tg mice (Figure 6.1a). Similarly, CBL-treated non tg mice had a slight increase in the numbers of BrdU+ cells when compared to the non tg vehicle-treated group (Figure 6.1a).

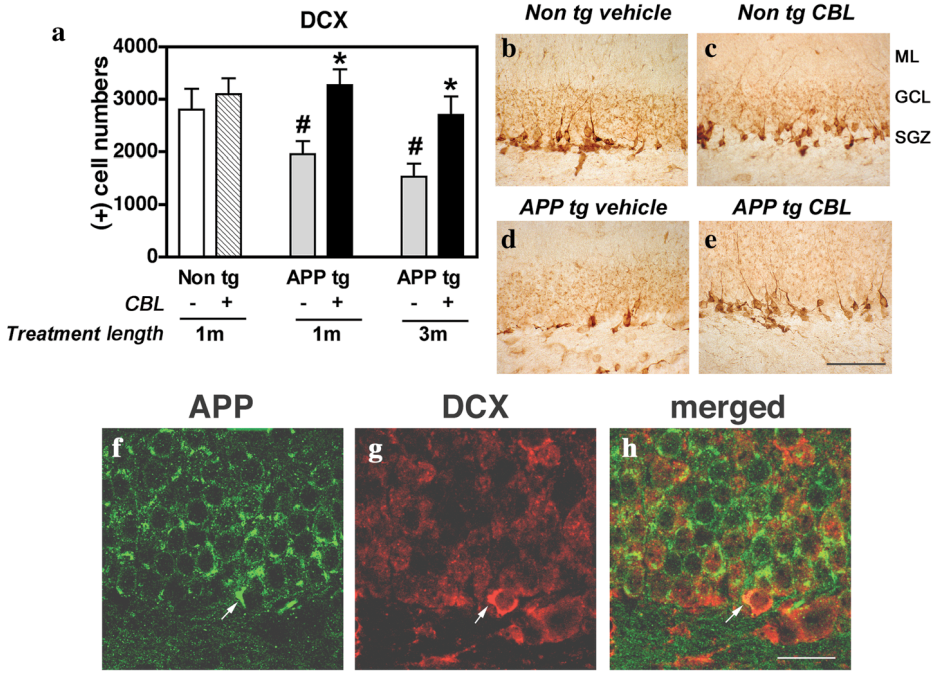

Figure 6.2 *Immunocytochemical analysis of doublecortin (DCX)-positive (+) cells in non transgenic (non tg) and amyloid precursor protein (APP) tg mice treated with Cerebrolysin (CBL).* **a** Quantitative analysis using the disector method in the subgranular zone (SGZ) shows decreased numbers of DCX+ neurons in vehicle-treated APP tg mice compared to non tg animals, while CBL-treated APP tg mice at 1 and 3 months (m) show increased levels of DCX+ neurons compared to vehicle-treated APP tg animals. #$p < 0.05$ compared to vehicle-treated non tg control by one-way ANOVA with post-hoc Dunnett's ($n = 6$); *$p < 0.05$ compared to vehicle-treated APP tg mice by one-way ANOVA with post-hoc Tukey-Kramer ($n = 6$). **b-e** All panels are representative images (400X) displaying the molecular layer (ML), GCL (granular cell layer), and SGZ of mice treated for 1 month. DCX+ neurons in the SGZ of vehicle-treated non tg mice (**b**), CBL-treated non tg mice (**c**), vehicle-treated APP tg mice (**d**), CBL-treated APP tg mice (**e**). *Scale bar* 60 μm. **f-e** All panels are representative images displaying the CGL and SGZ of a vehicle-treated APP tg mouse. Double-labeling analysis with antibodies against human APP (8E5, **f**) and DCX (**g**) shows colocalization (**h**) of the two markers in cells in the SGZ (arrows). Scale bar = 30 μm.

To investigate the relationship between APP expression and neurogenesis in the tg mice, double-labeled sections were analyzed with the confocal microscope. The APP tg mice express the human APP in the granular cell layer, moreover approximately

18% of the DCX+ NPC in the SGZ expressed human APP (Figure 6.2f-h). Amyloid deposits are observed at 4-6 months of age in the molecular layer of the DG but no deposits are detected in the SGZ in the vicinity of the NPC that are DCX+ (not shown).

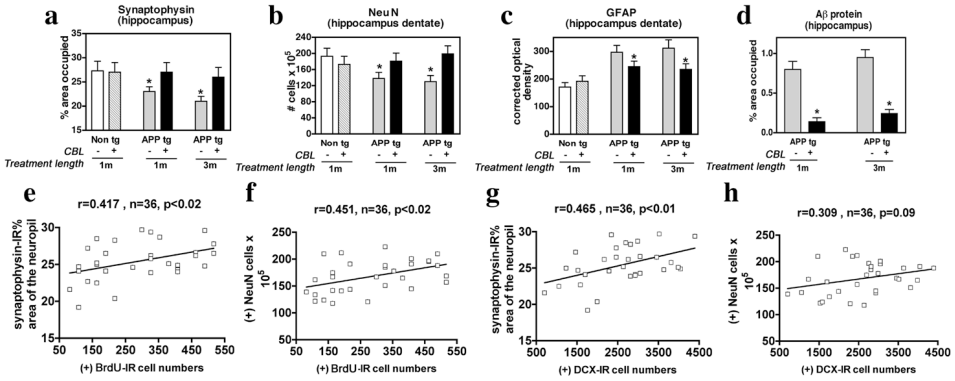

Figure 6.3 *Analysis of neurodegeneration and amyloid deposition and correlation with markers of neurogenesis in non transgenic (non tg) and amyloid precursor protein (APP) tg mice treated with Cerebrolysin (CBL).* **a** Percent area of the molecular layer of the hippocampal dentate gyrus covered by synaptophysin-immunoreactive terminals. **b** Estimates of the numbers of NeuN+ neurons in the hippocampal dentate gyrus using the disector method. **c** Levels of astrogliosis (glial fibrillary acidic protein [GFAP] immunoreactivity) in the hippocampal dentate gyrus. **d** Percent area of the hippocampus covered by amyloid-β (Aβ)-immunoreactive deposits. *p < 0.05 compared to vehicle-treated APP tg mice by one-way ANOVA with post-hoc Tukey-Kramer (n = 6). **e-h** Linear regression analysis between markers of neurogenesis (5-bromo-2-deoxyuridine [BrdU]- and doublecortin [DCX]-immunoreactive [IR] cells) and markers of neuronal preservation (synaptophysin and NeuN).

Consistent with the effects in neurogenesis, analysis of the nerve terminals by confocal microscopy showed that in the CBL-treated APP tg mice, levels of SYN-immunoreactive (IR) terminals (Figure 6.3a) and NeuN+ cells (Figure 6.3b) in the DG were comparable to non tg control mice. In contrast, in the DG of the vehicle-treated APP tg mice there were decreased levels of SYN-IR terminals (Figure 6.3a) [$F(3,18) = 5.75$, $p<0.01$] and NeuN+ cells (Figure 6.3b) [$F(3,18) = 16.9$, $p<0.001$] compared to CBL-treated APP tg mice. Neuropathological analysis of the APP tg mice showed that compared to the vehicle-treated group, after 1 and 3 months of CBL treatment, there

was a significant reduction in the levels of astrogliosis in the DG (Figure 6.3c) and in the percent area of the neuropil covered by Aβ immunoreactivity (Figure 6.3d). Linear regression analysis showed that the levels of SYN-IR terminals and NeuN+ cells in the DG were correlated with the numbers of BrdU+ (Figure 6.3e, f) and DCX+ (Figure 6.3g, h) cells in the SGZ.

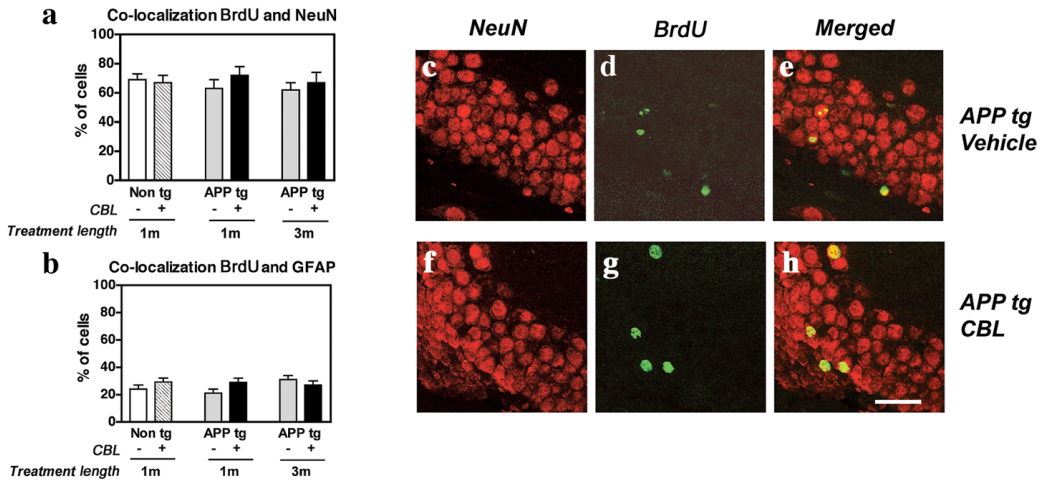

Figure 6.4 *Double-immunocytochemical analysis to determine the proportion of 5-bromo-2-deoxyuridine (BrdU)-positive (+) cells that are NeuN and glial fibrillary acidic protein (GFAP)-positive in non transgenic (non tg) and amyloid precursor protein (APP) tg mice treated with Cerebrolysin (CBL).* **a** Percent of BrdU+ cells that are NeuN+. **b** Percent of BrdU+ cells that are GFAP+. **c-h** Representative images obtained from confocal microscopy of sections double-labeled with antibodies against NeuN (red) and BrdU (green) in the hippocampal dentate gyrus of APP tg mice treated for 1 month (m) with vehicle (**c-e**) or CBL (**f-h**). Scale bar = 50 μm.

The effects of CBL on neurogenesis are associated with increased survival of hippocampal NPC

To determine if the effects of CBL were related to a correction in the baseline alterations in the proportion of NPC in the SGZ converting into neurons or astroglia in the APP tg mice, analysis of sections double-labeled for BrdU and NeuN or GFAP was performed. As expected, in non tg mice approximately 65% of the BrdU+ cells expressed NeuN (Figure 6.4a) and 25% expressed GFAP (Figure 6.4b).

Although in the vehicle-treated APP tg mice there were fewer BrdU+ (and total NeuN+ in the DG) nuclei, the proportion of cells expressing NeuN (Figure 6.4a, c-e) and GFAP (Figure 6.4b) was similar to the non tg controls. Moreover, CBL treatment did not alter this proportion (Figure 6.4b, f-h), suggesting that the effects of CBL on neurogenesis were not related to an enhanced differentiation of precursors into neurons but rather to increased proliferation or survival of NPC in the SGZ of the hippocampus. To investigate these possibilities, sections immunolabeled with an antibody against PCNA or stained with the Apoptag kit were analyzed.

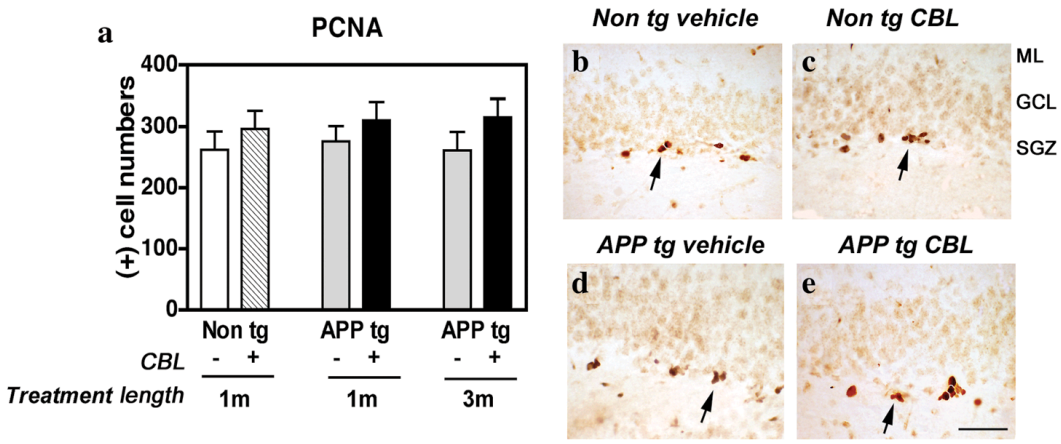

Figure 6.5 *Immunocytochemical analysis of proliferating cell nuclear antigen (PCNA)-positive (+) cells in non transgenic (non tg) and amyloid precursor protein (APP) tg mice treated with Cerebrolysin (CBL).* **a** Quantitative analysis using the disector method in the subgranular zone (SGZ) showing numbers of PCNA+ NPC. **b-e** All panels are representative images displaying the molecular layer (ML), GCL (granular cell layer), and SGZ at 400X magnification of mice treated for 1 month (m). PCNA+ NPC in the SGZ of vehicle-treated non tg mice (**b**), CBL-treated non tg mice (**c**), vehicle-treated APP tg mice (**d**), CBL-treated APP tg mice (**e**). Scale bar = 60 μm.

This study showed that vehicle- and CBL-treated mice showed comparable numbers of PCNA-IR cells in the SGZ (Figure 6.5a). Similarly, no significant differences were observed between vehicle-treated non tg and APP tg mice (Figure 6.5b-e). In contrast, vehicle-treated APP tg mice displayed increased numbers of

TUNEL+ cells in the SGZ compared to the vehicle- and CBL-treated non tg control group (Figure 6.6a, b-d) [$F(3,18) = 4.26$, $p<0.05$].

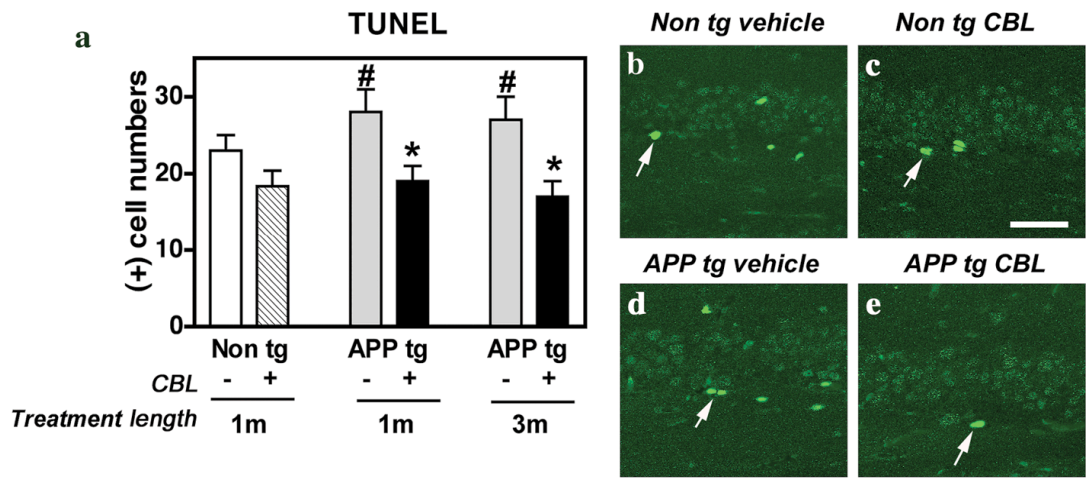

Figure 6.6 *Analysis of DNA fragmentation by terminal deoxynucleotidyl transferase dUTP Nick End Labeling (TUNEL) histochemistry in non transgenic (non tg) and amyloid precursor protein (APP) tg mice treated with Cerebrolysin (CBL).* **a** Quantitative analysis using the disector method in the subgranular zone (SGZ) to estimate the numbers of apoptotic nuclei show increased numbers of TUNEL+ neurons in vehicle-treated APP tg mice compared to non tg animals, while CBL-treated APP tg mice at 1 and 3 months (m) show decreased levels of TUNEL+ neurons compared to vehicle-treated APP tg animals. #$p < 0.05$ compared to vehicle-treated non tg control by one-way ANOVA with post-hoc Dunnett's ($n = 6$); *$p < 0.05$ compared to vehicle-treated APP tg mice by one-way ANOVA with post-hoc Tukey-Kramer ($n = 6$). **b-e** All panels are representative images displaying the molecular layer (ML), GCL (granular cell layer), and SGZ at 400X magnification of mice treated for 1 month. TUNEL+ neurons in the SGZ of vehicle-treated non tg mice (**b**), CBL-treated non tg mice (**c**), vehicle-treated APP tg mice (**d**), CBL-treated APP tg mice (**e**). Scale bar = 60 μm.

This increased mortality of NPC in APP tg mice (Figure 6.6d) was significantly reduced by CBL (Figure 6.6e) after 1 and 3 months of treatment (Figure 6.6a) [$F(3,18) = 7.69$, $p<0.01$]. To verify that NPC in the SGZ of the APP tg mice activate pathways involved in apoptosis, sections were doubled-labeled and analyzed by confocal microscopy. This study showed that in the non tg mice, approximately 3% of the DCX+ cells in the SGZ are immunoreactive for activated caspase-3, and in the APP tg mice, about 5% of the DCX+ cells co-expressed activated caspase-3 (Figure 6.7). In

contrast, in the APP tg mice treated with CBL, less than 2% of the DCX+ cells displayed caspase-3 activation (Figure 6.7). Together, these findings support the possibility that CBL rescues the defects in neurogenesis in APP tg mice by enhancing the *maturation and survival* (and reducing the rate of apoptosis) of the NPC in the hippocampus.

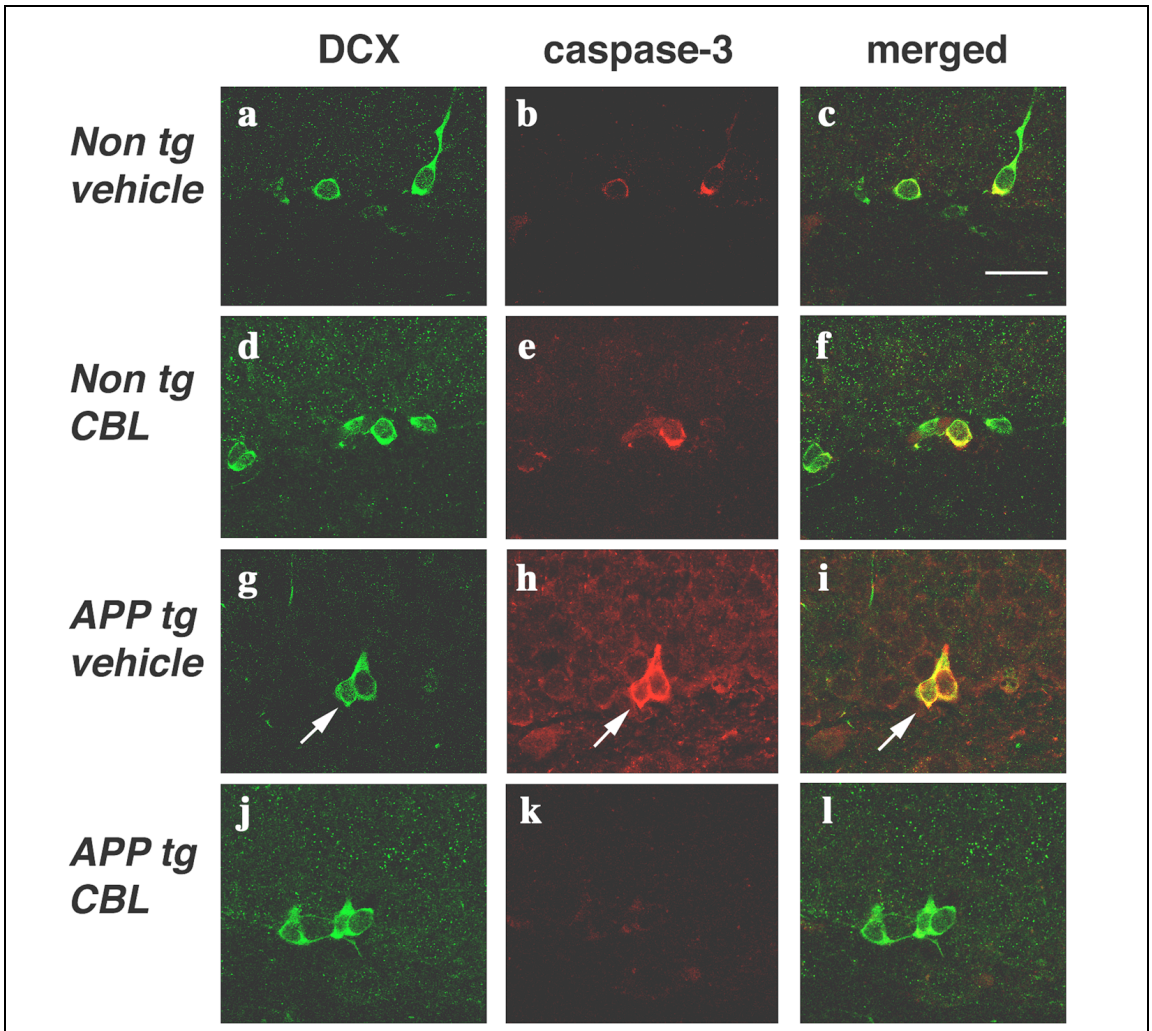

Figure 6.7 *Double-immunocytochemical analysis of activated caspase-3, in NPCs in amyloid precursor protein (APP) tg mice treated with Cerebrolysin (CBL).* All panels are representative images of the SGZ in mice treated for 1 month. Sections were imaged with the confocal microscope. The panels in red correspond to activated caspase-3 and the panels in green correspond to doublecortin (DCX). DCX and activated caspase-3 double-immunolabeling in vehicle-treated non tg mice (**a-c**), CBL-treated non tg mice (**d-f**), vehicle-treated amyloid precursor protein (APP) tg mice (**g-i**), and CBL-treated APP tg mice (**j-l**). Scale bar = 30μm.

Long-term Cerebrolysin treatment regulates kinases involved in AD pathogenesis

To investigate if Cerebrolysin's protective effects on neurogenesis might be related to normalization of signaling pathways that are overactive in AD, levels of active CDK5, GSK3β and another kinase SAPK1 were analyzed by immunoblot. For this purpose, brain homogenates were analyzed by Western blot with antibodies against total and phosphorylated CDK5, GSK3β and SAPK1 (Figure 6.8). While the antibodies against CDK5-p and SAPK1-p recognize the activated kinase, the one against GSK3β-p identifies the inactivated kinase (via the Akt pathway).

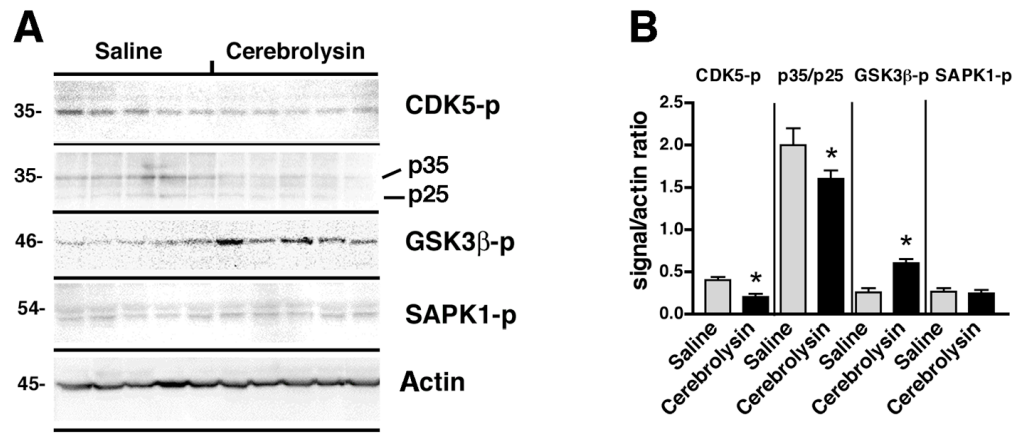

Figure 6.8 *Immunoblot analysis of the effects of Cerebrolysin on the levels of activation of amyloid precursor protein (APP)-phosphorylating kinases.* (A) Representative Western blot of the patterns of phosphorylated cyclin-dependent kinase-5 (CDK5-p), CDK5 activators p25 and p35, phosphorylated glycogen synthase kinase-3β (GSK3β-p) and phosphorylated stress-activated protein kinase-1 (SAPK1-p) immunoreactivity in homogenates from the frontal cortex of APP transgenic (tg) mice treated with saline or Cerebrolysin. (B) Image analysis of the levels of CDK5-p, GSK3β-p and SAPK1-p in the brains of APP tg mice. *$p < 0.05$ compared to saline-treated APP tg mice by unpaired two-tailed Student's t-test; n = 12 mice per group.

This study showed that Cerebrolysin treatment reduced the levels of CDK5-p (active form) and CDK5 activators p35 and p25, and increased the levels of GSK3β-p (inactive form), while the levels of SAPK1-p were unchanged (Figure 6.8A, B). These

results support the notion that by regulating overactive kinases such as CDK5 in AD, Cerebrolysin might protect against defective adult neurogenesis associated with the disorder.

DISCUSSION

The present study showed that CBL ameliorates the alterations in hippocampal neurogenesis in an APP tg model of AD neuropathology. The deficient neurogenesis in the SGZ of the DG found in our APP tg mice is consistent with studies in other lines of APP tg mice that deposit amyloid (Dong et al., 2004; Haughey et al., 2002b) and other models that do not deposit amyloid but express mutant variants of the presenilin gene associated with familial AD (Chevallier et al., 2005; Feng et al., 2001; Wang et al., 2004). These models have shown decreased markers of neurogenesis, such as BrdU+ and DCX+ cells, with an increase in the expression of markers of apoptosis (Dong et al., 2004; Feng et al., 2001; Haughey et al., 2002b; Wang et al., 2004). Although a different study reported increased neurogenesis in the PDAPP model (Jin et al., 2004a), a more recent and comprehensive analysis showed that while in the ML of the DG there is an increased number of NPC, in the SGZ markers of neurogenesis are decreased, indicating that in PDAPP animals there is altered migration and increased apoptosis of NPC that contributes to the deficits in neurogenesis (Donovan et al., 2006). A similar situation might be at play in AD patients since a previous study showed increased expression of markers of neurogenesis in the hippocampus (Jin et al., 2004a).

The increased neurogenesis in the SGZ in the CBL-treated mice was correlated with preservation of the neuronal and synaptic markers in the APP tg mice and with reduced deposition of amyloid aggregates. Moreover, CBL enhanced neurogenesis in the non tg mice. This is consistent with studies in aged rodents and in animals exposed to an enriched environment that have shown that enhanced neurogenesis promotes synaptogenesis and behavioral performance (Kempermann et al., 2002; van Praag et al., 1999). Although the animals used in the present study display a significant amyloid burden in the hippocampus (at 6 months of age amyloid occupies an average of 1% of the hippocampal area), the changes in hippocampal volume are mild and most likely related to the loss of neuropil. Therefore, changes in neurogenesis are unlikely to be a result of alterations in hippocampal volume.

The beneficial effects of CBL on neurogenesis in APP tg mice was linked with reduced apoptosis. Interestingly, BrdU uptake was increased in CBL-treated animals, however NPC proliferation as measured by PCNA immunolabeling was unchanged. This difference is likely a direct result of the decreased apoptosis, because while the BrdU labeling identifies dividing cells over the 5 days of injections and there is a 4-week time period between BrdU injection and euthanization, PCNA immunostaining only indicates NPCs in the cell cycle at the time of tissue fixation. Therefore, numbers of NPCs that take up BrdU appear increased because their rate of apoptosis during the 4 week treatment period is reduced, while instantaneous proliferation rates are unchanged. Since markers of NPC proliferation (e.g., PCNA) and differentiation (e.g., ratio of BrdU+/NeuN+ cells) were not altered in the APP tg mice and were not modified by CBL, we concluded that CBL rescues the defects in neurogenesis in APP

tg mice by enhancing the *maturation and survival* (and reducing the rate of apoptosis) of NPC in the hippocampus. However, the use of PCNA as an indicator of cell proliferation in the APP tg mice needs to be interpreted with caution because previous studies have shown that Aβ might affect PCNA expression (Wu et al., 2000).

The effects of CBL on NPC in APP tg mice is consistent with *in vitro* studies of neuronal cultures (Gutmann et al., 2002; Hartbauer et al., 2001) and *in vivo* studies in rodent NPC (Chen et al., 2006; Tatebayashi et al., 2003) that have shown that distinct from other neurotrophic factors, CBL influences neurogenesis by improving neuronal survival and decreasing apoptosis. The study by Tatebayashi and colleagues showed that CBL treatment resulted in an increase in the number of BrdU+ cells 12 days after treatment, and these effects were associated with an increase in the numbers of newborn NeuN+ neurons and improved performance in the Morris water maze (Tatebayashi et al., 2003). The effects of CBL in the *in vivo* models is also in agreement with studies in neuronal cultures and the mature CNS that have shown that CBL attenuates apoptosis (Rockenstein et al., 2003) resulting from a variety of neurotoxic challenges. The mechanisms through which CBL might regulate maturation and survival of NPC are unclear. Recent studies have shown that in the adult hippocampus the sonic hedgehog (Shh) gene (Ahn and Joyner, 2005; Kenney et al., 2004; Machold et al., 2003), and in the fetal brain the Notch signaling pathway (Androutsellis-Theotokis et al., 2006) play an important role in neurogenesis. In such a paradigm, it has been proposed that Notch activation in NPC activates Akt, mammalian target of rapamycin (mTor), and STAT3, followed by induction of Hes3 and Shh in a temporally controlled fashion (Androutsellis-Theotokis et al., 2006).

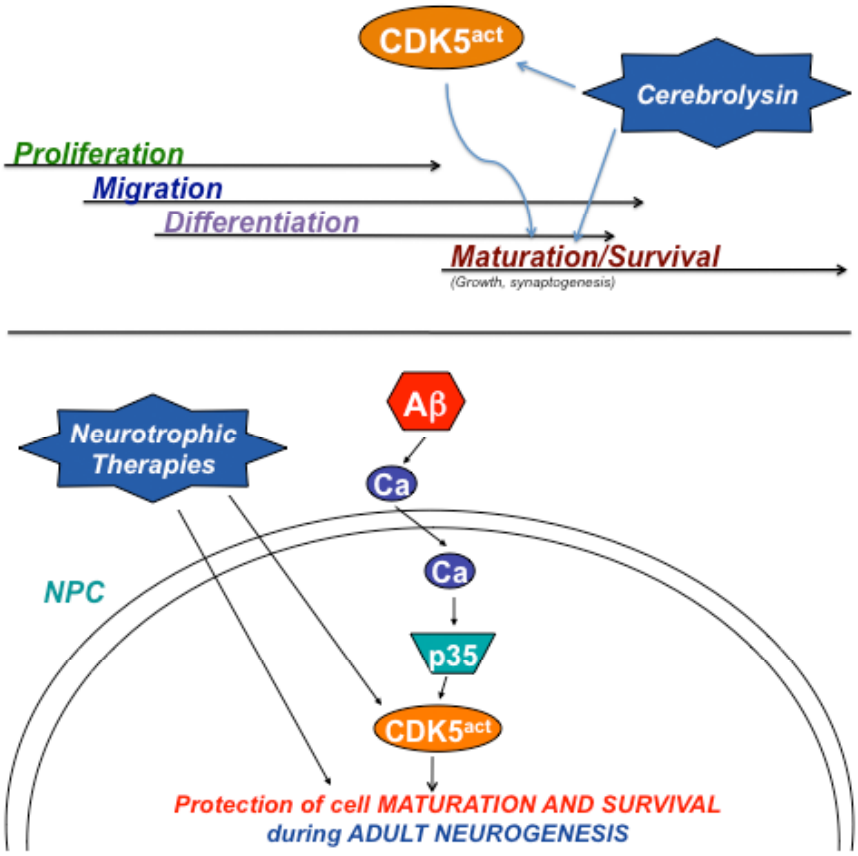

Figure 6.9 *Schematic model of potential mechanisms of therapeutic action of neurotrophic compounds (e.g. Cerebrolysin) that rescue deficient neurogenesis and protect against neurodegenerative alterations in AD.*

We have shown that CBL reduces amyloid production and neurodegeneration in APP tg mice by modulating glycogen synthase kinase-3β (GSK3β) and cyclin-dependent kinase-5 (CDK5) dependent phosphorylation (and maturation) of APP (Rockenstein et al., 2006). Both GSK3β and CDK5 interact with presenilin-1, which participates in the proteolysis of Notch and APP by activating this component of the γ-secretase complex (Ryder et al., 2003; Tesco and Tanzi, 2000). The GSK3β signaling pathway is regulated by Akt and has been shown to modulate the activity and expression of molecules involved in apoptosis and neuronal survival (Chin et al.,

2005) such as the glycoprotein neuronal pentraxin 1 (Enguita et al., 2005), and the transcription factor NFAT3 (Benedito et al., 2005). Moreover, GSK3β cross-talks with the wnt-1 (McManus et al., 2005) and Notch (McKenzie et al., 2006) signaling pathways. Taken together, these studies suggest that CBL might play a role in neurogenesis by regulating *maturation and survival* of NPC via modulation of CDK5 activity (Figure 6.9).

Alternatively, CBL might regulate other aspects of the apoptosis cascades including TNFα-receptor and caspase activation, cytochrome C release and formation of the Apaf-1 complex, among others (Yuan et al., 2003). Future studies will be necessary to investigate these possibilities and to elucidate if the mechanisms through which CBL regulates apoptosis differ between mature neurons and NPC.

Previous studies have suggested that CBL can exert a neurotrophic-like activity by promoting synaptic formation in 6-week-old (Windholz et al., 2000) and aged (Reinprecht et al., 1999) rats, protecting against excitotoxicity (Veinbergs et al., 2000), and ameliorating cognitive deficits and synaptic pathology in animal models of AD-related neurodegeneration (Masliah et al., 1999; Rockenstein et al., 2005a; Rockenstein et al., 2003; Rockenstein et al., 2002; Rockenstein et al., 2006). Furthermore, in a manner similar to nerve growth factor (NGF) (Rossner et al., 1998), CBL promotes neurite outgrowth and cholinergic fiber regeneration (Francis-Turner and Valouskova, 1996; Satou et al., 2000) and reduces the synaptic pathology and behavioral deficits in APP tg mice (Rockenstein et al., 2006). In support of these results, studies in patients with mild to moderate AD have shown that CBL improves cognitive performance and that these effects are maintained even 6 months after termination of therapy (Ruther et

al., 2000). In conclusion, these studies suggest that the combined effects of CBL on neurogenesis, signal transduction, and amyloid production might play a role in alleviating the synaptic and cognitive deficits in patients with AD (Figure 6.9).

ACKNOWLEDGEMENTS

Chapter 6, in part, is a reprint of the material as it appears in Acta Neuropathologica 2007. With kind permission from Springer Science+Business Media: Rockenstein E, Mante M, Adame A, Crews L, Moessler H, Masliah E (2007) Effects of Cerebrolysin on neurogenesis in an APP transgenic model of Alzheimer's disease. Acta Neuropathol (Berl) 113:265-275, Springer Berlin/Heidelberg. The dissertation author was co-author of this paper.

Chapter 6, in part, contains figures of the material as it appears in the Journal of Neuroscience Research 2006. With kind permission from John Wiley and Sons: Rockenstein E, Torrance M, Mante M, Adame A, Paulino A, Rose JB, Crews L, Moessler H, Masliah E (2006) Cerebrolysin decreases amyloid-beta production by regulating amyloid protein precursor maturation in a transgenic model of Alzheimer's disease. J Neurosci Res 83:1252-1261, John Wiley and Sons.

The work in Chapter 6 was supported by NIH grant AG05131 and by a grant from EBEWE Pharmaceuticals.

CHAPTER 7

CONCLUSIONS

Neurodegenerative disorders of the aging population affect over 5 million people in the US and Europe alone. The common feature is the progressive accumulation of misfolded proteins with the formation of toxic oligomers. Alzheimer's Disease (AD) is characterized by cognitive impairment, alterations in synaptic connectivity, progressive degeneration of neuronal populations in the neocortex and limbic system, and formation of amyloid-β (Aβ)-containing plaques and neurofibrillary tangles composed of hyperphsphorylated tau protein.

More recent studies in AD patients and in transgenic (tg) animal models expressing Aβ-precursor protein (APP) have revealed that neurodegeneration in AD is also associated with alterations in hippocampal neurogenesis. These deficits may play a critical role in the cognitive impairments and memory loss, which comprise some of the most devastating manifestations of the disease in afflicted patients. Promising results have been obtained utilizing APP tg models of AD to better understand the molecular mechanisms involved in neurodegeneration and defective neurogenesis associated with the pathogenesis of AD, however the precise signaling pathways and functional alterations involved remain unclear.

In this context, the main objectives of this dissertation were to *i) Investigate the cellular mechanisms involved in defective hippocampal neurogenesis in an animal model of FAD; ii) Elucidate the role of Aβ in altered neurogenesis in AD; iii) Examine*

the role of cyclin-dependent kinase-5 (CDK5) in neurogenesis and its relationship to Aβ-induced alterations in signaling in neuronal progenitor cells (NPCs); and iv) Identify molecular targets of CDK5, as well as other potential novel candidate regulators, and investigate their function in the mechanisms of defective neurogenesis in AD.

To address these aims, I first implemented *in vitro* and *in vivo* models of neurogenesis in AD for the study of neurogenic alterations associated with the pathogenesis of AD (Chapter 2). In order to establish models to investigate the molecular mechanisms that regulate this process, we characterized two *in vitro* cell models of neurogenesis and neuronal maturation. For the first, a mouse embryonic stem (mES) cell line was differentiated to induce neural progeny over a period of 18 days, and markers of neuronal differentiation were assessed by immunoblot and immunocytochemistry. At the end of the differentiation period, we found that cells displayed a neuronal morphology, and expressed markers of immature (β-III-Tubulin) and mature (NSE) neuronal states. However, this process was lengthy and the average cell yield from embryoid body dissociation tended to be low. To develop an alternative, more relevant *in vitro* system to study neurogenesis in the *adult* brain, for the second model, adult rat hippocampal neuronal progenitor cells (NPC) were cultured and differentiated to induce neural progeny over a period of 4 days, followed by immunoblot and immunocytochemical analyses. This procedure induced neurite outgrowth and yielded a high proportion of β-III-Tubulin-positive cells.

We determined that the NPC model was the most relevant for studying adult neurogenesis *in vitro*, so then we characterized the CDK5 signaling pathway in these

cells during induced neuronal differentiation (Chapter 2). For this purpose, first we showed by immunoblot, qRT-PCR and immunocytochemical analyses that CDK5 mRNA and protein levels were increased during the 4-day NPC neuronal differentiation procedure, and this increase occurred primarily between days 2 and 4. This is consistent with previous *in vitro* studies (Fu et al., 2002), and supports a role for CDK5 in the maturation of NPCs during adult neurogenesis.

Following this, next we determined the effects of CDK5 deficiency in adult neurogenesis, and then we then adapted this model to develop a paradigm of adult hippocampal neurogenesis in AD (Chapter 3). In support of the hypothesis that CDK5 plays an important role during adult hippocampal neurogenesis, in the adult rat NPC model of neurogenesis, pharmacological and siRNA knockdown approaches demonstrated that inhibition of CDK5 resulted in lower levels of neuronal markers such as β-III tubulin. Moreover, NPCs were arrested in their development and displayed numerous short processes even after 4 days of differentiation. In comparison, vehicle-treated controls at this stage were characterized by more complex, longer neurites. Similarly, in a heterozygous deficient mouse model of CDK5 inhibition ($CDK5^{+/-}$ mice), we showed that decreased levels of CDK5 were accompanied by a reduction in markers of neurogenesis in the hippocampal dentate gyrus of adult mice compared to wild-type controls.

Previous studies (Ohshima et al., 1996; Tanaka et al., 2001) and the results of the present study show that inhibition of CDK5 activity is by itself deleterious to neuronal survival and differentiation. Although CDK5 has been implicated in cell migration during developmental neurogenesis (Figure 7.1), less is known about this

signaling pathway in adult neurogenesis in the context of neurodegenerative disease. Two recent studies have shown that CDK5 is critical for adult neuronal differentiation (Jessberger et al., 2008; Lagace et al., 2008), however the role of this kinase in mediating neurogenic alterations in AD is unclear. Previous studies have clarified in some detail the mechanism through which hyperactivation of CDK5 plays a causal role in the pathogenesis of neurodegeneration AD. In this process, Aβ triggers calcium influx into neurons, which activates calpain activity and subsequent cleavage of p35 to p25, which is a more stable activator of CDK5 that promotes the hyperphosphorylation of downstream substrates of CDK5 (Lee et al., 2000). Similar pathways might be involved in the mechanisms of defective neurogenesis in AD, so we focused on the activation of this pathway to further probe the role of CDK5 in the maturation of developing NPCs (Figure 7.1).

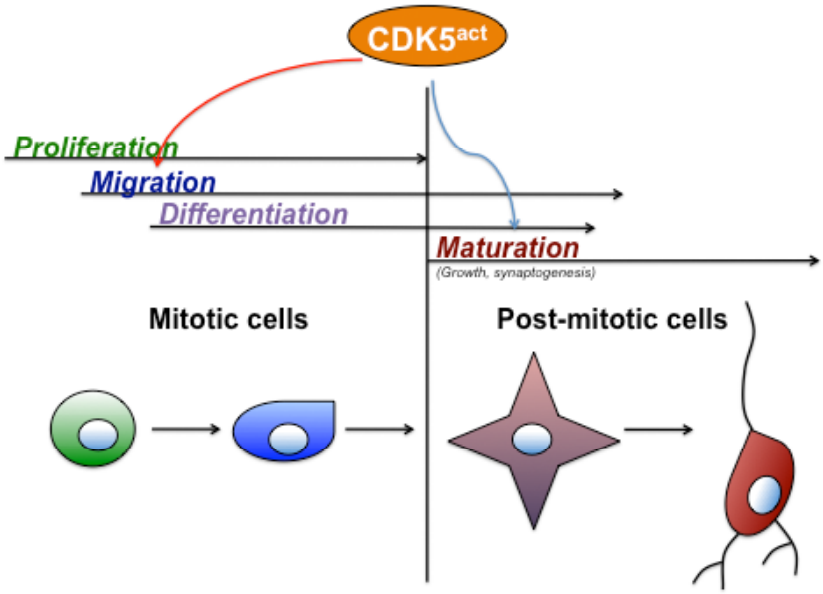

Figure 7.1 *Schematic model of the stages that comprise the neurogenic process in the adult brain, and the role of deregulated cyclin-dependent kinase-5 (CDK5) in this process*. CDK5 has been previously shown to regulate cell migration during developmental neurogenesis, and we provide evidence showing that it may also modulate other stages of neurogenesis, specifically maturation of NPCs.

To investigate this potential function of CDK5, we developed an *in vitro* neurogenesis model of CDK5 hyperactivation in AD (Chapter 3). For this purpose, we utilized the adult rat hippocampal NPC model infected with a viral vector expressing the CDK5 activator, p35. Since Aβ has been shown to abnormally stimulate the activity of this pathway, p35-expressing differentiating NPCs were treated with human $A\beta_{1\text{-}42}$ peptide to study the role of this AD-related protein in the CDK5 signaling pathway in neuronal maturation. In this *in vitro* model of CDK5 hyperactivation in adult neurogenesis in AD, expression of p35 resulted in high levels of p35 immunoreactivity by day four of differentiation, and combined treatment with sub-toxic concentrations of $A\beta_{1\text{-}42}$ for 24 hrs resulted in increased CDK5 activity. This was accompanied by a reduction in neurite outgrowth, and the arrest of neuronal maturation with the generation of progeny expressing multiple markers of progenitor and glial lineages. Taken together, these results support a role for CDK5 hyperactivation in impaired neurogenesis in AD.

Neurogenesis is a complex process characterized by several progressive steps, including NPC *proliferation*, *migration*, *differentiation* (cell fate commitment), and *maturation* (including growth and synaptogenesis) (Figure 7.1). Moreover, during any one of these stages, survival and apoptosis may play a role in the net outcome of neurogenesis and numbers of surviving neural progeny in the adult hippocampus. Furthermore, each of these phases may be regulated by distinct molecular mechanisms, and could be susceptible to changes induced by pathological conditions in disease states. In our model system of adult neurogenesis in AD, we induced CDK5 activation during the latter stage of the neuronal differentiation procedure, when cells

are exiting the proliferative phase and the majority express immature neuronal markers. Therefore we are specifically examining the *maturation* phase of adult NPCs in this culture model (Figure 7.1).

Next, to characterize an *in vivo* model of adult neurogenesis in AD, we examined neurogenesis in a tg mouse model that overexpresses mutant human APP and recapitulates several features of AD (Chapter 3). We showed by immunohistochemical analysis that in this model, there were reduced numbers of BrdU- and DCX-labeled cells in the adult hippocampus of APP tg mice compared to non-tg controls one month post-treatment, and this was accompanied by increased numbers of apoptotic cells in the subgranular zone (SGZ), suggesting that survival or maturation of immature neurons is impaired in these animals. The deficient neurogenesis in the SGZ of the dentate gyrus (DG) found in our APP tg mice (Rockenstein et al., 2007a) is consistent with studies in other lines of APP tg mice and other models of AD that have shown decreased markers of neurogenesis, with an increase in the expression of markers of apoptosis (Dong et al., 2004; Donovan et al., 2006; Feng et al., 2001; Haughey et al., 2002b; Wang et al., 2004). Furthermore, and in support of a role for Aβ in the mechanisms of defective neurogenesis in AD, previous studies in nestin-GFP x APP/PS1 mice showed reduced numbers of quiescent nestin-positive stem cells (Ermini et al., 2008), and these cells displayed an aberrant morphologic reaction toward congophilic amyloid-deposits. Taken together, these studies provide evidence for a disruption to NPCs in an amyloidogenic environment.

Our results support the contention that physiological CDK5 activity is necessary for the proper development of NPCs in the hippocampus, however increased

aberrant activity of CDK5 results in impaired maturation of NPCs in this neurogenic niche. It is important to take this into account when considering CDK5 as a target for therapeutic intervention in AD, as while CDK5 pathological activation associated with AD is detrimental, too little CDK5 activity has a significant negative impact as well (Figure 7.2). A previous work has aptly labeled CDK5 as a "Jekyll and Hyde kinase" (Cruz and Tsai, 2004). This reflects both the pathological hyperphosphorylation of CDK5 substrates associated with neurodegeneration in the pathogenesis of AD (Cruz et al., 2006) as well as the necessity of its physiological function in neuronal migration (Ohshima et al., 1996) and in synaptic integrity (Dhavan and Tsai, 2001; Matsubara et al., 1996) (Figure 7.2).

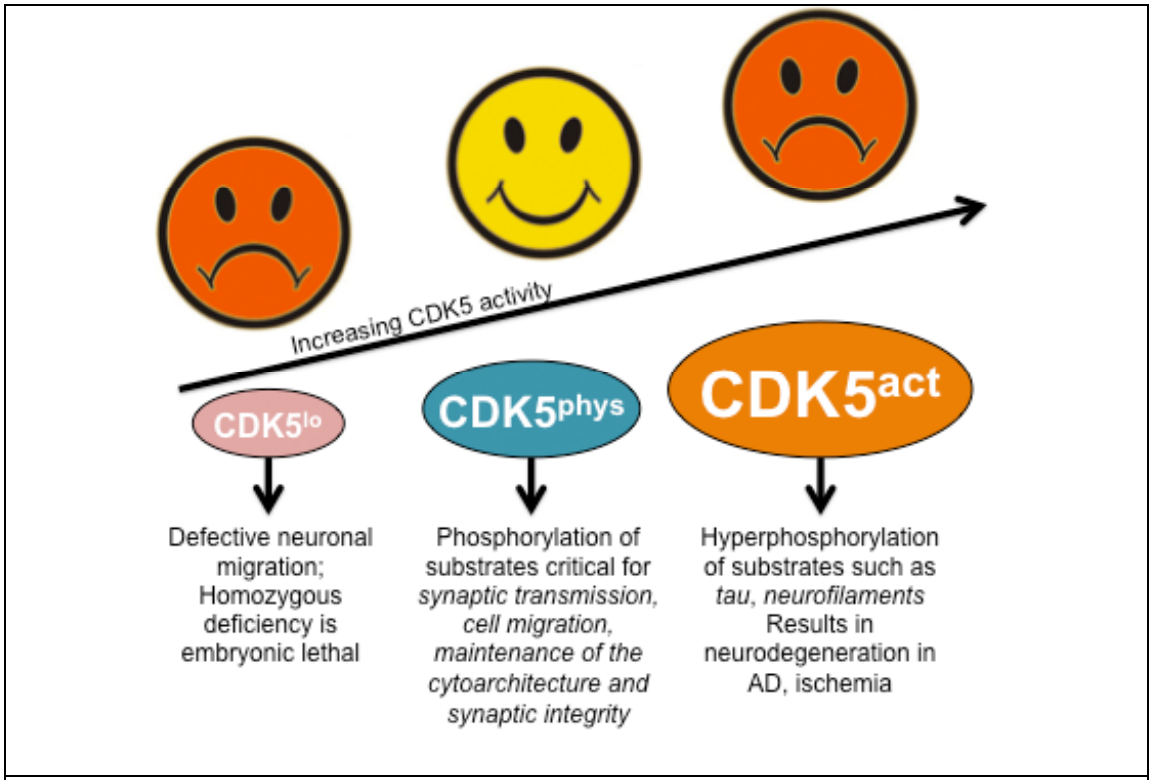

Figure 7.2 *Schematic model of the two "faces" of CDK5 activity*. Reduced CDK5 activity (CDK5 low, or $CDK5^{lo}$) impairs critical neuronal functions, while over-active CDK5 ($CDK5^{act}$) results in hyperphosphorylation of substrates contributing to neurodegeneration and defective neurogenesis in AD.

Having established that deregulation of CDK5 resulted in impaired *maturation* of NPCs in the adult hippocampus in *in vitro* and *in vivo* models of neurogenesis in AD, we next sought to *identify molecular targets of CDK5 that play a role in the mechanisms of defective neurogenesis in AD* (Chapter 4). During the pathogenesis of AD, both CDK5 and GSK3β have been shown to be deregulated, triggering a cascade of hyperphosphorylation of downstream targets of these kinases. Most studies have focused on the role of tau hyperphosphorylation in mediating the neurodegenerative effects of these hyperactive kinases (Cruz and Tsai, 2004), however given the large number of substrates phosphorylated by CDK5 alone, other downstream targets may be involved. In this context, we show here that aberrant phosphorylation of the growth cone signaling protein CRMP2 by CDK5 hyperactivation in an *in vitro* model of adult neurogenesis contributes to defective neurite outgrowth during neuronal maturation. Inhibition of CDK5 with the chemical compound Roscovitine or siRNA knockdown, or expression of a non-phosphorylatable S522A-CRMP2 mutant construct rescued the neurite defects associated with p35/Aβ-mediated activation of CDK5 in NPC-derived neural progeny.

In support of a role for CRMP2 in neurodegeneration in AD, previous studies have revealed that in AD patients and in the triple transgenic mouse model of FAD, hyperphosphorylated CRMP2 accumulates as a result of CDK5 hyperactivity (Soutar et al., 2009). In AD brains, phosphorylated CRMP2 associates with damaged neurites and neurofibrillary tangles (Cole et al., 2007; Yoshida et al., 1998), and builds up in neurons surrounding cortical amyloid plaques, an effect that has been associated with the activation of Rho kinase by Aβ (Petratos et al., 2008). However the role of CDK5

in this process is less clear, and the effects of AD-related, CDK5-directed CRMP2 hyperphosphorylation in adult neurogenesis have not been previously investigated.

Aberrant phosphorylation of CDK5 cytoskeletal substrates may also have an effect on structural elements of developing neurons, such as microtubules. In support of this possibility, we showed that the alterations in neurite outgrowth in p35/Aβ NPC-derived neural progeny were accompanied by defective microtubule polymerization compared to controls, as shown by a redistribution of β-tubulin from polymerized microtubule fractions to the soluble free-tubulin intracellular pool (Chapter 4). This is in accordance with previous studies of CDK5 hyperactivation in neurodegeneration showing that CDK5 can associate with microtubules indirectly (Sobue et al., 2000) and its substrates include microtubule-associated proteins (MAPs). Moreover, the Aβ/CDK5 neurotoxic pathway may involve the destabilization of microtubules (Li et al., 2003). Taken together, abnormal activation of CDK5 by Aβ, resulting in hyperphosphorylation of CRMP2 during the pathogenesis of AD, might impair the functioning of mature neurons and also contribute to alterations in neurogenesis by disturbing the development of stable microtubules in differentiating neurons.

In addition to the potential role that CDK5 may play in neurogenesis in AD, other signaling pathways may contribute to the Aβ-mediated alterations in neurogenesis. Interestingly, paralleling the decline in both the pool of NPCs and their proliferative potential in AD, the levels of various neurotrophic factors, including brain-derived neurotrophic factor (BDNF), stem cell factor (SCF), and neurosteroids among others, are deregulated in AD and FAD-linked models (Laske et al., 2008;

Weill-Engerer et al., 2002); for review see (Schindowski et al., 2008)). These studies suggest that the neurogenic niche is dramatically altered in the pathogenesis of AD, and other growth factors may be aberrantly regulated as well.

In this context, we sought to *identify novel potential regulators of neurogenesis that may play a role in the mechanisms of defective neurogenesis in AD* (Chapter 5). We identified the bone morphogenetic family of proteins (BMP) as candidate regulators of neurogenesis in aging, and found that reduced hippocampal neurogenesis in AD patients and in APP tg mice was accompanied by increased expression levels BMP6, as revealed by qRT-PCR, immunoblot and immunohistochemical analyses. Moreover, BMP6 deposits accumulated surrounding amyloid plaques in the hippocampus. Since BMP6 is a secreted protein, and its primary reported role in the brain is in regulating developmental neurogenesis, it is possible that abnormally elevated levels of this protein in AD might affect adult neurogenesis in the hippocampus. In support of this possibility, *in vitro* studies showed that Aβ exposure increased BMP6 expression levels in NPCs, and that recombinant BMP6 treatment reduced proliferation of NPCs, supporting a role for BMP6 in regulating the *proliferative* phase of neurogenesis in the hippocampus in AD.

In support of a role for BMPs in AD, two recent publications have shown that BMP4 levels are increased in the brains of an animal model of AD (Li et al., 2008b; Tang et al., 2009). High levels of BMP4 were associated with reduced neurogenesis in the DG of mice expressing mutant forms of APP and presenilin-1 (PS1) (Li et al., 2008b; Tang et al., 2009). Increased BMP4 expression was accompanied by reduced expression of the BMP inhibitor Noggin (Tang et al., 2009), however the precise

mechanisms through which BMP levels are increased during the pathogenesis of AD remain unclear. It is possible that normalization of BMP expression in models of AD may present a novel therapeutic approach for protecting against the neurogenic alterations in AD.

It is important to note that neurogenesis persists in the aged brain, however its rate declines with increasing age, as revealed by previous studies in rodents (Kempermann et al., 1998; Kuhn et al., 1996), non-human primates (Gould et al., 1999), and humans (Cameron and McKay, 1999). Despite this natural decline with age, previous studies have shown that the adult brain remains responsive to therapeutic interventions that enhance neurogenesis (Jin et al., 2003; Wise, 2003), and understanding the molecular mechanisms involved in AD-related alterations in neurogenesis might help guide the development of new therapies in this direction.

Additionally, the limited regions in which neurogenesis occurs in the adult brain and the natural reduction in neurogenesis with age might raise questions as to the importance of neurogenesis in the adult brain and in disease processes. However, given the critical role of the hippocampus in the processes of learning and memory, and the recent studies showing that neurogenesis plays an important part in these functions (van Praag et al., 2002), it is possible that modulation of neurogenesis in this area might have therapeutic potential. Moreover, it is important to consider the interconnected circuitry that characterizes the brain's architecture. Although AD pathology in the hippocampus primarily affects the non-neurogenic pyramidal cell layers, the granular cells extend processes into the pyramidal layers, and additionally affect the connectivity of the entorhinal cortex via the perforant pathway. Taken

together, much further work will be necessary to fully understand the role of neurogenesis in the pathogenesis of AD and the therapeutic potential of harnessing the regenerative capacity of progenitor cells.

Considering that numerous alterations have been observed in growth factors in the adult neurogenic niche of the hippocampus during AD, and in an effort to investigate the potential of neuroprotective therapies to rescue the neurogenic deficits associated with AD pathology, we performed an *in vivo* study of APP tg mice treated with a neurotrophic compound (Cerebrolysin) that has previously been shown to reduce neurodegeneration in this model (Chapter 6). This treatment recovered hippocampal neurogenesis in APP tg mice, and this effect was associated with down-regulation of the CDK5 signaling pathway. Taken together, these studies suggest that Cerebrolysin might play a role in neurogenesis by regulating CDK5 activity.

In conclusion, these studies demonstrate that the CDK5 and BMP signaling pathways play important roles in different phases in the process of hippocampal neurogenesis during the pathogenesis of AD. We have shown that a neurotrophic therapy aimed at rescuing the neurogenic deficits in AD is effective, and might exert its effects through down-regulation of aberrant signaling pathways including CDK5. Furthermore, we have demonstrated a role for CRMP2 hyperphosphorylation in the mechanisms of Aβ/CDK5-mediated defective neuronal maturation in the hippocampus in models of neurogenesis in AD. We have also provided evidence showing that Aβ might be directly involved in the mechanisms of BMP6 upregulation in AD. Additional future therapeutic approaches aimed at the normalization of aberrant signaling cascades including the CDK5 and BMP6 pathways could stimulate

endogenous neurogenesis in mouse models and in patients with AD. The rescue of cell proliferation and maturation in the neurogenic niche may be important both for the integrity of local NPCs as well as for the function of the mature neuronal circuitry of the hippocampus and connected regions.

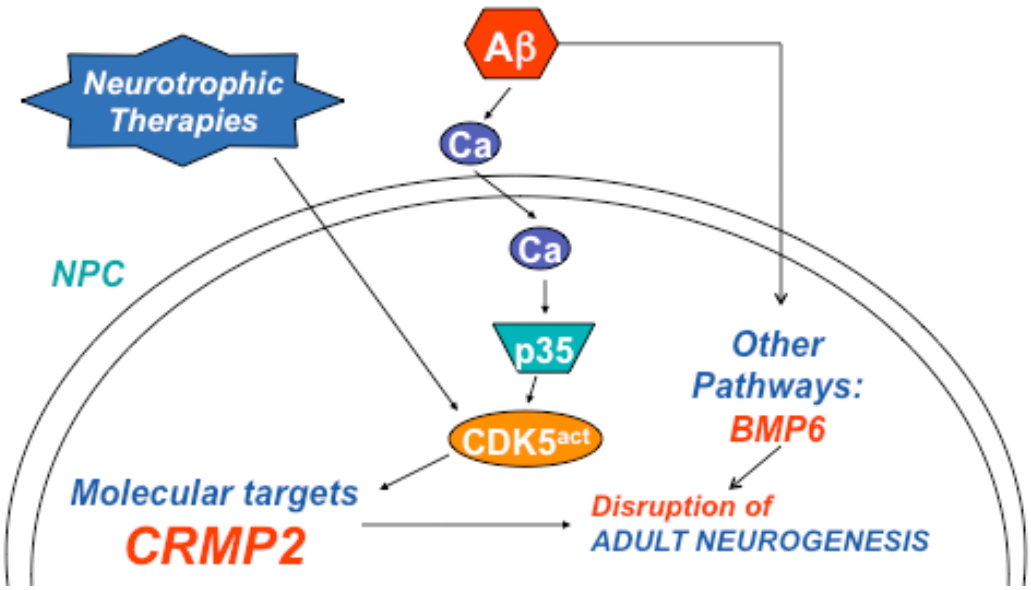

Figure 7.3. *Schematic model of potential Aβ-mediated signaling effects that result in impaired neurogenesis in AD.* Neurotrophic therapies might target these molecular mechanisms to rescue the neurogenic niche and mature neuronal circuitries.

REFERENCES

Ahlijanian, M. K., Barrezueta, N. X., Williams, R. D., Jakowski, A., Kowsz, K. P., McCarthy, S., Coskran, T., Carlo, A., Seymour, P. A., Burkhardt, J. E*., et al.* (2000). Hyperphosphorylated tau and neurofilament and cytoskeletal disruptions in mice overexpressing human p25, an activator of cdk5. Proc Natl Acad Sci U S A *97*, 2910-2915.

Ahn, S., and Joyner, A. L. (2005). In vivo analysis of quiescent adult neural stem cells responding to Sonic hedgehog. Nature *437*, 894-897.

Andra, K., Abramowski, D., Duke, M., Probst, A., Wiederholt, K., Burki, K., Goedert, M., Sommer, B., and Staufenbiel, M. (1996). Expression of APP in transgenic mice: a comparison of neuron-specific promoters. NeurobiolAging *17*, 183-190.

Androutsellis-Theotokis, A., Leker, R. R., Soldner, F., Hoeppner, D. J., Ravin, R., Poser, S. W., Rueger, M. A., Bae, S. K., Kittappa, R., and McKay, R. D. (2006). Notch signalling regulates stem cell numbers in vitro and in vivo. Nature.

Arimura, N., Inagaki, N., Chihara, K., Menager, C., Nakamura, N., Amano, M., Iwamatsu, A., Goshima, Y., and Kaibuchi, K. (2000). Phosphorylation of collapsin response mediator protein-2 by Rho-kinase. Evidence for two separate signaling pathways for growth cone collapse. J Biol Chem *275*, 23973-23980.

Arimura, N., Menager, C., Fukata, Y., and Kaibuchi, K. (2004). Role of CRMP-2 in neuronal polarity. J Neurobiol *58*, 34-47.

Ashford, J. W. (2004). APOE genotype effects on Alzheimer's disease onset and epidemiology. J Mol Neurosci *23*, 157-165.

Association, A. s. (2010). 2010 Alzheimer's disease facts and figures. Alzheimers Dement *6*, 158-194.

Barneda-Zahonero, B., Minano-Molina, A., Badiola, N., Fado, R., Xifro, X., Saura, C. A., and Rodriguez-Alvarez, J. (2009). Bone morphogenetic protein-6 promotes cerebellar granule neurons survival by activation of the MEK/ERK/CREB pathway. Mol Biol Cell *20*, 5051-5063.

Baum, L., Hansen, L., Masliah, E., and Saitoh, T. (1996). Glycogen synthase kinase 3 alteration in Alzheimer disease is related to neurofibrillary tangle formation. MolChemNeuropathol *29*, 253-261.

Beach, T., Walker, R., and McGeer, E. (1989). Patterns of gliosis in Alzheimer's disease and aging cerebrum. Glia *2*, 420-436.

Beatus, P., and Lendahl, U. (1998). Notch and neurogenesis. J Neurosci Res *54*, 125-136.

Benedito, A. B., Lehtinen, M., Massol, R., Lopes, U. G., Kirchhausen, T., Rao, A., and Bonni, A. (2005). The transcription factor NFAT3 mediates neuronal survival. J Biol Chem *280*, 2818-2825.

Bertoli-Avella, A. M., Oostra, B. A., and Heutink, P. (2004). Chasing genes in Alzheimer's and Parkinson's disease. Hum Genet *114*, 413-438.

Bibel, M., Richter, J., Schrenk, K., Tucker, K. L., Staiger, V., Korte, M., Goetz, M., and Barde, Y. A. (2004). Differentiation of mouse embryonic stem cells into a defined neuronal lineage. Nat Neurosci *7*, 1003-1009.

Biebl, M., Cooper, C. M., Winkler, J., and Kuhn, H. G. (2000). Analysis of neurogenesis and programmed cell death reveals a self-renewing capacity in the adult rat brain. Neurosci Lett *291*, 17-20.

Biebl, M., Winner, B., and Winkler, J. (2005). Caspase inhibition decreases cell death in regions of adult neurogenesis. Neuroreport *16*, 1147-1150.

Boekhoorn, K., Joels, M., and Lucassen, P. J. (2006). Increased proliferation reflects glial and vascular-associated changes, but not neurogenesis in the presenile Alzheimer hippocampus. Neurobiol Dis *24*, 1-14.

Borchelt, D., Ratovitski, T., van Lare, J., Lee, M., Gonzales, V., Jenkins, N., Copeland, N., Price, D., and Sisodia, S. (1997). Accelerated amyloid deposition in the brains of transgenic mice coexpressing mutamt presenilin 1 and amyloid precursor proteins. Neuron *19*, 939-945.

Breunig, J. J., Silbereis, J., Vaccarino, F. M., Sestan, N., and Rakic, P. (2007). Notch regulates cell fate and dendrite morphology of newborn neurons in the postnatal dentate gyrus. Proc Natl Acad Sci U S A *104*, 20558-20563.

Brown, J., Cooper-Kuhn, C. M., Kempermann, G., Van Praag, H., Winkler, J., Gage, F. H., and Kuhn, H. G. (2003). Enriched environment and physical activity stimulate hippocampal but not olfactory bulb neurogenesis. Eur J Neurosci *17*, 2042-2046.

Bruel-Jungerman, E., Laroche, S., and Rampon, C. (2005). New neurons in the dentate gyrus are involved in the expression of enhanced long-term memory following environmental enrichment. Eur J Neurosci *21*, 513-521.

Budson, A. E., and Price, B. H. (2005). Memory dysfunction. N Engl J Med *352*, 692-699.

Cai, H., Wang, Y., McCarthy, D., Wen, H., Borchelt, D. R., Price, D. L., and Wong, P. C. (2001). BACE1 is the major beta-secretase for generation of Abeta peptides by neurons. Nat Neurosci *4*, 233-234.

Cameron, H. A., and McKay, R. D. (1999). Restoring production of hippocampal neurons in old age. Nat Neurosci *2*, 894-897.

Chae, T., Kwon, Y. T., Bronson, R., Dikkes, P., Li, E., and Tsai, L. H. (1997). Mice lacking p35, a neuronal specific activator of Cdk5, display cortical lamination defects, seizures, and adult lethality. Neuron *18*, 29-42.

Chana, G., Everall, I. P., Crews, L., Langford, D., Adame, A., Grant, I., Cherner, M., Lazzaretto, D., Heaton, R., Ellis, R., and Masliah, E. (2006). Cognitive deficits and degeneration of interneurons in HIV+ methamphetamine users. Neurology *67*, 1486-1489.

Chana, G., Landau, S., Beasley, C., Everall, I. P., and Cotter, D. (2003). Two-dimensional assessment of cytoarchitecture in the anterior cingulate cortex in major depressive disorder, bipolar disorder, and schizophrenia: evidence for decreased neuronal somal size and increased neuronal density. Biol Psychiatry *53*, 1086-1098.

Chang, C. F., Lin, S. Z., Chiang, Y. H., Morales, M., Chou, J., Lein, P., Chen, H. L., Hoffer, B. J., and Wang, Y. (2003). Intravenous administration of bone morphogenetic protein-7 after ischemia improves motor function in stroke rats. Stroke *34*, 558-564.

Charytoniuk, D. A., Traiffort, E., Pinard, E., Issertial, O., Seylaz, J., and Ruat, M. (2000). Distribution of bone morphogenetic protein and bone morphogenetic protein receptor transcripts in the rodent nervous system and up-regulation of bone morphogenetic protein receptor type II in hippocampal dentate gyrus in a rat model of global cerebral ischemia. Neuroscience *100*, 33-43.

Chen, H., Tung, Y. C., Li, B., Iqbal, K., and Grundke-Iqbal, I. (2006). Trophic factors counteract elevated FGF-2-induced inhibition of adult neurogenesis. Neurobiol Aging.

Chevallier, N. L., Soriano, S., Kang, D. E., Masliah, E., Hu, G., and Koo, E. H. (2005). Perturbed neurogenesis in the adult hippocampus associated with presenilin-1 A246E mutation. Am J Pathol *167*, 151-159.

Chin, P. C., Majdzadeh, N., and D'Mello, S. R. (2005). Inhibition of GSK3beta is a common event in neuroprotection by different survival factors. Brain Res Mol Brain Res *137*, 193-201.

Chou, J., Harvey, B. K., Chang, C. F., Shen, H., Morales, M., and Wang, Y. (2006). Neuroregenerative effects of BMP7 after stroke in rats. J Neurol Sci *240*, 21-29.

Cicero, S., and Herrup, K. (2005). Cyclin-dependent kinase 5 is essential for neuronal cell cycle arrest and differentiation. J Neurosci *25*, 9658-9668.

Colak, D., Mori, T., Brill, M. S., Pfeifer, A., Falk, S., Deng, C., Monteiro, R., Mummery, C., Sommer, L., and Gotz, M. (2008). Adult neurogenesis requires Smad4-mediated bone morphogenic protein signaling in stem cells. J Neurosci *28*, 434-446.

Cole, A. R., Causeret, F., Yadirgi, G., Hastie, C. J., McLauchlan, H., McManus, E. J., Hernandez, F., Eickholt, B. J., Nikolic, M., and Sutherland, C. (2006). Distinct priming kinases contribute to differential regulation of collapsin response mediator proteins by glycogen synthase kinase-3 in vivo. J Biol Chem *281*, 16591-16598.

Cole, A. R., Knebel, A., Morrice, N. A., Robertson, L. A., Irving, A. J., Connolly, C. N., and Sutherland, C. (2004). GSK-3 phosphorylation of the Alzheimer epitope within collapsin response mediator proteins regulates axon elongation in primary neurons. J Biol Chem *279*, 50176-50180.

Cole, A. R., Noble, W., van Aalten, L., Plattner, F., Meimaridou, R., Hogan, D., Taylor, M., LaFrancois, J., Gunn-Moore, F., Verkhratsky, A.*, et al.* (2007). Collapsin response mediator protein-2 hyperphosphorylation is an early event in Alzheimer's disease progression. J Neurochem *103*, 1132-1144.

Cole, G., Dobkins, K., Hansen, L., Terry, R., and Saitoh, T. (1988). Decreased levels of protein kinase C in Alzheimer brain. Brain Res *452*, 165-170.

Cooper-Kuhn, C. M., and Kuhn, H. G. (2002). Is it all DNA repair? Methodological considerations for detecting neurogenesis in the adult brain. Brain Res Dev Brain Res *134*, 13-21.

Cotman, C., Cummings, B., and Pike, C. (1993). Molecular cascades in adaptive versus pathological plasticity. In Neurodegeneration, A. Gorio, ed. (New York, Raven Press), pp. 217-240.

Crews, L., Mizuno, H., Desplats, P., Rockenstein, E., Adame, A., Patrick, C., Winner, B., Winkler, J., and Masliah, E. (2008). Alpha-synuclein alters Notch-1 expression and neurogenesis in mouse embryonic stem cells and in the hippocampus of transgenic mice. J Neurosci *28*, 4250-4260.

Crews, L., Patrick, C., Rockenstein, E. M., Adame, A., and Masliah, E. (2010). Abeta-induced alterations in CDK5 signaling interfere with the maturation of neuronal progenitor cells. *In preparation*.

Crews, L., Rockenstein, E., and Masliah, E. (2009). APP transgenic modeling of Alzheimer's disease: mechanisms of neurodegeneration and aberrant neurogenesis. Brain Struct Funct.

Cruts, M., and Van Broeckhoven, C. (1998). Molecular genetics of Alzheimer's disease. Ann Med *30*, 560-565.

Cruz, J. C., Kim, D., Moy, L. Y., Dobbin, M. M., Sun, X., Bronson, R. T., and Tsai, L. H. (2006). p25/cyclin-dependent kinase 5 induces production and intraneuronal accumulation of amyloid beta in vivo. J Neurosci *26*, 10536-10541.

Cruz, J. C., and Tsai, L. H. (2004). A Jekyll and Hyde kinase: roles for Cdk5 in brain development and disease. Curr Opin Neurobiol *14*, 390-394.

Cuello, A. C. (2005). Intracellular and extracellular Abeta, a tale of two neuropathologies. Brain Pathol *15*, 66-71.

Davis, F. J., Pillai, J. B., Gupta, M., and Gupta, M. P. (2005). Concurrent opposite effects of trichostatin A, an inhibitor of histone deacetylases, on expression of alpha-MHC and cardiac tubulins: implication for gain in cardiac muscle contractility. Am J Physiol Heart Circ Physiol *288*, H1477-1490.

DeKosky, S., and Scheff, S. (1990). Synapse loss in frontal cortex biopsies in Alzheimer's disease: correlation with cognitive severity. AnnNeurol *27*, 457-464.

DeKosky, S. T., Scheff, S. W., and Styren, S. D. (1996). Structural correlates of cognition in dementia: quantification and assessment of synapse change. Neurodegeneration *5*, 417-421.

Dhavan, R., and Tsai, L. H. (2001). A decade of CDK5. Nat Rev Mol Cell Biol *2*, 749-759.

Dhikav, V., and Anand, K. S. (2007). Glucocorticoids may initiate Alzheimer's disease: a potential therapeutic role for mifepristone (RU-486). Med Hypotheses *68*, 1088-1092.

Dickson, D., Farlo, J., Davies, P., Crystal, H., Fuld, P., and Yen, S. (1988). Alzheimer disease. A double immunohistochemical study of senile plaques. AmJPathol *132*, 86-101.

Diez del Corral, R., and Storey, K. G. (2001). Markers in vertebrate neurogenesis. Nat Rev Neurosci *2*, 835-839.

Dong, H., Goico, B., Martin, M., Csernansky, C. A., Bertchume, A., and Csernansky, J. G. (2004). Modulation of hippocampal cell proliferation, memory, and amyloid

plaque deposition in APPsw (Tg2576) mutant mice by isolation stress. Neuroscience *127*, 601-609.

Donovan, M. H., Yazdani, U., Norris, R. D., Games, D., German, D. C., and Eisch, A. J. (2006). Decreased adult hippocampal neurogenesis in the PDAPP mouse model of Alzheimer's disease. J Comp Neurol *495*, 70-83.

Enguita, M., DeGregorio-Rocasolano, N., Abad, A., and Trullas, R. (2005). Glycogen synthase kinase 3 activity mediates neuronal pentraxin 1 expression and cell death induced by potassium deprivation in cerebellar granule cells. Mol Pharmacol *67*, 1237-1246.

Ermini, F. V., Grathwohl, S., Radde, R., Yamaguchi, M., Staufenbiel, M., Palmer, T. D., and Jucker, M. (2008). Neurogenesis and alterations of neural stem cells in mouse models of cerebral amyloidosis. Am J Pathol *172*, 1520-1528.

Feng, R., Rampon, C., Tang, Y. P., Shrom, D., Jin, J., Kyin, M., Sopher, B., Miller, M. W., Ware, C. B., Martin, G. M.*, et al.* (2001). Deficient neurogenesis in forebrain-specific presenilin-1 knockout mice is associated with reduced clearance of hippocampal memory traces. Neuron *32*, 911-926.

Fischer, A., Sananbenesi, F., Pang, P. T., Lu, B., and Tsai, L. H. (2005). Opposing roles of transient and prolonged expression of p25 in synaptic plasticity and hippocampus-dependent memory. Neuron *48*, 825-838.

Francis-Turner, L., and Valouskova, V. (1996). Nerve growth factor and nootropic drug Cerebrolysin but not fibroblast growth factor can reduce spatial memory impairment elicited by fimbria-fornix transection: short-term study. NeurosciLett *202*, 1-4.

Fu, W. Y., Wang, J. H., and Ip, N. Y. (2002). Expression of Cdk5 and its activators in NT2 cells during neuronal differentiation. J Neurochem *81*, 646-654.

Fukata, Y., Itoh, T. J., Kimura, T., Menager, C., Nishimura, T., Shiromizu, T., Watanabe, H., Inagaki, N., Iwamatsu, A., Hotani, H., and Kaibuchi, K. (2002). CRMP-2 binds to tubulin heterodimers to promote microtubule assembly. Nat Cell Biol *4*, 583-591.

Fukuda, S., Abematsu, M., Mori, H., Yanagisawa, M., Kagawa, T., Nakashima, K., Yoshimura, A., and Taga, T. (2007). Potentiation of astrogliogenesis by STAT3-mediated activation of bone morphogenetic protein-Smad signaling in neural stem cells. Mol Cell Biol *27*, 4931-4937.

Fukuda, S., and Taga, T. (2005). Cell fate determination regulated by a transcriptional signal network in the developing mouse brain. Anat Sci Int *80*, 12-18.

Gage, F. H., Kempermann, G., Palmer, T. D., Peterson, D. A., and Ray, J. (1998). Multipotent progenitor cells in the adult dentate gyrus. J Neurobiol *36*, 249-266.

Gamell, C., Osses, N., Bartrons, R., Ruckle, T., Camps, M., Rosa, J. L., and Ventura, F. (2008). BMP2 induction of actin cytoskeleton reorganization and cell migration requires PI3-kinase and Cdc42 activity. J Cell Sci *121*, 3960-3970.

Games, D., Adams, D., Alessandrini, R., Barbour, R., Berthelette, P., Blackwell, C., Carr, T., Clemes, J., Donaldson, T., Gillespie, F.*, et al.* (1995). Alzheimer-type neuropathology in transgenic mice overexpressing V717F b-amyloid precursor protein. Nature *373*, 523-527.

Games, D., Masliah, E., Lee, M., Johnson-Wood, K., and Schenk, D. (1997). Neurodegenerative Alzheimer-like pathology in PDAPP 717V-->F transgenic mice. In Connections, cognition and Alzheimer's disease, B. Hyman, C. Duyckaerts, and Y. Christen, eds. (Berlin, Springer-Verlag), pp. 105-119.

Gilmore, E. C., Ohshima, T., Goffinet, A. M., Kulkarni, A. B., and Herrup, K. (1998). Cyclin-dependent kinase 5-deficient mice demonstrate novel developmental arrest in cerebral cortex. J Neurosci *18*, 6370-6377.

Glabe, C. C. (2005). Amyloid accumulation and pathogensis of Alzheimer's disease: significance of monomeric, oligomeric and fibrillar Abeta. Subcell Biochem *38*, 167-177.

Glabe, C. G., and Kayed, R. (2006). Common structure and toxic function of amyloid oligomers implies a common mechanism of pathogenesis. Neurology *66*, S74-78.

Goshima, Y., Nakamura, F., Strittmatter, P., and Strittmatter, S. M. (1995). Collapsin-induced growth cone collapse mediated by an intracellular protein related to UNC-33. Nature *376*, 509-514.

Gould, E., Reeves, A. J., Fallah, M., Tanapat, P., Gross, C. G., and Fuchs, E. (1999). Hippocampal neurogenesis in adult Old World primates. Proc Natl Acad Sci U S A *96*, 5263-5267.

Grant, P., Sharma, P., and Pant, H. C. (2001). Cyclin-dependent protein kinase 5 (Cdk5) and the regulation of neurofilament metabolism. Eur J Biochem *268*, 1534-1546.

Gross, R. E., Mehler, M. F., Mabie, P. C., Zang, Z., Santschi, L., and Kessler, J. A. (1996). Bone morphogenetic proteins promote astroglial lineage commitment by mammalian subventricular zone progenitor cells. Neuron *17*, 595-606.

Gundersen, H. J., Bagger, P., Bendtsen, T. F., Evans, S. M., Korbo, L., Marcussen, N., Moller, A., Nielsen, K., Nyengaard, J. R., Pakkenberg, B., and et al. (1988). The new stereological tools: disector, fractionator, nucleator and point sampled intercepts and their use in pathological research and diagnosis. Apmis *96*, 857-881.

Gutmann, B., Hutter-Paier, B., Skofitsch, G., Windisch, M., and Gmeinbauer, R. (2002). In vitro models of brain ischemia: the peptidergic drug cerebrolysin protects cultured chick cortical neurons from cell death. Neurotox Res *4*, 59-65.

Hartbauer, M., Hutter-Paier, B., Skofitsch, G., and Windisch, M. (2001). Antiapoptotic effects of the peptidergic drug cerebrolysin on primary cultures of embryonic chick cortical neurons. J Neural Transm *108*, 459-473.

Harvey, B. K., Hoffer, B. J., and Wang, Y. (2005). Stroke and TGF-beta proteins: glial cell line-derived neurotrophic factor and bone morphogenetic protein. Pharmacol Ther *105*, 113-125.

Harvey, B. K., Mark, A., Chou, J., Chen, G. J., Hoffer, B. J., and Wang, Y. (2004). Neurotrophic effects of bone morphogenetic protein-7 in a rat model of Parkinson's disease. Brain Res *1022*, 88-95.

Hashimoto, M., Hernandez-Ruiz, S., Hsu, L., Sisk, A., Xia, Y., Takeda, A., Sundsmo, M., and Masliah, E. (1998). Human recombinant NACP/a-synuclein is aggregated and fibrillated in vitro: Relevance for Lewy body disease. Brain Res *799*, 301-306.

Haughey, N. J., Liu, D., Nath, A., Borchard, A. C., and Mattson, M. P. (2002a). Disruption of neurogenesis in the subventricular zone of adult mice, and in human cortical neuronal precursor cells in culture, by amyloid beta-peptide: implications for the pathogenesis of Alzheimer's disease. Neuromolecular Med *1*, 125-135.

Haughey, N. J., Nath, A., Chan, S. L., Borchard, A. C., Rao, M. S., and Mattson, M. P. (2002b). Disruption of neurogenesis by amyloid beta-peptide, and perturbed neural progenitor cell homeostasis, in models of Alzheimer's disease. J Neurochem *83*, 1509-1524.

Hebert, L. E., Scherr, P. A., Bienias, J. L., Bennett, D. A., and Evans, D. A. (2004). State-specific projections through 2025 of Alzheimer disease prevalence. Neurology *62*, 1645.

Hirota, Y., Ohshima, T., Kaneko, N., Ikeda, M., Iwasato, T., Kulkarni, A. B., Mikoshiba, K., Okano, H., and Sawamoto, K. (2007). Cyclin-dependent kinase 5 is required for control of neuroblast migration in the postnatal subventricular zone. J Neurosci *27*, 12829-12838.

Hof, P., Cox, K., and Morrison, J. (1990). Quantitative analysis of a vulnerable subset of pyramidal neurons in Alzheimer's disease: I. Superior frontal and inferior temporal cortex. JCompNeurol *301*, 44-54.

Hooper, C., Markevich, V., Plattner, F., Killick, R., Schofield, E., Engel, T., Hernandez, F., Anderton, B., Rosenblum, K., Bliss, T.*, et al.* (2007). Glycogen synthase kinase-3 inhibition is integral to long-term potentiation. Eur J Neurosci *25*, 81-86.

Hou, Z., Li, Q., He, L., Lim, H. Y., Fu, X., Cheung, N. S., Qi, D. X., and Qi, R. Z. (2007). Microtubule association of the neuronal p35 activator of Cdk5. J Biol Chem *282*, 18666-18670.

Hsiao, K., Chapman, P., Nilsen, S., Eckman, C., Harigaya, Y., Younkin, S., Yang, F., and Cole, G. (1996). Correlative memory deficits, Ab elevation, and amyloid plaques in transgenic mice. Science *274*, 99-102.

Hsiao, Y. H., Chen, P. S., Yeh, S. H., Lin, C. H., and Gean, P. W. (2008). N-acetylcysteine prevents beta-amyloid toxicity by a stimulatory effect on p35/cyclin-dependent kinase 5 activity in cultured cortical neurons. J Neurosci Res *86*, 2685-2695.

Hutton, M., and Hardy, J. (1997). The presenilins and Alzheimer's disease. Hum Mol Genet *6*, 1639-1646.

Hyman, B., and Gomez-Isla, T. (1994). Alzheimer's disease is a laminar regional and neural system specific disease, not a global brain disease. NeurobiolAging *15*, 353-354.

Hyman, B., VanHoesen, G., Damasio, A., and Barnes, C. (1984). Alzheimer's disease: Cell-specific pathology isolates the hippocampal formation. Science *225*, 1168-1170.

Jessberger, S., Aigner, S., Clemenson, G. D., Jr., Toni, N., Lie, D. C., Karalay, O., Overall, R., Kempermann, G., and Gage, F. H. (2008). Cdk5 regulates accurate maturation of newborn granule cells in the adult hippocampus. PLoS Biol *6*, e272.

Jessberger, S., Gage, F. H., Eisch, A. J., and Lagace, D. C. (2009). Making a neuron: Cdk5 in embryonic and adult neurogenesis. Trends Neurosci *32*, 575-582.

Jin, K., Galvan, V., Xie, L., Mao, X. O., Gorostiza, O. F., Bredesen, D. E., and Greenberg, D. A. (2004a). Enhanced neurogenesis in Alzheimer's disease transgenic (PDGF-APPSw,Ind) mice. Proc Natl Acad Sci U S A *101*, 13363-13367.

Jin, K., Peel, A. L., Mao, X. O., Xie, L., Cottrell, B. A., Henshall, D. C., and Greenberg, D. A. (2004b). Increased hippocampal neurogenesis in Alzheimer's disease. Proc Natl Acad Sci U S A *101*, 343-347.

Jin, K., Sun, Y., Xie, L., Batteur, S., Mao, X. O., Smelick, C., Logvinova, A., and Greenberg, D. A. (2003). Neurogenesis and aging: FGF-2 and HB-EGF restore neurogenesis in hippocampus and subventricular zone of aged mice. Aging Cell *2*, 175-183.

Johansson, J. U., Lilja, L., Chen, X. L., Higashida, H., Meister, B., Noda, M., Zhong, Z. G., Yokoyama, S., Berggren, P. O., and Bark, C. (2005). Cyclin-dependent kinase 5 activators p35 and p39 facilitate formation of functional synapses. Brain Res Mol Brain Res *138*, 215-227.

Johnson, M. A., Ables, J. L., and Eisch, A. J. (2009). Cell-intrinsic signals that regulate adult neurogenesis in vivo: insights from inducible approaches. BMB Rep *42*, 245-259.

Kamenetz, F., Tomita, T., Hsieh, H., Seabrook, G., Borchelt, D., Iwatsubo, T., Sisodia, S., and Malinow, R. (2003). APP Processing and Synaptic Function. Neuron *37*, 925-937.

Katzman, R. (1986). Alzheimer's disease. N Engl J Med *314*, 964-973.

Kawabata, M., Imamura, T., and Miyazono, K. (1998). Signal transduction by bone morphogenetic proteins. Cytokine Growth Factor Rev *9*, 49-61.

Kempermann, G., Gast, D., and Gage, F. H. (2002). Neuroplasticity in old age: sustained fivefold induction of hippocampal neurogenesis by long-term environmental enrichment. Ann Neurol *52*, 135-143.

Kempermann, G., Kuhn, H. G., and Gage, F. H. (1997). More hippocampal neurons in adult mice living in an enriched environment. Nature *386*, 493-495.

Kempermann, G., Kuhn, H. G., and Gage, F. H. (1998). Experience-induced neurogenesis in the senescent dentate gyrus. J Neurosci *18*, 3206-3212.

Kenney, A. M., Widlund, H. R., and Rowitch, D. H. (2004). Hedgehog and PI-3 kinase signaling converge on Nmyc1 to promote cell cycle progression in cerebellar neuronal precursors. Development *131*, 217-228.

Kuhn, H. G., Dickinson-Anson, H., and Gage, F. H. (1996). Neurogenesis in the dentate gyrus of the adult rat: age-related decrease of neuronal progenitor proliferation. J Neurosci *16*, 2027-2033.

Lacor, P. N., Buniel, M. C., Chang, L., Fernandez, S. J., Gong, Y., Viola, K. L., Lambert, M. P., Velasco, P. T., Bigio, E. H., Finch, C. E.*, et al.* (2004). Synaptic targeting by Alzheimer's-related amyloid beta oligomers. J Neurosci *24*, 10191-10200.

Lagace, D. C., Benavides, D. R., Kansy, J. W., Mapelli, M., Greengard, P., Bibb, J. A., and Eisch, A. J. (2008). Cdk5 is essential for adult hippocampal neurogenesis. Proc Natl Acad Sci U S A *105*, 18567-18571.

Lansbury, P. T., Jr. (1999). Evolution of amyloid: what normal protein folding may tell us about fibrillogenesis and disease. Proc Natl Acad Sci U S A *96*, 3342-3344.

Laske, C., Stellos, K., Stransky, E., Seizer, P., Akcay, O., Eschweiler, G. W., Leyhe, T., and Gawaz, M. (2008). Decreased plasma and cerebrospinal fluid levels of stem cell factor in patients with early Alzheimer's disease. J Alzheimers Dis *15*, 451-460.

Lazarov, O., and Marr, R. A. (2009). Neurogenesis and Alzheimer's disease: At the crossroads. Exp Neurol.

Lee, H. G., Moreira, P. I., Zhu, X., Smith, M. A., and Perry, G. (2004). Staying connected: synapses in Alzheimer disease. Am J Pathol *165*, 1461-1464.

Lee, K. Y., Clark, A. W., Rosales, J. L., Chapman, K., Fung, T., and Johnston, R. N. (1999). Elevated neuronal Cdc2-like kinase activity in the Alzheimer disease brain. Neurosci Res *34*, 21-29.

Lee, M. S., Kwon, Y. T., Li, M., Peng, J., Friedlander, R. M., and Tsai, L. H. (2000). Neurotoxicity induces cleavage of p35 to p25 by calpain. Nature *405*, 360-364.

Lesne, S., Koh, M. T., Kotilinek, L., Kayed, R., Glabe, C. G., Yang, A., Gallagher, M., and Ashe, K. H. (2006). A specific amyloid-beta protein assembly in the brain impairs memory. Nature *440*, 352-357.

Lewen, A., Soderstrom, S., Hillered, L., and Ebendal, T. (1997). Expression of serine/threonine kinase receptors in traumatic brain injury. Neuroreport *8*, 475-479.

Li, B., Yamamori, H., Tatebayashi, Y., Shafit-Zagardo, B., Tanimukai, H., Chen, S., Iqbal, K., and Grundke-Iqbal, I. (2008a). Failure of neuronal maturation in Alzheimer disease dentate gyrus. J Neuropathol Exp Neurol *67*, 78-84.

Li, D., Tang, J., Xu, H., Fan, X., Bai, Y., and Yang, L. (2008b). Decreased hippocampal cell proliferation correlates with increased expression of BMP4 in the APPswe/PS1DeltaE9 mouse model of Alzheimer's disease. Hippocampus *18*, 692-698.

Li, G., Faibushevich, A., Turunen, B. J., Yoon, S. O., Georg, G., Michaelis, M. L., and Dobrowsky, R. T. (2003). Stabilization of the cyclin-dependent kinase 5 activator, p35, by paclitaxel decreases beta-amyloid toxicity in cortical neurons. J Neurochem *84*, 347-362.

Lie, D. C., Colamarino, S. A., Song, H. J., Desire, L., Mira, H., Consiglio, A., Lein, E. S., Jessberger, S., Lansford, H., Dearie, A. R., and Gage, F. H. (2005). Wnt signalling regulates adult hippocampal neurogenesis. Nature *437*, 1370-1375.

Lim, D. A., Tramontin, A. D., Trevejo, J. M., Herrera, D. G., Garcia-Verdugo, J. M., and Alvarez-Buylla, A. (2000). Noggin antagonizes BMP signaling to create a niche for adult neurogenesis. Neuron *28*, 713-726.

Liu, F., Su, Y., Li, B., Zhou, Y., Ryder, J., Gonzalez-DeWhitt, P., May, P. C., and Ni, B. (2003). Regulation of amyloid precursor protein (APP) phosphorylation and processing by p35/Cdk5 and p25/Cdk5. FEBS Lett *547*, 193-196.

Liu, Y., Titus, L., Barghouthi, M., Viggeswarapu, M., Hair, G., and Boden, S. D. (2004). Glucocorticoid regulation of human BMP-6 transcription. Bone *35*, 673-681.

Lopes, J. P., Oliveira, C. R., and Agostinho, P. (2007). Role of cyclin-dependent kinase 5 in the neurodegenerative process triggered by amyloid-Beta and prion peptides: implications for Alzheimer's disease and prion-related encephalopathies. Cell Mol Neurobiol *27*, 943-957.

Luo, Y., Bolon, B., Kahn, S., Bennett, B. D., Babu-Khan, S., Denis, P., Fan, W., Kha, H., Zhang, J., Gong, Y*., et al.* (2001). Mice deficient in BACE1, the Alzheimer's beta-secretase, have normal phenotype and abolished beta-amyloid generation. Nat Neurosci *4*, 231-232.

Machold, R., Hayashi, S., Rutlin, M., Muzumdar, M. D., Nery, S., Corbin, J. G., Gritli-Linde, A., Dellovade, T., Porter, J. A., Rubin, L. L*., et al.* (2003). Sonic hedgehog is required for progenitor cell maintenance in telencephalic stem cell niches. Neuron *39*, 937-950.

Mallory, M., Honer, W., Hsu, L., Johnson, R., and Masliah, E. (1999). In vitro synaptotrophic effects of Cerebrolysin in NT2N cells. Acta Neuropathol *97*, 437-446.

Marongiu, R., Spencer, B., Crews, L., Adame, A., Patrick, C., Trejo, M., Dallapiccola, B., Valente, E. M., and Masliah, E. (2009). Mutant Pink1 induces mitochondrial dysfunction in a neuronal cell model of Parkinson's disease by disturbing calcium flux. J Neurochem *108*, 1561-1574.

Masliah, E. (1995). Mechanisms of synaptic dysfunction in Alzheimer's disease. HistolHistopathol *10*, 509-519.

Masliah, E. (2000). The role of synaptic proteins in Alzheimer's disease. Ann N Y Acad Sci *924*, 68-75.

Masliah, E. (2001). Recent advances in the understanding of the role of synaptic proteins in Alzheimer's Disease and other neurodegenerative disorders. J Alzheimers Dis *3*, 121-129.

Masliah, E., Alford, M., Adame, A., Rockenstein, E., Galasko, D., Salmon, D., Hansen, L. A., and Thal, L. J. (2003). Abeta1-42 promotes cholinergic sprouting in patients with AD and Lewy body variant of AD. Neurology *61*, 206-211.

Masliah, E., Armasolo, F., Veinbergs, I., Mallory, M., and Samuel, W. (1999). Cerebrolysin ameliorates performance deficits and neuronal damage in apolipoprotein E-deficient mice. PharmacolBiochemBeh *62*, 239-245.

Masliah, E., Mallory, M., Alford, M., DeTeresa, R., Hansen, L. A., McKeel, D. W., Jr., and Morris, J. C. (2001). Altered expression of synaptic proteins occurs early during progression of Alzheimer's disease. Neurology *56*, 127-129.

Masliah, E., Mallory, M., Alford, M., DeTeresa, R., Iwai, A., and Saitoh, T. (1997). Molecular mechanisms of synaptic disconnection in Alzheimer's disease. In Connections, cognition and Alzheimer's disease, B. Hyman, C. Duyckaerts, and Y. Christen, eds. (Berlin, Springer-Verlag), pp. 121-140.

Masliah, E., Mallory, M., Hansen, L., Alford, M., Albright, T., Terry, R., Shapiro, P., Sundsmo, M., and Saitoh, T. (1991). Immunoreactivity of CD45, a protein phosphotyrosine phosphatase, in Alzheimer disease. Acta Neuropathol *83*, 12-20.

Masliah, E., Mallory, M., Hansen, L., Alford, M., DeTeresa, R., and Terry, R. (1993). An antibody against phosphorylated neurofilaments identifies a subset of damaged association axons in Alzheimer's disease. AmJPathol *142*, 871-882.

Masliah, E., Rockenstein, E., Veinbergs, I., Mallory, M., Hashimoto, M., Takeda, A., Sagara, Sisk, A., and Mucke, L. (2000). Dopaminergic loss and inclusion body formation in alpha-synuclein mice: Implications for neurodegenerative disorders. Science *287*, 1265-1269.

Masliah, E., Sisk, A., Mallory, M., Mucke, L., Schenk, D., and Games, D. (1996). Comparison of neurodegenerative pathology in transgenic mice overexpressing V717F b-amyloid precursor protein and Alzheimer's disease. JNeurosci *16*, 5795-5811.

Masliah, E., and Terry, R. (1994). The role of synaptic pathology in the mechanisms of dementia in Alzheimer's disease. ClinNeurosci *1*, 192-198.

Matsubara, M., Kusubata, M., Ishiguro, K., Uchida, T., Titani, K., and Taniguchi, H. (1996). Site-specific phosphorylation of synapsin I by mitogen-activated protein kinase and Cdk5 and its effects on physiological functions. J Biol Chem *271*, 21108-21113.

McKenzie, G., Ward, G., Stallwood, Y., Briend, E., Papadia, S., Lennard, A., Turner, M., Champion, B., and Hardingham, G. E. (2006). Cellular Notch responsiveness is defined by phosphoinositide 3-kinase-dependent signals. BMC Cell Biol *7*, 10.

McManus, E. J., Sakamoto, K., Armit, L. J., Ronaldson, L., Shpiro, N., Marquez, R., and Alessi, D. R. (2005). Role that phosphorylation of GSK3 plays in insulin and Wnt signalling defined by knockin analysis. Embo J *24*, 1571-1583.

Mehler, M. F., Mabie, P. C., Zhang, D., and Kessler, J. A. (1997). Bone morphogenetic proteins in the nervous system. Trends Neurosci *20*, 309-317.

Moolman, D. L., Vitolo, O. V., Vonsattel, J. P., and Shelanski, M. L. (2004). Dendrite and dendritic spine alterations in Alzheimer models. J Neurocytol *33*, 377-387.

Mucke, L., Abraham, C., Ruppe, M., Rockenstein, E., Toggas, S., Alford, M., and Masliah, E. (1995). Protection against HIV-1 gp120-induced brain damage by neuronal overexpression of human amyloid precursor protein (hAPP). JExpMed *181*, 1551-1556.

Mucke, L., Masliah, E., Yu, G. Q., Mallory, M., Rockenstein, E. M., Tatsuno, G., Hu, K., Kholodenko, D., Johnson-Wood, K., and McConlogue, L. (2000). High-level neuronal expression of abeta 1-42 in wild-type human amyloid protein precursor transgenic mice: synaptotoxicity without plaque formation. J Neurosci *20*, 4050-4058.

Nakashima, K., and Taga, T. (2002). Mechanisms underlying cytokine-mediated cell-fate regulation in the nervous system. Mol Neurobiol *25*, 233-244.

Nikolic, M., Dudek, H., Kwon, Y. T., Ramos, Y. F., and Tsai, L. H. (1996). The cdk5/p35 kinase is essential for neurite outgrowth during neuronal differentiation. Genes Dev *10*, 816-825.

Ohshima, T., Gilmore, E. C., Longenecker, G., Jacobowitz, D. M., Brady, R. O., Herrup, K., and Kulkarni, A. B. (1999). Migration defects of cdk5(-/-) neurons in the developing cerebellum is cell autonomous. J Neurosci *19*, 6017-6026.

Ohshima, T., Hirasawa, M., Tabata, H., Mutoh, T., Adachi, T., Suzuki, H., Saruta, K., Iwasato, T., Itohara, S., Hashimoto, M.*, et al.* (2007). Cdk5 is required for multipolar-to-bipolar transition during radial neuronal migration and proper dendrite development of pyramidal neurons in the cerebral cortex. Development *134*, 2273-2282.

Ohshima, T., Ward, J. M., Huh, C. G., Longenecker, G., Veeranna, Pant, H. C., Brady, R. O., Martin, L. J., and Kulkarni, A. B. (1996). Targeted disruption of the cyclin-dependent kinase 5 gene results in abnormal corticogenesis, neuronal pathology and perinatal death. Proc Natl Acad Sci U S A *93*, 11173-11178.

Olson, A. K., Eadie, B. D., Ernst, C., and Christie, B. R. (2006). Environmental enrichment and voluntary exercise massively increase neurogenesis in the adult hippocampus via dissociable pathways. Hippocampus *16*, 250-260.

Palmer, A., and Gershon, S. (1990). Is the neuronal basis of Alzheimer's disease cholinergic or glutamatergic? FASEB J *4*, 2745-2752.

Pastor, P., and Goate, A. M. (2004). Molecular genetics of Alzheimer's disease. Curr Psychiatry Rep *6*, 125-133.

Patrick, G. N., Zukerberg, L., Nikolic, M., de la Monte, S., Dikkes, P., and Tsai, L. H. (1999). Conversion of p35 to p25 deregulates Cdk5 activity and promotes neurodegeneration. Nature *402*, 615-622.

Pernas-Alonso, R., Morelli, F., di Porzio, U., and Perrone-Capano, C. (1999). Multiplex semi-quantitative reverse transcriptase-polymerase chain reaction of low abundance neuronal mRNAs. Brain Res Brain Res Protoc *4*, 395-406.

Perry, E., Perry, R., Blessed, G., and Tomlinson, B. (1977). Neurotransmitter enzyme abnormalities in senile dementia: CAT and GAD activities in necropsy tissue. JNeurolSci *34*, 247-265.

Petratos, S., Li, Q. X., George, A. J., Hou, X., Kerr, M. L., Unabia, S. E., Hatzinisiriou, I., Maksel, D., Aguilar, M. I., and Small, D. H. (2008). The beta-amyloid protein of Alzheimer's disease increases neuronal CRMP-2 phosphorylation by a Rho-GTP mechanism. Brain *131*, 90-108.

Pigino, G., Paglini, G., Ulloa, L., Avila, J., and Caceres, A. (1997). Analysis of the expression, distribution and function of cyclin dependent kinase 5 (cdk5) in developing cerebellar macroneurons. J Cell Sci *110 (Pt 2)*, 257-270.

Price, D. L., Wong, P. C., Markowska, A. L., Lee, M. K., Thinakaren, G., Cleveland, D. W., Sisodia, S. S., and Borchelt, D. R. (2000). The value of transgenic models for the study of neurodegenerative diseases. Ann N Y Acad Sci *920*, 179-191.

Raff, M. C., Whitmore, A. V., and Finn, J. T. (2002). Axonal self-destruction and neurodegeneration. Science *296*, 868-871.

Rao, M. S., and Shetty, A. K. (2004). Efficacy of doublecortin as a marker to analyse the absolute number and dendritic growth of newly generated neurons in the adult dentate gyrus. Eur J Neurosci *19*, 234-246.

Ray, J., and Gage, F. H. (2006). Differential properties of adult rat and mouse brain-derived neural stem/progenitor cells. Mol Cell Neurosci *31*, 560-573.

Ray, J., Raymon, H. K., and Gage, F. H. (1995). Generation and culturing of precursor cells and neuroblasts from embryonic and adult central nervous system. Methods Enzymol *254*, 20-37.

Reinprecht, I., Gschanes, A., Windisch, M., and Fachbach, G. (1999). Two peptidergic drugs increase the synaptophysin immunoreactivity in brains of 24-month-old rats. Histochem J *31*, 395-401.

Ren, J., Kaplan, P. L., Charette, M. F., Speller, H., and Finklestein, S. P. (2000). Time window of intracisternal osteogenic protein-1 in enhancing functional recovery after stroke. Neuropharmacology *39*, 860-865.

Rocchi, A., Pellegrini, S., Siciliano, G., and Murri, L. (2003). Causative and susceptibility genes for Alzheimer's disease: a review. Brain Res Bull *61*, 1-24.

Rockenstein, E., Adame, A., Mante, M., Larrea, G., Crews, L., Windisch, M., Moessler, H., and Masliah, E. (2005a). Amelioration of the cerebrovascular amyloidosis in a transgenic model of Alzheimer's disease with the neurotrophic compound cerebrolysin. J Neural Transm *112*, 269-282.

Rockenstein, E., Adame, A., Mante, M., Moessler, H., Windisch, M., and Masliah, E. (2003). The neuroprotective effects of Cerebrolysin trade mark in a transgenic model of Alzheimer's disease are associated with improved behavioral performance. J Neural Transm *110*, 1313-1327.

Rockenstein, E., Mallory, M., Mante, M., Alford, M., Windisch, M., Moessler, H., and Masliah, E. (2002). Effects of Cerebrolysin on amyloid-beta deposition in a transgenic model of Alzheimer's disease. J Neural Transm Suppl, 327-336.

Rockenstein, E., Mallory, M., Mante, M., Sisk, A., and Masliah, E. (2001). Early formation of mature amyloid-b proteins deposits in a mutant APP transgenic model depends on levels of Ab1-42. J neurosci Res *66*, 573-582.

Rockenstein, E., Mante, M., Adame, A., Crews, L., Moessler, H., and Masliah, E. (2007a). Effects of Cerebrolysintrade mark on neurogenesis in an APP transgenic model of Alzheimer's disease. Acta Neuropathol (Berl) *113*, 265-275.

Rockenstein, E., Mante, M., Alford, M., Adame, A., Crews, L., Hashimoto, M., Esposito, L., Mucke, L., and Masliah, E. (2005b). High beta-secretase activity elicits neurodegeneration in transgenic mice despite reductions in amyloid-beta levels: implications for the treatment of Alzheimer disease. J Biol Chem *280*, 32957-32967.

Rockenstein, E., McConlogue, L., Tan, H., Power, M., Masliah, E., and Mucke, L. (1995). Levels and alternative splicing of amyloid b protein precursor (APP) transcripts in brains of APP transgenic mice and humans with Alzheimer's disease. JBiolChem *270*, 28257-28267.

Rockenstein, E., Torrance, M., Adame, A., Mante, M., Bar-on, P., Rose, J. B., Crews, L., and Masliah, E. (2007b). Neuroprotective effects of regulators of the glycogen synthase kinase-3beta signaling pathway in a transgenic model of Alzheimer's disease are associated with reduced amyloid precursor protein phosphorylation. J Neurosci *27*, 1981-1991.

Rockenstein, E., Torrance, M., Mante, M., Adame, A., Paulino, A., Rose, J. B., Crews, L., Moessler, H., and Masliah, E. (2006). Cerebrolysin decreases amyloid-beta production by regulating amyloid protein precursor maturation in a transgenic model of Alzheimer's disease. J Neurosci Res *83*, 1252-1261.

Rogers, J., Luber-Narod, J., Styren, S., and Civin, W. (1988). Expression of immune system-associated antigens by cells of the human central nervous system: relationship to the pathology of Alzheimer's disease. NeurobiolAging *9*, 339-349.

Rossner, S., Ueberham, U., Schliebs, R., Perez-Polo, J. R., and Bigl, V. (1998). The regulation of amyloid precursor protein metabolism by cholinergic mechanisms and neurotrophin receptor signaling. Prog Neurobiol *56*, 541-569.

Rowe, W. B., Blalock, E. M., Chen, K. C., Kadish, I., Wang, D., Barrett, J. E., Thibault, O., Porter, N. M., Rose, G. M., and Landfield, P. W. (2007). Hippocampal expression analyses reveal selective association of immediate-early, neuroenergetic, and myelinogenic pathways with cognitive impairment in aged rats. J Neurosci *27*, 3098-3110.

Ruther, E., Ritter, R., Apecechea, M., Freitag, S., and Windisch, M. (1994a). Efficacy of Cerebrolysin in Alzheimer's disease. In New trends in the diagnosis and therapy of Alzheimer's disease, K. Jellinger, G. Ladurner, and M. Windisch, eds. (Vienna, Springer-Verlag), pp. 131-141.

Ruther, E., Ritter, R., Apecechea, M., Freytag, S., Gmeinbauer, R., and Windisch, M. (2000). Sustained improvements in patients with dementia of Alzheimer's type (DAT) 6 months after termination of Cerebrolysin therapy. J Neural Transm *107*, 815-829.

Ruther, E., Ritter, R., Apecechea, M., Freytag, S., and Windisch, M. (1994b). Efficacy of the peptidergic nootropic drug cerebrolysin in patients with senile dementia of the Alzheimer's type (SDAT). Pharmacopsychiatry *27*, 32-40.

Ryder, J., Su, Y., Liu, F., Li, B., Zhou, Y., and Ni, B. (2003). Divergent roles of GSK3 and CDK5 in APP processing. Biochem Biophys Res Commun *312*, 922-929.

Sahlgren, C. M., Mikhailov, A., Vaittinen, S., Pallari, H. M., Kalimo, H., Pant, H. C., and Eriksson, J. E. (2003). Cdk5 regulates the organization of Nestin and its association with p35. Mol Cell Biol *23*, 5090-5106.

Satou, T., Itoh, T., Tamai, Y., Ohde, H., Anderson, A. J., and Hashimoto, S. (2000). Neurotrophic effects of FPF-1070 (Cerebrolysin) on cultured neurons from chicken embryo dorsal root ganglia, ciliary ganglia, and sympathetic trunks. J Neural Transm *107*, 1253-1262.

Scheff, S. W., and Price, D. A. (2001). Alzheimer's disease-related synapse loss in the cingulate cortex. J Alzheimers Dis *3*, 495-505.

Scheff, S. W., and Price, D. A. (2003). Synaptic pathology in Alzheimer's disease: a review of ultrastructural studies. Neurobiol Aging *24*, 1029-1046.

Schindowski, K., Belarbi, K., and Buee, L. (2008). Neurotrophic factors in Alzheimer's disease: role of axonal transport. Genes Brain Behav *7 Suppl 1*, 43-56.

Scholzen, T., and Gerdes, J. (2000). The Ki-67 protein: from the known and the unknown. J Cell Physiol *182*, 311-322.

Selkoe, D. (1989). Amyloid b protein precursor and the pathogenesis of Alzheimer's disease. Cell *58*, 611-612.

Selkoe, D. J. (1999). Translating cell biology into therapeutic advances in Alzheimer's disease. Nature *399*, A23-31.

Selkoe, D. J., Yamazaki, T., Citron, M., Podlisny, M. B., Koo, E. H., Teplow, D. B., and Haass, C. (1996). The role of APP processing and trafficking pathways in the formation of amyloid beta-protein. Ann N Y Acad Sci *777*, 57-64.

Shelton, S. B., and Johnson, G. V. (2004). Cyclin-dependent kinase-5 in neurodegeneration. J Neurochem *88*, 1313-1326.

Sinha, S., Anderson, J., John, V., McConlogue, L., Basi, G., Thorsett, E., and Schenk, D. (2000). Recent advances in the understanding of the processing of APP to beta amyloid peptide. Ann N Y Acad Sci *920*, 206-208.

Sinha, S., Anderson, J. P., Barbour, R., Basi, G. S., Caccavello, R., Davis, D., Doan, M., Dovey, H. F., Frigon, N., Hong, J.*, et al.* (1999). Purification and cloning of amyloid precursor protein beta-secretase from human brain. Nature *402*, 537-540.

Smith, D. S., Greer, P. L., and Tsai, L. H. (2001). Cdk5 on the brain. Cell Growth Differ *12*, 277-283.

Smith, P. D., Crocker, S. J., Jackson-Lewis, V., Jordan-Sciutto, K. L., Hayley, S., Mount, M. P., O'Hare, M. J., Callaghan, S., Slack, R. S., Przedborski, S.*, et al.* (2003). Cyclin-dependent kinase 5 is a mediator of dopaminergic neuron loss in a mouse model of Parkinson's disease. Proc Natl Acad Sci U S A *100*, 13650-13655.

Sobue, K., Agarwal-Mawal, A., Li, W., Sun, W., Miura, Y., and Paudel, H. K. (2000). Interaction of neuronal Cdc2-like protein kinase with microtubule-associated protein tau. J Biol Chem *275*, 16673-16680.

Soutar, M. P., Thornhill, P., Cole, A. R., and Sutherland, C. (2009). Increased CRMP2 phosphorylation is observed in Alzheimer's disease; does this tell us anything about disease development? Curr Alzheimer Res *6*, 269-278.

Sun, M., Thomas, M. J., Herder, R., Bofenkamp, M. L., Selleck, S. B., and O'Connor, M. B. (2007). Presynaptic contributions of chordin to hippocampal plasticity and spatial learning. J Neurosci *27*, 7740-7750.

Tanaka, T., Veeranna, Ohshima, T., Rajan, P., Amin, N. D., Cho, A., Sreenath, T., Pant, H. C., Brady, R. O., and Kulkarni, A. B. (2001). Neuronal cyclin-dependent kinase 5 activity is critical for survival. J Neurosci *21*, 550-558.

Tang, J., Song, M., Wang, Y., Fan, X., Xu, H., and Bai, Y. (2009). Noggin and BMP4 co-modulate adult hippocampal neurogenesis in the APP(swe)/PS1(DeltaE9) transgenic mouse model of Alzheimer's disease. Biochem Biophys Res Commun.

Tang, X., Wang, X., Gong, X., Tong, M., Park, D., Xia, Z., and Mao, Z. (2005). Cyclin-dependent kinase 5 mediates neurotoxin-induced degradation of the transcription factor myocyte enhancer factor 2. J Neurosci *25*, 4823-4834.

Tatebayashi, Y., Lee, M. H., Li, L., Iqbal, K., and Grundke-Iqbal, I. (2003). The dentate gyrus neurogenesis: a therapeutic target for Alzheimer's disease. Acta Neuropathol (Berl) *105*, 225-232.

Terry, R., Hansen, L., and Masliah, E. (1994). Structural basis of the cognitive alterations in Alzheimer disease. In Alzheimer disease, R. Terry, and R. Katzman, eds. (New York, Raven Press), pp. 179-196.

Terry, R., Peck, A., DeTeresa, R., Schechter, R., and Horoupian, D. (1981). Some morphometric aspects of the brain in senile dementia of the Alzheimer type. AnnNeurol *10*, 184-192.

Terry, R. D., Masliah, E., Salmon, D. P., Butters, N., DeTeresa, R., Hill, R., Hansen, L. A., and Katzman, R. (1991). Physical basis of cognitive alterations in Alzheimer's disease: synapse loss is the major correlate of cognitive impairment. Ann Neurol *30*, 572-580.

Tesco, G., and Tanzi, R. E. (2000). GSK3 beta forms a tetrameric complex with endogenous PS1-CTF/NTF and beta-catenin. Effects of the D257/D385A and FAD-linked mutations. Ann N Y Acad Sci *920*, 227-232.

Tesseur, I., and Wyss-Coray, T. (2006). A role for TGF-beta signaling in neurodegeneration: evidence from genetically engineered models. Curr Alzheimer Res *3*, 505-513.

Toggas, S., Masliah, E., Rockenstein, E., and Mucke, L. (1994). Central nervous system damage produced by expression of the HIV-1 coat protein gp120 in transgenic mice. Nature *367*, 188-193.

Trojanowski, J. Q., and Lee, V. M. (2000). "Fatal attractions" of proteins. A comprehensive hypothetical mechanism underlying Alzheimer's disease and other neurodegenerative disorders. Ann N Y Acad Sci *924*, 62-67.

Tsai, L. H., Delalle, I., Caviness, V. S., Jr., Chae, T., and Harlow, E. (1994). p35 is a neural-specific regulatory subunit of cyclin-dependent kinase 5. Nature *371*, 419-423.

Tsigelny, I. F., Crews, L., Desplats, P., Shaked, G. M., Sharikov, Y., Mizuno, H., Spencer, B., Rockenstein, E., Trejo, M., Platoshyn, O.*, et al.* (2008). Mechanisms of hybrid oligomer formation in the pathogenesis of combined Alzheimer's and Parkinson's diseases. PLoS ONE *3*, e3135.

Uchida, Y., Ohshima, T., Sasaki, Y., Suzuki, H., Yanai, S., Yamashita, N., Nakamura, F., Takei, K., Ihara, Y., Mikoshiba, K.*, et al.* (2005). Semaphorin3A signalling is mediated via sequential Cdk5 and GSK3beta phosphorylation of CRMP2: implication of common phosphorylating mechanism underlying axon guidance and Alzheimer's disease. Genes Cells *10*, 165-179.

van Praag, H., Christie, B. R., Sejnowski, T. J., and Gage, F. H. (1999). Running enhances neurogenesis, learning, and long-term potentiation in mice. Proc Natl Acad Sci U S A *96*, 13427-13431.

van Praag, H., Schinder, A. F., Christie, B. R., Toni, N., Palmer, T. D., and Gage, F. H. (2002). Functional neurogenesis in the adult hippocampus. Nature *415*, 1030-1034.

Vassar, R. (2005). beta-Secretase, APP and Abeta in Alzheimer's disease. Subcell Biochem *38*, 79-103.

Vassar, R., Bennett, B. D., Babu-Khan, S., Kahn, S., Mendiaz, E. A., Denis, P., Teplow, D. B., Ross, S., Amarante, P., Loeloff, R.*, et al.* (1999). Beta-secretase cleavage of Alzheimer's amyloid precursor protein by the transmembrane aspartic protease BACE. Science *286*, 735-741.

Veinbergs, I., Mante, M., Mallory, M., and Masliah, E. (2000). Neurotrophic effects of Cerebrolysin in animal models of excitotoxicity. J Neural Transm Suppl *59*, 273-280.

Verwer, R. W., Sluiter, A. A., Balesar, R. A., Baayen, J. C., Noske, D. P., Dirven, C. M., Wouda, J., van Dam, A. M., Lucassen, P. J., and Swaab, D. F. (2007). Mature astrocytes in the adult human neocortex express the early neuronal marker doublecortin. Brain *130*, 3321-3335.

Vogl, T., Ludwig, S., Goebeler, M., Strey, A., Thorey, I. S., Reichelt, R., Foell, D., Gerke, V., Manitz, M. P., Nacken, W.*, et al.* (2004). MRP8 and MRP14 control microtubule reorganization during transendothelial migration of phagocytes. Blood *104*, 4260-4268.

Volles, M. J., and Lansbury, P. T., Jr. (2002). Vesicle permeabilization by protofibrillar alpha-synuclein is sensitive to Parkinson's disease-linked mutations and occurs by a pore-like mechanism. Biochemistry *41*, 4595-4602.

Volles, M. J., Lee, S. J., Rochet, J. C., Shtilerman, M. D., Ding, T. T., Kessler, J. C., and Lansbury, P. T., Jr. (2001). Vesicle permeabilization by protofibrillar alpha-synuclein: implications for the pathogenesis and treatment of Parkinson's disease. Biochemistry *40*, 7812-7819.

Walsh, D., Tseng, B., Rydel, R., Podlisny, M., and Selkoe, D. (2000). The oligomerization of amyloid beta-protein begins intracellularly in cells derived from human brain. Biochemistry *39*, 10831-10839.

Walsh, D. M., Klyubin, I., Fadeeva, J. V., Rowan, M. J., and Selkoe, D. J. (2002). Amyloid-beta oligomers: their production, toxicity and therapeutic inhibition. Biochem Soc Trans *30*, 552-557.

Walsh, D. M., and Selkoe, D. J. (2004). Oligomers on the brain: the emerging role of soluble protein aggregates in neurodegeneration. Protein Pept Lett *11*, 213-228.

Wang, L. H., and Strittmatter, S. M. (1997). Brain CRMP forms heterotetramers similar to liver dihydropyrimidinase. J Neurochem *69*, 2261-2269.

Wang, R., Dineley, K. T., Sweatt, J. D., and Zheng, H. (2004). Presenilin 1 familial Alzheimer's disease mutation leads to defective associative learning and impaired adult neurogenesis. Neuroscience *126*, 305-312.

Wang, X., Shaw, W. R., Tsang, H. T., Reid, E., and O'Kane, C. J. (2007). Drosophila spichthyin inhibits BMP signaling and regulates synaptic growth and axonal microtubules. Nat Neurosci *10*, 177-185.

Weill-Engerer, S., David, J. P., Sazdovitch, V., Liere, P., Eychenne, B., Pianos, A., Schumacher, M., Delacourte, A., Baulieu, E. E., and Akwa, Y. (2002). Neurosteroid quantification in human brain regions: comparison between Alzheimer's and nondemented patients. J Clin Endocrinol Metab *87*, 5138-5143.

Wen, P. H., Hof, P. R., Chen, X., Gluck, K., Austin, G., Younkin, S. G., Younkin, L. H., DeGasperi, R., Gama Sosa, M. A., Robakis, N. K.*, et al.* (2004). The presenilin-1 familial Alzheimer disease mutant P117L impairs neurogenesis in the hippocampus of adult mice. Exp Neurol *188*, 224-237.

Wilcock, G. K., Esiri, M. M., Bowen, D. M., and Hughes, A. O. (1988). The differential involvement of subcortical nuclei in senile dementia of Alzheimer's type. J Neurol Neurosurg Psychiatry *51*, 842-849.

Williams, R. W., and Rakic, P. (1988). Three-dimensional counting: an accurate and direct method to estimate numbers of cells in sectioned material. J Comp Neurol *278*, 344-352.

Windholz, E., Gschanes, A., Windisch, M., and Fachbach, G. (2000). Two peptidergic drugs increase the synaptophysin immunoreactivity in brains of 6-week-old rats. Histochem J *32*, 79-84.

Winner, B., Lie, D. C., Rockenstein, E., Aigner, R., Aigner, L., Masliah, E., Kuhn, H. G., and Winkler, J. (2004). Human wild-type alpha-synuclein impairs neurogenesis. J Neuropathol Exp Neurol *63*, 1155-1166.

Winner, B., Rockenstein, E., Lie, D. C., Aigner, R., Mante, M., Bogdahn, U., Couillard-Despres, S., Masliah, E., and Winkler, J. (2008). Mutant alpha-synuclein exacerbates age-related decrease of neurogenesis. Neurobiol Aging *29*, 913-925.

Wise, P. M. (2003). Creating new neurons in old brains. Sci Aging Knowledge Environ *2003*, PE13.

Wordinger, R. J., and Clark, A. F. (2007). Bone morphogenetic proteins and their receptors in the eye. Exp Biol Med (Maywood) *232*, 979-992.

Wu, Q., Combs, C., Cannady, S. B., Geldmacher, D. S., and Herrup, K. (2000). Beta-amyloid activated microglia induce cell cycling and cell death in cultured cortical neurons. Neurobiol Aging *21*, 797-806.

Yoshida, H., Watanabe, A., and Ihara, Y. (1998). Collapsin response mediator protein-2 is associated with neurofibrillary tangles in Alzheimer's disease. J Biol Chem *273*, 9761-9768.

Yuan, J., Lipinski, M., and Degterev, A. (2003). Diversity in the mechanisms of neuronal cell death. Neuron *40*, 401-413.

Zhang, M., Yan, J. D., Zhang, L., Wang, Q., Lu, S. J., Zhang, J., and Zhu, T. H. (2005). Activation of bone morphogenetic protein-6 gene transcription in MCF-7 cells by estrogen. Chin Med J (Engl) *118*, 1629-1636.

Zhao, C., Deng, W., and Gage, F. H. (2008). Mechanisms and functional implications of adult neurogenesis. Cell *132*, 645-660.